

Soft tissue preservation in amber
a comparative study on the taphonomy and
limits of fossilisation of resin embedded
arthropods

Dissertation

zur

Erlangung des Doktorgrades (Dr. rer. nat.)

der

Mathematisch-Naturwissenschaftlichen Fakultät

der

Rheinischen Friedrich-Wilhelms-Universität Bonn

vorgelegt von

Hans Jonas Barthel

aus

Emmerich am Rhein

Bonn, 2021

Angefertigt mit Genehmigung der Mathematisch-Naturwissenschaftlichen Fakultät der
Rheinischen Friedrich-Wilhelms-Universität Bonn

1. Gutachter

Prof. Dr. Jes Rust

2. Gutachter

Prof. Dr. Tomas Martin

Tag der Promotion:

31.03.2022

Erscheinungsjahr: 2022

For Betty, Heidi & Jürgen

Gone but not forgotten

Zusammenfassung

Diese Doktorarbeit befasst sich mit den Grenzen der morphologischen und biomolekularen Erhaltung von Fossilien in Bernstein und liefert neue Informationen zu ihrer Taphonomie. Ein besonderer Schwerpunkt liegt auf Arthropodeneinschlüssen aus den Bernsteinvorkommen von Cambay und Zhangpu, welche sich chemisch von zuvor untersuchten Bernsteinablagerungen unterscheiden. Dabei konnten zum ersten Mal anhand elektronenmikroskopischer Methoden subzelluläre Strukturen in Fossilien aus dem eozänen Cambay-Bernstein aus Indien nachgewiesen werden. Eine Untersuchung von Arthropoden aus dem miozänen Zhangpu-Bernstein aus China zeigt, dass die Häufigkeit und das Ausmaß der Erhaltung der inneren Gewebe nicht zufällig verteilt sind, sondern in erster Linie durch eine Kombination von organismischen Eigenschaften und ursprünglicher Harzchemie beeinflusst werden. Muskelgewebe, Tracheenreste und Nervengewebe sind am häufigsten erhalten, wohingegen abdominales Gewebe seltener nachweisbar ist. Dieses Muster wird durch das Eindringen flüchtiger Harzverbindungen entlang des Tracheensystems eingeschlossener Arthropoden erklärt.

Chemische Analysen ergaben, dass Bernsteinfossilien mineralischen Ausfällungen von Calcit und Quarz ausgesetzt sein können, was zeigt, dass die geologische Umgebung einen starken Einfluss auf das Potenzial der Erhaltung von Gewebe oder Biomolekülen haben kann. Dies wird weiter durch einen Eidechsenknochen aus Dominikanischem Bernstein bestätigt, in dem der ursprüngliche Bioapatit in Fluorapatit umgewandelt ist. Raman-Spektren derselben Probe zeigten einen intensiven Abbau von Kollagen zu amorphen Kohlenstoffverbindungen, was auf die Abwesenheit intakter Biomoleküle hinweist.

Im Gegensatz dazu können ursprüngliche einzelne Aminosäuren von Fossilien aus Cambay und Zhangpu Bernstein extrahiert werden, die immer noch Rückschlüsse auf deren Phylogenie ermöglichen. Frühere Studien und die Ergebnisse dieser Arbeit legen nahe, dass Aminosäuren die Grenze der Konservierung von Peptiden in Bernstein darstellen.

In Bezug auf DNA-Konservierung in Bernstein wird gezeigt, dass intakte DNA zumindest aus heutigen, in Harz eingebetteten Arthropoden gewonnen werden kann. Dies bietet eine erste Grundlage um schrittweise die Konservierungsgrenze von DNA in Bernstein zu ermitteln. Zahlreiche Details im Hinblick auf die Fossilisation in Bernstein sind noch nicht untersucht worden und beinhalten ein großes Potenzial für zukünftige Studien.

Summary

This doctoral thesis deals with the limits of morphological and biomolecular preservation of fossils in amber and provides new information on their taphonomy. A particular focus lies on arthropod inclusions from Cambay and Zhangpu amber deposits, which both are chemically distinct from previously studied amber occurrences.

For the first time, subcellular structures could be evidenced in fossils from Eocene Cambay amber from India with electron microscopic methods. An examination of arthropods from Miocene Zhangpu amber from China shows that the frequency and extent of internal tissue preservation is not randomly distributed, but impacted by a combination of organismal characteristics and original resin chemistry. Muscle tissue, tracheal remains, and nervous tissue are the most commonly preserved, whereas abdominal tissue is infrequently detectable. This pattern is explained by an infiltration of volatile resin compounds along the tracheal system of entrapped arthropods.

Chemical analyses revealed that amber fossils can be exposed to mineral precipitations of calcite and quartz, which shows that the geological environment can have a strong influence on the potential of tissue or biomolecular preservation. This is further confirmed by a lizard bone from Dominican amber in which the original bioapatite was transformed into fluorapatite. Raman spectra of the same specimen showed an intense degradation of collagen into amorphous carbon compounds, indicating a lack of intact biomolecules.

In contrast to this, original single amino acids are extracted from Cambay and Zhangpu amber fossils which still enable conclusions about their phylogeny. Previous studies and the results of this thesis suggest that amino acids represent the limit of peptide preservation in amber. With respect to DNA preservation in amber, it is shown that intact DNA can be retrieved from extant resin-embedded arthropods. This provides an initial basis for step-by-step approaches towards the DNA preservation limit in amber. Numerous details regarding fossilisation in amber have not yet been investigated and hold great potential for future studies.

Acknowledgements

I am extremely grateful to my supervisor Jes Rust for his support in the last few years and his confidence in me. Without him, this doctoral thesis would be non-existing. I thank Thomas Martin for his engagement on being the second reviewer of this thesis, and also Tom McCann Herbert Koch, and Torsten Wappler for their interest in my work and their willingness to complete the doctoral committee. I am grateful to the former and current members of the DFG research unit FOR 2685 and to the members of the AG Rust for many fruitful discussions, interesting talks, and happy memories. I also want to thank the co-authors of my publications for the great collaboration. It was a pleasure to work with you!

I am grateful to the secretary and technical staff of the Institute of Geosciences, namely Dagmar Hambach, Beate Mühlens, Peter Göddertz, and Georg Oleschinski for helping me countless times. Further, I want to thank the people that contributed to the different unpublished aspects of this thesis. I am looking forward to continue our research! Samantha Presslee and Kirsty Penkman carried out the HPLC analysis, whereas Tatjana Bartz prepared most of the TEM samples. I thank Mara Lönartz for helping me with any issues regarding Raman spectroscopy and for reserving measuring time whenever possible. I am grateful to Thomas van de Kamp for his time and effort he put into scanning so much Zhangpu amber inclusions. I also thank Professor Bo Wang for providing me with the Zhangpu material.

Special thanks go to my friends and colleagues Tory McCoy, David Peris, Jens Lallensack, Thomas Engler, and Bastian Mähler for the great memories. You are awesome! In particular, I want to thank Tory McCoy and Jens Lallensack for their proofreads and critical comments on the drafts of this thesis. Especially, I thank my office mate Bastian Mähler. I really enjoyed our time! Thank you so much for lots of fruitful discussions, funny moments, and supporting me in any regards of my research projects.

I am grateful to the members of the Eulenparlament for countless great evenings. I am happy to be friends with so many fantastic people. I thank my parents Regina and Jürgen for promoting my curiosity in natural sciences and my family for the support and interest in my work.

Lastly, I want to thank the person who constantly encouraged me and kept my back free. Thank you, Jessica for your love, support, and patience.

Table of Contents

Structure of the thesis	1
1.0 General Introduction.....	2
1.1 Project background.....	2
1.2 Exceptional preservation in the fossil record	2
1.3. Amber & resins – a definition	5
1.3.1 Resin composition	8
1.3.2 Chemical analyses of resin and amber	13
1.4 Amber deposits and their occurrence through earth’s history	18
1.5. Amber taphonomy	22
1.5.1 Resin production.....	22
1.5.2 Fossilisation in amber.....	26
2.0 Exceptional preservation in amber: state of the art	31
2.1 Tissue preservation in amber – previous studies.....	31
2.2 Chemical preservation in amber – previous studies.....	33
3.0 Aims of the thesis	35
4.0 Material and methods	36
4.1. Sample origin and geology	36
4.2 Methods.....	39
5.0 Examination of amber taphonomy.....	42
5.1 Microscopic examinations of Cambay amber fossils.....	42
5.2 Raman spectroscopy of resin-embedded insects.....	49
5.2.1 Raman spectroscopy of <i>Hymenaea</i> resins and inclusions	49
5.2.2 Raman spectroscopy of collection material	62
5.3 Synchrotron examination of Zhangpu amber inclusions.....	65
5.4 Amino acid racemization in class II ambers	74
5.4.1 Introduction: fossil amino acids & proteins in the rock record	74
5.4.2 Fossil amino acids and proteins in amber	76
5.4.3 Analysis of amino acid compositions of fossils from class II ambers	77
5.5 DNA extraction of resin-entombed beetles.....	86
5.6 Examination of a lizard forelimb in Dominican amber.....	91
6.0 Synthesis	96
6.1 Taphonomy of amber arthropods.....	96
6.1.1 Early entrapment and mode of fossilisation.....	96
6.1.2 Amber fossil types and their diagenetic history	100

6.1.2 Differences in tissue preservation of amber fossils	104
6.2 Evaluation and future perspectives	109
7.0 Conclusions	111
8.0 References	112
9.0 Appendix	132
9.1 TEM protocol for amber samples	132
9.2 Bio-Rad spectra	134
9.3 HPLC results	136
10.0 Publications	141
10.1 Publicaton 1	141
10.2 Publication 2	172
10.3 Publication 3	207

Structure of the thesis

This thesis is written as a cumulative work, with individual studies submitted and published in international peer-reviewed journals and books. Where applicable, this is mentioned at the beginning of the specific chapter. Minor formal deviations (e.g., in abbreviations) may occur between individual chapters due to the utilization of different journal author guidelines to prepare the publications.

This thesis is divided into seven major sections. Section 1 provides a general introduction to exceptional preservation in the fossil record and several aspects of amber research (geology, analysis, taphonomy). Section 2 summarises previous studies that deal in particular with exceptional preservation in amber. Section 3 discusses open questions and driving hypotheses in amber taphonomy; these are then addressed in the following sections. Material and methods are listed in section 4. Section 5 comprises the new research that was performed by the author in the framework of this thesis. The chapters therein represent either unpublished results or summarised versions of already published works which can be found in the Publications section (10). To date, three chapters have been published in peer-reviewed scientific journals and books and two more will be submitted after performing some final adjustments. In section 6, the new findings are integrated and synthesised with results from previous studies to demonstrate how this work contributes to the understanding of amber taphonomy and if and how the aims of this thesis have been met. Section 7 summarises the main conclusions of this thesis.

1.0 General Introduction

1.1 Project background

This PhD thesis was funded by the Deutsche Forschungsgemeinschaft (DFG; German Research Foundation) and is content-affiliated to the project C2 of the DFG Research Unit FOR 2685: The limits of the fossil record: analytical and experimental approaches towards the understanding of fossilization. FOR 2685 focusses on the formation and taphonomy of vertebrate, arthropod, and plant fossils, and was founded to improve the understanding of fossilisation processes, thereby providing a better characterisation of the material nature of these ancient remains of former life on earth. In total, nine projects, categorised into three clusters, are involved. Cluster A comprises four projects which deal with the preservation of mineralised tissues such as bones, eggs, and teeth. The three projects in Cluster B examine the permineralisation of non-mineralised tissues of plants, crustaceans, and fish. Cluster C comprises two projects which focus on the alteration of non-mineralized tissues: project C1 focusses on secondary plant compounds whereas project C2 deals with soft tissue preservation in amber.

1.2 Exceptional preservation in the fossil record

In the last few decades, numerous studies reported the preservation of soft tissue in the fossil record (e.g. Trinajstić et al., 2007; Manning et al., 2009; McNamara et al., 2010; Li et al., 2010; Haug et al., 2013). The term “soft tissue preservation” traditionally refers to the persistence in a fossil of organismal parts that are not biomineralised during the life of the organism such as skin, muscles, or gut remains (Schweitzer, 2011). From a descriptive point of view, soft tissue preservation can simply be understood to imply the preservation of soft-bodied parts or organisms (= non-mineralised) but the term intermixes various types of preservation: soft tissues can be preserved as impressions of non-mineralised tissue in the sediment (such as footprints), as products of replacement mechanisms, or as original compounds which can only be evidenced via analytical tools (Schweitzer, 2011). Therefore, nowadays a subdivision into morphological, exceptional, and organic preservation is preferred (Schweitzer, 2011). In many cases of traditional “soft tissue preservation,” it is unclear if the material of a fossil is original or not. As long as it has not been proven to be original, the term morphological preservation is preferred over soft tissue preservation (Schweitzer, 2011).

Examples of morphological preservation include soft-bodied organisms such as priapulids from the Cambrian or the wide variety of organisms making up the famous Ediacaran biota (Hofmann et al., 1983; Conway Morris & Robison, 1986). Another common phenomenon is the preservation of the skin as a dark silhouette ('Hautschatten') around the bones, representing the original body outline; this is reported from many different vertebrate groups such as ichthyosaurs and mammals (Franzen, 1985; Storch et al., 1996; Bardet & Fernandez, 2000). Morphological preservation can extend to the tissue or subcellular level (in which case it can be called 'exceptional') and is reported, for example, in the form of cells, collagen fibrils or vessels from dinosaur bones (Pawlicki et al., 1966; Schweitzer et al., 2005). Such examples of morphological (and exceptional) preservation are often the product of replacement mechanisms such as calcification, phosphatisation, or pyritisation of once non-mineralised tissues (Briggs, 1991; Wilby et al., 1996; Briggs, 2003; Briggs et al., 2005; Zhu et al., 2005).

Beyond morphological preservation, extensive evidence of ancient biomolecule preservation in various fossils and depositional environments has been reported in recent years, including porphyrins (Greenwalt et al., 2013; Tahoun et al., 2021), lipids (Bobrovskiy et al., 2018), chitin (Stankiewicz et al., 1997; Ehrlich et al., 2013), amino acids (Manning et al., 2009; Lindgren et al., 2011; Saitta et al., 2020), proteins (Asara et al., 2007; Schweitzer et al., 2009; Bertazzo et al., 2015; Schweitzer et al., 2019; Bailleul et al., 2020; Dutta et al., 2020), and DNA (Poinar et al., 1998; Bailleul et al., 2020). These examples are completed by reports on skin remains and blood cells with some kind of original organic composition (Pawlicki & Nowogrodzka-Zagórska, 1998; Edwards et al., 2011). In such cases, the terms "exceptional" and "organic" preservation are appropriate to describe the fossils (Schweitzer, 2011). Exceptional preservation is a mode of fossilisation where original hard part mineralogy, soft tissue detail, primary organic molecules, cellular or subcellular detail is conserved. Organic preservation is a special type of exceptional preservation, implying that original components are still present in the fossil (Schweitzer, 2011). However, it is vital to distinguish between assuming originality on the basis of morphological similarity to components in living animals and supporting this assertion by applying analytical methods (Schweitzer, 2011).

Studies reporting exceptional or organic preservation are the expression of significant advances in analytical tools, which led to a new interdisciplinary field, termed "Molecular Palaeontology" (Schweitzer, 2004, 2011). Molecular palaeontology is strongly linked with the discipline of taphonomy (literally "laws of burial") which deals with the transition of organic remains into the lithosphere (Martin, 1999). Thus, it deals with processes of fossilisation, which take place

from the point of the death of an organism onwards and track its fate after burial (Martínez-Delclòs et al., 2004). Taphonomic studies are usually experimental and examine how organisms decay and which processes lead to their conservation for millions of years (Martin, 1999). Mineralized tissues such as bones and teeth are commonly found in the fossil record, but the non-mineralised materials are scarce in comparison. Therefore, evidence of original material in fossils is particularly interesting with respect to the limits of fossilisation: what processes lead to the preservation of original molecules? Are some biomolecules more likely to be preserved than others? What are the time constraints on the preservation of biomolecules?

There seems to be no overall mechanism that explains the preservation of biomolecules (organic preservation); rather, various hypotheses exist for different compounds (Schweitzer et al., 2019). One pathway to preserve organic molecules over geological timescales involves their binding to minerals or inorganic compounds, or vice versa (Collins et al., 2000). For example, Schweitzer et al. (2013) and Greenwalt et al. (2013) suggested that iron plays a role in preserving proteins and pigments from fossil tissues. Isolated vessels extracted from *Tyrannosaurus rex* and *Brachylophosaurus canadensis* bones were associated with iron-rich nanoparticles, and in an ostrich blood vessel model, haemoglobin significantly increased tissue stability (Schweitzer et al., 2013). Furthermore, experiments on proteins in eggshell samples revealed differential protein survivability, with the proteins strongly bound to the calcite surface being more persistent (Demarchi et al., 2016). In addition, hydroxyapatite, which is the primary constituent of the mineral phase of bones and dentin, has a strong affinity for binding to DNA, making this labile biomolecule more resistant to decay (Brundin et al., 2013). For melanosomes, a diagenetic incorporation of sulphur (sulphurisation) has been suggested as a pathway of preservation (McNamara et al., 2016).

Another pathway of biomolecular preservation involves glycooxidation and lipoxidation (Wiemann et al., 2020). These Maillard reactions turn proteins, fats, and sugars into tough, complex polymers resulting in the “trapping” of these compounds within humic acid-like geopolymers, which are recognisable as brownish residues (Bada, 1991; Bada et al., 1999, Wiemann et al., 2018). With the help of specific cleaving agents, the incorporated biomolecules can be recovered again, as successfully demonstrated by Poinar et al. (1998) for DNA from an extinct ground sloth. Thus, it is possible to distinguish between different modes of organic fossilisation, although their detailed mechanisms and order of events are yet to be fully understood in most cases.

Occurrences of soft tissue preservation (as morphological, exceptional and/or organic preservation) in the fossil record are restricted to Konservat-Lagerstätten, which represent exceptional conditions in the earth's history (Seilacher, 1970; Seilacher et al., 1985; Allison, 1988). Famous examples include the Cambrian Burgess Shale and Chenjiang Lagerstätte, as well as the Carboniferous Mazon Creek and the Eocene Messel Pit (Selden & Nudds, 2012). Amber deposits represent a unique type of Konservat-Lagerstätten: the fossil inclusions are not directly in contact with the sediment. Instead, the inclusions are in contact with a complex chemical material, which is itself a fossil (specifically a type of “chemofossil”): fossilised tree resin. Amber is famous for its three-dimensional preservation of entrapped organisms, including minute details. Ancient molecules from conventional Konservat-Lagerstätten are usually modified via diagenetic processes (Briggs, 1999; McNamara et al., 2016). But to what extent are biomolecules degraded in inclusions in amber? Previous studies have shown that the quality of preservation is not uniform and varies between deposits (Grimaldi et al., 1994; Stankiewicz et al., 1998; Koller et al., 2005; Soriano et al., 2010; McCoy et al., 2018a). It ranges from complete body fossils to hollow inclusions where just remains of the cuticle are present. This thesis offers new insights into the fossilisation of amber inclusions and their variable preservation quality as well as into the limits of amber preservation in general.

1.3. Amber & resins – a definition

A plethora of plants are capable of producing substances that are stored in pores, ducts, or canals and that can be exuded through the outer surface of the plant, including gums, waxes, mucilages, latex, and resins. These exudates are defined by their composition, secretory tissue, and biosynthetic pathway (Table 1), and have a variety of ecological functions, from growth regulation to energy storage to defensive mechanisms (Langenheim, 1994, 2003). Resins are secreted by canals, pockets (cysts), cavities, epidermal cells or trichomes, and mainly comprise terpenoid or phenolic compounds. Resins have the best fossilisation potential among plant exudates, because their compounds are able to polymerise and cross-link, making them more resistant to decay (Langenheim, 1990; Vávra, 2009). However, resins widely vary in their composition, which means that their fossilisation potential is also variable. Probably the best-known resin producers today are conifers of the families Pinaceae, Araucariaceae, and Cupressaceae. But even among the extant angiosperms, many taxa, such as *Hymenaea* or *Shorea*, are able to produce resin. A more detailed description of resin production in the past and present is given in chapters 1.4 and 1.5.

Table 1. Characteristics of different plant exudates. From Langenheim (2003).

	PRIMARY COMPONENTS	SOLUBILITY	SECRETORY TISSUE
Resins	Terpenoids; phenolic compounds	Lipid soluble	Canals, pockets, cavities, trichomes, epidermal cells
Gums	Polysaccharides	Water soluble	Cavities
Mucilages	Polysaccharides	Water soluble	Idioblasts, epidermal cells, trichomes, ducts, cavities
Oils (fats)	Fatty acids and glycerol	Lipid soluble	None
Waxes	Fatty acids esterified with long-chain alcohols	Lipid soluble	Unspecialized epidermal cells
Latex	Complex mixture, may include terpenoids, phenolic compounds, proteins, carbohydrates, etc.	Lipid soluble	Laticifers

Distinguishing resin, copal, and amber

By definition, amber is fossilised plant resin (Andrée 1951; Langenheim, 2003; Martínez-Delclòs et al., 2004; Ragazzi & Schmidt, 2011; Seyfullah et al., 2018a). In order to enable the preservation of resinous remains over geological time scales, favourable conditions are needed (e.g. chapter 1.5). The transformation from resin into amber is hypothesised to continue for millions of years, and includes processes such as hardening, polymerisation, and crosslinking of its compounds (Cunningham et al., 1983; Mills et al., 1984; Cunningham et al., 1987). This process is called ‘amberisation’ and further includes the burial of the material in sediments where it is exposed to elevated pressure and temperature (Iturralde-Vinent, 2001). Poinar (1992) described the general physical properties of amber with a melting point between 200°C and 380°C, a hardness of 2.0 – 3.0 on Moh’s scale, a specific gravity of 1.04 – 1.10, and a refractive index of 1.5 – 1.6. Amber lacks cleavage and does not have a crystalline structure, but shows conchoidal fracture. The fossilised resin is usually indurate, massive, and resistant to organic solvents, whereas weathered material can be brittle and crumbly (Poinar, 1992). Amber can be translucent or opaque and offers a wide colour spectrum: it ranges from frequent translucent yellow, reddish, or brown to white, but rare occurrences of blue amber have been reported as well (Iturralde-Vinent, 2001). Elemental analyses indicated a composition in the range of 75-87% carbon, 8.5-11% hydrogen, and 5-15% oxygen with occasional occurrences of sulphur (up

to 1.7%) and other elements (Grimalt et al., 1987; Ragazzi et al., 2003; Ragazzi & Schmidt, 2011).

In addition to resin and amber, there is also sub-fossilised resin termed “copal” which is assumed to be a diagenetic precursor of amber (Langenheim, 1990; Iturralde-Vinent, 2001; Vávra, 2009). The loosely usage of the term copal in scientific studies has led to much confusion: “copal” has different meanings and was used to describe both modern and fossil resin, depending on the cultural context and study area (Langenheim, 1995). A recent example on this issue was presented by Delclòs et al. (2020), who showed that “Madagascar copal” is a modern resin with a maximum age of roughly 300 years rather than sub-fossil.

However, there is no clear boundary between sub-fossilised resin (occasionally called copal) and amber, which is why the definitions of these terms have been discussed extensively (Anderson, 1996; Vávra, 2009; Seyfullah et al., 2018a). Previous studies attempted to distinguish the different materials via chemical and physical properties such as melting point and microhardness which were thought to be a function of age (Poinar, 1992; Feist et al., 2007; Czapla et al., 2016; Stach et al., 2019). However, these characteristics depend less on age than on diagenetic processes and the original composition of the exudate (Stach et al., 2019).

The same is true for the maturity of the resin, which is indicated by the grade of polymerisation. For example, the Cambay amber, which was produced roughly 53 million years ago by trees of the family Dipterocarpaceae, has an extremely low degree of polymerisation and behaves brittlely (Rust et al., 2010; Mazur et al., 2014) whereas modern *Hymenaea* trees (Leguminosae) produce resin that polymerises quickly to a very high degree, so that even resin pieces (as opposed to copal or amber) from these trees can be very hard (Langenheim, 2003). Therefore, the maturity of the resin alone is not suited for distinguishing between amber and copal, and depends on the diagenetic history of the sample and its botanic origin (Brody et al., 2001).

Even though there is no set age at which copal becomes amber (Penney & Green, 2010; Penney & Preziosi, 2010; Penney & Green, 2012), distinguishing amber, copal, and resin solely on the basis of age provides a general framework for discussion (Schlee & Glöckner, 1978; Anderson, 1996).

This thesis follows the most recent approach of Solórzano Kraemer et al. (2020), who established a new classification based on radiocarbon (^{14}C) dating (Fig. 1). These authors suggest a distinction between amber, Pleistocene copal, Holocene copal, and Defaunation resin. In consequence, amber is defined as fossilised plant resin older than 2.58 Ma. Copal can be considered as ancient resin having an age between 2.58 Ma and 1760 AD. A subdivision into

Pleistocene copal (2.58 - 0.0117 Ma) and Holocene copal (0.0117 - 1760 AD) is preferred. The novel term “Defaunation resin” comprises all resins exuded after 1760 AD and is based on the defaunation concept according to Dirzo et al. (2014).

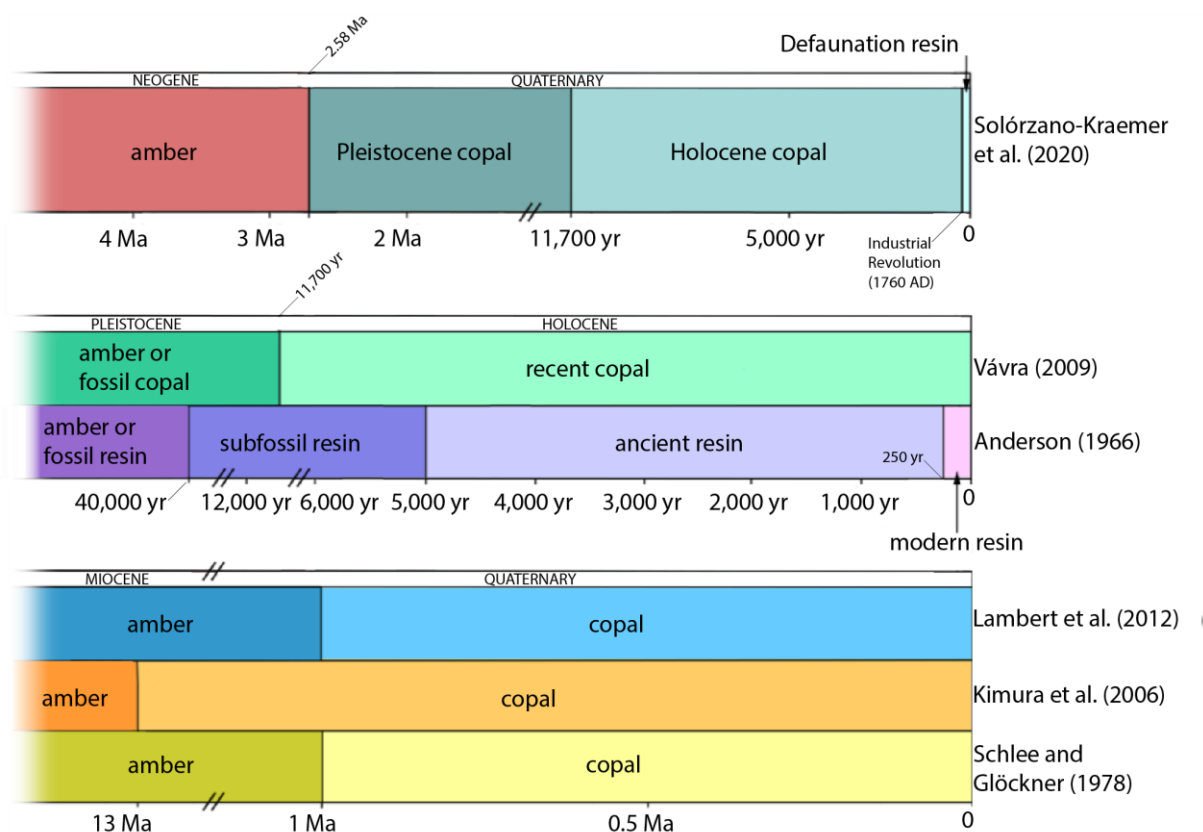


Figure 1. Age based definitions of amber, resin, and copal by various authors in the past. This thesis follows the scheme at the top, established by Solórzano-Kraemer et al. (2020). Modified from Solórzano-Kraemer et al. (2020).

1.3.1 Resin composition

Terpenoid resins

Plant resins in general are defined as a lipid-soluble mixture of volatile and non-volatile terpenoid (mono-, sesqui-, di-, and triterpenoids) and/or phenolic secondary compounds (Langenheim, 1969, 2003). Plant secondary compounds do not directly contribute towards the growth or development of the plant (as primary compounds do) but play important roles in ecological interactions with other organisms, including defence mechanisms or attraction of pollinators. Alcohols, aldehydes, esters, and resenes (amorphous, unsaponifiable neutral substances) may also be included in the resinous mixture (Langenheim, 1969). Moreover, resins are either synthesised internally by secretory structures called resin canals and cysts or may be secreted externally by glandular trichomes (Langenheim, 2003).

Terpenoids attain their greatest structural and functional diversity in plants, but occur in all living organisms (Langenheim, 1969, 2003). They are distinguished from the closely related terpenes by having functional groups, whereas terpenes are pure hydrocarbons. The terms terpenoids and terpenes are often used interchangeably and synonymously in the literature. With roughly 30,000 terpenoid and 8,000 terpene compounds known, they constitute the largest and most diverse class of plant compounds (Langenheim, 2003; Breitmaier, 2006). An overview of different terpenoids that are common in plants and/or are used commercially is given in Figure 2. Some of these, such as cadalane and α -muurolene, have also been detected in amber.

Terpenoids and terpenes derive from isoprene monomers (C_5H_8 , more specifically 2-methyl-1,3-butadiene) and are built up as metabolites in plants via the Mevalonic acid and/or Deoxyxylose 5-phosphate pathways (Langenheim, 1969; Eisenreich et al., 1998). The number of connected isoprene monomers determines the name and type of the compound: monoterpenoids consist of two isoprene units (C_{10}), diterpenoids (C_{20}) consist of four isoprene units, triterpenoids (C_{30}) consist of six isoprene units, and so forth. Tetraterpenes (C_{40}) include the carotenoids, important pigments for photosynthesis, but they are not present in resins. Terpenes have a high structural variation and exist as linear, acyclic, and cyclic (mono-, bi-, tri, etc.) molecules.

With regard to resins, terpenoids can be subdivided into volatile and non-volatile fractions (Langenheim, 1969). Depending on the producing plant, the volatile fraction is primarily made up of mono-, or sesquiterpenoids (C_{15}), but occasionally volatile diterpene hydrocarbons may be present as well (Otto & Wilde, 2001; Langenheim, 2003). Monoterpenoids such as α -Pinene and β -Myrcene dominate the volatile fraction of conifer resins, whereas sesquiterpenoids are the primary compounds in angiosperm resins of Fabaceae and Dipterocarpaceae origin (Langenheim, 2003). Volatile terpenoids have a plethora of ecological functions in plants: they act as natural insecticides, can inhibit the growth of insect larvae, and have antimicrobial properties (chapter 1.5.1). Due to their biological activity, volatile terpenoids are used commercially as pharmaceuticals whereas many aromatic compounds find applications in perfume production (Langenheim, 2003).

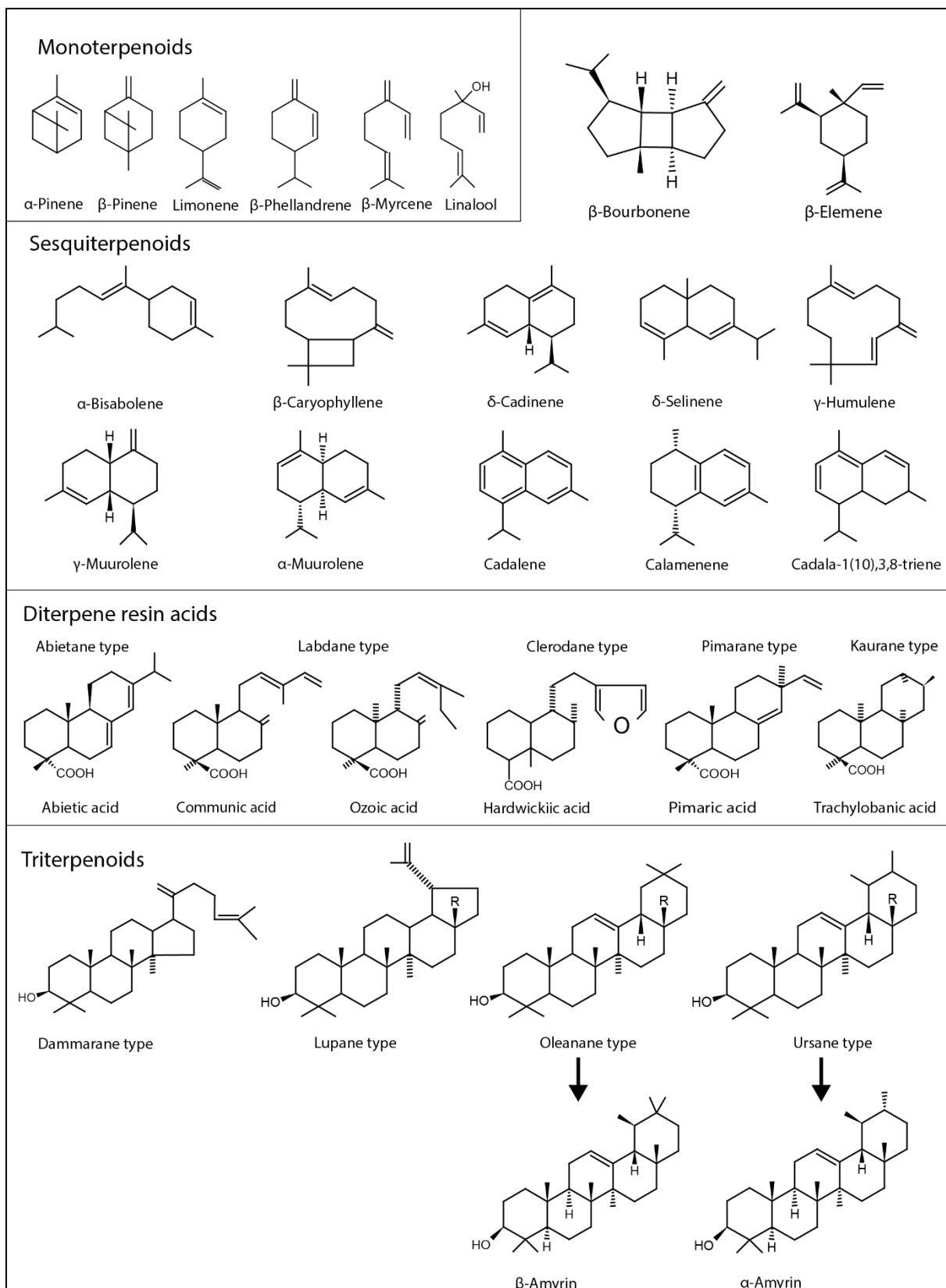


Figure 2. Common terpenoids in extant and fossil plants and resins. Compounds were redrawn or taken from Grimalt et al. (1987), Langenheim (2003), Dutta et al. (2009), Mallick et al. (2014), and da Silva Oliveira et al. (2018).

The non-volatile fraction in tree resin consists primarily of diterpenoid and triterpenoid compounds (Fig. 2) but can also include small proportions of alcohols, esters, and amorphous neutral substances (Otto & Wilde, 2001; Langenheim, 2003). In conifers, three main types of diterpene skeletons characterise the non-volatile fraction: abietane, pimarane, and labdane (Fig. 2). Their occurrence varies quantitatively in conifer families and has an influence on the hardness of the resin (Langenheim, 2003). Labdane-type acids are the primary diterpene constituents in Cupressaceae, whereas a combination of abietane- and pimarane-type acids is typical for Pinaceae. All three types occur in resins of Araucariaceae with especially large quantities of labdanes in *Agathis*. Labdane-type acids (such as communic acid) readily polymerise, allowing the production of very hard copals and ambers (Langenheim, 2003).

In angiosperms the non-volatile fraction can be composed of diterpenoid or triterpenoid compounds. Very hard copals are produced by trees of the family Fabaceae (formerly Leguminosae) due to the presence of labdane-type diterpenoid acids which are enantiomers of communic acid (Cunningham et al., 1973; Langenheim, 2003; da Silva Oliveira et al., 2018). Like in the conifer *Agathis*, these compounds can lead to fossilisation of the resin in the legume *Hymenaea*. Resins from Burseraceae exhibit a complex mixture of triterpenoid skeletal types such as euphane, lupine, ursane, and oleanane (Langenheim, 2003). The non-volatile fraction of Dipterocarpaceae consists of triterpenoids as well, but here compounds of the tetracyclic dammarane series are predominant (Hota & Bapuji, 1993; Langenheim, 2003).

The proportion of volatile to non-volatile compounds determines the fluidity, viscosity and polymerisation rate of the resin and may vary between species of the same genus (Langenheim, 2003). In terms of fossilisation, the volatile fraction does not polymerise: these compounds function as solvents and natural plasticisers that readily react with their environment (Cunningham, 1983). Although these compounds are capable of becoming fossilised in rare circumstances in their original state (Dutta & Mallick, 2017), the majority are gradually lost as the resin hardened, once the material is exposed to air (Cunningham et al., 1983; Poulin & Helwig, 2015). In addition, it has been shown that the occurrence of sesquiterpenes in modern and fossil dammar resins varies widely, indicating diagenetic alteration of the original compounds (Mallick et al., 2014). The first steps of resin fossilisation occur within the non-volatile fraction: soon after exposure to air and sun radiation, the high molecular terpenoids (di and triterpenoids; especially diterpenoid resin acids) will start to polymerise and crosslink, hardening the material and making it stable enough to be preserved for millions of years (Cunningham et al., 1983; Clifford & Hatcher, 1995).

Not all resins have the same fossilisation potential and most actually get broken down and washed away by rain or rivers (Ross, 1997). Modern-day producers of copious quantities of resin that have the potential to become fossilised in the future are the Kauri pine (*Agathis australis*) of New Zealand, species of the legume *Hymenaea* in East Africa and South and Central America, and producers of “dammar” type resin such as the dipterocarps *Shorea* and *Hopea* in South East Asia (Anderson et al., 1992; Ross, 1997).

Phenolic resins & oleoresins

Terpenoid resins are not the only resins secreted by plants. Some flowering plants produce phenolic resins containing phenolic compounds, which are characterised by an aromatic ring structure with at least one attached hydroxyl group (Langenheim, 2003). As with terpenoid resin, phenolic resin is diverse in function: it provides structural support, protection from antioxidants and ultraviolet light, and functions in signalling, pigmentation, and plant defence (Langenheim, 2003). In contrast to terpenoid resins that are metabolised through the mevalonic acid and deoxyxylulose 5-phosphate pathways, phenolic resins are synthesised through the shikimic and malonic acid pathway (Langenheim, 2003; Santos-Sánchez et al., 2019).

Oleoresins (occasionally called oily resins) are composed of terpenoid components, but have a higher ratio of volatile to non-volatile terpenoids than common terpenoid resins. In consequence, they are highly fluid, and are often considered interchangeably with balsams or oils (Langenheim, 2003). The volatile fraction of oleoresins consists of mono- and sesquiterpenoids, and is sometimes referred to as essential oil (Joye & Lawrence, 1967; Janssen et al., 1987; Langenheim, 2003; Bassolé & Juliani, 2012). The primary constituents of the non-volatile fraction are diterpenoids in conifers and most angiosperms, and triterpenoids in Dipterocarpaceae (Otto & Wilde, 2001; Langenheim, 2003). Hitherto, no oleo-resin is known to be a source of amber (Langenheim, 1995).

1.3.2 Chemical analyses of resin and amber

In plants, the high molecular-weight terpenoids are the product of complex metabolic pathways; therefore some compounds are taxon-specific and can be used for systematic classification at the genus- and family-level (Lambert et al., 1990, 1999; Otto & Wilde, 2001; Tappert et al., 2011). However, classification based on resin composition becomes less accurate with decreasing molecular weight, because mono- and sesquiterpenoids are basic compounds which can be produced by a variety of plants.

Due to their compositional complexity, resin and amber have been examined with multiple analytical tools such as various chromatographic (Mills & Werner, 1955; Bisset, et al., 1971; Aksamija et al., 2012) and mass spectrometric methods, Nuclear Magnetic Resonance spectroscopy (NMR), Infrared spectroscopy (IR), Raman spectroscopy, and in rare cases Fluorescence spectroscopy (Drzewicz et al., 2016; Seyfullah et al., 2018a). These methods were either applied to identify the structure of certain compounds (mass spectrometry & chromatography) or help in terms of authentication, provenance or botanical source of the sample (NMR, IR). A summary of chromatographic and fluorescence spectroscopic studies on amber is given in Drzewicz et al. (2016).

With the exception of Raman spectroscopy, all of the previously named methods require proper, and destructive, sample preparation, which means that they are most commonly applied to the resin itself but not to its inclusions. Although there have been some attempts to apply Raman spectroscopy to amber classification and characterisation (Edwards & Farwell, 1996; Brody et al., 2001; Winkler et al., 2001; Vandenabeele et al., 2003; Jehlička et al., 2004; Edwards et al., 2007; Jehlička et al., 2009; Vítek et al., 2012; Rao et al., 2013; Truică et al., 2014), it turned out to have limited utility for identifying the provenance of a piece (Brody et al., 2001). However, Raman spectroscopy has the advantage over other analytical methods in the characterisation of chemical compounds of the inclusions (Edwards et al., 2007, Hartl et al., 2015) and the identification of the sample maturity (Winkler et al., 2001).

Laser spectroscopy (IR and Raman) and ^{13}C NMR characterise the bulk composition of amber and provide a spectroscopic “fingerprint” of the material (Lambert et al., 2008). The wide application of IR and ^{13}C NMR has shaped the field of chemical and physical characterisation of resins, subfossil resins, and amber, resulting in an extensive literature on these topics. An incomplete list on IR literature comprises Beck et al. (1964), Langenheim & Beck (1965), Cunningham et al. (1983), Grimalt et al. (1987), Rao et al. (2013), Truică et al. (2014), Beltran et al. (2016), and for NMR Lambert & Frye (1982), Lambert et al. (1990, 1995, 1999), Anderson & Muntean (2000), and Lambert et al. (2005, 2007, 2013, 2015).

Mass spectrometry, especially Pyrolysis-Gas chromatography / Mass spectrometry (PyGCMS), is also widely applied to the analysis of resinous material (Mills et al., 1984; Grimalt et al., 1987; Anderson & Winans, 1991; Anderson, et al., 1992; Anderson & Botto, 1993; Anderson, 1994; Stacey et al., 2006; Dutta et al., 2009, 2011; Poulin & Helwig, 2012; Poulin & Helwig, 2015; McCoy et al., 2017; Dutta & Mallick, 2017). Mass spectrometry provides an analysis at the molecular level and allows the identification of individual components within the material (Lambert et al., 2008; Drzewicz et al., 2016).

Resin classification

There are three existing classification schemes for resinous materials. The first one is established by Anderson et al. (1992) based on PyGCMS, which links certain compounds to extant resins and amber deposits (Table 2). Since then, the original classification received some minor revisions but it still presents an important groundwork for amber related studies (Anderson & Botto, 1993; Anderson, 1994; Langenheim, 2003; Poulin & Helwig, 2012; Seyfullah et al., 2018a). The fossilisation potential widely varies between classes and is strongly dependant on the capability of compounds to polymerise (Langenheim, 2003). Therefore, extensive fossilised resin accumulations, or amber deposits, are restricted to resin class I and II. However, under favourable conditions resins from classes III to V may fossilise as well (Anderson & Botto, 1993).

Class I is the largest of the five classes and comprises the vast majority of amber deposits known today. All resins in this class derive from labdanoid diterpenes, including especially labdatriene carboxylic acids, alcohols and hydrocarbons (Anderson; 1994). Class I is subdivided into the four subclasses Ia, Ib, Ic, and Id. Resins of class Ia derive from polymers of labdanoid diterpenes with a regular configuration, including communic acid and communal (Table 2). The most striking characteristic is the incorporation of succinic acid: this compound is common in Baltic amber and many other European ambers and is lacking in resins of subclasses Ib and Ic (Anderson; 1994). Succinic acid plays a key role in cross-linking the macromolecular structures of resin from class Ia and Id (Poulin & Helwig, 2014).

Table 2. The current scheme of resin classes based on PyGCMS. It was established by Anderson et al. (1992) and has been expanded by several authors within the last years. From Seyfullah et al. (2018a).

Class	Characteristics	Examples	Inferred botanical affinity
Class I	Polymeric skeleton of labdanoid diterpenes, including especially labdatriene carboxylic acids, alcohols and hydrocarbons		
Class Ia	Based on polymers and copolymers of labdanoid diterpenes (regular configuration), including communic acid and communal; incorporation of significant amounts of succinic acid	Succinite: Baltic shore area, Samland Glessite	Pinaceae? Araucariaceae? Sciadopityaceae? Burseraceae, <i>Betula</i> (Betulaceae)
Class Ib	Based on polymers and copolymers of labdanoid diterpenes (regular configuration), including/not limited to communic acid, communal and biformene; devoid of succinic acid	Raritan amber Burmese amber New Zealand amber	Cupressaceae <i>Agathis</i> (Araucariaceae) <i>Agathis</i> (Araucariaceae)
Class Ic	Based on polymers and copolymers of labdanoid diterpenes (enantio configuration), including/not limited to ozic acid, ozol and enantio bioformenes; devoid of succinic acid	Mexican amber Dominican amber African amber (Zanzibar, Kenya) Carboniferous amber from Illinois	<i>Hymenaea mexicana</i> (Fabaceae) <i>Hymenaea protera</i> (Fabaceae) Pre-conifer gymnosperm
Class Id	Based on polymers and copolymers of labdanoid diterpenes with <i>enantio</i> configuration; incorporating significant amounts of succinic acid	Canadian Arctic (Nunavut) and British Columbia	unknown
Class II	Polymeric skeleton of bicyclic sesquiterpenoid hydrocarbons, especially cadinene; triterpenoid including di-sesquiterpenoid component as occluded material	Indian amber	Dipterocarpaceae (<i>Shorea</i>)
Class III	Polymeric skeleton; basic structural feature is polystyrene	Siegburgite: Siegburg and Bitterfeld (in part) some New Jersey ambers	Hamamelidaceae (<i>Liquidambar</i>)
Class IV	Non-polymeric, basic structural feature is sesquiterpenoid, based on cedrane (IX) skeleton	Ionite: Pliocene of California	unknown
Class V	Non-polymeric diterpenoid carboxylic acid, especially based on abietane, pimarane and iso-pimarane carbon skeletons	Highgate Copalite: Eocene of Highgate Hill area, London Settlingite: Northumberland, UK	Pinaceae

Class Ib resins derive from labdanoid diterpenes (communic acid, communal, biformene) as well, but lack succinic acid. These resins can undergo self-crosslinking of the polylabdane matrix between the communal and communic acid moieties (Poulin & Helwig, 2015). Class Ib resins are known from New Zealand (Kauri resin) and Australia (Victorian brown coal).

Polymers of labdanoid diterpenes with an *enantio* configuration, such as ozic acid and zanzibaric acid, are specific to resins of class Ic (Anderson, 1994). This class comprises important amber and copal deposits such as the Dominican and Mexican amber, and Zanzibaric copal.

In 2012, Poulin & Helwig established class Id after examining samples from three deposits in Canada. The fossil resins are based on labdanoid diteterpenes which have an enantiomeric configuration (instead of a regular configuration as in class Ia), including ozic acid, ozol and enantio biformenes (Poulin & Helwig, 2012). Furthermore, the pieces contain succinic acid which separates them from class Ib, and Ic.

The plants that produce class I amber most probably belong to Araucariaceae (*Agathis*), Leguminosae (*Hymenaea*, *Copaifera*), Cupressaceae, and Taxodiaceae. However, some other families have also been suggested, especially with respect to the dubious botanical affiliation of Baltic amber.

Class II resins commonly derive from polymers of bicyclic sesquiterpenoid compounds (especially cadinene), but functional triterpenoids (di-sesquiterpenoid components) may be occasionally included as well (Table 2). The nearest modern equivalent is “dammar” type resin, which is produced by dipterocarp trees (especially *Shorea*) in South-East Asia and Borneo. Fossil representatives are the Cambay and Zhangpu amber from India and China (Rust et al., 2010; Shi et al., 2014a; Dutta & Mallick, 2017).

Class III resins resemble natural polystyrene and are reported from New Jersey (Grimaldi et al., 1989; Langenheim, 1969) and Germany (Siegburgite). The most probable botanical affinity is Hamamelidaceae, especially *Liquidambar*.

Characteristic of class IV resins are sesquiterpenoid compounds, but in contrast to class II resins, they are primarily based on the cedrane skeleton (Table 2). These resins do not polymerise and thus fossilise only in rare circumstances. Ionite (Pliocene, California (US); Grantham & Douglas, 1980) and Moravian resins (Eocene, Czech Republic; Havelcová et al., 2019) belong to this group, but no botanical affinity has been proposed so far (Anderson et al., 1992).

Class V resins consist of non-polymeric mixtures of diterpenoid resin acids, primarily abietic, pimaric, and iso-pimaric types, as well as n-alkanoic acids and n-alkanes. The only member of this class is “Highgate Copalite” which is most likely derived from an undetermined pine species (Anderson & Botto, 1993).

The second classification scheme is based on ^{13}C NMR spectra and was established by Lambert & Poinar (2002) as a complementary approach to the PyGMCS based classification. In total, five groups of resins can be distinguished that widely overlap with the classes of Anderson et al., (1992). Group A consists of resins that are affiliated with the genus *Agathis*, starting in the

Cretaceous and continuing today with extant species (Lambert & Poinar, 2002). This group corresponds to class Ib of Anderson et al. (1992). The resins in group B could not be traced to a specific modern genus, but their widespread occurrence in the Paleogene from India and North America argues for a correspondence to class II. Group C contains Baltic amber and similar resins and corresponds to class Ia of Anderson's classification. Baltic amber likely had a coniferous source of either Pinaceae or Araucariaceae and may even have the same origin as group A but with a lesser degree of chemical degradation. Group D resins derive from *Hymenaea* and are found in the Americas and in Africa. Consequently, this group corresponds to class Ic resins (Anderson et al., 1992). Group E contains amber composed of polystyrene from the Cretaceous of New Jersey, which was likely produced by trees of the family Hamamelidaceae (Anderson et al., 1992; Lambert et al., 2015). This corresponds to class III resins after the classification of Anderson et al. (1992).

The third and somewhat informal classification scheme is not based on chemical analysis and divides fossiliferous ambers into named types based on similarities of entombed biota, geographical location, and age (Penney, 2010a; McCoy et al., 2018a). Famous examples include Baltic amber, Burmese amber, Dominican amber, and Lebanese amber. These are subsets of chemical groups, and the sites within a named type are generally more chemically similar to each other than to other sites in the same chemical group (Lambert et al., 2015; McCoy et al., 2018a).

1.4 Amber deposits and their occurrence through earth's history

Amber has a strong cultural connection to humans, as it was a traded in ancient times and is collected and used for jewelry even today (de Navarro, 1925; Poinar, 1992; Murillo-Barroso & Martín-Torres, 2012; Murillo-Barroso et al., 2018). With regard to their scientific value, amber fossils greatly contribute to taxonomic, taphonomic, palaeogeographical, and palaeobiological studies. Amber deposits are relatively young in earth's history and not evenly distributed in space and time (Martínez-Delclòs et al., 2004; Labandeira, 2014, Seyfullah et al., 2018a). Roughly 630 amber deposits are reported in the literature and distributed all around the globe, but they are not necessarily fossiliferous (Langenheim, 2003; Martínez-Delclòs et al., 2004; Lambert et al., 2012; McCoy et al., 2018a). This thesis focusses on deposits that yielded great quantities of material and/or had a significant scientific impact on our general understanding of resin production in the past. For also information about smaller and less extensively documented deposits, see Langenheim (2003), Lambert et al. (2012), McCoy et al. (2018a), and Seyfullah et al. (2018a).

Labandeira (2014) uses four criteria to distinguish four major phases in the amber fossil record. These criteria are (i) the abundance and diversity of inclusions, (ii) an important biogeographic placement, (iii) an occurrence that fills a major gap in the fossil record, and (iv) the potential for capturing important, early terrestrial organisms.

According to Labandeira (2014), the four phases occur in the Carboniferous, Triassic to mid-Cretaceous, mid-Cretaceous to K/P boundary, and Cenozoic. In addition to the phases presented by Labandeira, Seyfullah et al. (2018a) identified four major 'bursts' of amber production in the past. These bursts reflect to some extent the phases introduced by Labandeira, and are associated with climatic changes and/or biotic turnovers. For a general structure, the four phases in the amber record are described in the following but where applicable, information on the amber bursts is also given.

Palaeozoic (Carboniferous) amber

The first phase of the fossil record of amber dates back to the Carboniferous. It comprises occurrences of small resin rodlets ('resinite') within Pennsylvanian to late Permian strata from Europe and North America, which are either attributed to extinct early seed plants or are of unknown botanical affiliation (Jones & Murchison, 1963; Phillips et al., 1976; Lyons et al., 1982; Bray and Anderson, 2009; Labandeira, 2014; and references therein). With an age of 320 Million years, the oldest amber is reported within coal seams from the Tradewater Formation

of Illinois, USA (Kosanke & Harrison, 1957; Bray & Anderson, 2009). The millimetre-sized amber clasts are attributed to class Ic ambers, but their botanical affiliation remains unknown (Bray & Anderson, 2009). Another occurrence stems from Middle to Late Pennsylvanian coal-ball floras of the Central Appalachian basin and consists of small, cylindrical resin rodlets (Lyons et al., 1982). They frequently occur in fusain layers or lenses of carbominerite and appear to be equivalent to the ones from the Tradewater Formation (Lyons et al., 1982). Moreover, resin rodlets from the Appalachian basin are likely attributed to *Medullosa*, an extinct seed fern, although a production by Cordaitales is discussed as well (Lyons et al., 1982). Jones & Murchison (1963) report amber from bituminous coals of Yorkshire and Northumberland in Northern England. It is found as tiny globules which in some cases are filling cleats of the coal, indicating a diagenetic migration (Jones & Murchison, 1963; Lyons et al., 1982). Microscopic examination points to a member of the Cordaitales as a source plant (James & Murchison, 1963), at least for the coal from Northumberland, and therefore also possibly for the amber contained within the coal. Rodlets from the Yorkshire coal are attributed to a medullosan pteridosperm, and have composition unlike any other vascular plant resin produced today (van Bergen et al., 1995). Even though the exact source plant remains unidentified in the previous examples, it is safe to state that the amber from this first phase of production has no parallel in modern plants, and may represent biomolecules that did not survive into the Mesozoic (Labandeira, 2014). It is important to note that no inclusions have been reported from Palaeozoic ambers so far. In addition, Palaeozoic ambers appear to represent local accumulations rather than a worldwide phenomenon. Finally, these ambers cannot be considered real *exudates* because they are found inside plant remains without exception, and were therefore never exuded. As a result, Seyfullah et al. (2018a) do not recognise these early amber occurrences as one of the major amber bursts.

Mesozoic amber

The second phase of the amber record began in the Triassic (1st amber burst; Gianolla et al., 1998) and continued into the mid-Cretaceous (2nd amber burst; Labandeira, 2014; Seyfullah et al., 2018a). During this phase, more copious amber was produced than during the Paleozoic, resulting in significant accumulations (Labandeira, 2014; Seyfullah et al., 2018b). This is contextualised within the expansion of new, resin-producing conifer clades, such as Araucariaceae (Litwin & Ash, 1991), Cheirolepidicaeae (Roghi et al., 2006; Schmidt et al., 2012), and probably Voltziaceae (Labandeira, 2006, 2014).

Moreover, ambers from this second phase are the first to include inclusions, although they have a lower biodiversity than inclusions in ambers from the third or fourth phases (Schmidt et al., 2012). The pieces can be found in lignitic strata or associated lag deposits (Schmidt et al., 2012), in association with *Agathoxylon* logs (Litwin & Ash, 1991) or as amber replacements of the vacuities that resulted from the consumption of ovulate tissue by an unknown seed predator (Labandeira, 2014). For several deposits, larger amber clasts in the range around 5 cm are reported (Grimaldi, 1996; Philippe et al., 2005; Azar et al., 2010a).

The occurrence of Late Triassic (Carnian) amber has been studied extensively in the last few years (Gianolla et al., 1998; Schmidt et al., 2012; Seyfullah et al., 2018b; Dal Corso et al., 2020). This first burst of amber production falls within the Carnian Pluvial Episode (CPE) and is associated with massive volcanic activity that led to profound biotic changes (Dal Corso et al., 2020). The CPE gave rise to major radiations in many groups which play important roles in modern ecosystems, such as scleractinian corals and several conifer families (Dal Corso et al., 2020).

Phase three of the amber record spans from the mid-Cretaceous to the K/P boundary. Even though this interval includes the expansion of angiosperms, they do not become copious resin producers until the Paleogene (Labandeira, 2014). Although Araucariaceae and Cheirolepidaceae were occasional resin producers during the Cretaceous, the predominant resin producers of the third phase are pinalean conifers, particularly Cupressaceae and Pinaceae (Labandeira, 2014). Within this phase, the amount of resin production increased significantly as did the compositional diversity of resins (Labandeira, 2014). All of the famous and intensively studied Cretaceous amber deposits belong to this phase. With an age of roughly 120 million years, the earliest amber occurrence within this phase is the Lebanese amber, which represents the oldest amber-fossilised example of a complex forest ecosystem (Schlee & Dietrich, 1970). It is followed by Álava amber (Albian, Spain; Peñalver & Delclòs, 2010), Burmese amber (uppermost Albian to lowermost Cenomanian, Myanmar; Grimaldi et al., 2002), Charentes amber (Albian-Cenomanian boundary, France; Perrichot et al., 2007), Raritan amber (Turonian, USA; Grimaldi et al., 1989), and Canadian amber (Campanian, Alberta and Manitoba; McKellar & Wolfe, 2010).

Late Cretaceous ambers like the Raritan amber are not considered to reflect a burst in amber production but rather represent local accumulations (Seyfullah et al., 2018a). Therefore, the second burst in production is identified by Seyfullah et al. (2018a) in the Early to Mid-Cretaceous.

Cenozoic amber

The fourth phase starts immediately after the K-Pg boundary and is associated with new groups of angiosperms that became copious resin producers in the Cenozoic (Labandeira, 2014). In the Paleogene, a combination of gymnosperm (Araucariaceae, Cupressaceae, Pinaceae) and angiosperm (Dipterocarpaceae, Combretaceae, Hamamelidaceae) taxa appear as resin producers (Rust et al., 2010; Labandeira, 2014; Shi et al., 2014a). However, Eocene Baltic amber, the deposit with the greatest diversity and abundance of inclusions, was mainly produced by conifers, although angiosperm taxa produced minor amounts of Baltic amber (Anderson & LePage, 1995; Wolfe et al., 2009; Weitschat & Wichard, 2010). Eocene amber deposits represent the third burst of amber production according to Seyfullah et al. (2018a).

By the time of the Neogene (4th burst), resin production heavily shifted towards angiosperms, dominated by plants of the Fabaceae (Leguminosae), especially *Hymenaea*. *Hymenaea* is the source plant of the famous Dominican and Mexican amber deposits (Hueber & Langenheim, 1986; Penney, 2010b; Solórzano Kraemer, 2010) and is responsible for significant subfossil and modern resin accumulations from the Pliocene to Holocene of Colombia, Tanzania, and Madagascar (Schlüter & von Gnielinski, 1980; Penney & Preziosi, 2010; Delclòs et al., 2020).

1.5. Amber taphonomy

1.5.1 Resin production

Resins are produced by many plant taxa in modern ecosystems, but their physiological role is not entirely known (Langenheim, 1995; Seyfullah et al., 2018a). About 10% of extant plant families produce resin in appreciable quantities, of which two-thirds grow in tropical conditions (Langenheim, 1990). Not all resins produced by plants today are stable enough to enter the fossil record. Therefore, the following examples focus on taxa that produce resins and are associated with amber deposits.

Within the gymnosperms, all conifers are resinous, but only the Araucariaceae, Cupressaceae, and Pinaceae are of particular interest with respect to amber formation (Langenheim, 1990, 2003; Seyfullah et al., 2018a). In particular, high modern production is reported from Araucariaceae from New Zealand (*Agathis*, *Wollemia*) where these trees are the source of “kauri” resin (class Ic), which has industrial value in the production of lacquers and varnishes (Langenheim, 2003). Pinaceae also produce high amounts of resin (class V), but it does not preserve well due to its limited capability to polymerise, even though some rare occurrences in the fossil record are reported (Anderson & Botto, 1993; Anderson, 1994; Seyfullah et al., 2018a). Cupressaceae are less resinous today, but they are discussed as the source of some amber deposits from the Cretaceous onwards (Mustoe et al., 1985; Wang et al., 2014; Sadowski et al., 2017).

Angiosperm lineages which exude large amounts of resin mostly live in tropical to warm-temperate areas, and comprise Burseraceae, Combretaceae, Dipterocarpaceae, Fabaceae, and Hamamelidaceae (Langenheim, 2003; Nel et al., 2004; Seyfullah et al., 2018a). Dipterocarpaceae of South-East Asia produce copious amounts of “dammar” type resin (class II), whereas resin of Fabaceae (especially *Hymenaea*, class Ic) is noted from Tanzania, Kenya, Madagascar, and Colombia (Schlüter & von Gnielinski, 1980; Anderson et al., 1992; Penney & Green, 2012). Both resin types are used in the production of lacquers and varnishes, or have applications in medicine (Langenheim, 2003). Dipterocarpaceae, in particular *Shorea* and *Hopea*, are the source of Eocene and Miocene amber from India (Rust et al., 2010), China (Shi et al., 2014a), Australia (Sonibare et al., 2014), and possibly Arkansas (Saunders et al., 1974). In the Cenozoic, *Hymenaea* trees are responsible for large amber and sub-fossil resin accumulations in the Caribbean, Central to South America, and East Africa (Iturralde-Vinent, 2001; Langenheim, 2003; Penney & Green, 2012).

The exact mechanism of resin production and the storage of resin differ in specific details between gymnosperms and angiosperms (Langenheim, 2003), but in both groups resin may accumulate in multiple separate locations in the tree. Large portions of resin are commonly exuded from the bark, but resin may also be secreted by roots or accumulate in pods or pockets under the bark or heartwood as well (Langenheim, 1995).

Ecological roles of plant resins

To explain why plants exude resin at all, it is necessary to take a closer look on its ecological roles. Possibly, the terpenoids of early plants originally represented metabolic end products, which were needed to dispose of excess acetate products in order to prevent self-poisoning (Sandermann, 1962; Langenheim, 1969, 2003). The incidental properties, which find expression in the numerous ecological roles of resin, must have been so favourable that the production of resin was maintained throughout plant evolution.

Suggested ecological functions of resin comprise physical sealing in response to wounding (Farrell et al., 1991; Henwood, 1993), preventing pathogen or insect attacks (Langenheim et al., 1986; Henwood, 1993; Grimaldi & Engel, 2005), storing cellular waste products (Henwood, 1993), or attracting particular pollinators (Armbruster, 1993). Moreover, resin plays an important role in chemical plant defence (Phillips & Croteau, 1999; Trapp & Croteau, 2001) and influences interactions among plants and between plants and other organisms (Langenheim, 1994, 1995, 2003). In addition, resin inhibits herbivory and parasitism (Litvak & Monson, 1998; Farrell et al., 1991) and may act as a barrier to limit temperature and water loss (Dell & McComb, 1978). Some resin compounds have antiseptic properties and can prevent a widespread infection of the plant (Bridges, 1987; Poehland et al., 1987; Moleyar & Narasimham, 1992; Savluchinske Feio et al., 1999; McKay et al., 2003). However, it is unclear which of these functions were the major drivers to maintain resin production in plants (Langenheim, 1969).

Resin production today

The overall production of resin depends on environmental factors such as light, temperature, moisture, soil type and nutrients (Lorio & Hodges, 1968; Langenheim, 1995; Seyfullah et al., 2018a). As resin production is linked to ecological functions, resin composition varies between

different tissues or parts of the plant (Anderson et al., 1969; Thomas, 1969, 1970; Langenheim, 1995, 2003). Besides the basic rate of resin production, several factors may significantly affect the production, including elevated temperatures, climate change, physical damage (storms and insect feeding), wildfires, disasters, diseases, and water stress (Martínez-Delclòs et al., 2004; Beimforde et al., 2017; Seyfullah et al., 2018a).

Resins are most famous for their role in the defensive strategies of plants (Berryman, 1972; Messer et al., 1990; Phillips & Croteau, 1999; Langenheim 1994; Tomlin et al., 2000; Trapp & Croteau, 2001; Langenheim, 2003), which is why it is not surprising that the exudation of resin is triggered by insect attack and fungal infection (Beimforde et al., 2017; Seyfullah et al., 2018a). Certain compounds like humulene and kaurenoic acids are lethal to larvae and imagos of many insects, or inhibit their growth (Elliger et al., 1976; Lincoln, 1985; Messer et al., 1990). Besides the overall resin production, the resin composition (particularly mono- and sesquiterpenoids) can be rapidly modified towards certain threats, especially bark boring insects and fungi (Sturgeon, 1979; Raffa & Berryman, 1982; Phillips & Croteau, 1999; Tomlin et al., 2003; Trapp & Croteau, 2001; McKay et al., 2003).

Moreover, one of the oldest explanations for the Baltic amber deposit refers to a disease – “succinosis” (Conwentz, 1890; Seyfullah et al., 2018a). This assumed disease caused massive resin exudation and is thought to be linked with a larger disaster that allowed the disease to take place (Conwentz, 1890; Seyfullah et al., 2018a). As demonstrated by *Agathis australis* specimens from New Zealand, there is no doubt that extant trees exude resin in response to diseases (Seyfullah et al., 2018a). Infestation with the oomycete *Phytophthora agathidicida* caused a yellowing of the leaves, a thinning of the canopy, and lesioning on the lower stem which were the places of enhanced resin production (Seyfullah et al., 2018a). This enhanced resin production is called hyper-resinosis and was repeatedly suggested to be the source of amber deposits, as suggested by Conwentz (1890).

Resin production in the past

Why amber deposits surpass by far the resin accumulation of modern ecosystems is still not clear. There is an ongoing and vigorous debate on the factors that might have led to the extensive preservation of amber (Seyfullah et al., 2018a). It is assumed that a generally higher production rate of resin was achieved due to environmental and biological factors in the past. Remarkably, all of the four phases of amber production fall into geological times with hot climate conditions, which appear to constitute a favourable prerequisite for extensive resin

exudation (Labandeira, 2014; Seyfullah et al., 2018a). As concluded from amber pieces and modern observations, large accumulations of amber might be attributed to water stress and wildfires as well (Brasier et al., 2009; Najarro et al., 2010; Peris et al., 2016; Seyfullah et al., 2018a). In addition, fungal infestation and insect attacks (especially of xylophagous beetles) have been considered possible explanations for large amounts of amber (Grimaldi et al., 2000; McKellar et al., 2011; Beimforde et al., 2017; Seyfullah et al., 2018a).

Beimforde et al. (2017) report extensive resin exudation from extant *Araucaria humboldtensis* trees of New Caledonia infected with the larvae of weevils (Araucarini) and long horn beetles (Cerambycidae). In addition, the infestation led to the production of resin drops similar in size and shape to amber pieces from the Triassic, Late Cretaceous, and Eocene ambers of Europe (Schmidt et al., 2006; Néraudeau, 2017; Beimforde et al., 2017). However, the modern New Caledonia damage was restricted to single branches and not the entire tree. Even though exudation is promoted in this case, it is unlikely that the massive resin production in the past was caused solely by beetle infestation (Beimforde et al., 2017; Peris et al., 2016; Peris & Rust, 2020).

The observed impact on modern resin production by water stress, wildfires and pests led to the assumption that amber deposits reflect abnormal “disaster” forests instead of healthy ecosystems (Najarro et al., 2010; Dal Corso et al., 2013, 2015; Seyfullah et al., 2018a). Apart from a higher production rate of resin, there are geologic factors which may explain the extensive preservation of amber as well. In a recent study, Delclòs et al. (2020) showed that the soil type and composition can prohibit the preservation of resin. Their study area of Madagascar is well-known as the habitat of *Hymenaea* trees, which are copious resin producers today and were the source plants of Neogene Dominican and Mexican amber. In the particular case of Delclòs et al. (2020), it was evidenced that the resin produced by living *Hymenaea* trees is only stable in the soil for about 300 years. So, even if promoted exudation takes place, it is not guaranteed that the produced resin enters the fossil record. This emphasises the importance of the depositional environment and shows that resin needs either to accumulate in suitable areas or be transported to them (Martínez-Delclòs et al., 2004). As a summary, large amber accumulations are not explainable on a monocausal base. It seems like a variety of conditions must come together to enable both copious exudation and the preservation of resin over geological time scales which may not be present today.

1.5.2 Fossilisation in amber

Resin and its embedded inclusions represent a unique and complex mode of fossilisation. Traditionally, taphonomy is separated into three phases: necrolysis, biostratinomy, and diagenesis (Martin, 1999). Necrolysis represents death and its causes. The second phase, called biostratinomy, comprises all processes that take place after the death of an organism until its deposition, such as autolysis, scavenging, microbial decomposition and transportation. Diagenesis is the third phase of taphonomy and includes the possible fossilisation of the carcass. This phase comprises processes that take place after the deposition of the carcass and either lead to its destruction or preservation over geological timescales. Diagenetic (or fossilisation) processes can last for millions of years and may include mineralisation, compression, and heating. It must be emphasised that the remains of a carcass can be lost at any point during biostratinomy or diagenesis for several reasons – in fact, the degradation of organic material represents the default pathway in nature. Therefore, fossils represent an exception to the rule and are the result of inhibited or retarded decay processes.

Several previous studies summarised the taphonomy of amber and its inclusions with slight differences in respect to the various phases (Martínez-Delclòs et al., 2004, Ragazzi & Schmidt, 2011; Labandeira, 2014). The taphonomy of amber and its embedded organisms are closely related to each other which is why it makes sense to treat both as a single unit in terms of fossilisation. Because the beginning of necrolysis (only for the inclusion), biostratinomy and diagenesis are shifted by definition for the resin and its inclusion, they cannot be regarded as occurring contemporaneously. Therefore, a deviation from the traditional model is suggested in the following with a subdivision into entrapment, early, and late diagenesis. The entrapment phase includes resin exudation and the trapping of an organism which usually leads to its death (necrolysis). Early diagenesis includes the entombment of the organism, the start of resin polymerisation while it is still rich in volatiles, and transportation processes that affect the whole piece. Late diagenesis includes processes that take place after initial deposition of the piece in the sediment and are referred to as ‘maturation’ or ‘amberisation’ (Clifford & Hatcher, 1995; Iturralde-Vinent, 2001; Seyfullah et al., 2018a). Within this phase, chemical modifications of the resinous material take place and it may be reworked several times. The boundary between early and late diagenesis is not clearly defined (Labandeira, 2014).

Entrapment

With regard to amber taphonomy, entrapment is the best studied phase (Martínez-Delclòs et al., 2004; Solórzano Kraemer et al., 2015, 2018). After exudation, resin may form stalactites, drops, and flows that have the chance to trap organisms (Weitschat & Wichard, 1998; Martínez-Delclòs et al., 2004). Once in contact with the sticky resin, organisms or parts of them can be entirely covered by further resin flows, so that inclusions are usually found at the boundaries between successive resin flows (Ragazzi & Schmidt, 2011). The stickiness of resin limits the chances of escape for many arthropods, which die of asphyxia after they have been entirely embedded. The majority of resin solidifies at the forest floor and not on the bark (Henwood, 1993; Schmidt & Dilcher, 2007). Therefore, aquatic organisms can be commonly found in amber (Schmidt & Dilcher, 2007; Wichard et al., 2009), and in cases where the trees grew directly at the coast, it is possible to find marine inclusions as well (Vonk & Schram, 2007; Girard et al., 2008; Yu et al., 2019).

Resin trapping is heavily biased towards certain organisms through a number of factors. These include resin viscosity, plant defence, overall resin production, and organismal behaviour and habitat (Martínez-Delclòs et al., 2004; Ragazzi & Schmidt, 2011; Solórzano Kraemer et al., 2015, 2018). The resin viscosity depends on temperature and internal sap pressure, which are both higher during spring and summer in seasonal climates (Langenheim, 2003; Seyfullah et al., 2018a). The higher the surface tension of the resin (which increases with viscosity of the resin), the lower the probability that it becomes penetrated by insects (Martínez-Delclòs et al., 2004). Large insects penetrate resin more easily, but they are more likely to struggle free, although there are a few records of large insects and small vertebrates in amber (Klebs, 1910; Xing et al., 2016; Barthel et al., 2020). Consequently, amber inclusions are dominated by small arthropods of less than 5 mm, but the ratio of small to large organisms differs between deposits and depends on the viscosity of the resin and the durability of the amber (Poinar, 1992; Martínez-Delclòs et al., 2004; Weitschat & Wichard, 2010).

Insect behaviour influences the chance of entrapment as well. Swarming insects, such as Chironomidae, Dolichopodidae, and Formicidae, or xylophagous insects are more at risk than others (Poinar & Poinar, 1999; Martínez-Delclòs et al., 2004). In addition, some insects forage for resin: a common example is the bee *Problebeia*, which is the most abundant bee in Dominican amber (Camargo et al., 2000; Martínez-Delclòs et al., 2004). Moreover, the small size of many insects increases their likelihood of being carried into the resin by wind (Martínez-Delclòs et al., 2004). Arthropods that live around resin-producing trees are more likely to be entrapped than arthropods with a different lifestyle. Therefore, the habitat has a great impact on

the overall amount of entrapped arthropods. Plant defence plays an important role as well, as volatile resin compounds deter or attract some groups of arthropods (Armbruster, 1984; Tomlin et al., 2000; Trapp & Croteau, 2001). Lastly, the overall resin production also influences the likelihood of entrapment: the more resin exuded, the higher the chance of entrapment.

Early diagenesis

As soon as the resin exudes out of the bark, di- or triterpenoid non-volatile compounds will start to polymerise due to free radicals, resulting in the hardening of the material (Cunningham et al., 1983). Diterpene resin acids play an especially key role in the polymerisation of resin (Poulin & Helwig, 2014). In contrast, while a small fraction of volatile compounds may randomly become integrated in the polymerising matrix (Poulin & Helwig, 2015), the majority plays no role in resin maturation (Cunningham, 1983; Langenheim, 2003). Polymerisation starts soon after exudation, but it continues even after the final deposition of the piece which is why it can extend into the late diagenetic phase as well. The maturation process of resins and amber is accompanied by the progressive loss of exomethylene groups and the loss of carboxyl groups in diterpene resin acids (Lyons et al., 2009).

Resin is affected by processes of weathering and degradation rapidly after exposure to air and sunlight, which is why long-term preservation requires redeposition into marine sediments or coverage by anoxic sediment (Martínez-Delclòs et al., 2004; Ragazzi & Schmidt, 2011). Resin may accumulate in the soil around the producing tree or get washed away by rivers or rain (Ross, 1997, Langenheim, 2003).

Soon after entrapment, but before burial, organisms begin to decay within the resinous matrix, a process which includes dehydration and carbonisation of the material (Martínez-Delclòs et al., 2004). A common phenomenon, especially in Baltic amber, is the presence of a whitish aureole around the carcass called ‘Verlumung’ (Martínez-Delclòs et al., 2004). While formerly interpreted as microscopic air bubbles (Mierzejewski, 1978, Weitschat & Wichard, 1998), this occurrence is nowadays regarded as the result of decay fluids reacting with sugars and terpenes of the resin (Martínez-Delclòs et al., 2004).

Although insect remains in amber are usually restricted to cuticles, their early anaerobic decay through autolysis and endogenous bacteria is likely inhibited (Martínez-Delclòs et al., 2004): resin has natural embalming properties due to antiseptic activity and creates a dehydrated environment within itself, favourable preconditions for fossilisation (Langenheim, 2003; Ragazzi & Schmidt, 2011). However, while most amber fossils appear to be hollow inside

(McCoy et al., 2018a), some studies report the preservation of labile tissue, in rare cases down to subcellular level (Henwood, 1992a, 1992b; Grimaldi et al., 1994; Tanaka et al., 2009).

With regard to resin chemistry, it is suggested that volatile mono- and sesquiterpenoids react with the tissue of the animal in a type of perfusion reaction that stabilises the material over geologic timescales (Grimaldi et al., 1994). Another suggestion by Poinar & Hess (1982) on this phenomenon is the case of an extreme inert dehydration of the tissue, caused by sugars and terpenes in the matrix combining with the water from the tissues. Although the exact mechanisms are still unclear, experiments by Henwood (1992a) and McCoy et al. (2018b) clearly showed that the embedding medium has a significant influence on the decay rate. However, their results are contradictory: while Henwood (1992a) argued that insects with well-preserved internal organs represent individuals with a high degree of dehydration prior to the entombment, McCoy et al. (2018b) showed that an initial dehydration hampers the preservation of labile tissues. Nevertheless, the preservation of arthropod tissues in resin is doubtless the result of reactions with resin compounds, although the details remain to be elucidated (Martínez-Delclòs et al., 2004).

Late diagenesis

Although amber may become redeposited several times during diagenesis (Weitschat & Wichard, 2010), the processes that lead to the progressive transformation from subfossil resin to amber take place after the final deposition in the sediment and are summarised by the term ‘maturation’ or ‘amberisation’ (Cunningham et al., 1983; Iturralde-Vinent, 2001; Winkler et al., 2001; Ragazzi & Schmidt, 2011). During maturation/amberisation, the amber structure is modified by chemical reactions such as cross-linking, isomerisation, and cyclisation (Clifford and Hatcher, 1995; Clifford et al., 1997), which lead to a progressive loss of unsaturated bonds, a decrease in functionalised groups and an increased proportion of aromatised groups (Grimalt et al., 1988).

For geologic conditions, the major processes affecting amber-bearing deposits are overburden pressure, elevated temperatures as a consequence of sediment upload (Iturralde-Vinent, 2001), and tectonic deformation (Grimaldi, 1995; Martínez-Delclòs et al., 2004). In addition, amber inclusions are affected by liquid phases, as indicated by the presence of pyrite in some amber insects and the fluoridation of bone tissue, which might be the result of microfractures that connect the inclusion to the surface of the amber piece (Baroni Urbani & Graeser, 1987; Schlüter, 1989; Martínez-Delclòs et al., 2004; Ragazzi & Schmidt, 2011; Barthel et al., 2020).

The majority of resin deposits are allochthonous, but a few occurrences are found *in situ* (Iturralde-Vinent, 2001; Martínez-Delclòs et al., 2004; Rust et al., 2010, Seyfullah et al., 2018a). Due to its low density, reworked amber nearly floats in salt water and can easily be transported by disturbed water for several kilometres (Ragazzi & Schmidt, 2011). Indeed, allochthonous amber can be found in fluvial sediments as well as in lagoonal to coastal marine environments, including deltas and coastal swamps (Iturralde-Vinent, 2001, Azar et al., 2010b). In many cases it is unclear whether the amber from swamp environments is found *in situ* or has been transported short distances (McKellar & Wolfe, 2010; Seyfullah et al., 2018a). Rare occurrences of autochthonous amber are associated with lignite and are either intercalated with brown coal seams or found within them, which means that the fossil resin is found within the remains of its source forest (Nissenbaum & Horowitz, 1992; Rust et al., 2010).

Once excavated, amber oxidises and weathers rapidly under atmospheric conditions, which is correlated to a darkening of the material and the formation of surface crazing (Martínez-Delclòs et al., 2004, Labandeira, 2014). Therefore, amber in scientific collections is nowadays stored under constant oxygen and ultra-violet radiation free conditions, and occasionally embedded in artificial resin (Penney & Preziosi, 2010; Bisulca et al., 2012; Labandeira, 2014).

2.0 Exceptional preservation in amber: state of the art

This chapter provides a short overview of previous studies on exceptional preservation in amber. It can be present in two forms: either as the morphological preservation of tissues and ultrastructure, or as the analytical proof of original compounds. A more detailed review of this topic was published by the author of this thesis in the following peer-reviewed research article:

Barthel, H.J., McCoy, V.E., Rust, J., 2021. From ultrastructure to biomolecular composition: taphonomic patterns of tissue preservation in arthropod inclusions in amber, in: Gee, C.T., McCoy, V.E., Sander, P.M. (Eds.), *Fossilization: Understanding the Material Nature of Ancient Plants and Animals*. Johns Hopkins University Press, Baltimore, pp. 115–138.

The original manuscript is attached in the Publications section (10.1).

2.1 Tissue preservation in amber – previous studies

The first report of internal tissues from amber inclusions dates back to 1903 and was achieved by Kornilowitsch through thin sectioning neuropteran and dipteran inclusions from Baltic amber (Grimaldi et al., 1994). Kornilowitsch found striated muscle tissue in the legs from both insect taxa, but his results were not widely accepted in the scientific community mainly due to the poor quality of his images. Furthermore, his amber pieces exhibited surface crazing, which was thought to be specific to copal alteration at this time. A better supported report on striated muscle tissue in amber was presented by Petrunkevitch (1935) on a fungus-gnat in Baltic amber. His sample showed preserved muscle tissue in all legs when examined under a microscope.

Tracheal parts were initially extracted from Baltic amber beetles by von Lengerken (1922). A detailed description of the remains is lacking because the author focused on the chemical preservation of the chitin.

Andrée & Keilbach (1936) reported the preservation of parts of the tracheal system, musculature, gut material, ovarioles, and chitin of braconids and Ceratopogonidae from Baltic amber. Unfortunately, they did not clearly state their methods, although Voigt (1937) notes that their results were achieved by dissolving the amber, without further information on the solvent. Voigt (1937) himself applied his development of a ‘laquer film method’ (previously used in sedimentary examinations) to numerous pieces of arthropods, plants, and fecal pellets from Baltic amber. He identified muscle tissue, trachea, and gland epithelia from the insect inclusions

and noted that the small insects seem to be better preserved than the larger ones (Voigt, 1937). Traditional microscopic slices of Baltic amber spiders were examined by Petrunkevitch (1950) and revealed exceptional preservation in several specimens. In one case, the preservation of hypodermal cells in the integument is reported, whereas another spider contained a wealth of tissues in the opisthosoma, including the heart (Petrunkevitch, 1950).

Mierzejewski (1976a, b) was the first to use SEM to examine tissue ultrastructure from amber. After initial grinding, he accessed the tissue of arthropod and wood inclusions from Baltic amber with a thin needle. Mierzejewski noted ultrastructural details of the wood of *Pinus succinifera*, the eye of a dolichopodid fly, the elytra of a beetle, and the book lung of a spider. The ultrastructure of a fungus gnat from Baltic amber was revealed in detail via TEM by Poinar & Hess (1982, 1985), and Poinar (1992): muscle fibers, nuclei, ribosomes, endoplasmic reticula, lipid droplets, and mitochondria were identified. In addition, Poinar (1992) found cellular-level structures in the abdomen of a braconid wasp from Cretaceous amber of Canada. A pyritised cast of an ant from Baltic amber was described by Baroni Urbani & Graeser (1987), and it turned out that the pyrite replicated surface microsculptural features of the integument. SEM investigations on the wing venation of termites from Cenomanian amber of France were carried out by Schlüter (1989). One of these samples was covered by marcasite and pyrite, and in the same study, Schlüter (1989) showed images of mineralised beetle elytra and an unidentified insect head.

All of these previous studies demonstrated exceptional microscopic details in fossils from different amber deposits, including Eocene Baltic amber, and Cretaceous amber from France and Canada. Furthermore, the authors emphasised that the fossil ultrastructures were identical to extant groups. The investigation and comparison of modern to fossil tissue intensified from this point on with various authors contributing to the body of evidence. Henwood (1992a) removed inclusions from Dominican amber by cutting and fracturing the material through the insect body and investigated the remains via TEM and SEM. In addition, she carried out decomposition experiments under varying conditions and compared the results with the tissue yielded from the amber (Henwood, 1992a). Muscle fibers and cristae were still preserved in the fossils, but they did not match the structures of freshly dead flies. Nevertheless, they are comparable to structures that underwent experimental decay. Henwood concluded that the experiments involving dehydration resulted in the best-preserved tissues. In another study, Henwood (1992b) successfully demonstrated the preservation of organ systems of a beetle from Dominican amber.

While addressing the question of consistency, the most comprehensive study of internal tissue preservation in amber was carried out by Grimaldi et al. (1994). The sample set included 16 arthropod specimens with variations in size and cuticle sclerotisation from Baltic and Dominican amber and eight botanical remains of *Hymenaea* from Dominican amber. Grimaldi et al. (1994) noted that soft tissue preservation is more common in Dominican amber (all of the specimens) than Baltic amber (two out of four samples), but if present, ultrastructural details can be found in their original insertions in both ambers. In addition, membranous material seems to be better preserved than proteinaceous tissue (Grimaldi et al., 1994).

Finally, studies on ultrastructural preservation in amber are rounded out by Poinar et al. (1996), Kohring (1998), Kowalewska & Szwedó (2009), and Tanaka et al. (2009). TEM investigations of *Hymenaea protera* leaflets from Dominican amber revealed the preservation of chloroplasts, mitochondria with associated endoplasmic reticulum, nuclei, and xylem tissue (Poinar et al., 1996). Kohring (1998) documents the preservation of various arthropod structures such as trachea, muscle tissue, and alae from Baltic, Bitterfeld, and Dominican amber. With a combination of SEM with EDS analysis, Kowalewska & Szwedó (2009) revealed the presence of marcasite on a leaf hopper from Baltic amber. In the same year, Tanaka et al. (2009) studied dolichopodid fly eyes from Baltic amber and revealed the presence of pigment cells, rhabdomeres, trachea, and the basement membrane.

In summary, all of these studies indicate a dichotomy in the preservation of tissue ultrastructure: either soft tissue preservation is absent, or the structures are exquisitely preserved. Furthermore, this dichotomy is apparent within the same amber site. There seems to be a difference in the preservation quality and/or chance of different tissues: muscle tissue and trachea are most commonly reported and may be more stable in terms of fossilisation than other tissues.

2.2 Chemical preservation in amber – previous studies

The question of chemical preservation, in particular the conservation of original biomolecules, was raised early on in the scientific history of amber studies. Tornquist (1910) hypothesised that no original material is preserved in amber. In the same year, a study on a lizard in amber revealed that coaly remains were present inside the inclusion, but no further analysis was carried out (Klebs, 1910). Von Lengerken (1913, 1922) was the first to examine chitin preservation in amber. He successfully extracted chitin from a Baltic amber piece which was stored under dry

conditions, and furthermore reported preserved abdominal segments. The chitin in this sample was not strongly altered, although in some places it had been transformed into brown coal. In contrast, pieces of amber which were stored in alcohol for several years did not contain any bioinclusions with preserved chitin (von Lengerken, 1913). With needle preparation, von Lengerken (1922) extracted remains of beetles from Baltic amber and observed chitin and tracheal remains under the microscope.

More recent studies on the tissue composition of fossil inclusions employed techniques such as pyrolysis gas chromatography-mass spectrometry (PyGCMS), Raman spectroscopy, and histochemical staining. A PyGCMS-based study on inclusions in Dominican amber and resin from Kenya did not detect chitin and proteins in the fossil samples, but rather found only straight chain hydrocarbons (Stankiewicz et al., 1998). An analysis using Raman spectroscopy led to some contradictory results: no original biomolecules could be detected from an insect in Baltic amber, but spectra of an insect from Mexican amber indicated the presence of severely altered proteins (Edwards et al., 2007). The cortex and medulla of lichens in Baltic amber could be distinguished from each other by Raman spectroscopy as well, but it is questionable if these differing spectra indicate that the tissues retain some remnants of original chemistry (Hartl et al., 2015). Koller et al. (2005) demonstrated the presence of unidentified tissue biomolecules in a cypress twig from Baltic amber via histochemical staining. It is suggested that these remains represent original tissue, but it is not clear to what extent the stains would also react to diagenetic altered biomolecules (Koller et al., 2005). Chitin remains could be evidenced by Speranza et al. (2015) with fluorescence markers and confocal laser scanning microscopy on fungal inclusions in Cretaceous Spanish amber. These represent the oldest records of β -1,3 and β -1,4-linked polysaccharides and residues of *N*-acetylglucosamine (monomeric unit of chitin). The aforementioned studies are inconclusive regarding chemical preservation in amber and are focused mainly on chitin, a polysaccharide which is one of the major compounds of the insect cuticle. In general, they indicate a significant alteration or loss of original tissue chemistry, but also offer hope that some trace remnants of biomolecules may be preserved.

Another approach to finding biochemical remnants is based on targeted techniques to isolate and characterise specific molecules of interest. These comprise DNA and amino acid studies which are introduced in their respective chapters later on. While DNA preservation is presumably attributed to modern contamination, amino acids could be successfully extracted from inclusions of different amber deposits (chapter 5.4; McCoy et al., 2019). However, it appears that the molecular preservation in amber follows the pattern observed in tissue preservation: it varies between amber deposits and between fossils from the same deposit.

3.0 Aims of the thesis

Previous studies on morphological and chemical preservation in amber give an indistinct idea on the mechanisms that influence amber taphonomy. Although many of these studies are outstanding in their methodology and significance, the majority describes a specific phenomenon with limited relevance for the greater picture. Therefore, the four major goals of this thesis are to:

- (I) Describe and document the exceptional preservation of amber fossils
- (II) Improve the understanding of the taphonomy of resin-embedded arthropods
- (III) Compare the preservation quality between different deposits
- (IV) Examine the limits of fossilisation in amber

To achieve these aims, several subprojects were carried out which are briefly introduced in the following paragraphs. Information on amber preservation is significantly biased towards class I ambers. The majority of famous amber deposits belongs to this chemical subgroup, such as Baltic, Dominican, Lebanese, Burmese, French, and Spanish amber. However, in recent years several excavations led to the collection of large amounts of class II ambers from India (Cambay) and China (Zhangpu). To enhance the comparability of class I and class II amber inclusions, this thesis includes the largest tomographic data set of a single class II amber deposit (chapter 5.3). Although class II ambers contain complete body fossils (Rust et al., 2010; Mazur et al., 2014) their grade of morphological and biomolecular preservation has not been examined before. This thesis offers the first insights on both of these subjects. The morphological preservation of class II insect inclusions is described for the first time in chapter 5.1 and 5.3. Chemical analyses of inclusions from different ambers and copal are presented in chapter 5.2 and show that the fossils may be exposed to mineral formations.

Dehydration of amber fossils is noted by several authors, but whether it is beneficial or unfavourable to preservation is disputed (Grimaldi et al., 1994; Henwood, 1992; McCoy et al., 2018b; Coty et al., 2014). Through examinations of platypodid beetles from Madagascan Defaunation resin, this thesis offers new insights on tissue dehydration in resinous environments (chapter 5.2 and 5.5).

Moreover, it is shown that DNA can be extracted from these extant resin-embedded organisms (chapter 5.5). The success of this procedure has been questioned due to the problematic early studies claiming the extraction of original DNA from amber. This approach yields new opportunities for the stepwise assessment of ancient DNA from amber.

In addition, this thesis reports on the first successful extraction of original amino acids from class II inclusions (chapter 5.4), showing that amino acid preservation is not restricted to class I amber deposits and may represent the limit of peptide preservation in this material.

The degree of chemical preservation of bone tissue in amber is also unknown. In this thesis, a lizard forelimb in Dominican amber is analysed by various methods, revealing distinctive alteration of the mineral and organic phases (chapter 5.6).

4.0 Material and methods

A general material and methods section is provided here. The samples and methods utilised for published articles of section 5.0 are reported in detail in their respective publications, which are listed in the Publications section (10.0).

4.1. Sample origin and geology

Cambay amber

The majority of samples stem from Cenozoic amber deposits, particularly the Lower Eocene Cambay amber deposits in India and the Miocene deposit of Zhangpu amber in China. Cambay amber fossils were made available to the author as the result of an international collaboration between the American Museum of Natural History (New York; USA), the Birbal Sahni Institute of Palaeobotany (Lucknow; India) and the Institute of Geosciences of the University of Bonn (Germany). Fieldwork in India, carried out by the author's supervisor and colleagues from the named institutes, resulted in the collection of large amounts of Lower Eocene Cambay amber, a small fraction of which is still housed in the Institute of Geosciences.

The collected material stems from the Vastan (N 21° 25.239, E 073° 07.249) and Tadkeshwar (N 21° 21.400, E 073° 04.532) lignite mines which are located between the Narma and Tapi rivers, approximately 30 km away from Surat (Gujarat state) in western India (Alimohammadian et al., 2005; McCann, 2010; Rust et al., 2010). This region belongs to the NNW-SSE trending Cambay basin, which covers an area of roughly 59000 km² (McCann, 2010). With a basin fill of up to 5.5 km, the Cambay basin directly overlies the Deccan traps (Banerjee et al., 2001; Sharma & Sircar, 2019).

The lignite-bearing strata of both mines are part of the Cambay shale Formation, the most prominent shale reserve of India (McCann, 2010; Sharma & Sircar, 2019). This shale represents

a 75-1500m thick layer of dense glauconitic clay with lignite seams (Rust et al., 2010). Associated shark teeth and microfossils indicate a mid-to early Ypresian (~50-52 Ma) age for these rocks, which coincides with the collision of the Indian land mass with Asia (Rana et al., 2004; Sahni et al., 2006; Garg et al., 2008; Punekar & Saraswati, 2010; Rust et al., 2010). The amber is accumulated in several light, parallel, 5-10 cm thick layers (“amber conglomerate”) within the lignite strata (Rust et al., 2010). The lignite consists of organic plant material remains that accumulated within a marsh-like environment (McCann, 2010). Most amber pieces range from sand grain sized to several millimetres in size, but scattered pieces of up to 5-10 cm in length are also found (Rust et al., 2010). These amber conglomerates are interpreted as stranded shoreline wrack concentrated by low-energy transgressions and regressions that imply brackish water conditions with some marine incursions (McCann et al., 2010; Rust et al., 2010). Remarkably, the presence of *in situ* preserved flows of amber indicates that at least some of the material has not been reworked (Rust et al., 2010). However, it is not clear from which layers exactly the material of this thesis was collected. Although Rust et al. (2010) mention that the bulk of amber of the first field season stems from “lignite 1” and “lignite 2” (exposed sequences in the Vastan mine), subsequent expeditions might have sampled different layers, especially since the lignite mines are active mining areas.

In contrast to other amber deposits, the botanical source of Cambay amber could be identified via chemical analyses and plant fossils. Various mass spectrometric methods and FTIR revealed cadalene-based bicyclic sesquiterpenoids, bicadinanes, and bicadinenes typical of dammar resin (Dutta et al., 2009; Mallick et al., 2009, 2014). According to Anderson et al. (1992), dammar resin is categorised into the chemical subgroup class II and was produced by trees of the family Dipterocarpaceae (Dutta et al., 2009; Mallick et al., 2009, 2014). A dipterocarp origin for Cambay amber was further validated by the wood anatomy of plant fragments found in association with amber pieces (Rust et al., 2010).

Approximately 100 arthropod species within 55 families of 14 orders were initially reported from Cambay amber (Rust et al., 2010). Since then, numerous studies on Cambay amber fossils have provided insight into the biodiversity, biogeography, and evolution of several taxa (e.g. Engel et al., 2011; Stebner et al., 2016, 2017; Nadein & Perkovsky, 2019).

Zhangpu amber

Prof. Dr. Wang (State Key Laboratory of Palaeobiology and Stratigraphy, Nanjing Institute of Geology and Palaeontology) kindly provided hundreds of pieces of Zhangpu amber for this thesis which were collected near Qianting town (N 24°16′03″, E 117°59′01″) in China, Fujian province (Shi et al., 2014a). The amber host rocks belong to the Fotan Group which consists of three basaltic and three sedimentary layers of terrestrial origin (Zheng & Wang, 1994). The amber occurs within coal seams and diatomite from the second sedimentary layers that directly underlie layers with abundant plant material (Zheng et al., 2019). Based on these plant fossils, Zheng & Wang (1994) suggested a middle to late Miocene age of the Fotan Group. A recent study based on argon isotopes confirms this and yields an absolute age of 14.7± 0.4 Ma (Zheng et al., 2019). Zhangpu amber is identified as a class II resin by its terpenoid composition characterised by sesquiterpenoids and triterpenoids (Shi et al., 2014a). The dipterocarp origin suggested by chemical analysis (Shi et al., 2014a) was confirmed by fossil fruit wings of *Shorea* and *Dipterocarpus* (both Dipterocarpaceae) from the same region (Shi & Li, 2010; Shi et al., 2014b). Thousands of collected Zhangpu amber pieces suggest, upon preliminary examinations, the presence of a highly diverse biota, but the scientific evaluation is in the early stages (Wang, pers. comm.).

Baltic & Dominican amber

A few pieces of Baltic and Dominican amber have been examined using Raman spectroscopy (chapter 5.1). They are part of the collection of the Goldfuß-Museum (University of Bonn) and were obtained a number of years ago from a private collector. Baltic and Dominican amber are among the most significant amber deposits with respect to their abundant collection material and scientific history, which is why only a short introduction is given here. Baltic amber (class Ia) has been re-deposited several times through glacial activity during the Pleistocene, resulting in wide-ranging modern occurrences that extend from the English coast into Russia and the German Hill Region (Weitschat & Wichard, 2010). The main region of Baltic amber mining is the Samland Peninsula where amber can be found in the ‘blue earth’ strata consisting of marine sands enriched in glauconite (Weitschat & Wichard, 2010). Baltic amber is most likely of Eocene age, but absolute dating remains problematic. Age determinations provide a Lutetian age of the ‘blue earth’ sediments, but underlying amber bearing strata indicate that the amber had already been deposited about 50 million years ago (Weitschat & Wichard, 2010). Recent studies by Sadowski et al. (2017) suggest that the vast amount of amber was not produced by a

single plant taxon, but rather multiple species of Pinaceae, Araucariaceae, and Sciadopityceae. In addition, these authors suggest a late Eocene origin of Baltic amber based on its conifer fossil assemblage.

Dominican amber is of Miocene age (~15-20 Ma) and found in the Cordillera Septentrional (northern mining district) and the Cordillera Oriental (eastern mining district) of the Dominican Republic (Iturralde-Vinent, 2001; Penney, 2010b). The La Toca Formation of the northern mining district consists mainly of sandstone with occasional conglomerates and thin lamellae of lignite in which the amber can be found. The amber bearing rocks of the eastern mining district are sandy clay and lignite (Yanigua Formation). Both amber occurrences (class Ic) were deposited in the same sedimentary basin and were produced by the extinct angiosperm species *Hymenaea protera* (Poinar, 1991; Anderson et al., 1992; Penney, 2010b). Various extant species of the genus *Hymenaea* still produce very similar resin today (Langenheim, 2003).

Madagascar “copal” & Defaunation resin

Several pieces of allegedly Madagascar “copal” containing platypodid beetles were purchased online in order to compare them with modern Defaunation resin from the same region (chapter 5.2). Pieces of modern Defaunation resin from Madagascar contained platypodid beetles as well and were kindly provided by Dr. Solórzano-Kraemer (Senckenberg Institut Frankfurt) who collected the material during fieldwork in 2017. Like Dominican amber, “copal” and Defaunation resin from Madagascar are produced by angiosperm trees of the genus *Hymenaea* (Penney & Preziosi, 2010; Delclòs et al., 2020). These trees grow in coastal lowland tropical forests along the eastern margin of the island (Delclòs et al., 2020).

4.2 Methods

Imaging

Images of the samples were taken with a Keyence VHX-1000 digital microscope and a Leica Stereomicroscope MZ16 with a JVC ky-F70B digital camera attachment. The raw files have been processed subsequently with Adobe Photoshop CS5.1 and Adobe Illustrator CS 5.1.

Extraction of amber inclusions

Microscopic analyses: The fossil arthropods utilised for microscopic analyses (light microscopy, SEM, TEM) are from Eocene Cambay amber (~ 52 Ma). For each of these samples, orange oil (CASRN: 8008-57-9) was used to dissolve the surrounding amber at room temperature. Depending on the size of the piece, this procedure took about 2-5 hours and enabled the extraction of the fossils. The samples were either transferred with fine brushes made of single eye lashes or through pipettes.

Amino acid racemisation: Five fossils each of Zhangpu and Cambay amber were extracted with HPLC grade toluene (CASRN: 108-88-03). Toluene was preferred in this case, because it represents a “clean” solvent, consisting only of the same type of molecules. Orange oil consists of several compounds in varying concentrations that might hamper mass spectrometric methods by adding too much noise. The samples were placed in petri dishes with toluene and could be extracted about 45-60 minutes later.

Scanning electron microscopy (SEM)

After extraction, fossils were directly placed on SEM sample holders and sputter coated with gold particles for 30 seconds. Subsequent analyses were carried out in the Institute of Geosciences, University Bonn, with a VegaTescan TS5130LM electron microscope at a high-voltage of 20 kV under vacuum conditions.

Transmission electron microscopy (TEM)

TEM preparation and analysis were performed in the Institute of Evolutionary Biology and Ecology, University of Bonn. Eight fossils, comprising one jumping spider, one torymid wasp, four dipterans, and one beetle were prepared using a modified protocol for modern samples (Appendix 9.1). Ultramicrotome slices have been produced from the spider and one dipteran (Chironomidae) whereas the other samples are still preserved in araldite and can be utilised for future experiments. Cutting of the samples was performed with a diamond knife on a Leica Ultracut S ultramicrotome. The subsequent analysis of the sections was carried out with a Zeiss EM10 A/B.

Raman spectroscopy

Raman measurements were conducted with a confocal Horiba Scientific Labram HR800 Raman spectrometer equipped with an Olympus BX41 microscope. The instrument is located at the Institute of Geosciences of the University of Bonn, Germany. For all measurements, a HeNe Laser 632,81 nm operating at a maximum power of 17 mW was used. The scattered light was detected in a 180° backscattering geometry by an electron multiplier charge-coupled device detector after having passed a 1000 µm confocal aperture and a 100 µm spectrometer entrance slit, and being dispersed by a grating of 600 grooves/mm. A 100x objective with a numerical aperture of 0.9 was used, yielding a theoretical lateral resolution in the order of 1 µm (859 nm). To avoid any thermal degradation of the enclosed tissue, the laser power was adjusted to 50 % of the total laser output power. All samples were measured in the wavenumber range between 200 – 1800 cm⁻¹. For a better signal-noise ratio, up to 60 accumulations of scans were performed. The measuring time varied between 150 – 1200 s, depending on the sample characteristics and chosen numbers of accumulations. The measured Raman intensities were corrected for the wavelength-dependent instrumental sensitivity (white light correction) and the background signals (stray light, fluorescence) which were fitted with a third order polynomial function. To identify single Raman modes, the bands were fitted with Gauss-Lorentz function.

Synchrotron X-ray microtomography

Synchrotron X-ray microtomography (SR-µCT) of Zhangpu amber fossils was performed at the UFO imaging station of the KARA Synchrotron Radiation Facility at Karlsruhe Institute of Technology (KIT). A parallel polychromatic X-ray beam was spectrally filtered by 0.2 mm Al to obtain a peak at about 15 keV. At a rate of 70 frames per second, 3,000 radiographic projections were acquired over a range of 180°. The detector consisted of a thin, plan-parallel lutetium aluminum garnet single crystal scintillator doped with cerium (LuAG:Ce), optically coupled via a Nikon Nikkor 85/1.4 photo-lens to a pco.dimax camera with a pixel matrix of 2008 × 2008 pixels. Depending on the size of the inclusion, a 5x or 10x setup (4.4 x 4.4 mm and 2.2 x 2.2 mm field of view) has been used. The image stacks were examined with the software ImageJ 1.53c and compared to ones of a modern chalcidoid wasp (*Nasonia vitripennis*) that was analysed under the same conditions. The modern wasp has been fixed in 100% ethanol prior to synchrotron examination.

5.0 Examination of amber taphonomy

The chapters of this section represent individual studies carried out within the framework of this thesis. Most of them are at different stages of preparation for publication whereas two have been already published. When chapters refer to published material, this is mentioned at the beginning. The related research articles are attached in the Publications section (10.0).

5.1 Microscopic examinations of Cambay amber fossils

The preservation of tissues and cellular compounds from fossil inclusions in amber has been reported in several studies within the last few decades (chapter 2.0; reviewed in Barthel et al., 2021). However, all of these previous findings stem from a type of amber mainly built from monoterpenoids and diterpenoid acids (class I amber). As the preservation of the inclusions is strongly affected by the chemistry of the surrounding amber (Henwood, 1992a; McCoy et al., 2018a), it is questionable to what degree these previous conclusions can be extrapolated to fossils from different types of amber. This chapter presents results of electron microscopic studies on several arthropod samples from Eocene Cambay amber, which, as a class II amber, is chemically distinct from the previously studied ambers, to determine if cellular structures are also preserved therein. In addition, some comments on remarkable observations are given.

Results

Scanning electron microscopy of a spider inclusion from Cambay amber revealed exceptional preservation of various structures (Fig. 3). The prosoma (anterior part of the body) includes the head and legs of a spider. Here, sensory hairs can be recognised along the legs and pedipalps (Fig. 3). In addition, eight eye lenses are preserved. The posterior part of a spider's body, called the opisthosoma, contains the reproductive, digestive, and respiratory systems along with the heart and silk glands. The opisthosoma of the fossil sample ruptured during preparation, allowing insight into the body cavity (Fig. 3). The ventral part consists of wrinkled homogeneous tissue structures that do not enable an identification of specific structures. In contrast, the dorsal part of the opisthosoma (Fig. 3) shows canal like structures and openings that can be identified as digestive tubules. These tubules extend in modern spiders from the intestine throughout the opisthosoma. Overall, the body of the spider, including the chelicerae and legs, is sunken, which may have resulted from dehydrating effects of the extraction solvent.

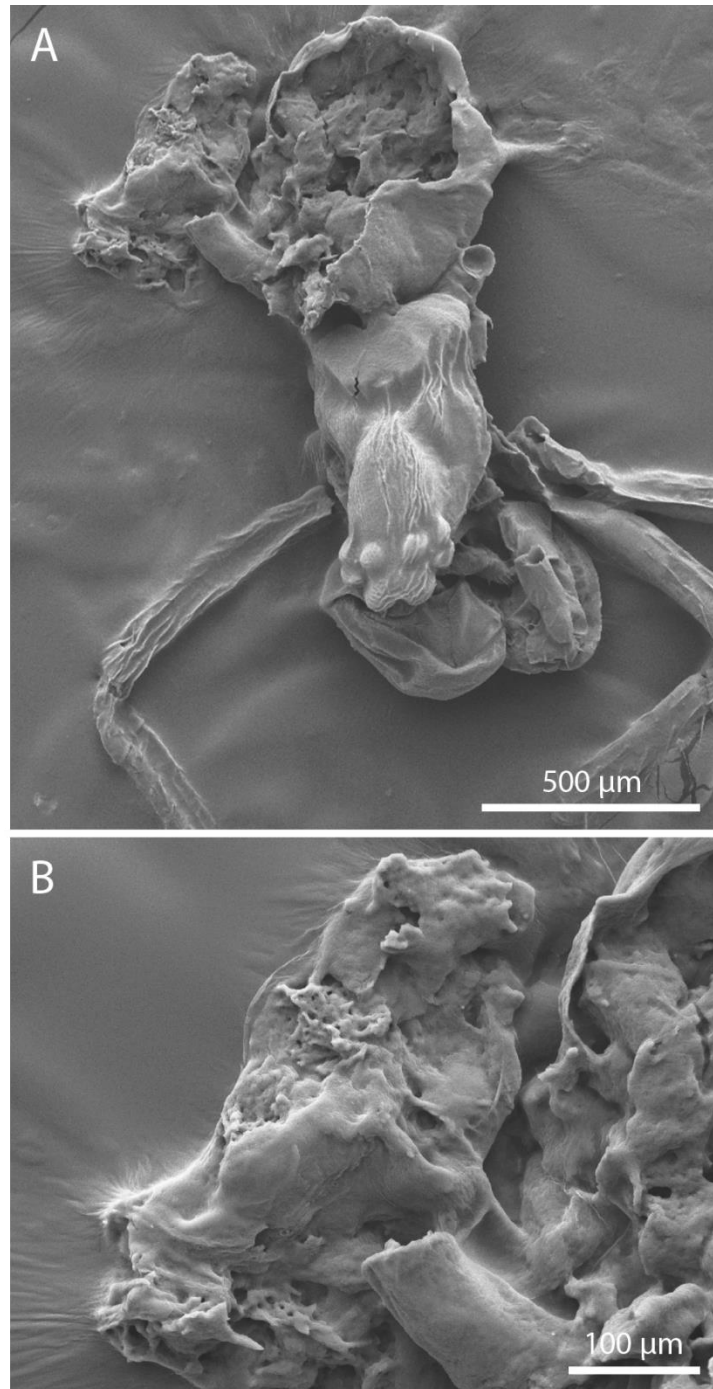


Figure 3. SEM images of a spider extracted from Eocene Cambay amber. (A) The opisthosoma ruptured dorsally and allows insight into the body cavity. Although, certain structures cannot be identified, the body cavity is not an empty void but filled with formerly intact tissues. (B) The ruptured part of the opisthosoma contains small, tubular shaped structures that are interpreted as parts of the digestive tissue.

The cuticle and inner parts of the opisthosoma of another Cambay amber spider could be examined via TEM (Fig. 4). Arthropod cuticle normally consists of three major layers: the epi-, exo-, and endocuticle. These are underlain by epidermal cells and separated from the body cavity through a basement membrane. Only the most distal epicuticle appears to be preserved without any identifiable sublayers (Fig. 4A). No exocuticle, endocuticle, basement membrane

or epidermal cells can be recognised. In addition, a grain like matrix of whitish to dark colour is present in the TEM figures. This matrix consists of binding complexes of metal ions (from the fixative) with degraded organic structures.

Remarkably, parts of the respiratory system of the spider, namely the book lung and some trachea, are preserved (Fig. 4) and surrounded by the same matrix. Parts of the book lung are associated with some unidentified structures (Fig. 4D). It appears that in the case of the spider, the preservation is biased towards membranous (distal) structures that are close to or in contact with the amber.

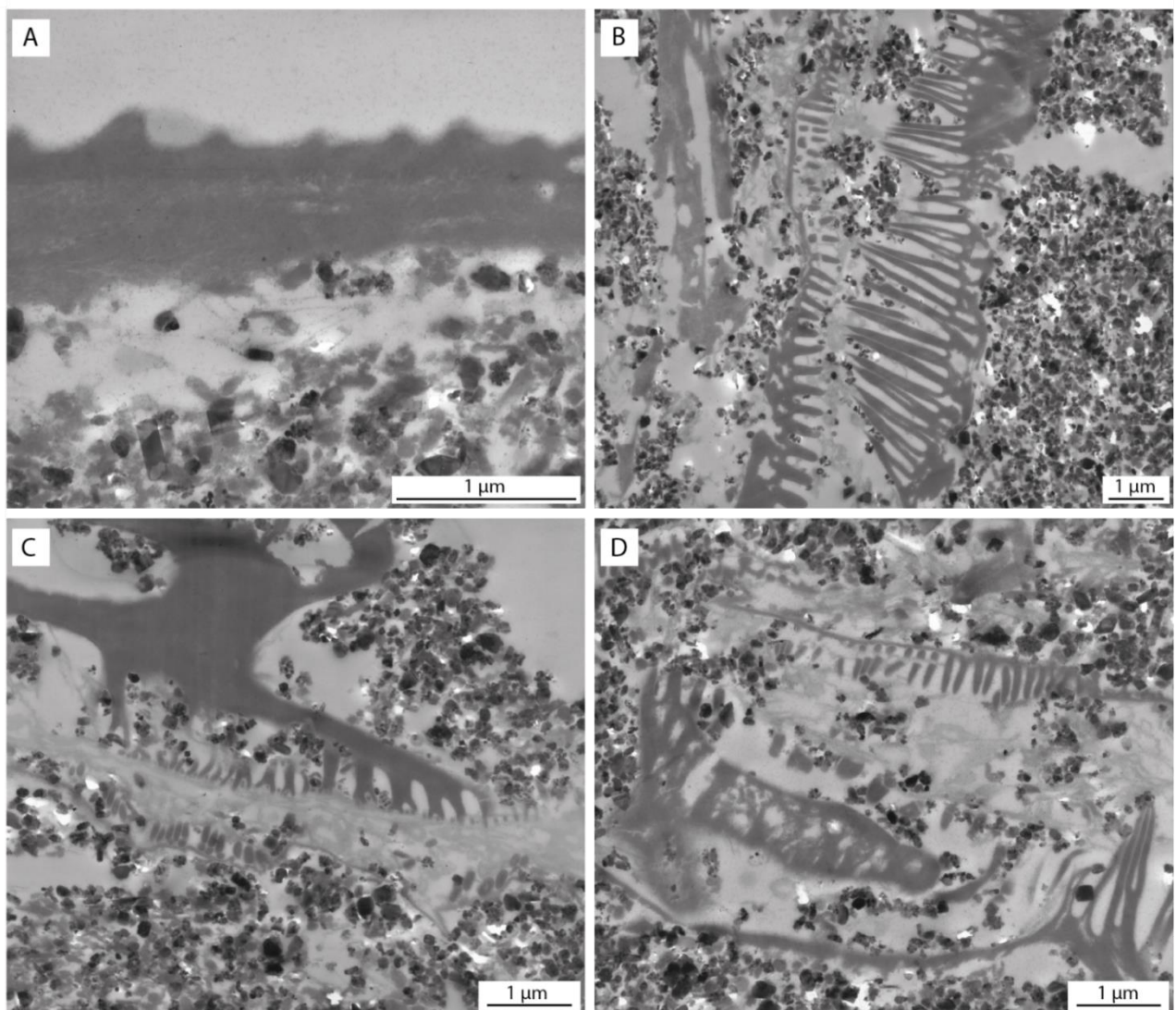


Figure 4. TEM images of a spider from Eocene Cambay amber. The epicuticle (A), and book lung (B) can be recognised. (C) A tracheol branches into a large tubular shaped structure that likely represents parts of the digestive tissue. (D) Unidentified structures and lamellae of the book lung.

TEM slices of a nematoceran head yielded well preserved eye lenses and abundant mitochondria (Fig. 5). It has to be noted that this sample was extremely fragile after extraction which led to the disintegration of the head when embedded in artificial resin. Therefore, more ultrastructures might have been present originally but lost during preparation. Regarding the eyes, only the distal parts of each ommatidium (cornea) can be observed. No crystal cones, pigment cells or axons are present. The mitochondria can be found proximally to the lenses in a region that could represent the former cerebral ganglia of the insect. Besides the mitochondria, no ultrastructures could be evidenced in this region. The inner (cristae) and outer membranes of mitochondria are composed of double layered phospholids. In contrast to mitochondria of modern samples, the boundaries of the fossil membranes are not as clearly defined when examined with higher magnifications, indicating some degree of alteration. The outer membrane and the cristae express the same degree of preservation. Due to their abundance and position in the slice, it can be assumed that these mitochondria represent remains of sensory or nervous tissue, probably the cerebral ganglia. The cuticle of the nematoceran shows the same kind of preservation as the spider: only the epicuticle is present without any sublayers.

Notably, the TEM arthropod samples used in this study were only partially filled with artificial resin. This is a common problem in modern arthropod preparation and is due to the repelling characteristic of the cuticle, which makes a proper infiltration challenging. Apparently, resin cannot enter the body cavity of the animal as long as the cuticle is intact. During TEM preparation of the spider sample (Fig. 4), the legs and opisthosoma appeared to be hollow inside and were not filled by resin, but were coated with a greyish material that did not seem to represent original tissue. However, TEM later revealed the preservation of ultrastructures from the same region of the opisthosoma. This is similar to a case where Poinar & Hess (1982, 1985) reported on ultrastructures, which they found in a small strip of tissue next to the cuticle in a fungus gnat abdomen. It appears that parts of the original tissue are present in this region even when the inclusion looks hollow. While screening through amber collections, it became evident that samples that were damaged during grinding never contained resin remains inside of their body parts. Instead, in some cases the complete body cavity or part of it were filled with material that was later analysed via Raman spectroscopy (chapter 5.2.2).

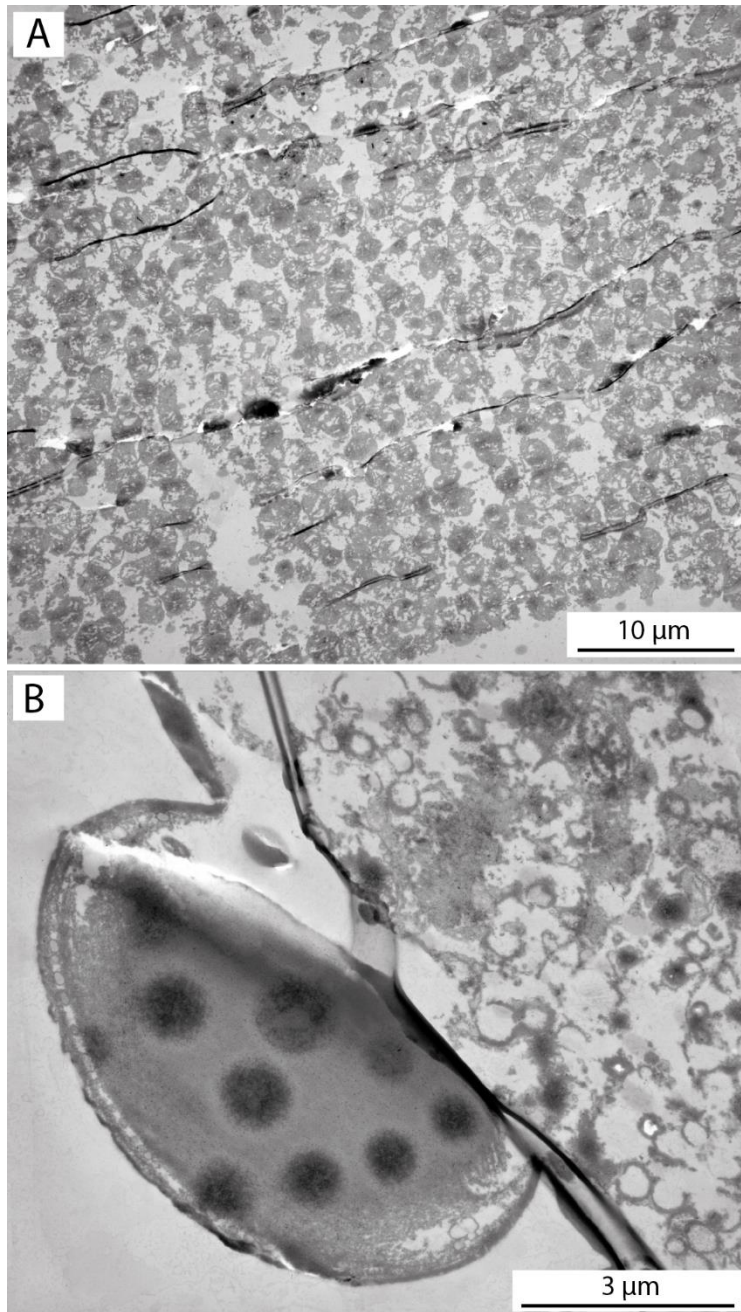


Figure 5. TEM images of the cephalon region of a nonbiting midge (Chironomidae) in Eocene Cambay amber. (A) Accumulations of mitochondria. (B) Eye lens with black dots. Ommatidia are not present in the underlying tissue.

Although ultrastructural compounds are evidenced from different samples of Cambay amber inclusions, the majority of tissues is severely damaged or lost during fossilisation. The quality and amount of ultrastructural preservation is not equal in the examined specimens and shows that the degree of preservation cannot only depend on the depositional environment or resin chemistry, but must also be attributed to the individual fate of the inclusion before and after entrapment. These observations gave rise to a large-scale synchrotron examination of amber fossils (chapter 5.3).

Further notes on Cambay amber material

When examining TEM samples with a light microscope, it became evident that there is no hint towards the structural integrity of them prior to the dissolving of the amber matrix. This was especially the case for a chalcidoid wasp that appeared completely intact before preparation (Fig. 6). However, after exposure to orange oil in order to dissolve the amber around it, the wasp completely disintegrated and was not suited for subsequent analysis. Therefore, to save collection material, it should be tested if the physical integrity of a fossil can be assessed by other methods before invasive methods are applied.



Figure 6. Chalcidoid wasp in Eocene Cambay amber. Although it appears to be intact, this sample completely disintegrated after exposure to orange oil. It is therefore not possible to assess the stability of an inclusion solely by light-microscopy.

Another remarkable point on Cambay amber material regards occurrences of whitish radial crystals within the matrix (Fig. 7). These crystals can be extremely abundant in the matrix, but have so far not been observed to grow on inclusions. Such crystals are not described from other amber deposits and seem to be the result of special diagenetic processes. Electron microprobe measurements revealed that they consist of C, S, and Na with low amounts of Al, but their exact crystal structure is not known. P, Si, K, and Fe could not be evidenced. The crystals must have formed in an early diagenetic phase, because they did not grow within voids of the piece, but within the matrix. More analyses are necessary to reveal the structure and origin of these crystals.

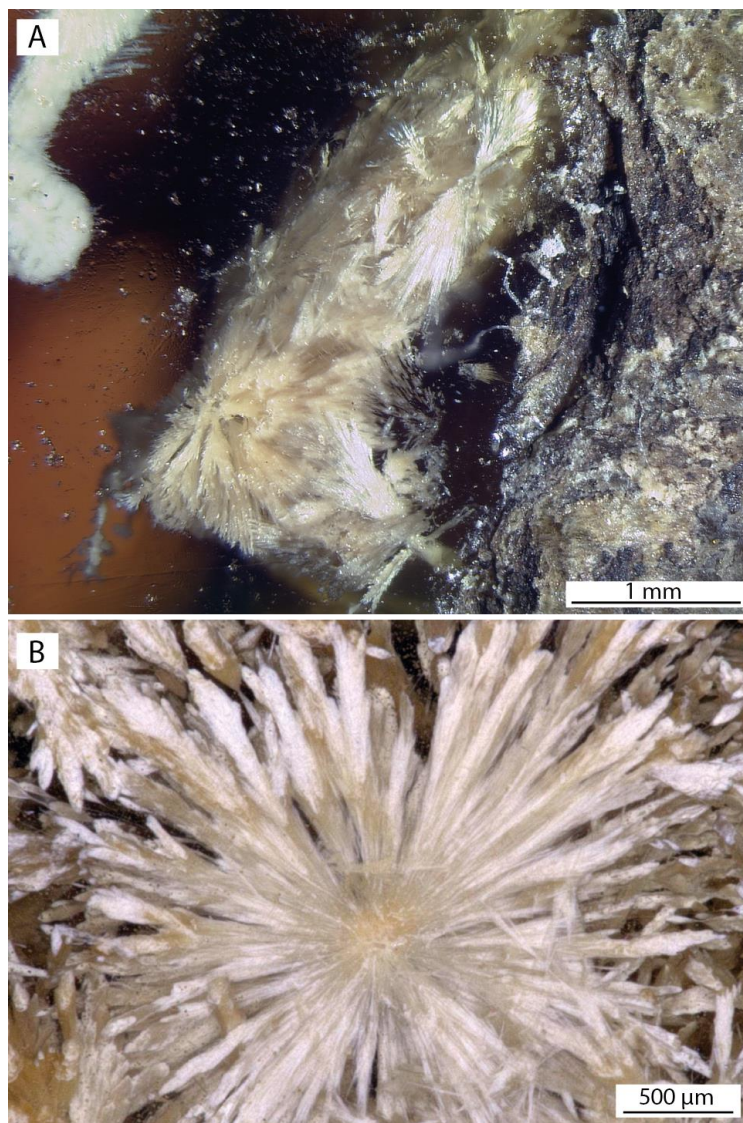


Figure 7. Crystal structures in Cambay amber. (A) Overview image. The crystals are located in the resin matrix and directly underlie the weathering crust in this sample. (B) Detailed image of another sample. Column-like structures formed radially around the nucleus and increase in diameter towards their distal end. These crystals are commonly found in Cambay amber pieces and consist of C, S, and Na.

5.2 Raman spectroscopy of resin-embedded insects

This chapter comprises Raman spectroscopic analyses of various resin-embedded insects. The first part deals with platypodid beetles in *Hymenaea* resins whereas the second part reports on general observations that were made while screening material of the Goldfuß-Museum (University of Bonn) amber collection.

5.2.1 Raman spectroscopy of *Hymenaea* resins and inclusions

Introduction

Amber inclusions provide information about ecosystems in deep time and represent the result of a diagenetic process that lasts for millions of years. In contrast, Holocene copal (sensu Solórzano-Kraemer et al., 2020) gives insight into much younger ecosystems of some thousands of years old up to the present. In the past, copal was deemed to be not of significance for evolutionary or biogeographic studies due to its young age (Penney & Preziosi, 2010). Scientific interest has increased within the last few years when studies showed that copal preserves arthropod taxa that became extinct in historical times or may be undescribed from the recent fauna (Hinojosa-Díaz & Engel, 2007; Penney et al., 2013a). Copal is an excellent source of information to analyse faunal changes during the Anthropocene, a geologically short epoch from the industrial revolution to the present (Delclòs et al., 2020). With respect to this thesis, copal is especially interesting because under the right conditions, modern day accumulations of copal might form amber deposits in the future, which is why they have the potential to provide insights into early diagenetic fossilisation processes (Penney & Preziosi, 2010).

To track down the changes that may occur to resin embedded arthropods and their surrounding matrix in the early diagenetic stage, quaternary inclusions from Madagascar are analysed via Raman spectroscopy. This non-invasive method is useful for analysing amber and copal material by providing a general overview on the maturity of the resinous matrix and limited information on the geographical origin of the sample (Edwards & Farwell, 1996; Brody et al., 2001; Winkler et al., 2001; Vandenabeele et al., 2003; Rao et al., 2013, Barthel et al., 2020). Edwards et al. (2007) expanded this approach and applied for the first time Raman spectroscopy to arthropod inclusions from amber. Their spectra of insect tissues from one piece each of Mexican and Baltic amber were interpreted to represent significant protein degradation in the Mexican amber piece. For the specimen from Baltic amber, well preserved keratotic signatures have been reported (Edwards et al., 2007). Herein, Raman spectra of Defaunation resin and

Holocene copal from Madagascar are compared to spectra of Dominican amber. The Defaunation resin and Holocene copal pieces contained arthropod inclusions that were analysed via Raman spectroscopy as well. In the following sections, the terms “Defaunation resin” and “Holocene copal” are abbreviated to “resin” and “copal” respectively, but refer to the original definition by Solórzano-Kraemer et al. (2020).

Results

Plant resins are composed of terpenoids, which are built up of isoprene subunits (C_5H_8). Therefore, Raman spectra of resinous materials (independent of age) share many features and are dominated by characteristic vibrational modes of carbon, hydrogen, and oxygen bonds. The chosen measurement range of 200 cm^{-1} to 1800 cm^{-1} contains the most distinctive spectral features of resinous material. Shifts in band positions may occur between samples of different geographic origin and may also be the result of methodological deviations or environmental influences. All measured bands are given in Table 3. After dealing with the main vibrational modes of resin matrix spectra that are suited to distinguish between different materials, additional spectral features are discussed ordered by their wavelength in the subsequent section.

Main vibrational modes in the matrix spectra

The most prominent bands in the matrix spectra are located near 1440 cm^{-1} and 1645 cm^{-1} (Fig. 8, Table 3). The band at $\sim 1646\text{ cm}^{-1}$ is directly related to the terpenoid “backbone” of the matrix because the same band is present in Raman spectra of isoprene (SDBSWeb, 2021), which is the polymeric building block of plant resins. It results from the stretching of non-conjugated $\nu(C=C)$ and forms a shoulder with a band at 1660 cm^{-1} that can be assigned to stretching modes of trans conjugated CC double bonds (Table 3; Brody et al., 2001). The 1440 cm^{-1} band is caused by a scissoring type deformation $\delta(CH_2)$ and $\delta(CH_3)$ in the resin structure (Brody et al., 2001) and forms two shoulders to higher frequencies at 1460 cm^{-1} and 1470 cm^{-1} (Fig. 8). These bands are assigned to different deformation modes of methyl and methylene (Table 3).

The intensity ratio of the 1646 cm^{-1} and 1450 cm^{-1} band positions (I^{1646}/I^{1450}) can be used as an indicator of resin maturation and is linked to the loss of C=C unsaturation during diagenesis (Edwards & Farwell, 1996). The progressive loss of C=C bonds (decrease of 1646 cm^{-1} band intensity) is balanced by the formation of CH_2 and CH_3 groups (increase of 1450 cm^{-1} band intensity). Although no absolute age is acquired with this method, it is possible to distinguish between mature (= fossil) and immature resins. Mature resins (amber) have a I^{1640}/I^{1450} ratio

smaller than 1.0 (Edwards & Farwell, 1996; Brody et al., 2001; Winkler et al., 2001). In contrast, immature resin, such as modern resin and Holocene copal, shows I^{1646}/I^{1440} values greater than 1.0 (Edwards & Farwell, 1996; Brody et al., 2001; Winkler et al., 2001). In this study, the higher maturation ratio of amber was directly recognisable in comparison to copal and resin. To determine the ratio of maturation, the according bands were fitted with an asymmetric Gauss-Lorentz function estimating the full width at half maximum.

For the Dominican amber sample, a I^{1643}/I^{1440} ratio of 0.64 was measured. This value is in the range of amber pieces from other deposits, but much lower than previously documented ratios of about 0.9 for Dominican amber samples (Brody et al., 2001). The low value of 0.64 may be due to additional shoulders in the Dominican amber spectra that can occur at higher wavenumbers and influence the integrated areas (Edwards & Farwell, 1996). In any case, the I^{1643}/I^{1440} of the Dominican amber sample clearly separates it from the younger material: the resin and copal samples have I^{1644}/I^{1442} ratios of 1.2 and 1.4, respectively. These ratios fall within the range of previously published values for resinous material from East Africa (Brody et al., 2001) and are sufficient to distinguish between the amber and more recent material (copal and resin).

Additional spectral features that can also be used to distinguish between the fossilised amber and recent material are located in the region of ~ 700 to 750 cm^{-1} . Here, the Dominican amber spectrum (Fig. 8) shows a triplet of bands ($696\text{ cm}^{-1} / 720\text{ cm}^{-1} / 744\text{ cm}^{-1}$), which represents the fingerprint region of this material (Brody et al., 2001; Winkler et al., 2001). The band at 722 cm^{-1} is present in the amber and absent from the copal or resin spectra, which are instead characterized by a doublet at 696 cm^{-1} and 744 cm^{-1} in the same region (Fig 8). The 720 cm^{-1} and 744 cm^{-1} bands can be assigned to $\nu(\text{C-C})$ stretching vibrations (Table 3, Brody et al., 2001). The 696 cm^{-1} band is not assigned to a distinct type of vibrational mode, but its position in argues for a mode related to C-C bonds in the resin matrix.

The band at 720 cm^{-1} is the result of amber maturation (Brody et al., 2001) and is not present in the copal and resin material. In fact, multiple spectra of Dominican amber samples show that another weak band can be identified at 713 cm^{-1} (Fig. 8B). Thus, the fingerprint region in our measurements of Dominican amber is characterised by four bands (“quartet”) instead of three. This observation has not been described in previous studies and may provide further information on the structural changes of the matrix in consequence of diagenesis. More

experiments are needed to assess this matter, because the small “fourth” band could also have been caused by methodological deviations.

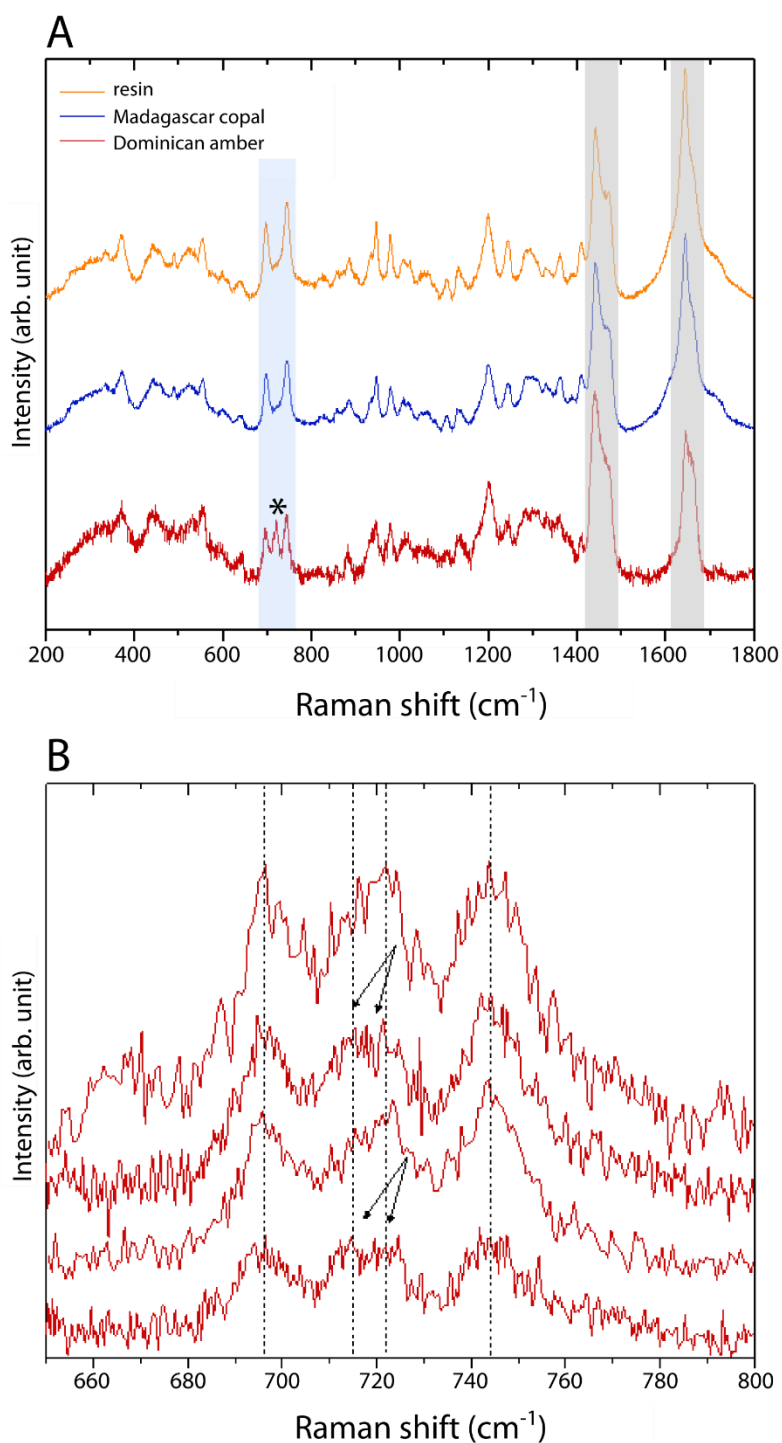


Figure 8: Raman spectra of resin and copal from Madagascar and Dominican amber. (A) Comparison of resin, copal, and Dominican amber spectra. Highlighted in gray are the band positions that are used to determine the maturity of the samples. The fingerprint region of the Dominican amber is highlighted in blue. * = wavenumber region shown in B. (B) Detailed Dominican amber spectra in the wavenumber region of 660 – 680 cm⁻¹. The black arrows point towards spectra in which a splitting from a triplet into a quartet is indicated. See text for further discussions and Table 3 for band assignments.

Additional spectral features

In the region below 700 cm^{-1} , two bands at 370 cm^{-1} and around 450 cm^{-1} are assigned to $\delta(\text{CCO})$ deformation modes (Brody et al., 2001; Vandenabeele et al., 2003). Additional bands at 263 cm^{-1} , 336 cm^{-1} , 490 cm^{-1} , 523 cm^{-1} , 554 cm^{-1} , 599 cm^{-1} , and 640 cm^{-1} were unassignable. A very weak, broad band can be identified in all matrix spectra at roughly 823 cm^{-1} . This band is slightly shifted towards lower wave numbers (819 cm^{-1}) in the amber spectrum, but cannot be assigned to a distinct vibrational mode. In the region from 800 cm^{-1} to 1000 cm^{-1} several strong bands at 885 cm^{-1} , 934 cm^{-1} , and 978 cm^{-1} represent $\rho(\text{CH}_2)$ and $\rho(\text{CH}_3)$ rocking vibrations.

The band at 885 cm^{-1} forms a weak shoulder with an unassignable band at 858 cm^{-1} in the resin and copal spectra, but in the amber spectrum both bands are clearly separated. In addition, the band at 934 cm^{-1} forms a shoulder with a sharp, strong unassigned band at 947 cm^{-1} in the copal and resin spectra, whereas these two bands are difficult to distinguish in the amber spectrum. From the bands in the region of 1000 cm^{-1} to 1200 cm^{-1} , only three can be assigned to specific vibrational modes. Although definitive band assignments cannot be made for the spectral features at 1008 cm^{-1} and 1022 cm^{-1} in the copal and resin spectrum, it is assumed that they are related to additional $\nu(\text{CC})$ and $\nu(\text{CO})$ stretching modes (Vandenabeele et al., 2003). The amber spectrum shows a single broad band in this region instead of two separate bands.

In contrast to Brody et al. (2001), who described a weak band at 1063 cm^{-1} in their Dominican amber spectra, the matrix spectra only show a broad, weak band between 1046 cm^{-1} and 1065 cm^{-1} . This band is likely related to $\nu(\text{CC})$ and $\nu(\text{COH})$ stretching (Brody et al., 2001). The bands at 1106 cm^{-1} and 1133 cm^{-1} are attributable to CC bond vibrations, namely $\nu(\text{C-C})$ stretching and $\nu(\text{C-C})$ ring breathing of cyclic terpenoid compounds (Table 3). The broad asymmetric band at 1200 cm^{-1} is the result of two vibrational modes; $\delta(\text{CCH})$ and $\delta(\text{C-O})$, respectively.

The region from 1200 cm^{-1} to 1500 cm^{-1} is dominated by methyl (CH_3) and methylene (CH_2) deformations that are expressed especially by broad and weak bands between 1290 cm^{-1} and 1350 cm^{-1} , and two strong bands at 1360 cm^{-1} and 1410 cm^{-1} . The band at 1244 cm^{-1} represents the *cis* ($\text{HC}=\text{CH}$) symmetric rocking mode (Vandenabeele et al., 2003).

Table 3. Wavenumber (cm⁻¹) and vibrational mode assignments for the Raman spectra obtained from amber, copal and resin. Information on band assignments were collected from Brody et al. (2001) on data of Dominican amber, Mexican and East African copal, and Vandenaabee et al. (2003) on data of Mexican copal. ν = stretching mode, δ = deformation mode, ρ = rocking mode.

Band positions (cm ⁻¹)			Band assignments
Dominican amber	Madagascar copal	Defaunation resin	
1715	1711	1713	?
1662	1663	1664	$\nu(\text{C}=\text{C})$ trans conjugated
1644	1643	1643	$\nu(\text{C}=\text{C})$ non-conjugated
1475	1472	1474	$\delta(\text{CH}_2)$, $\delta(\text{CH}_3)$
1460	1456	1453	$\delta(\text{CH}_2)$, $\delta(\text{CH}_3)$
1438	1440	1441	$\delta(\text{CH}_2)$, $\delta(\text{CH}_3)$ scissors
1408	1410	1408	$\delta(\text{CH}_2)$, $\delta(\text{CH}_3)$
1386	1389	1387	$\delta(\text{CH}_2)$, $\delta(\text{CH}_3)$
1358	1362	1362	$\delta(\text{CH}_2)$, $\delta(\text{CH}_3)$
1331	1327	1330	$\delta(\text{CH}_2)$, $\delta(\text{CH}_3)$
1311			$\delta(\text{CH}_2)$, $\delta(\text{CH}_3)$
1299	1300	1294	$\delta(\text{CH}_2)$, $\delta(\text{CH}_3)$ twisty
1282	1282		$\delta(\text{CH}_2)$, $\delta(\text{CH}_3)$
1243	1244	1243	<i>cis</i> $\rho_s(\text{HC}=\text{CH})$
1202	1201	1200	$\delta(\text{CCH})$, $\delta(\text{C-O})$
1136	1135	1135	$\nu(\text{CC})$ ring breathing
1106	1104	1106	$\nu(\text{CC})$
1066	1064	1057	$\nu(\text{CC})$; $\nu(\text{COH})$
1039	1048	1048	$\nu(\text{CC})$ or $\nu(\text{CO})$
1021	1021	1023	$\nu(\text{CC})$ or $\nu(\text{CO})$
1008	1007	1007	$\nu(\text{CC})$ or $\nu(\text{CO})$
979	980	979	$\rho(\text{CH}_2)$, $\rho(\text{CH}_3)$
937	935	932	$\rho(\text{CH}_2)$
884	886	886	$\rho(\text{CH}_2)$
856	858	858	?
819	823	825	?
744	746	745	$\nu(\text{CC})$ isolated
720			$\nu(\text{CC})$ isolated
696	696	697	?
638	640	639	?
595	601	601	?
525	524	526	?
486	489	488	?
	462	457	?
442	442	445	$\delta(\text{CCO})$
371	372	372	$\delta(\text{CCO})$
329	334	338	?
254	263	265	?

Comparison of matrix spectra

Except for the fingerprint triplet, every band found in the amber sample can be observed in the more recent spectra as well (Fig. 8, Table 3). Notably, while measured under the same conditions, the amber spectrum yielded lower intensity values than the copal and resin samples. This was also observed in previous studies and is interpreted as the result of increasing resin maturation (Winkler et al., 2001).

The copal spectrum differs from that of amber in several major and minor aspects (Fig. 8). Major aspects comprise the higher (I^{1646}/I^{1440}) intensity ratio in the copal spectrum (1.4), and the presence of a doublet in the 700 cm^{-1} to 750 cm^{-1} region instead of a triplet like in the amber spectrum. These major aspects are clearly the result of increasing maturation, as demonstrated by previous studies (Edwards & Farwell, 1996; Brody et al., 2001; Winkler et al., 2001). Minor aspects comprise a band at 600 cm^{-1} in the copal spectrum, which is only weakly developed in the amber spectrum (Fig. 8). Although this band has been noted previously (Brody et al., 2001), it was not possible to assign it to certain vibrational modes. Other minor differences comprise the 823 cm^{-1} band position, the weak shoulders at 885 cm^{-1} , 934 cm^{-1} , and 1294 cm^{-1} , and additional weak bands at 1008 cm^{-1} and 1022 cm^{-1} in the copal spectrum. It can be assumed, that these small differences stem from the varying degrees of maturation between the copal and amber. For example, shoulders in the copal spectrum are separated into single bands in the amber spectrum, which argues for a structural separation of specific compounds over time. Strikingly, the Raman spectra of the modern resin and copal show no significant differences, as the same Raman bands can be found in both spectra (Fig. 8). Furthermore, the I^{1646}/I^{1440} ratio of 1.2 in the extant resin is close to the ratio for the copal sample, indicating the same degree of maturation. At this point, it is not possible to distinguish between these two materials with regard to Raman spectroscopy. However, the distinction between amber and the younger copal and resin was carried out successfully.

Tissue section

In addition to their surrounding matrix, two platypodid beetles (“pin hole borers”) from the previously analysed Madagascar copal and resin were also examined via Raman spectroscopy. The cuticle of the head region was removed via grinding to allow sampling of the underlying tissue (Fig. 9).

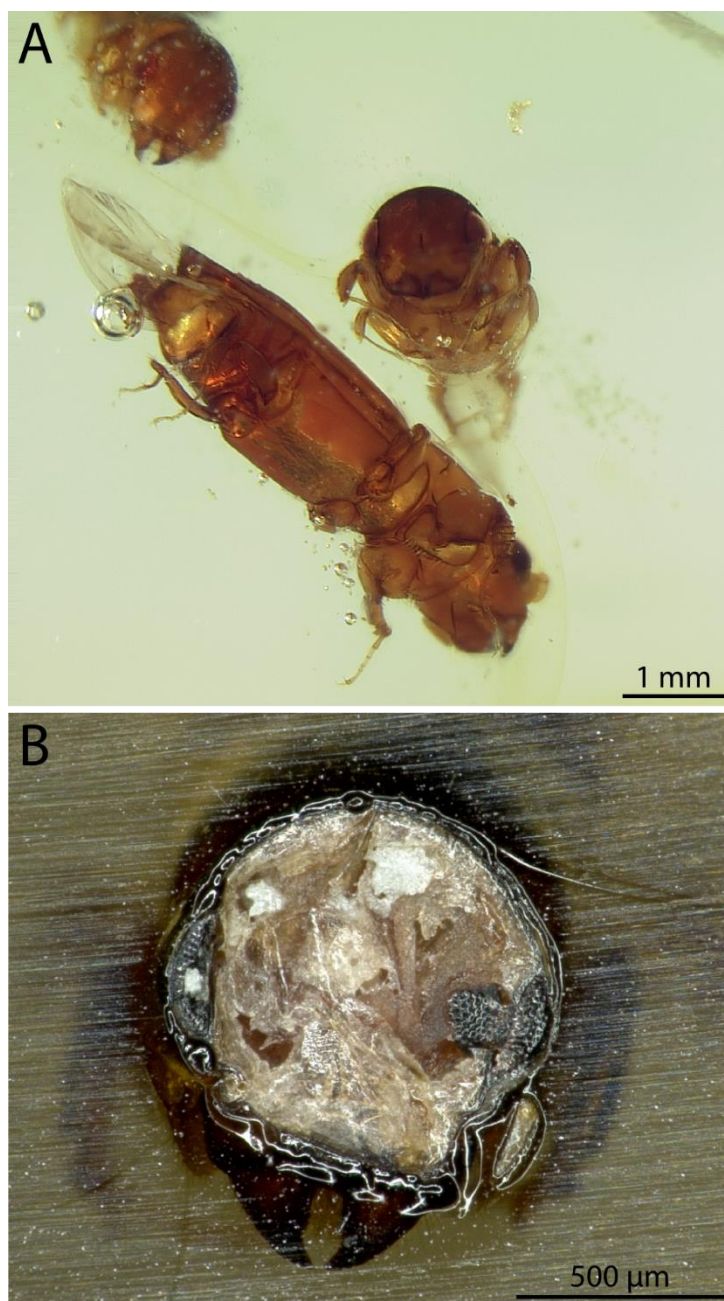


Figure 9. Platypodid beetles in Madagascar copal and Defaunation resin. (A) Surface ground copal and resin pieces contain abundant platypodid beetle individuals. (B) Ground specimen. The internal tissues of the head capsule are nicely preserved.

The collected Raman spectra of the beetle tissues from Madagascar copal and modern resin show prominent, sharp bands at 621 cm^{-1} , 1002 cm^{-1} , and 1031 cm^{-1} (Fig. 10). Another sharp but smaller band can be recognised at 1585 cm^{-1} . Low intensity bands are located at 798 cm^{-1} , 1156 cm^{-1} , 1183 cm^{-1} , 1201 cm^{-1} , 1329 cm^{-1} , and 1450 cm^{-1} , and in the region between 1280 cm^{-1} and 1400 cm^{-1} .

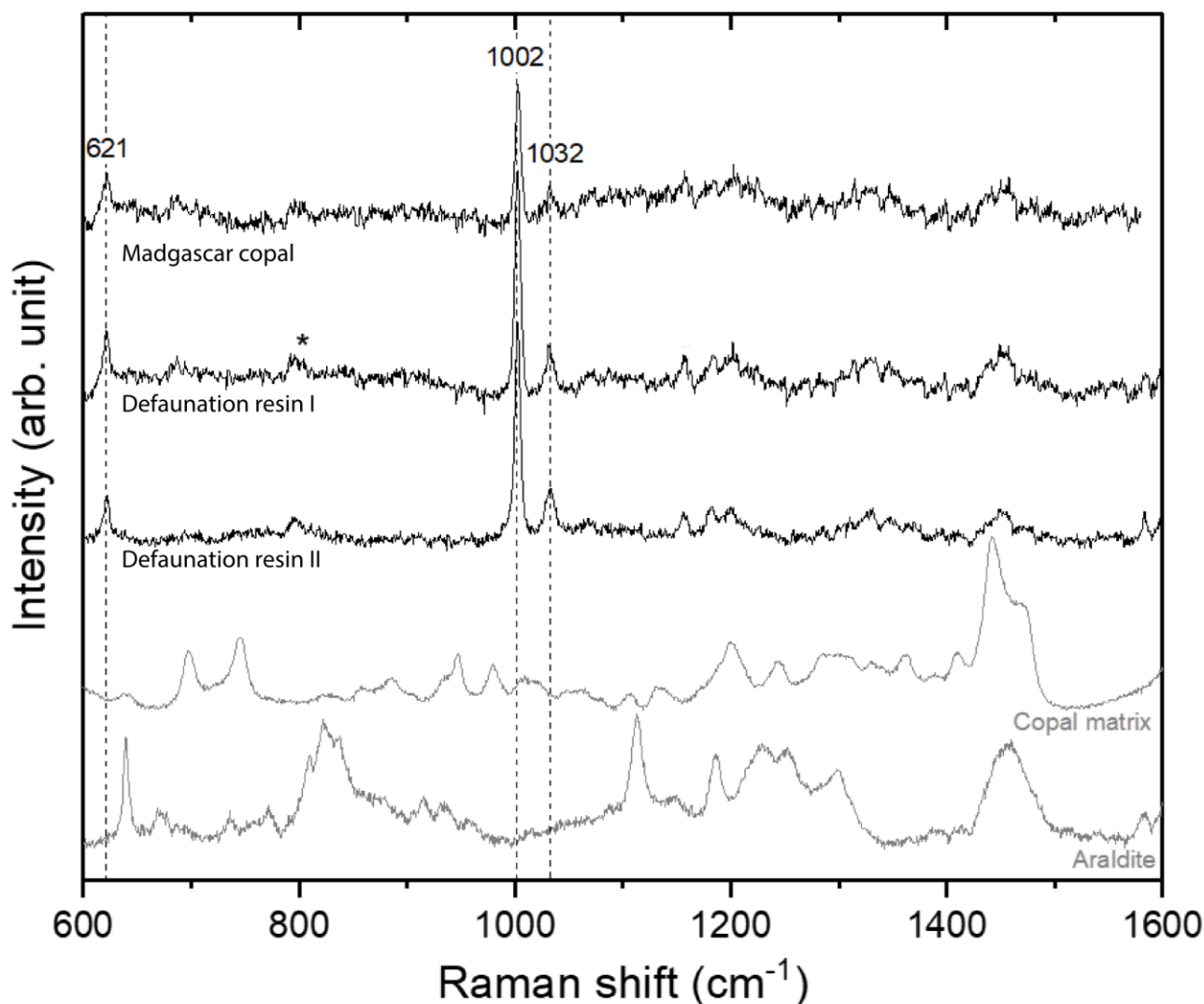


Figure 10. The upper three Raman spectra show band positions in beetle tissue from Madagascar copal and Defaunation resin. The two gray spectra at the bottom belong to materials that might interfere with signals in the tissue spectra. The tissue spectra clearly show sharp bands that are assigned to phenylalanine. These bands do not derive from araldite (epoxy resin) or the matrix of the surrounding copal and argue for the authenticity of the band intensities. * = unassigned band position. Defaunation resin I and II refer to different samples of the same material. See text for further information.

The intense bands at 621 cm^{-1} (phenyl ring breathing mode), 1002 cm^{-1} (phenyl ring angular bending), 1032 cm^{-1} (phenyl ring CC stretching and bending), and 1585 cm^{-1} (phenyl ring bond-stretching vibrations) can be clearly assigned to various vibrational modes of the phenyl ring structure in the side chain of the amino acid phenylalanine (Table 4; Fischer & Eysel, 1992; Hernández et al., 2013). Another band at 1201 cm^{-1} is likely attributed to additional $\nu(\text{CC})$ vibrations in the phenyl ring (Hernández et al., 2013) and points additionally towards the presence of phenylalanine in the samples. These five band positions (plus another one that was out of measuring range) are called the characteristic Raman lines (F1-F6) of phenylalanine and are present in free amino acids as well as in long-chain peptides such as somatostatin and bovine serum (Hernández et al., 2013). Weaker bands providing additional information on the side chain are located at 1156 cm^{-1} and 1329 cm^{-1} by $\delta(\text{CCH})$ deformation and $\rho(\text{CH}_2)$ rocking modes (Table 4). The 1329 cm^{-1} is not present in the tissue from the resin sample, but this is likely due to background noise. The weak band at 1450 cm^{-1} possibly derives from $\delta(\text{NH}_3)$ deformation, but it may be also the result of a mixed spectrum with resin signals, namely $\delta(\text{CH}_2)$ and $\delta(\text{CH}_3)$ deformations. For the smaller bands at 798 cm^{-1} and 1183 cm^{-1} , a clear assignment cannot be provided, but at least the latter appears in typical phenylalanine spectra (De Gelder et al., 2007). This band is also not present in the resin sample spectra, which again might be caused by high background noise. Overall, no significant spectral differences are present in the tissue spectra regardless of their proposed age.

Table 4. Band positions and their assignments of the beetle tissue spectra from Madagascar copal and Defaunation resin. Band assignments were made according to De Gelder et al. (2007), Edwards et al. (2007), and Hernández et al. (2013). F1 Raman line is out of measuring range. ν = stretching mode, δ = deformation mode, ρ = rocking mode.

Band positions (cm ⁻¹)		Band assignments
beetle tissue A (Madagascar copal)	beetle tissue B (Defaunation resin)	
1585	1585	$\nu(\text{CC})$ phenyl ring; F2 Raman line
1457	1457	?; possibly $\delta(\text{CH}_2)$ and $\delta(\text{CH}_3)$ of the matrix
1440 - 1449	1438 - 1451	$\delta(\text{NH}_3^+)$; $\rho(\text{NH}_3^+)$; or matrix $\delta(\text{CH}_2)$ and $\delta(\text{CH}_3)$ scissors
1326		$\rho(\text{CH}_2)$; $\delta(\text{CCH})$
1201	1205	$\nu(\text{CC})$ sidechain coupled with $\nu(\text{CC})$ in-phase motions; F3 Raman line
1183		phenylalanine, unassigned; $\delta(\text{CCH})$ bending
1156	1157	$\delta(\text{CCH})$ bending
1031	1031	$\nu(\text{CC})$ in-phase motion coupled with $\delta(\text{CCH})$ in-phase motions in the phenyl ring; F4 Raman line
1002	1003	phenyl ring $\delta(\text{CCC})$ angular bending vibrations; F5 Raman line
798	803	?
621	622	phenyl ring breathing; F6 Raman line

Discussion

Remarkably, no structural changes are present between the copal and extant resin spectra (Fig. 10). In addition, the I^{1464}/I^{1450} ratios of 1.2 and 1.4 (typical for modern resins, see Brody et al., 2001) are almost same for both samples. The tissue spectra look alike as well and without prior knowledge, it is not possible to assign a single spectrum to its original material. In consequence, it can be argued that copal and resin samples from Madagascar are synonymous and represent the same material, in this case Defaunation resin *sensu* Solórzano-Kraemer et al. (2020). This is in accordance with previous radiocarbon data that suggested a maximum age of 50 years for copal from East Africa (Burleigh & Whalley, 1983). Unfortunately, while preparing the original manuscript of this subproject, the fact that ‘Madagascar copal’ does not represent a subfossil resin but rather modern Defaunation resin has been published by Delclòs et al. (2020). In any case, even though it is not possible to track down diagenetic changes over longer time spans from modern to subfossil to fossil *Hymenaea* resins in a stepwise approach, Defaunation resin

from Madagascar can still provide crucial insights into processes that take place in an early diagenetic stage of amber formation.

While measuring the beetle tissue, it was notable that the material appeared heterogenic and that in many cases the spectra were of poor quality and not suited for a deeper analysis. However, when suited measuring points were found, the collected spectra expressed five band positions (621 cm^{-1} , 1002 cm^{-1} , 1032 cm^{-1} , 1201 cm^{-1} , 1585 cm^{-1}) characteristic of phenylalanine (Hernández et al., 2013).

The observed spectral features of phenylalanine are not shared by other aromatic amino acids, namely tryptophan, tyrosine, and histidine (De Gelder et al., 2007; Freire et al., 2017); these amino acids can be excluded as a possible source of misinterpretation. An online comparison with the Bio-Rad KnowItAll[®] spectral database software yielded two phenolic compounds (*N*-Benzylethylenediamine and Diphenylborinic acid) that show similarities at the 621 cm^{-1} , 1002 cm^{-1} , 1032 cm^{-1} , and 1585 cm^{-1} band positions with the tissue spectra but deviate slightly in other spectral regions (Appendix 9.2). In modern bone tissue, the high intensity bands at $\sim 1002\text{ cm}^{-1}$ and $\sim 1032\text{ cm}^{-1}$ can be detected, but no other distinctive features of amino acids are present (Barthel et al., 2020). These observations show that the intensities at $\sim 621\text{ cm}^{-1}$, $\sim 1002\text{ cm}^{-1}$, $\sim 1030\text{ cm}^{-1}$, and $\sim 1585\text{ cm}^{-1}$ have excellent Raman scattering properties but are rather characteristic for the phenyl ring structure, instead of phenylalanine as supposed by Hernández et al. (2013). In any case, the complete spectral information argues for the presence of phenylalanine in the beetle tissues and show that these signals do not derive from the matrix or preparation material (Fig. 10).

According to Hernández et al. (2013), bands associated with vibrational modes of nitrogen bonds should be present at 856 cm^{-1} , 1068 cm^{-1} , 1360 cm^{-1} , and 1446 cm^{-1} . Only the latter can be observed in the tissue spectra (Fig. 10). Raman spectra of proteins and tissues are complex due to the large diversity of compounds and the bonds they are composed of, leading in some cases to overlapping signals and complex interactions. The measurements were carried out with a 633 nm laser in all cases for consistency and to enhance comparability between resin and tissue spectra. A laser of a different excitation energy might have resulted in optimised tissue spectra that reveal additional low intensity bands.

Interestingly, a Raman spectrum of an insect inclusion from Miocene Mexican amber presents similar spectral features to the ones of the beetle tissues (Edwards et al., 2007): the prominent band intensities at $\sim 1002\text{ cm}^{-1}$ and $\sim 1030\text{ cm}^{-1}$ can be clearly identified. Additional band assignments (such as the probable phenyl ring breathing mode at 621 cm^{-1}) are difficult due to the incomplete data description. The band positions point towards the presence of phenolic compounds in this sample (Edwards et al., 2007), but it remains unclear whether these signals represent original phenylalanine. Several amino acids (including phenylalanine) have been extracted from much older material (chapter 5.4) which supports the possibility that the measured spectral features can be assigned to unaltered phenylalanine.

Except for phenylalanine, no additional amino acids could be evidenced via Raman spectroscopy in beetles from Defaunation resin, even though the age of the samples does not prohibit their presence. It is possible that additional amino acids are present in these samples, but simply not detected in the Raman spectra due to the chosen experimental settings. An excitation laser in the ultraviolet region might be suited to detect band positions of amino acids that do have lower Raman scattering characteristics. In addition, the samples were irradiated with a maximum laser power of 50%, which means that phenylalanine, as a good Raman scattering material, yields much higher intensities when compared to other amino acids. It may be possible that the phenolic signal can be used as an indicator of amino acids preservation in materials of different ages due to its high Raman scattering capacity, but this matter needs to be addressed by future experiments.

5.2.2 Raman spectroscopy of collection material

During the screening of amber material from the scientific collection of the Goldfuß-Museum (University Bonn), several inclusions exhibited whitish fillings of the body cavity (e.g. Fig. 11). In order to characterise the physical and chemical characteristics of these infillings, Raman spectroscopic measurements were performed on three samples of Dominican (Do38; Do67) and Baltic amber (Ba102). In all of these cases, the inclusions are located partially at the surface of the amber matrix and are not completely surrounded by resin.

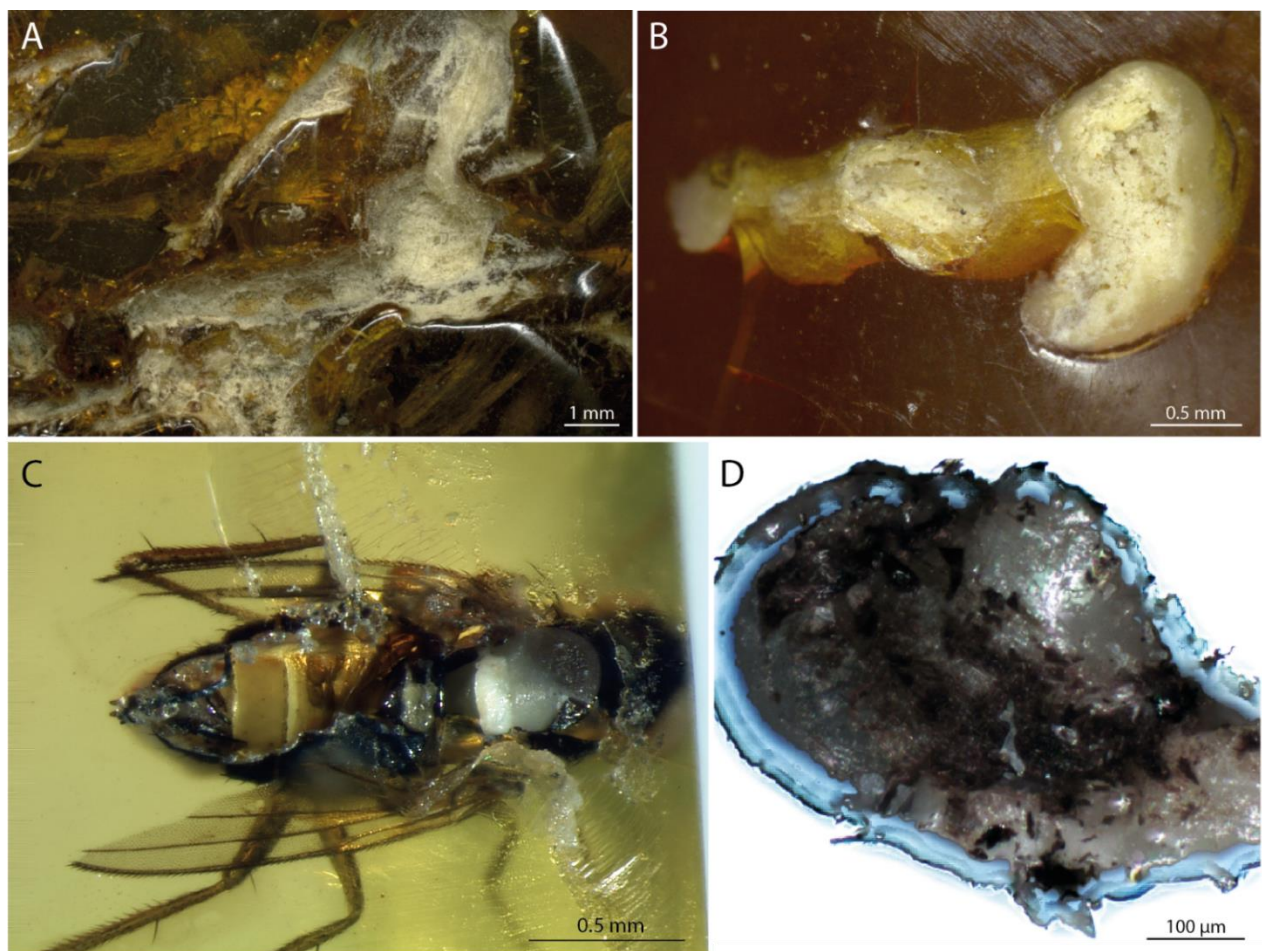


Figure 11. Samples examined by Raman spectroscopy. (A) Plant fragments in a Baltic amber piece (Ba102) that are exposed to the surface and filled with whitish material. (B) An inclusion of unknown origin from Dominican amber (Do67). In the right part of the inclusion, aggregates of the filling material can be recognized, implying a mineral structure. (C) A fly in Dominican amber (Do38). Both the thorax and abdomen are exposed, but only the former is filled. (D) Detailed image of the thoracic tissue seen in C after extraction with a scalpel.

Results & Discussion

The Raman spectrum of Ba102 shows three distinct bands at 128 cm^{-1} , 207 cm^{-1} , and 466 cm^{-1} that characterise this material as being composed of quartz (Fig. 12). The prominent band at 466 cm^{-1} is assigned to oxygen breathing modes (stretching) whereas the weaker bands represent rotational modes of the SiO_4 tetrahedron (Fig. 12).

In contrast, the Raman spectrum of the filling of Do67 (Fig. 12) contains three distinct bands at 154 cm^{-1} , 281 cm^{-1} , and 1085 cm^{-1} . The band at 1085 cm^{-1} represents the fully symmetric $\nu(\text{CO}_3)$ stretching which - accompanied by lattice modes (154 cm^{-1} and 281 cm^{-1}) - identifies this material as well-ordered calcite (Wang et al., 2012). In consequence, the whitish fillings of Ba102 and Do67 can be assigned to different mineral phases (Fig. 12). A comparison with the RRUFF Database (Fig. 12; Lafuente et al., 2015) validates this observation.

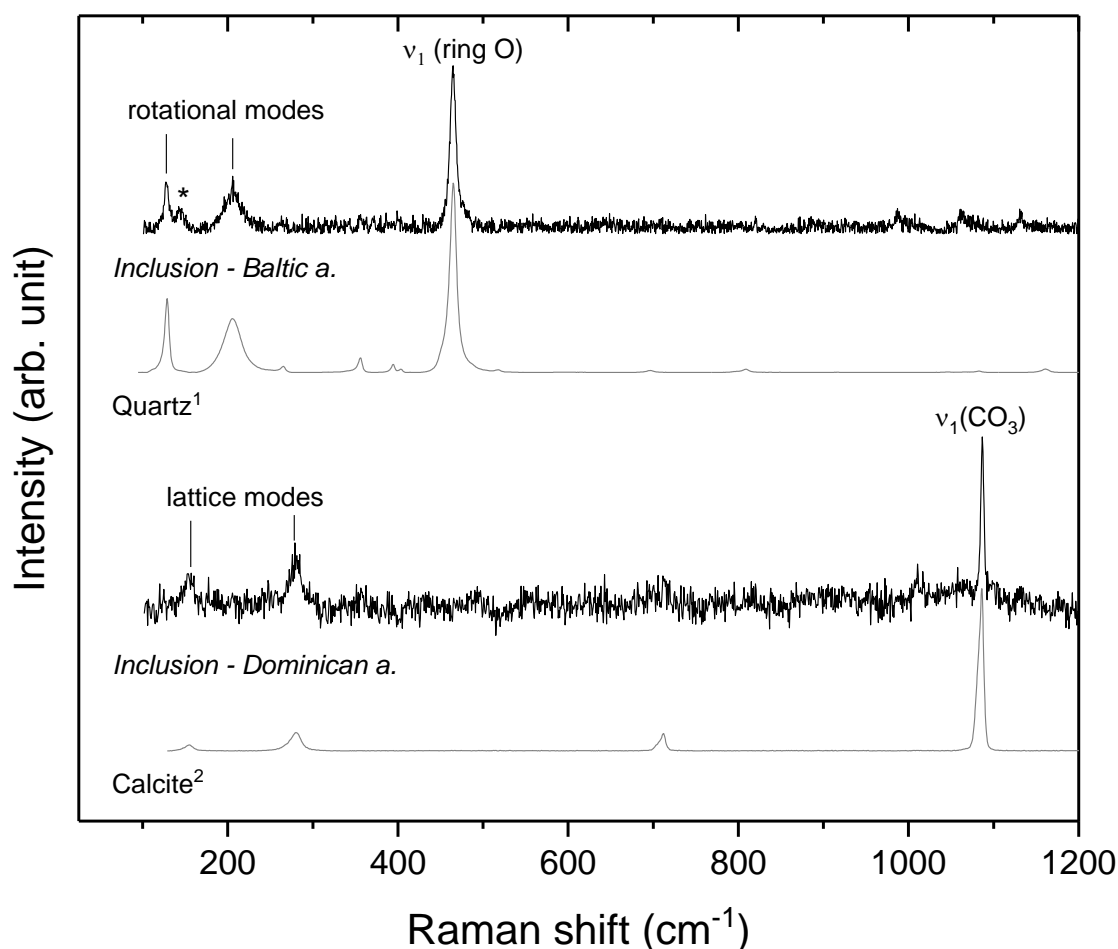


Figure 12. Raman spectra of whitish infillings of amber inclusions. The bold black spectra represent the measured samples, whereas the light grey spectra were adopted from the RRUFF Raman spectral database (Lafuente et al., 2015). The spectrum at the top was acquired from plant fragments in Baltic amber (Ba102) and represents characteristic vibrational modes of quartz. The bottom spectrum stems from an unidentified Dominican amber inclusion (Do67) and shows that the material consists of well-ordered calcite. * = unassigned band position.

The presence of mineral phases is of particular interest with respect to the permeability of amber. Previous studies (e.g. McCoy et al., 2018a) and the research performed in this thesis show that many fossils from different amber deposits are empty inside. For these empty inclusions, the idea that mineral phases precipitated in the body cavity can be excluded. Mineral phases are easily distinguished (although not specifically identified) in tomographic slices because of their high density compared to the amber matrix and organismal remains. Such mineral phases were only evident in a few samples of Zhangpu amber fossils when analysed with synchrotron radiation whereas all other bioinclusions were either empty inside or contained internal tissues (chapter 5.3). Therefore, it can be argued that amber has excellent water repelling characteristics as long as the integrity of the material is intact and not compromised by (micro-)fissures. This is also indicated by the presence of fluorine in a Dominican amber lizard (Barthel et al., 2020; chapter 5.6). Amber inclusions with mineral fillings must be the result of physical diagenetic stress that caused fracturing of the material and allowed ion rich fluids (e.g. groundwater) to interact with the fossil remains. The timing of this process may vary from sample to sample and could be of either early or late diagenetic origin.

Apart from mineral phases, organic phases may also be present in the body cavities of inclusions. The whitish filling in the thoracic region of Do38 (Fig. 12) was extracted with a scalpel and analysed with Raman spectroscopy. Its spectral features clearly indicate the material as being Dominican amber. The different colours of the amber inside and outside of the body cavity argue for a second resin flow that diffused into the thoracic region after the inclusion was located on the resin surface for an uncertain amount of time. However, this process likely happened in an early diagenetic stage before transportation took place, but after the hardening of the initial flow. The filling appears to replicate the original body compartments of Do38, which implies that remains of the segmental membranes were still present at the time that the specimen made contact with a subsequent resin flow.

Fragments of the cuticle adhered to the extracted amber filling and were analysed with Raman spectroscopy as well. The spectra point to the presence of unorganised, aliphatic carbon which is in accordance with mass spectrometric analyses by Stankiewicz et al. (1998) that showed only the preservation of straight chained hydrocarbons in fossils from Dominican amber. The absence of macromolecules and their degradation products in damaged (Do38) and undamaged (Stankiewicz et al., 1998) Dominican amber insects show that this deposit comprises unfavourable conditions with respect to biomolecular preservation.

5.3 Synchrotron examination of Zhangpu amber inclusions

Introduction

The preservation of amber inclusions varies widely between deposits and between samples from the same location (Grimaldi et al., 1994; McCoy et al., 2018a; Barthel et al., 2021). Initial tomographic studies on the distribution and occurrence of internal tissue preservation show that lots of inclusions represent empty molds with just cuticle preservation (Lak et al., 2008; McCoy et al., 2018a). The occurrence of internal tissues in inclusions across various class I amber sources ranged between 0% in Charentes amber to 95 % in Dominican amber for sample sizes of over ten (McCoy et al., 2018a). To gain a deeper insight into the overall frequency of internal tissue preservation in amber, an analysis of class II inclusions would be helpful. Within this thesis, 149 inclusions of class II Miocene Zhangpu amber were analysed via synchrotron X-ray microtomography (SR- μ CT) at the Karlsruhe Institute of Technology (KIT).

Even though the synchrotron experiments are in the early stages, they represent the largest database of tomographic data of class II amber inclusions. To assess the frequency and abundance of internal tissue preservation in Zhangpu amber, image stacks of the fossils have been compared to a modern wasp (*Nasonia vitripennis*) that was fixated in 100% ethanol and analysed under the same conditions. Each individual image stack of a sample was examined manually for the presence of various tissues.

Results & Discussion

The tomographic images of the modern *Nasonia vitripennis* clearly show the preservation of the cuticle and different kinds of soft tissues in the head, thoracic and abdominal region (Fig. 13). These include muscle bundles, the cerebral ganglia and digestive tissues.

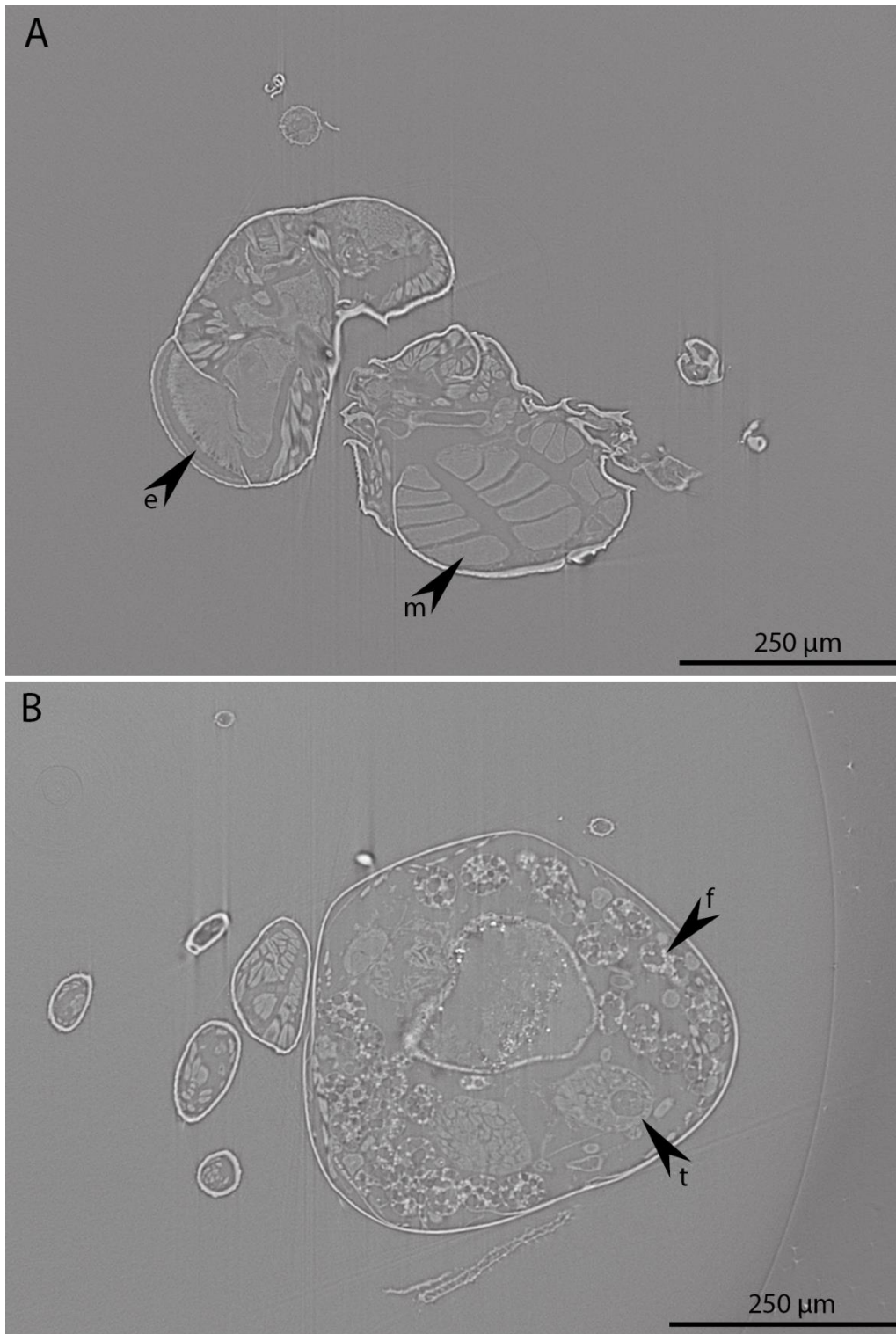


Figure 13. Synchrotron scans of an extant *Nasonia vitripennis* (Hymenoptera: Chalcidoidea). (A) Head capsule and thorax with internal tissues. Within the head capsule, the cerebral ganglia, optic neuropils, and ommatidia can be identified. Several muscle pads that belong to the flight-muscle complex are present in the thorax. (B) The abdominal region contains extensive internal tissues as well. Here, the most prominent structures are the testicles, and the fat body. e = eye apparatus, f = fat body, t = testicle, m = muscle tissue.

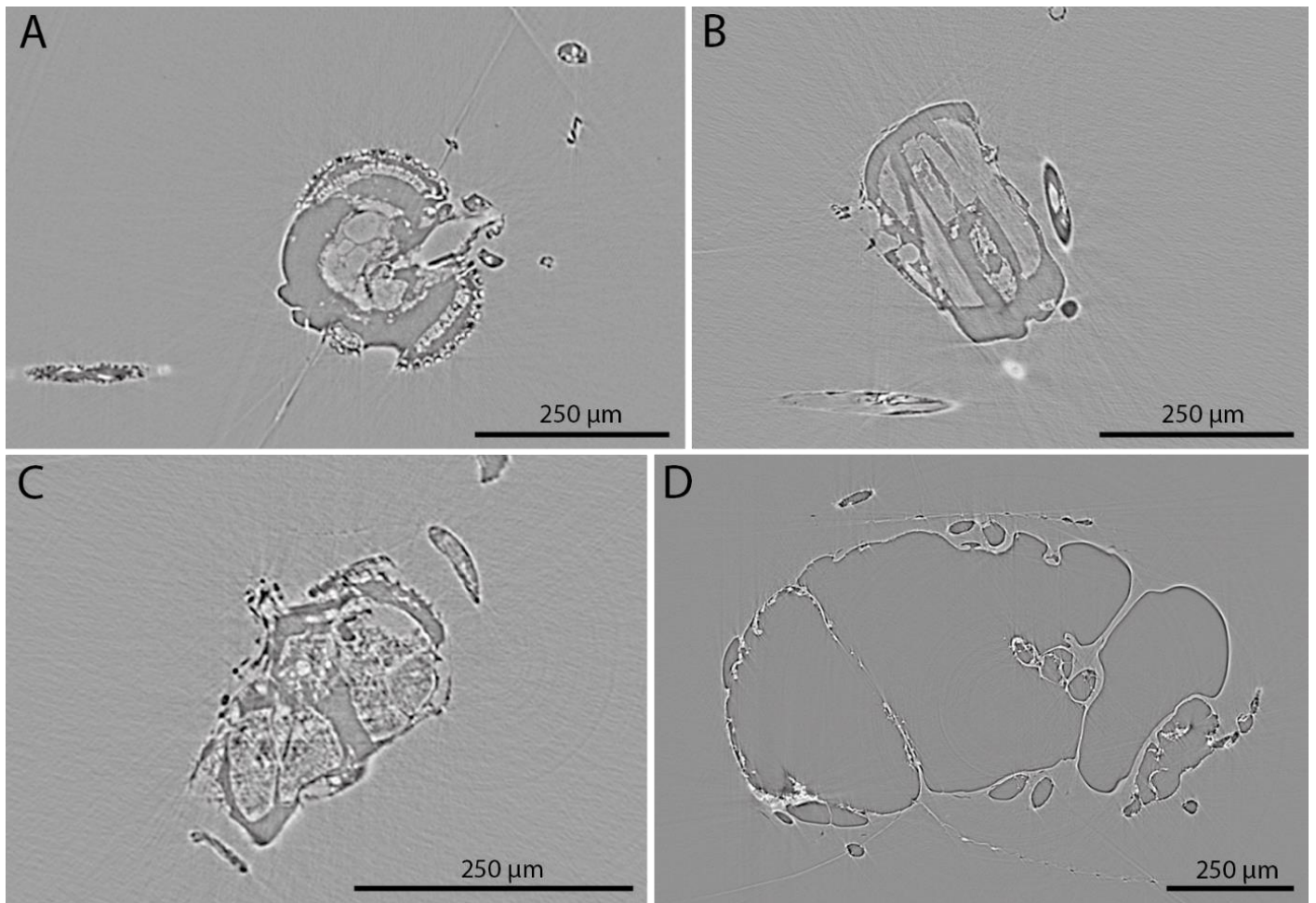


Figure 14. Synchrotron images of Zhangpu amber samples of PC A (A, B, C) and PC E (D). (A) Head capsule with preserved cerebral ganglia, eye lenses and ommatidia. Various other tissues of unknown origin are present as well. (B) Thoracic part of a dipteran with prominently developed flight muscles. (C) Abdominal region of the same sample as in B with various tissues. (D) A fungus-gnat of PC E in lateral view. The fossil does not contain internal tissues in any body part.

The Zhangpu amber inclusions show different degrees of preservation (Fig. 14) and are categorised into five different preservation classes (PCs) based on their abundance and occurrence of internal tissues (Table 5). It must be emphasised that the respiratory system could not be clearly assessed with this method, which is why it does not contribute to the categorisation of the preservation classes. Although it would be possible to recognise respiratory structures (and other tissues) under higher magnifications, this experimental setup was designed for a high sample throughput in order to screen the samples rather than generating images of extraordinary resolution. For the same reason, distinguishing between different tissues in the abdominal region was difficult in most cases (preservation class B-E). Therefore, these structures are summarised as “abdominal” tissues unless specific structures can be identified.

Table 5: Preservation classes (PCs) of Zhangpu amber inclusions. The PCs A-E represent the framework for the assessment of internal tissue preservation in Zhangpu amber and are distinguishable by their grade of tissue preservation in different body parts of analysed arthropods. See text for further information.

preservation classes of Zhangpu amber inclusions		
preservation classes	count (n = 149)	grade of tissue preservation in head, thorax and abdomen
A	33 (22.2%)	identifiable tissues in all three body parts (preservation of sensory tissue, muscles, and digestive tissue)
B	51 (34.2%)	identifiable tissue in two of three body parts
C	21 (14.1%)	identifiable tissue in one of three body parts (preservation of sensory tissue or muscles, and unidentified tissue)
D	29 (19.5%)	preservation of unidentified tissue in any body part
E	15 (10.1%)	only cuticle preservation, no tissues present

Inclusions in PC A show the highest (“best”) degree of tissue preservation (Table 5). These inclusions exhibit internal structures in every major body segment (head capsule, thorax, abdomen) that furthermore can be assigned to specific structures. For example, in the head capsule, the brain and the compound eye with preserved optic neuropils are present (Fig. 14). In the thorax, the flight muscles can be identified, more specifically the dorsal longitudinal muscles and the dorso-ventral muscles of the metathorax and mesothorax (Fig. 14). In the abdomen of PC A inclusions, the midgut and/or hindgut can be recognised.

PC B inclusions are characterised by the preservation of distinguishable internal tissues in the head capsule and thorax, but structures in the abdomen cannot be assigned to specific tissues (Table 5). When inclusions only exhibited either nervous tissue in the head or muscle tissue in the thorax and unidentified structures in any other body part, they were categorised into PC C (Table 5). Inclusions of PC D show the preservation of only unidentified structures in any single or multiple body parts (Table 5). Some inclusions revealed no internal structures at all, in which case, they were categorised as PC E (Fig. 14, Table 5). Due to the fact that some structures and tissues are better distinguishable (muscle tissue, brain) than the ones of the abdomen, the categorisation of the data is biased. Inclusions of PC B, C, or D may rank higher if abdominal tissues could be identified properly.

For syninclusions, it could be observed that the PC of the individual fossils may deviate within the same amber piece. Another remarkable observation is the small amount of only 15 (10%) inclusions without any internal tissues (Table 6).

Table 6. Frequency of internal tissue preservation in Zhangpu amber inclusions in total and of different preservation classes (PCs). See text for further information.

total frequency of tissue preservation (n = 149)	
samples (A-C) with muscular preservation	97 (65%)
samples (A-C) with sensory tissue	86 (58%)
samples (A-C) with digestive tissue	39 (26%)
samples (A-D) with any kind of tissue	134 (90%)
samples (E) without any internal tissue	15 (10%)

PC A: frequency of tissue preservation (n = 33)	
samples with muscular preservation	33 (100%)
samples with sensory tissue	33 (100%)
samples with digestive tissue	33 (100%)

PC B: frequency of tissue preservation (n = 51)	
samples with muscular preservation	50 (98%)
samples with sensory tissue	46 (90%)
samples with digestive tissue	6 (12%)

PC C: frequency of tissue preservation (n = 21)	
samples with muscular preservation	14 (67%)
samples with sensory tissue	7 (33%)
samples with digestive tissue	0 (0%)

In a comparable study, McCoy et al. (2018a) analysed the occurrence of internal tissue preservation in various class I ambers based on micro-CT, synchrotron, and light microscopy data in the scientific literature. For each deposit where more than ten samples could be analysed, McCoy et al. (2018a) showed that Dominican amber yields the highest frequency of internal tissue preservation. The high value of 90% of Zhangpu amber inclusions containing internal tissues comes close to the 94% published for Dominican amber samples (McCoy et al., 2018b). The non-volatile fraction of the original resin differs largely among these deposits which indicates that as long as it forms a physical barrier, its specific composition is not an important factor in terms of fossilisation.

Further, the data of McCoy et al. (2018a) and the ones presented herein imply that the preservation potential of internal structures cannot be solely explained by resin chemistry and that other factors must have a strong impact as well.

In the Zhangpu material, the frequency of preservation varies between tissue types (Table 6): for the whole data set, muscle tissue is most commonly preserved (65% of inclusions), closely

followed by nervous tissue (58% of inclusions). Digestive tissue could be identified in only 26% of all inclusions. The same pattern of decreasing preservation from muscles, to sensory to digestive tissue can be observed in PC B and C as well (Table 6). In PC B, 98% of inclusions exhibit muscular tissue, whereas sensory tissue can be detected in 90%, and digestive tissue in 12%. Interestingly, of the 51 inclusions in PC B, 45 (88%) showed identifiable tissue in the head capsule and thorax. Five of these inclusions (10%) revealed tissue in the thorax and abdomen, and only one sample (2%) contained tissue in the head capsule and abdomen. In PC C, 67% of the samples revealed muscular tissue, 33% sensory, and 0% digestive tissue (Table 6).

These observations implicate that the preservation potential is not randomly distributed between tissues and body parts. For sensory tissue, the cerebral ganglia (brain) and the optic neuropils are most commonly preserved. It was not possible to assess the preservation of the thoracic ganglia and the nerve chord. Therefore, information on sensory tissue preservation is limited to occurrences in the head capsule.

The vast majority of analysed Zhangpu amber inclusions consists of diptera, of which modern relatives possess well developed flight muscles. Accordingly, the most commonly preserved muscle tissues are the dorsal longitudinal and the dorso-ventral flight muscles in the thoracic region of inclusions in PC A, B, and C (Table 7). Even in PC A, only a small number of inclusions showed muscle tissue in the legs (15%), head capsule (6%), and antennae (6%), and the same trend can be observed in PC B and C (Table 7).

Table 7. Detailed examination of the frequency and locality of muscle tissue preservation in Zhanpugu amber inclusions of PCs A-C. See text for further information.

PC A: distribution of muscle tissue preservation (n = 33)	
location of preserved muscle tissue	number of samples (total/percent)
thorax	33 (100%)
legs	5 (15%)
head capsule	2 (6%)
antennae	2 (6%)

PC B: distribution of muscle tissue preservation (n = 50)	
location of preserved muscle tissue	number of samples (total/percent)
thorax	49 (98%)
legs	2 (4%)
head capsule	5 (10%)
antennae	0 (0%)

PC C: distribution of muscle tissue preservation (n = 14)	
location of preserved muscle tissue	number of samples (total/percent)
thorax	14 (100%)
legs	0 (0%)
head capsule	0 (0%)
antennae	0 (0%)

The chance of muscle preservation appears to be coupled to the size of the original tissue: larger structures have better chances to be identified in tomographic scans and in addition, these larger structures may decay to parts that are still more clearly visible than originally smaller tissues. In consequence, the location and frequency of muscle preservation is biased towards the behaviour and nutrition of the entrapped organism. In the head capsule of chewing insects, strongly developed muscles are associated with movements of the mandibles. Diptera commonly have a piercing-sucking type of food uptake and therefore do not possess a strongly developed musculature in their head capsule, which explains the rare occurrences of muscle preservation in this body part. The same conclusion can be drawn for the leg musculature that only plays a minor role in dipteran lifestyles compared to fossorial, jumping, or cursorial insects.

As mentioned before, the occurrence of tissues in the abdomen could not be assessed in the same way as tissues in the head capsule or thoracic region. In some cases, the mid and hindgut were observable, but other structures could not be identified. The overall loss of abdominal tissues becomes apparent when comparing the fossil tomographs to those of the modern wasp *Nasonia vitripennis* (Fig. 13 & 14).

The rare preservation of abdominal tissues in the Zhangpu amber inclusions may be the result of bacterial decomposition and autolysis processes that take place after the insect has been trapped in resin. Autolysis is caused by enzymes that remain in the body cavity and react with various tissues even after the death of the organism. Bacterial decomposition, as the main factor of organic material decomposition, is suggested to be strongly inhibited for resin embedded arthropods due to the antibacterial properties of several resin compounds (e.g. McCoy et al., 2018b). Therefore, autolysis may be the main factor to influence the degradation of original tissues in amber fossils and is suited to explain the observed pattern of preservation: it is most evident in digestive tissues, which are concentrated in the abdomen, whereas the head capsule and thorax are not that heavily affected.

Another explanation for the observed pattern of tissue preservation derives from the tracheal system of insects. Experiments with dieldrin ($C_{12}H_8Cl_6O$) - a contact insecticide that acts on the insects' ganglia - showed that after exposure, the insecticide accumulates in the integument probably at the endocuticle-hypodermis region where it is transported laterally through the insect's body (Gerolt, 1969). Instead of a direct diffusion into the haemolymph, dieldrin reaches its site of action along the tracheal system, which branches within integument (Gerolt, 1969). The path of dieldrin uptake is likely the same as for volatile resin compounds and explains the pattern of tissue preservation observed in Zhangpu amber fossils. Tissues that are extensively supplied with oxygen by tracheoles might therefore be better preserved than others. In case of diptera, these comprise the nervous system and flight muscles. When applied as a dry deposit to housefly larvae, ^{14}C -dieldrin showed an increasing concentration with the length of exposure in audioradiograms of tracheal remains whereas Malpighian tubes, fat body, and haemolymph gave no detectable image (Gerolt, 1969). This mode of infiltration contrasts the model of Grimaldi et al. (1994) who suggested that volatile resin compounds directly diffuse into the tissue through the integument, probably at the intersegmental membranes.

The fate of tissue preservation in amber inclusions is also coupled to the occurrence of fissures and micro cracks in the hardened resin. Resin within the fossils was only found in some heavily degraded remains that must have been laying on a hardened resin surface before getting enclosed by a subsequent resin flow. While crosschecking inclusions of PC A and E via light microscopy it became evident that micro cracks run through several fossils. In addition, body parts, especially the wings and legs, may extend to the edge of the amber piece, where they are in direct contact with air. Cracks and exposed body parts represent favoured pathways for fluid phases and microbial influx, both of which lead to tissue degradation. Because both conditions

– resin cracks and exposed appendages – are observed in PC A and E inclusions, it is hypothesised that their timely occurrence is crucial for the extent of tissue preservation. Cracks in PC E inclusions are interpreted as being of early diagenetic origin, whereas the cracks in PC A inclusions formed during the late diagenesis, in some cases even after excavation as indicated by their degree of tissue preservation which should be better in freshly damaged samples (PC A). The same is expected for the occurrence of exposed appendages that can be caused by friction during transportation processes or may derive from preparation handling of the piece.

In summary, the majority of Zhangpu amber inclusions (90%) contain internal tissues, which is close to the value of 94% recorded in Dominican amber from a much lower sample size (McCoy et al., 2018a). The extremely good preservation of Zhangpu amber inclusions is not only caused by the presence of biologically active mono-, sesqui-, and triterpenoids in the resin matrix, but is also due to favourable diagenetic conditions. The overall degree of tissue preservation in amber is linked (in addition to previously reported factors) to the organisation of the tracheal system, the behaviour of the embedded arthropod, and also to the physical integrity of the hardened resin. Autolysis appears to be the main factor in terms of tissue degradation in amber. However, the complex interactions between these observations need to be addressed in the future as well as the identification of “favourable” diagenetic conditions in terms of soft tissue preservation in amber.

5.4 Amino acid racemization in class II ambers

5.4.1 Introduction: fossil amino acids & proteins in the rock record

In contrast to the instinctive expectation that amino acids are highly labile, several studies report on amino acid and protein preservation in the fossil record from various environments and taxonomic groups. This chapter briefly summarises reports of amino acid and protein preservation in the sedimentary rock record (i.e., not in amber); amino acids and proteins in amber are described in detail in the following chapter. In the years since the first extraction of amino acids from fossils in 1954 (Abelson, 1954), this procedure has become more common and was particularly and recently improved with the development of new analytical tools. For example, Manning et al. (2009) examined a mummified hadrosaur from Hell Creek Formation with FTIR and carried out amino acid analyses of the skin. FTIR revealed the presence of amide groups in the ungual phalanx, but the unusual racemisation of some amino acids might indicate contamination by modern bacteria. In a mosasaur bone from the Maastrichtian Ciply-Malogne Phosphatic Chalk Formation of Belgium, the most abundant amino acids were aspartic acid, serine, glutamic acid, glycine, and alanine (Lindgren et al., 2011). These amino acids make up roughly 60% of the residues in modern collagen, which is the most abundant structural protein in modern bones. Therefore, Lindgren et al. (2011) argue that their findings represent remains of collagen I. Saitta et al. (2020) analysed roughly 80-million-year-old titanosaur egg shells and found that the calcitic layer was enriched in glutamic acid, glycine, alanine, and possibly valine. These amino acids are some of the most stable with respect to diagenetic alteration (Saitta et al., 2020). Most other amino acids were either fully racemised or absent in the titanosaur samples, which implies that these amino acids are completely hydrolysed or degraded during diagenesis (Saitta et al., 2020).

The longevity of single amino acids (apart from environmental factors) depends on their side chain chemistry, which defines the chemical characteristics of the molecule. Bada (1991) notes four processes that affect amino acids during diagenesis: peptide bond hydrolysis, decomposition, condensation reactions, and racemisation. The impact of these factors is different for each amino acid or peptide bond; amino acids that are more resistant to a certain factor might be less resistant to another.

The process of amino acid racemisation, the random transformation from L to D configuration, takes place rapidly under natural conditions and is observed in fossil organisms, but in rare and specific circumstances also occur in living animals (Bada, 1991). The D/L ratios of amino acids have been used for age determination of archaeological and geological samples (Bada &

Schroeder, 1975; Schroeder & Bada, 1976), but this approach can be misleading because racemisation rates not only depend on age, but also on diagenetic influences like environmental pH (Collins et al., 2009; Demarchi et al., 2013). The rate of racemisation strongly depends on material, temperature and environment and often surpasses the rate of decomposition, so that even young samples can contain only small amounts of D amino acids (Bada, 1971; 1991). Racemisation rates differ between amino acid under equal conditions. For example, the racemisation half-lives differed in aqueous solutions at neutral pH and 100°C from 30 days for aspartic acid to 300 days for isoleucine (Bada, 1991). On the surface of the earth, L amino acids produced by living organisms are totally racemised after one hundred thousand to one million years (Bada, 1991; Bada et al., 1994). Racemisation happens much more rapidly for free amino acids than for amino acids in proteins (which are predominantly left-handed). Proteins in older samples are more degraded, meaning there are more free amino acids, and therefore more right-handed amino acids, than in younger samples. Although exact dating of fossil material through racemisation rates is not possible, the more ancient the material, the closer to 1.0 the D/L ratio (Bada et al., 1973).

Beyond single amino acids, the preservation of proteins or protein sequences from fossils has been reported (Tuross & Stathoplos, 1993; Schweitzer et al., 2019). Most reports of ancient proteins are associated with dinosaur fossils and are attributed to the preservation of collagen I - the most common structural protein in bones, which seems to be quite resistant to decay (Tuross & Stathoplos, 1993; Asara et al., 2007; Schweitzer et al., 2009; Bertazzo et al., 2015; Buckley et al., 2019; Bailleul et al., 2020).

With respect to this thesis, the most interesting report of protein preservation stems from a fish vertebra from the Vastan lignite mine in India (Dutta et al., 2020). The Vastan lignite mine is an important source of Cambay amber and some of the pieces used in this thesis come from this locality. The fish vertebrae were found in a lignite-bearing sequence of the Cambay Formation (Ypresian stage), but a complete description of the sampling site is still missing. As with the dinosaur fossils, the protein that was found in the fish vertebrae is collagen. Pyrolysis-comprehensive two-dimensional gas chromatography time-of-flight mass spectrometry (py-GCxGC-TOGMS) of these vertebrae revealed the same prominent pyrolysis products found during comparative pyrolysis of modern fish vertebrae (e.g. pyridines, acetic acid, succinimide, Dutta et al., 2020). The modern fish contained abundant fatty acids that could not be detected in the fossils (Dutta et al., 2020), but the presence of cyclic dipeptides in the fossils indicates that collagen is preserved with structural accuracy. Dutta et al. (2020) conclude that the

preservation of collagen I is due to the encapsulation of soft tissue within the hydroxyapatite of the bone. Moreover, the preservation of collagen in the fish vertebrae implies that the environment of the Vastan lignite mine is favourable for the preservation of biomolecules, although some variation is evident. However, the degree of protein and amino acid preservation in Cambay amber is questionable, because the resinous matrix provides different preconditions compared to the rocks from where the fish vertebrae derive. Interestingly, proteins are poorly preserved in mammal bone fragments from the same location, which is interpreted as being the result of different microbial degradation pathways (Dutta et al., 2020).

5.4.2 Fossil amino acids and proteins in amber

Compared to reports from rocks, only a few studies have dealt with the preservation of amino acids and proteins in amber (Bada et al., 1994; Wang et al., 1995; Smejkal et al., 2011; McCoy et al., 2019).

Bada et al. (1994) and Wang et al. (1995) were the first to report the preservation of amino acids in amber. They analysed inclusions from different copal and amber sources ranging in age from 130 Million years old to modern Defaunation resin, but only published the numerical values for a fly inclusion from Eocene Baltic amber and a bee from Miocene Dominican amber. The analysis through HPLC with fluorescence detection showed that amino acid concentrations of the inclusions were significantly higher than in the surrounding amber matrix. However, a Mexican amber piece included in the first study only yielded amino acid amounts close to the procedural blank. Bada et al. (1994) and Wang et al. (1995) observed a net loss in amino acids over time, ranging from 15–20% in a modern fly, to 2–10% in Defaunation resin, and 0.1–1% in amber. The D/L ratios of aspartic acid, alanine, and valine (all under 0.05) from the amber fly were similar to the values of the modern fly, and even in the sample from Lebanese amber (~130 Ma), there was little racemisation (Bada et al., 1994). The Baltic amber fly appears to be enriched in serine, glutamic acid, and glycine whereas the relative amounts of aspartic acid, alanine, and valine are lower compared to a modern fly (Wang et al., 1995). The same pattern could be recognised for the bee from Dominican amber. The presence of serine in the fossils is remarkable, because it is recognised as one of the least stable amino acids (Bada, 1991).

In both studies it was concluded that racemisation processes are greatly retarded in amber due to the anhydrous nature of the amber matrix. The absence of water furthermore enabled the

preservation of serine, which is usually rapidly hydrolysed (Bada et al., 1994; Wang et al., 1995). The amino acid patterns of fossils in amber might therefore deviate from those in aqueous environments.

A more recent study on amino acid racemisation of feathers from Baltic, Burmese, and Spanish amber exhibited large differences in the presence of 13 original amino acids (McCoy et al., 2019): Cretaceous Spanish amber had no amino acids; one out of six samples of Burmese amber had low concentrations of original feather amino acids; and one sample of Baltic amber had higher concentrations of original feather amino acids. However, the amino acid compositions, and some variation in the D/L ratios of different amino acids, suggested that the different amber sites had different pathways of degradation. McCoy et al. (2019) proposed that varying decay rates between the deposits caused by varying antimicrobial compounds in the resins are responsible for their results.

Only one study reported the preservation of amino acids in amber in such an abundance that peptide sequencing was possible: Smejkal et al. (2011) identified several proteins of the yeast *Saccharomyces* in Miocene Dominican amber. If not caused by contamination, these results imply that it should be also possible to sequence peptides from other ambers as well. However, these results should be taken with some caution, because in all other previous studies (and the results presented herein) the concentration of amino acids is too low to allow for peptide sequencing.

5.4.3 Analysis of amino acid compositions of fossils from class II ambers

The amber samples in previous studies on amino acid preservation, ranging in age from the Cretaceous to the Miocene, have been attributed to class I based on their diterpenoid skeleton, and stem from several gymnosperm and angiosperm taxa (Anderson et al., 1992; Penney, 2010a). This thesis examines for the first time the amino acid composition and racemisation of inclusions from class II ambers.

Material and methods

In total, ten fossils from Eocene Cambay (India) and Miocene Zhangpu amber (China) were analysed (Table 8), comprising five dipterans, one spider, one mite, one unidentified arachnid, and two plant fragments (Fig. 15). To minimise the risk of contamination, only inclusions completely surrounded by resin (not lying on the surface of the piece) without any cracks running through the fossil or within 2 mm of it were selected. The two specimens with plants were the only ones without any visible cracks, but the others had no cracks near the inclusions.

Table 8: Samples analysed for amino acid racemisation. Samples marked in green show a normal L-hArg signal and were used for further analyses. See text for more information.

Collection number	Description	Amber deposit
10013	Brachycera	Zhangpu amber
10040	Nematocera	Zhangpu amber
11614	plant fragment	Zhangpu amber
11697	Nematocera	Zhangpu amber
11706	Nematocera	Zhangpu amber
STB-011-T'10	Acari	Cambay amber
STB-039-T'12	Araneae	Cambay amber
STB-0041-T'12	plant fragment	Cambay amber
STB-0291-T'09	Nematocera	Cambay amber
Tad'10 spider	Arachnida indet.	Cambay amber

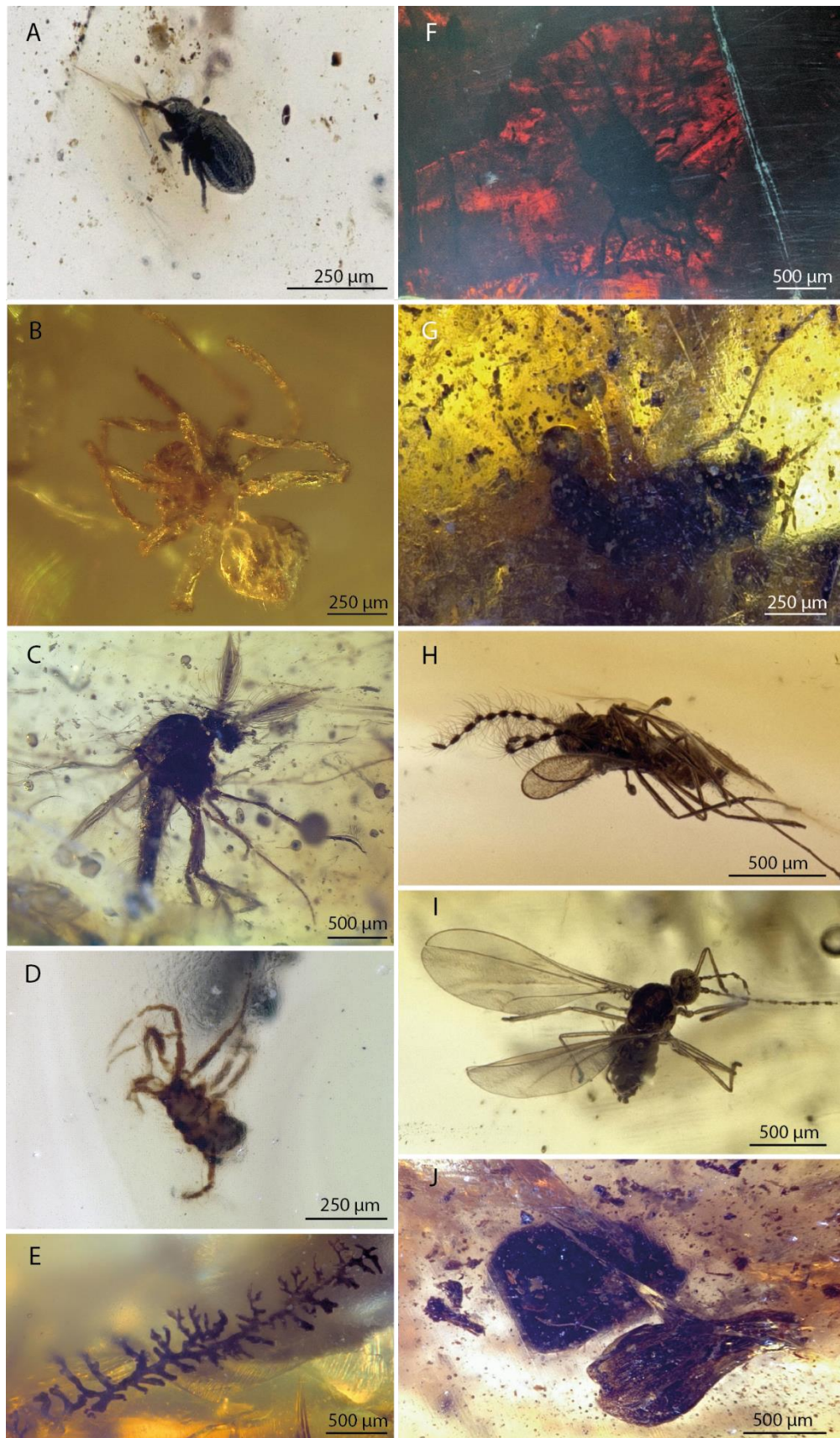


Figure 15: Images of fossils used for amino acid racemisation analysis. Fossils on the left are from Cambay amber; fossils on the right from Zhangpu amber. Collection numbers: STB-011-T'10 (A), STB-039-T'12 (B), STB-291-T'09 (C), Tad'10 spider (D), STB-0041-T'12 (E), 10013 (F), 10040 (G), 11697 (H), 11706 (I), and 11614 (J).

Sample preparation

Each specimen was initially cut into a ~3 mm cube centred on the inclusion of interest, to remove excess amber and extraneous inclusions. These cubes were then moved to the clean preparation area. The preparation of samples was carried out in a class 1000 biologically clean laminar flow hood. All tools, beakers, vials, and petri dishes that made contact with the amber were chemically cleaned to remove modern contaminants: all tools were placed in 12% NaOCl overnight for 15 hours and were subsequently cleaned further with HPLC-grade Acetone and HPLC-grade Methanol. HPLC-grade water was used to wash the tools between each cleaning step.

Once within the clean preparation area, the 3 mm cubes were further mechanically prepared by grinding an extra millimetre from each surface using a Dremel grinding stone, cleaned following the procedure described above. This removes surface contaminants and, by decreasing the amount of amber even further, hastens the dissolution process and minimises the number of particles in the final solution. These smaller amber cubes were placed into petri dishes and flooded with HPLC-grade Toluene until all amber had dissolved and the inclusions were floating free, which takes about an hour. The inclusions, although they appear complete while in the amber, rarely retain their structural integrity once the amber is removed which hampers sampling and necessitates extensive microscopic examination of each petri dish to identify all the fossil fragments. These fragments were removed from the petri dishes using a sterile pipette and transferred to sterile glass vials for amino acid racemisation. The toluene was flushed from these vials using HPLC grade acetone. Subsequently, the samples were sent to the Department of Chemistry of the University of York where they were analysed according to McCoy et al. (2019) via RP-HPLC (reverse phase – high-performance liquid chromatography) for 13 amino acids (Fig. 16; Appendix 9.3). The D and L enantiomers cannot be distinguished for four of these 13 amino acids, and so D/L ratios are only reported for nine amino acids. Each specimen was sampled in at least two experimental runs (Fig. 16).

Results & Discussion

All of the ten fossils yield concentrations of different amino acids of up to 5427 picomoles/gram (Appendix 9.3, Table 1), but in five of them the L-homo-arginine (L-hArg) standard is repressed. L-homo-arginine is a non-protein amino acid which is added during RP-HPLC preparation to quantify amino acid concentrations in the samples (e.g. McCoy et al., 2019). The repression of the standard may be due to interactions with the cleaning solvents or the toluene that was used to extract the fossils and must be addressed by future experiments and improved methods. Therefore, the description of the data continues only with the five samples that do not show a repressed standard.

The five samples with an unaffected L-hArg signal show varying amino acid compositions between fossils and experimental runs (Fig. 16; Appendix 9.3, Table 2). The differences in amino acid concentrations between experimental runs of the same sample do not exceed 4% and argue for the consistent application of the protocol (Appendix 9.3, Table 2). With a concentration of 27–42%, Glycine is the most abundant amino acid in each sample (Fig. 16A). The same observation has been reported in previous studies on amino acids in amber (Bada et al., 1994; Wang et al., 1995; McCoy et al., 2019). Glycine is the smallest amino acid and contains a single hydrogen atom in its side chain. It is reported that proteins, peptides, and large amino acids degrade into smaller fragments as a result of diagenetic alteration (Bada, 1991). Therefore, the prominent Glycine content in the samples likely represents decay products of formerly larger amino acids and peptides.

Tyrosine was detected only in two samples from Zhangpu amber (Fig. 16A; Appendix 9.3). The concentration ranged from 1% in a fly (sample 10013) to 2% in a nematoceran (sample 11697). Comparable data by McCoy et al. (2019) show that tyrosine was preserved in only small amounts in Baltic and Burmese amber as well. It appears that the preservation of tyrosine is not favoured in amber. The survivability of amino acids depends on their side chain chemistry in combination with environmental factors that may interact in complex ways. In freeze-dried samples from various marine environments, tyrosine decreased rapidly during the initial stages of alteration (Dauwe et al., 1999). With respect to geologic timescales, the preservation potential of tyrosine seems to be strongly limited.

Serine is described as a reactive amino acid that rapidly undergoes racemisation and alteration (Bada, 1991). Its preservation is reported in previous amber studies (Bada et al., 1994; Wang et al., 1995; McCoy et al., 2019) and serine could also be found in each of the recently analysed samples, where it ranges in concentration from 7–13% (Fig. 16A).

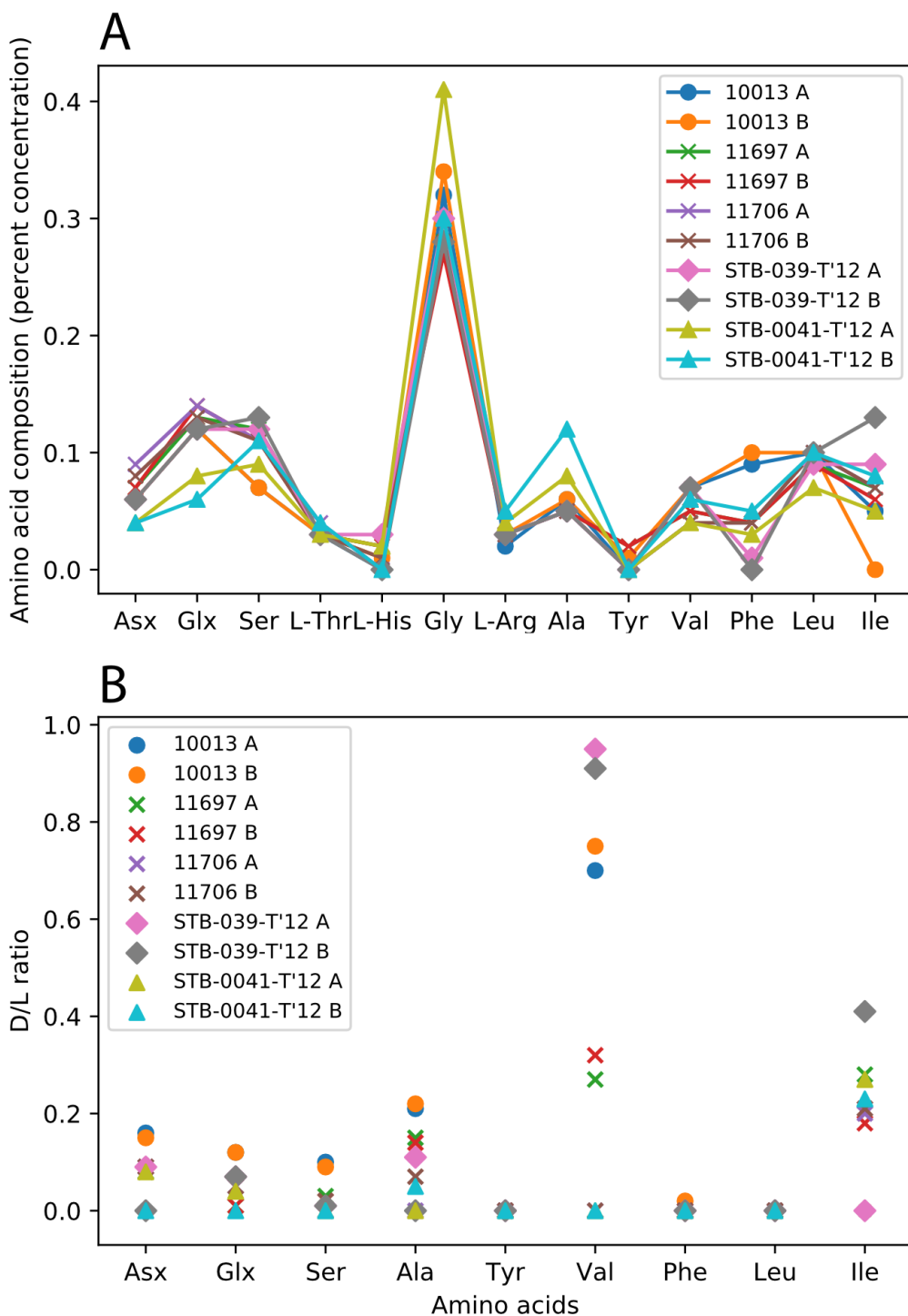


Figure 16. Plotted RS-HPLC results of inclusions from Cambay and Zhangpu amber. (A) Percent concentration of tested amino acids. (B) D/L ratios of tested amino acids. Capital letters in the sample description attribute to the two experimental runs. Raw data sheets are found in the Appendix 9.3 (Table 1-4).

The presence of serine implies the inhibition of racemisation rates in resins, at least for some amino acids, which seem to be quite different to the processes in aqueous environments (Bada et al., 1994; Wang et al., 1995).

The D/L ratios of selected amino acids range from 0.0 to 0.95 (Fig. 16B). The amino acids with a D/L ratio of 0 are interpreted as modern contaminants or might reflect freshly cleaved components from the peptide bond. The highest ratio of 0.95 is attributed to valine from a spider sample (Appendix 9.3, Table 4). Usually, the high D/L ratio of valine would argue for the age and authenticity of the material, but the values differ largely between samples from the same deposit. There is no explanation for this phenomenon at the moment, but it is possible that the application of toluene in the process of sample preparation had an impact on this matter.

The majority of D/L values of the other tested amino acids are up to 0.3 (Fig. 16B) and thus are much higher than reported values of insects from Baltic amber: D/L ratios of alanine, valine, and aspartic acid were each less than 0.05 (Bada et al., 1994). It could be assumed that Baltic amber or its depositional environment has a stronger effect on racemisation rates than class II amber, but it is more likely that the discrepancy derives from methodological differences or modern contamination in the samples of Bada et al. (1994). Although they tried to reduce the risk of contamination via preparational methods, they did not use a clean lab for their extractions. D/L ratios of the class II amber samples are more similar to values published by McCoy et al. (2019) on feathers from Baltic amber (Fig. 17). The samples of McCoy et al. (2019) and the ones presented herein have both been analysed in the same lab (Department of Chemistry, University of York) and differ only in preparation prior to RP-HPLC: instead of being extracted with solvents, samples of McCoy et al. (2019) were crushed with a pestle and mortar.

Based on percent concentrations of the studied amino acids, a principal component analysis (PCA) was carried out in collaboration with MCCOY (Fig. 18). It clearly distinguishes the samples of this thesis from the ones of McCoy et al. (2019) and from common contamination sources and represents a strong argument for authenticity of the material. Moreover, the PCA results imply that the amino acids of the thesis samples still contain biological information: phylogenetically closely related taxa plot near to each other in the graph meaning that they are similar in their amino acid composition. This is even the case for samples stemming from two different deposits, implying that the differences in amino acid compositions derive from the fossils rather than environmental influences (Fig. 18). A larger set of data would help to validate this finding.

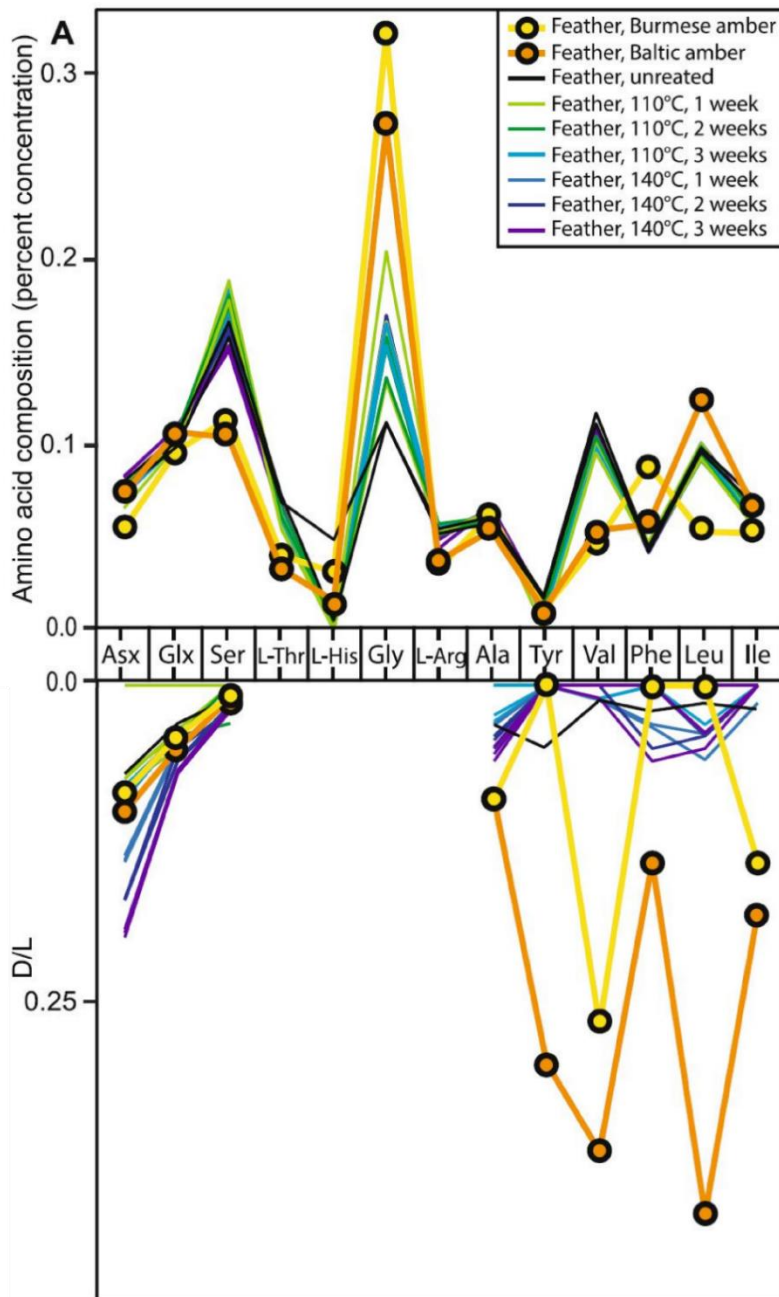


Figure 17. RS-HPLC results of modern and fossil feathers in artificial resin and amber. Note that D/L ratios of Baltic amber fossils (Eocene) are higher than for Burmese amber fossils (Cretaceous). From McCoy et al. (2019).

The experiments of this thesis can be regarded as a first step towards the analysis of amino acids from class II ambers. These preliminary results should be taken with caution, because in five out of ten fossils the L-hArg standard was repressed. The interactions of the cleaning solvents with amino acids have to be examined before a large-scale analysis can be carried out in the future. As evidenced by previous studies and supported by the results within this thesis, amber fossils from different deposits still contain original amino acids. In fact, this thesis represents the first proven finding of ancient amino acids in amber insects, since previous studies were likely biased by modern contamination as indicated by extremely low rates of racemisation (Bada et al., 1994; Wang et al., 1995). It is remarkable that serine could be documented from Burmese, Baltic, Dominican, Cambay and Zhangpu amber, regardless of extraction method. The preservation of serine and other amino acids in amber is partially explained by the anhydrous nature of the resinous matrix, which inhibits peptide bond hydrolysis (Bada et al., 1994; Wang et al., 1995). Other factors have to be elucidated by future experiments.

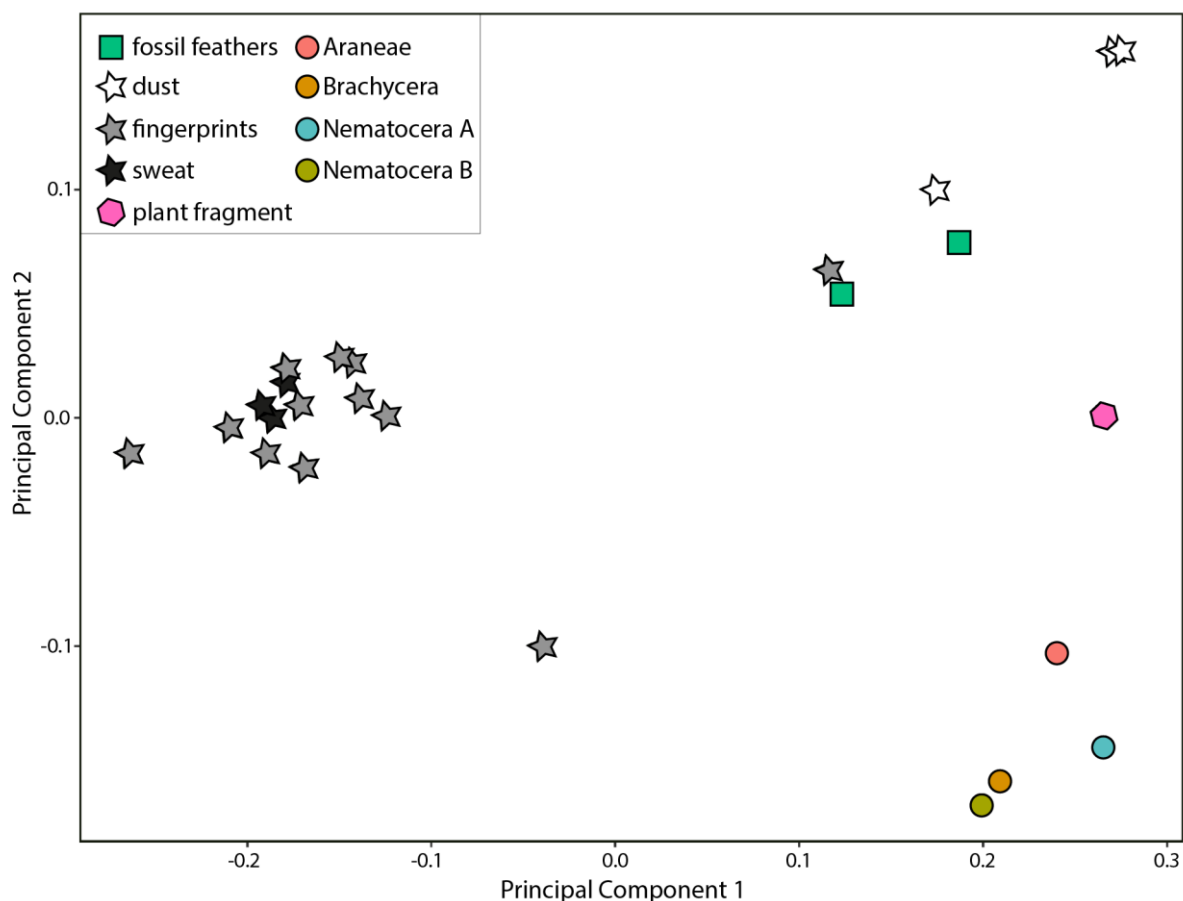


Figure 18: PCA of amino acid racemisation in amber fossils. The samples examined in this thesis (circles, hexagon) are well distinguished by contamination sources (stars) and fossil amber feathers (squares). In addition, the arthropod samples plot closer to each other than to the plant remain, indicating that the amino acids still contain biological information. Collection numbers: plant remain = STB-0041-T'12; Araneae = STB-039-T'12; Brachycera = 10013; Nematocera A = 11706; Nematocera B = 1169.

5.5 DNA extraction of resin-entombed beetles

This chapter represents a short summary on DNA preservation in resinous environments and provides new results on its potential limits. It is based on the following peer-reviewed and published research article to which the author of this thesis contributed:

Peris, D., Janssen, K., Barthel, H.J., Bierbaum, G., Delclòs, X., Peñalver, E., Solórzano-Kraemer, M.M., Jordal, B.H., Rust, J., 2020. DNA from resin-embedded organisms: Past, present and future. PLoS ONE 15, e0239521. <https://doi.org/10.1371/journal.pone.0239521>

The original manuscript is attached in the Publications section (10.2).

Introduction

In the early nineties of the 20th century, several studies reported the extraction of DNA from various amber entombed organisms such as bees, termites, and bacteria of up to 20 million years old (Cano et al., 1992a, b; De Salle et al., 1992; Cano et al., 1993; Poinar et al., 1993; Cano et al., 1994). These initially exciting results soon turned out to be caused by modern contamination, were not reproducible in subsequent studies, or were achieved with a problematic methodology (Lindahl 1993a, b; Austin et al., 1997a; Smith & Austin, 1997; Walden & Robertson, 1997; Pääbo et al., 2004; Hebsgaard et al., 2005; Willerslev & Cooper, 2005; Rosselló, 2014). Even the extraction of DNA from subfossil resin inclusions was not successful (Austin et al., 1997b; Penney et al., 2013b) and raised further questions about the preservation potential of DNA in resins. In a more recent approach, Büsse et al., (2017) report the successful amplification of DNA from two embedded beetles in Holocene copal that could be dated to 790-700 years BP and 4030-3900 years BP. Unfortunately, these authors do not provide any information on authentication procedures. Due to the indistinctive picture on DNA preservation in amber and resin in the past, we decided to explore its potential limits in a step-by-step approach and to develop a standardised protocol for comparative studies. The main question is, if DNA in resins has a poor preservation potential in general, or if the extraction methodology is limited in some way. We started our investigations with ten platypodid beetles of the genus *Mitosoma* collected in 2013 and 2017, which were embedded in *Hymenaea verrucosa* Defaunation resin from Madagascar (Fig. 19). For comparative reasons, four *Mitosoma* specimens that were collected in 2012 and stored in ethanol were sampled as well.

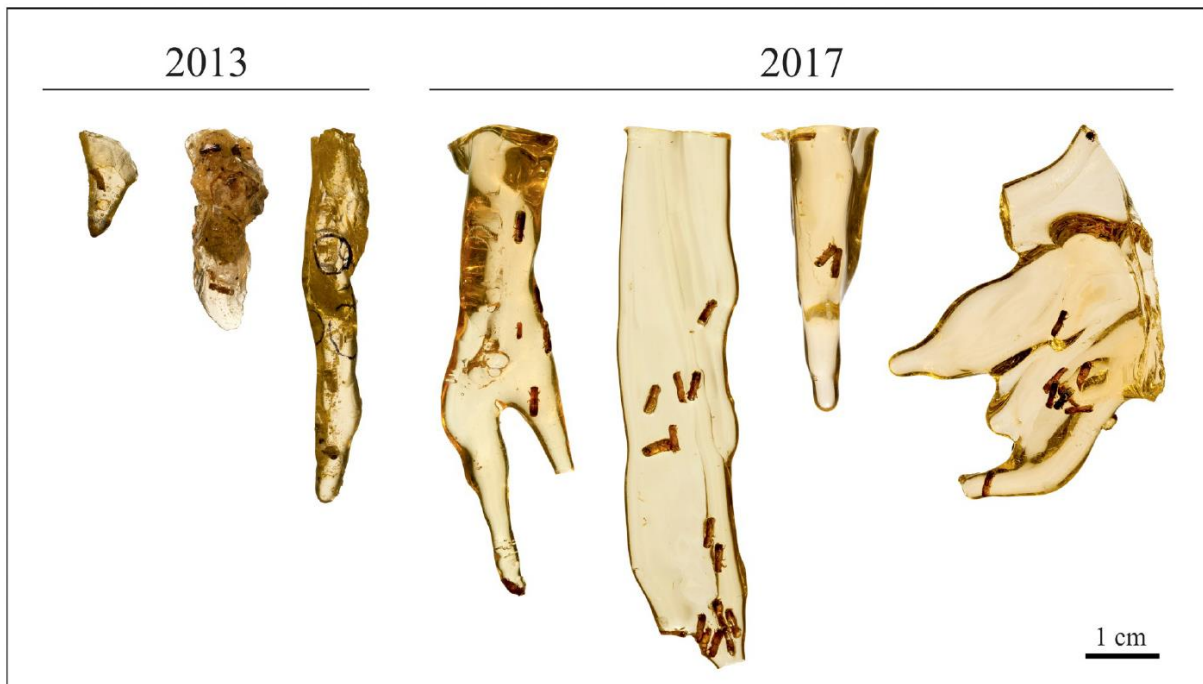


Figure 19. Photographs of *Mitosoma* sp. samples before destructive sampling. The beetles are embedded in Defaunation resin pieces from Madagascar. From Peris et al. (2020).

DNA extraction was performed by Kathrin Janssen and Gabriele Bierbaum at the Institute of Immunology, Medical Microbiology, and Parasitology (University Clinic Bonn, Germany). For the extraction of beetle DNA, the commercial DNeasy® Blood & Tissue Kit (Qiagen Germany) was used because its effectiveness has been validated in studies on extant beetles (McKenna & Farrell, 2005; Mugu et al., 2018). Six different primers were used in our study to detect DNA fragments. One primer pair (S3690F and A4285R) targets the large nuclear ribosomal subunit (28s), whereas the other primer pair (S2442F and A3014R) targets the 3' end of the mitochondrial cytochrome oxidase I (COI). Both pairs were successfully tested in previous studies on extant coleopteran samples (McKenna & Farrell, 2005; Mugu et al., 2018) and therefore chosen for our experiments. These original primers yielded DNA fragment sizes of ~600 (COI) to 800 (28S) base pairs. In addition, two newly designed, modified COI primers were used which are based on the sequence of the mitochondrial cytochrome oxidase I (COIRes F and COIRes R2).

Results & Discussion

We successfully amplified DNA with all tested primers from resin-embedded beetles that were collected in 2013 and 2017. DNA concentrations differed significantly between ethanol-stored and resin-embedded samples (Fig. 20). In addition, a non-significant time-correlated decrease in the amount of DNA obtained from resin beetles was observed.

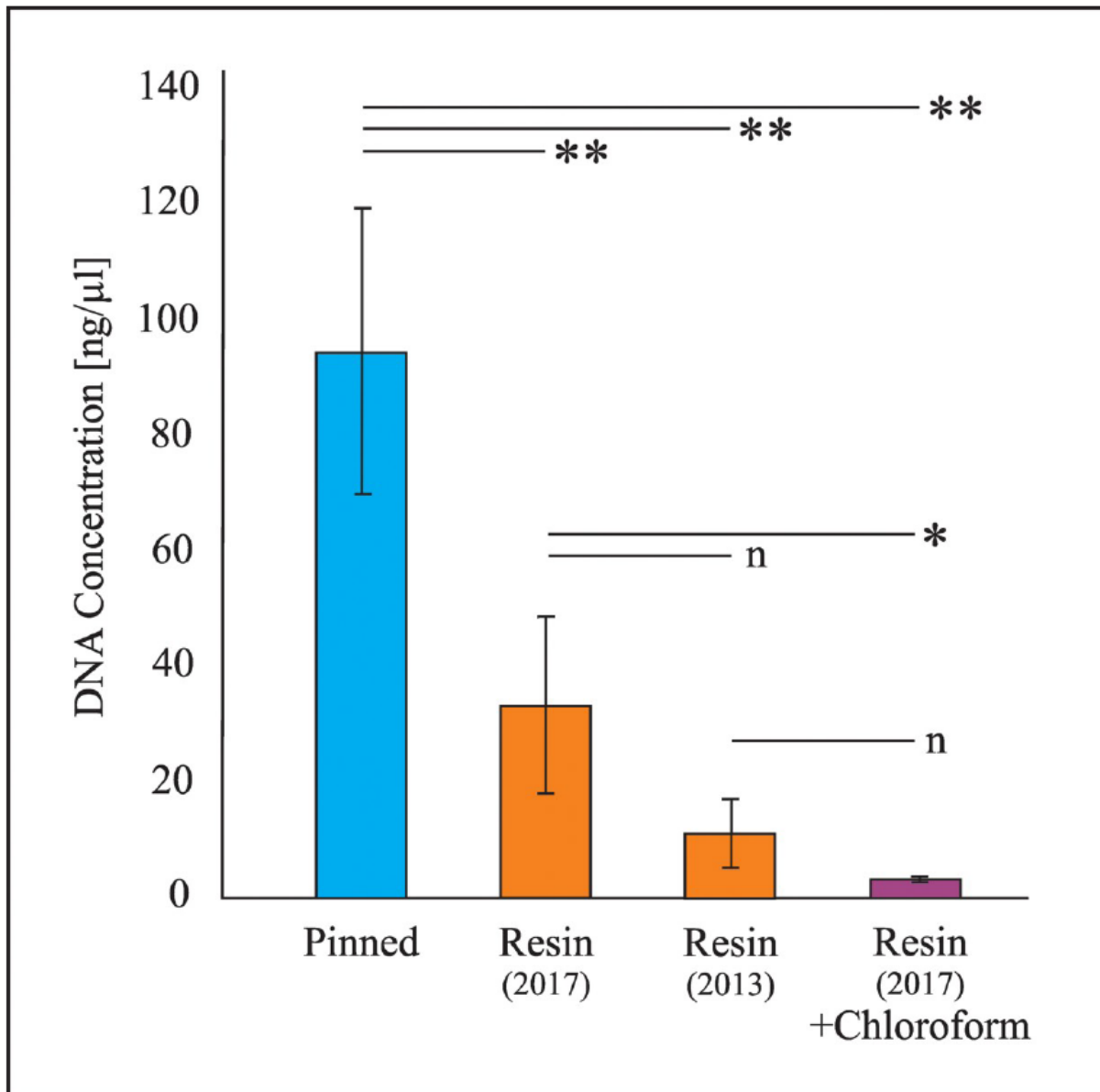


Figure 20. Mean DNA concentrations in the different samples analysed. * = Significant differences $P < 0.05$; ** = Significant differences $P < 0.01$; n = Non-significant differences. From Peris et al. (2020).

However, applying a standard PCR protocol to the resin-embedded samples resulted in unsuccessful initial attempts of DNA amplification. In contrast, the amplification of DNA from the ethanol samples was positive when carried out with the original primers. Due to the initial failure to amplify DNA in the resin samples, the PCR procedure was adapted and tested in two different approaches to increase the amount of amplicates. The first approach was to increase the number of PCR cycles up to 50. The second approach based on two consecutive PCR runs of 30 cycles each with a purification step in between. Both approaches turned out to be successful. Amplification was also successful with the new primers COIRes F and COIRes R2, which yield DNA fragment sizes of ~ 160 base pairs. These primers should be better suited to detect fragmented DNA in older samples.

The authentication of the specificity of the detected DNA fragments was performed via Sanger sequencing and multiple alignments with modern samples. This procedure should especially exclude the putative risk of inter-sample contaminations. In addition, if Bovine serum albumin (BSA) was added during a PCR (even with a reduced amount of 30 cycles), positive amplification was observed in the COI primers, but not 28a primers. BSA is a blood plasma protein that is commonly used in amplification procedures because it binds to inhibitors and prevents their negative effect on the polymerase. Furthermore, we did not detect any evidences for an inhibition of PCR through resin compounds in preliminary experiments.

It was shown in previous studies that it is possible to extract intact inclusions from amber and copal by dissolving the resinous matrix with chloroform (Azar, 1997; Penney et al., 2013a). This method is not invasive with regard to the inclusion and can represent a suited basis for further investigations, especially of analytical approaches. Since the sample does not need to be grinded, the chance of resin compounds contaminating the sample is highly reduced.

In our study, three out of ten resin-embedded beetles have been extracted with chloroform prior to PCR instead of grinding them. Interestingly, all three samples contained a lower concentration of extracted DNA (Fig. 20), which could indicate that chloroform has a negative effect on this procedure. The use of chloroform in the study of Penney et al. (2013a) is probably a reason for their unsuccessful DNA amplification from copal inclusions which were younger than 60 years.

While preparing the samples for pre-experiments, it could be observed that the internal tissues of the beetles are still nicely preserved and not shrunken or displaced. This could be proven by later micro-CT data which were not included in the original manuscript. Shrunken tissues are representative for dehydration, which has been proposed as one of the most important mechanisms with respect to exceptional preservation in amber (Poinar & Hess, 1985; Grimaldi et al., 1994; Martínez-Delclòs et al., 2004). Our results show that the idea of a rapid, thorough dehydration in resin-embedded arthropods needs to be revised. According to our observations, water might be available in resin-embedded arthropods for longer timespans than previously thought, which would have a negative impact on the limit of DNA preservation in amber.

In summary, PCR of tissues from resin-embedded organisms is not inhibited through resin compounds. Earlier, unsuccessful attempts on DNA extraction from Holocene copal samples could derive from methodological deviations, most probably the use of chloroform prior to sample extraction. The choice of primers and DNA extraction kits has a major impact on the results and it is crucial to adapt this choice towards the type of sample: we used a protocol that has been recommended in previous studies on extant platypodid beetles (McKenna & Farrell, 2005; Mugu et al., 2018). Our study represents an initial base on which further investigations on more ancient DNA in resins can be carried out in the future, including two newly designed primers and a preparation protocol that enhances the comparability of results and limits the risk of contamination.

5.6 Examination of a lizard forelimb in Dominican amber

This chapter is a summary of a published research article that represents the first analytical characterisation of a vertebrate fossil in amber. It is based on the following peer-reviewed and published research article to which the author of this thesis contributed:

Barthel, H.J., Fougereuse, D., Geisler, T., Rust, J., 2020. Fluoridation of a lizard bone embedded in Dominican amber suggests open-system behavior. PLoS ONE 15, e0228843. <https://doi.org/10.1371/journal.pone.0228843>.

The original manuscript is attached in the Publications section (10.3).

Introduction

The record of amber fossils does not only comprise arthropods, plants, and bacteria, but also tiny vertebrates (Klebs, 1910; Xing et al., 2016, 2017). Although findings of vertebrate remnants in amber became more common within the last few years, such fossils are still rare compared to the total number of known inclusions. Among these, small arboreal lizards, especially of the family Gekkonidae and the genus *Anolis* (Iguania) are the most commonly found (Klebs, 1910; Lazell, 1965; Rieppel, 1980; Borsuk-Bialynicka et al., 1999; Arnold et al., 2002; Böhme & Weitschat, 2002; Bauer et al., 2005; Arnold et al., 2008; Daza & Bauer, 2012; Polcyn et al., 2012; Sherratt et al., 2015; Daza et al., 2016). Due to the intensive trading on black markets of highly valuable amber vertebrates, only a small number are currently found in scientific collections.

X-ray scans of some lizard fossils revealed that parts of their skeletons are preserved (Polcyn et al., 2012; Daza et al., 2013; Sherratt et al., 2015; Daza et al., 2016), but despite this observation, nothing is known about the degree of preservation of bone tissue in amber. Bone is a complex hierarchical composite material consisting of a mineral phase (bioapatite) embedded in an organic fibrous matrix that is mainly built up of collagen fibrils and some subordinate lipids, proteins, and peptides such as osteocalcin (Pasteris et al., 2008). It can be expected that amber shields the bone material against aqueous solutions, which would result in a high degree of preservation, including of the bone's collagen matrix. The bioapatite in bone is a solid solution and its reactive sites allow for extensive ionic substitutions during diagenesis

(Hughes & Rakovan, 2002; Wopenka & Pasteris, 2005). Fossil bone specimens are often characterised by a larger than average crystallite size, a higher crystallinity, and a different apatite chemistry when compared to extant material (Pucéat et al., 2004; Trueman et al., 2004; Piga et al., 2009; Dumont et al., 2011). It is questionable whether bone tissue in amber differs from bone tissue in other depositional environments, as, to date, no data on this topic exist.

To clarify the composition and characteristics of fossil bone tissue in amber, we analysed a fossil forelimb of an *Anolis* lizard from Miocene Dominican amber with various imaging and analytical techniques. After initial imaging and CT-scanning, the humerus was cut along its cross-section to apply several analytical methods and to prepare microtome slices.

Results & Discussion

The visual examination of the amber piece reveals, several major resin flows in the matrix (Fig. 21). A mymarid wasp is embedded beside the *Anolis* forelimb but lies within a separate flow structure. The presence of multiple resin flows within the same piece of amber is called “Schlauben” and suggests that the piece formed along the stem of the tree. The matrix contains numerous bubbles, some of which consist of air, and others of unknown denser material. Two cracks run across the amber piece and cut through the anole forelimb in two points of the radius and ulna. The humeral head lies open in the resin matrix, but the rest of the limb is still covered by integument. Micro-CT scans revealed that the humerus is broken and furthermore showed an edema in the humeral integument, which was not observable via light microscopy. The edema must have been caused by trauma during or after trapping of the lizard in the original liquid resin, probably by a predator as indicated by the broken humerus. The bone tissue behaved in a brittle manner during preparation of microscopic and microtome slices which implies a severe grade of alteration in the material. This observation was later confirmed by analytical methods.

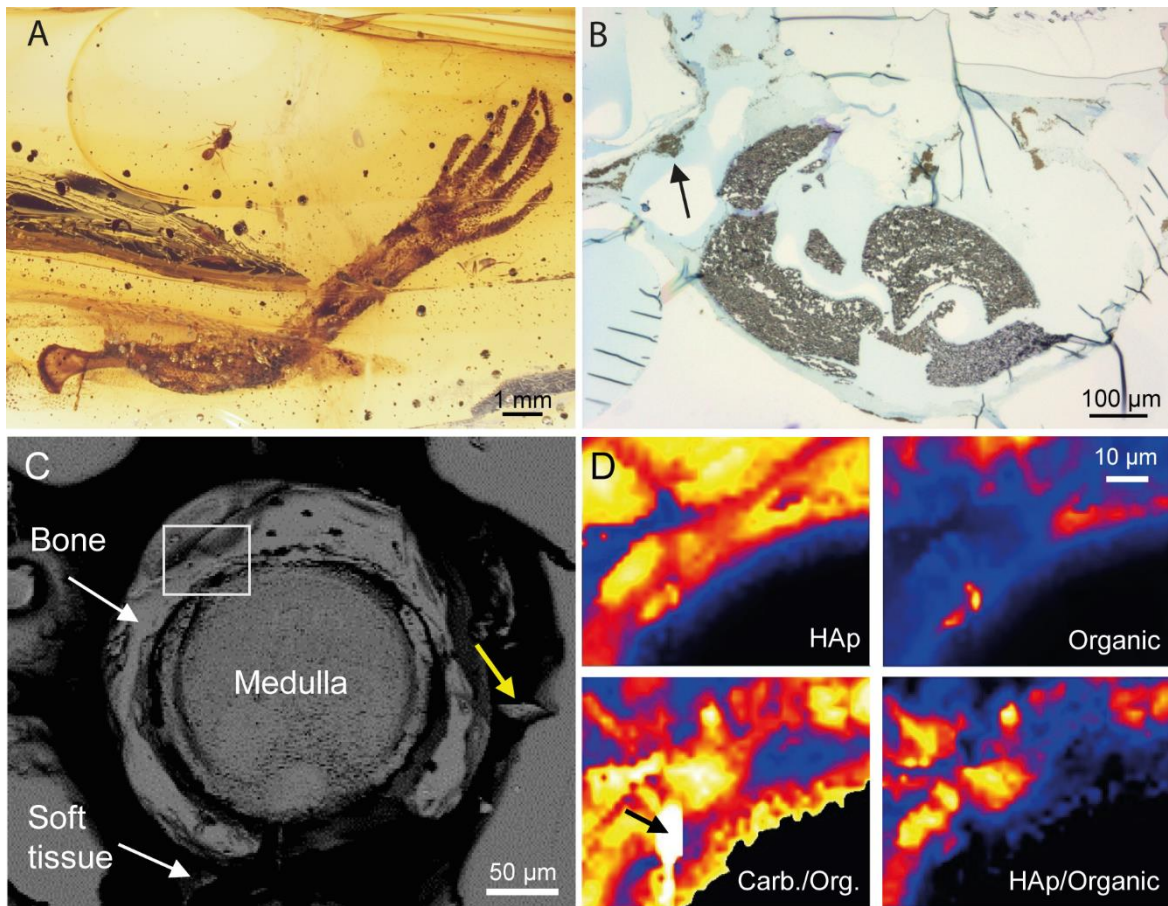


Figure 21. (A) Light microscopic image of the investigated amber piece. It contains a fairy wasp and the left forelimb of an anole lizard. Several flow structures can be recognised in the resin. (B) Microtome slice of the cross-sectioned bone showing fragmented bone material. The black arrow points towards epidermal remains in the matrix. (C) Backscattered electron image of the fossil bone surface. The yellow arrow shows a bone fragment that was pressed into the material during preparation of the sample. The white rectangle marks the area that was imaged by Raman spectroscopy. (D) False-coloured hyperspectral images of a bone area showing (upper left) the integrated intensity of the $\nu_1(\text{PO}_4)$ apatite band ($A_{\nu_1(\text{PO}_4)}$), (lower left) the intensity ratio of the $\nu_1(\text{CO}_3)$ band of carbonate near 1070 cm^{-1} ($A_{\nu_1(\text{CO}_3)}$) and the total intensity between 1150 cm^{-1} and 1700 cm^{-1} , reflecting the organic content ($A_{1150-1700}$) (upper right) $A_{1150-1700}$ and (lower right) $A_{\nu_1(\text{PO}_4)} / A_{1150-1700}$. An unknown carbonate phase is marked by a black arrow. From Barthel et al. (2020).

Raman spectroscopy of the fossil bone tissue showed the same bands of the mineral phase as modern *Anolis* bone tissue (Fig. 22). The prominent band at $\sim 960\text{ cm}^{-1}$ is assigned to the $\nu_1(\text{PO}_4)$ stretching mode of the phosphate tetrahedra, whereas a strong band at $\sim 1070\text{ cm}^{-1}$ represents the $\nu_1(\text{CO}_3)$ vibration of the carbonate group in the apatite structure. However, in the fossil sample, the 960 cm^{-1} band is shifted towards higher wave numbers (964 cm^{-1}). In addition, it is less intensive, narrower and on average less asymmetric when compared to the extant sample. These observations indicate a change in the chemical composition of the bone and argue for an incorporation of fluorine (Pasteris & Ding, 2009), which has been confirmed by EMP measurements (Fig. 22).

Similar to the mineral phase, Raman spectra of the organic phases reveal large differences between the extant and modern bone tissue (Fig. 22). Intact collagen in the modern bone is indicated by the presence of several bands assignable to phenylalanine (1033 cm^{-1}), amide III ($1243\text{-}1320\text{ cm}^{-1}$), CH stretch ($\sim 2940\text{ cm}^{-1}$), methylene side chains (CH_2 at 1450 cm^{-1}), proline (921 cm^{-1} and 855 cm^{-1}), and hydroxyproline (876 cm^{-1}) vibrational modes. The fossil bone spectrum does not show any of these characteristic bands and instead consists of two broad bands between 1200 cm^{-1} and 1500 cm^{-1} . In some spectra additional bands can be observed in the fossil bone (Fig. 22), but regardless of the exact composition and structure of these compounds, they do not represent typical collagen degradation products.

In consequence, the mineral and organic phase of the fossil bone have been intensively modified compared to their original state and an uptake of fluorine could be evidenced. The transformation of bioapatite to fluorapatite is a well-known phenomenon in fossil bones from the rock record and is associated with infiltration of F-rich ground or soil water accompanied by a loss of incorporated carbonate groups and the collagen matrix (Dwivedi et al., 1997; Pfretzschner, 2004; Wopenka & Pasteris, 2005). Our ToF-SIMS (time-of-flight secondary ion mass spectrometry) data suggest that fluorine most likely entered the bone through aqueous solutions along one of the cracks in the amber piece, although other possibilities cannot be fully excluded. The time at which this event occurred cannot be exactly dated, but it must have taken place after the hardening of the resin. Besides the crack in the amber matrix, the diagenetic fate of the sample may have been influenced by body fluids that were trapped inside the resin and reacted with various tissues. This is indicated by the presence of an edema, which must have formed during the time when the resin was still viscous. Our data on severely altered bone tissue are in accordance with results from Stankiewicz et al. (1998) who showed that the chitin in insects from the same amber deposit is largely degraded. Therefore, we propose that the chance to find intact macromolecular compounds in Dominican amber fossils is minimal.

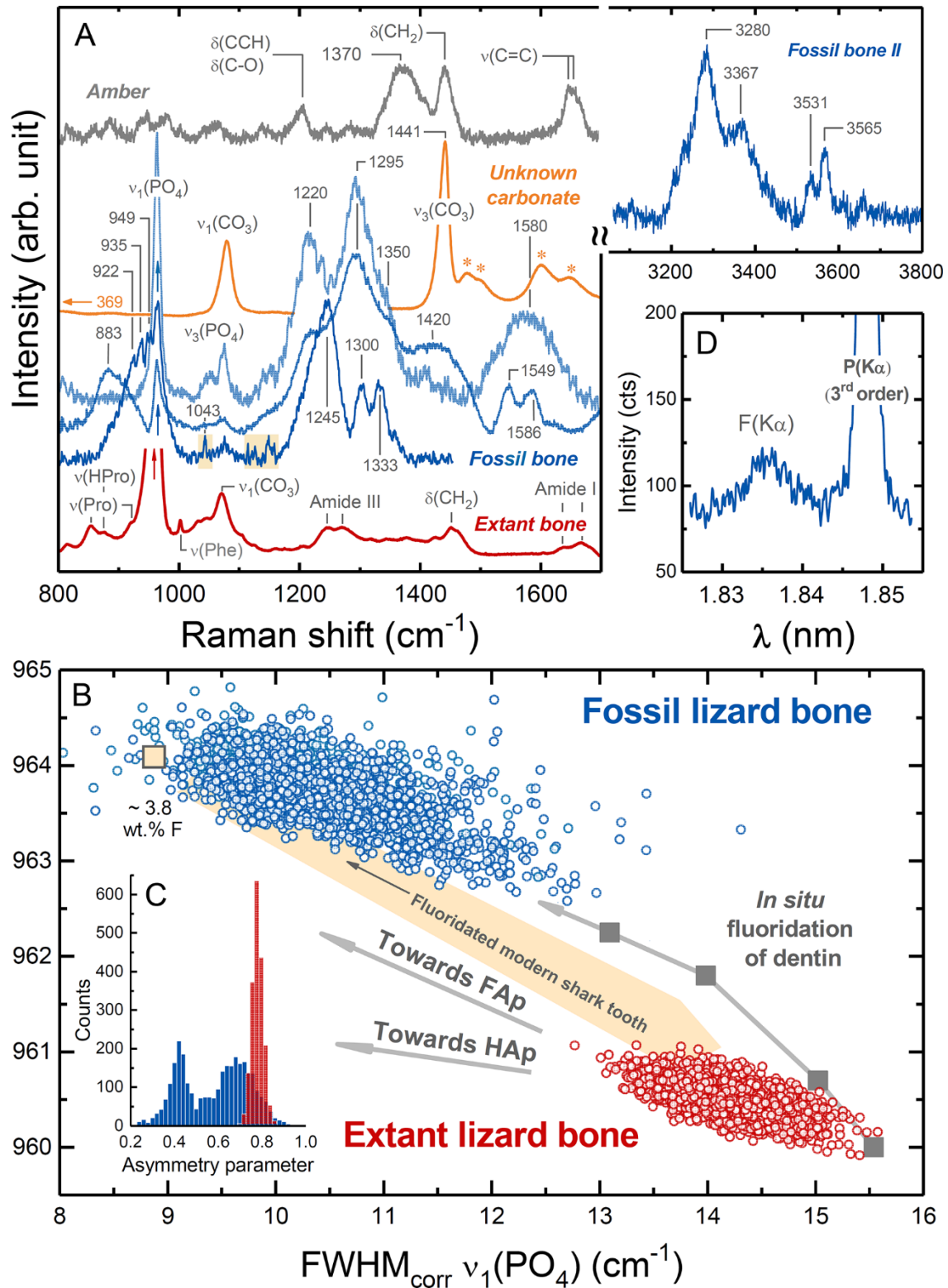


Figure 22. (A) Raman spectra of the fossil bone (blue), extant bone (red), the unknown carbonate (yellow) and the amber matrix (grey). (B) The relationship between the width, given as full width at half maximum (FWHM), and frequency of the $\nu_1(\text{PO}_4)$ mode for bone apatite shows that the fossil bone (4,323 analyses) is associated with higher frequencies and overall smaller FWHM values compared to the extant sample (2,527 analyses). In comparison with data from an extant shark tooth and experimental bone fluoridation data (Pasteris & Ding, 2009), this observation suggests the formation of fluorapatite. (C) The distribution of the asymmetry parameter of the $\nu_1(\text{PO}_4)$ band of fossil and extant bone spectra. The asymmetry parameter of the fitted asymmetric Gauss-Lorentz function varies between -1 and +1 with 0 referring to a symmetric profile. Negative values skew the spectrum toward higher wavenumbers, whereas positive values (as observed here) skew it toward lower wavenumbers. The multimodal distribution observed for the fossil bone indicates variable degrees of crystallinity and/or crystallite size. (D) An electron microprobe wavelength-dispersive X-ray scan from the fossil bone, which further verifies the occurrence of F in the material. From Barthel et al. (2020).

6.0 Synthesis

In the first part of this section, the results from the sub-projects are combined with results from previous studies to create new ideas and an improved model on the taphonomy of amber inclusions and to discuss several factors that may influence this process. The second part of this section shows how the main results contribute to the aims of this thesis.

6.1 Taphonomy of amber arthropods

According to the model of amber taphonomy by Martínez-Delclòs et al. (2004), the first part of this chapter deals with the mode of fossilisation that is already established in the earliest phase, namely the entrapment phase. The early and late diagenetic factors are discussed in the second part of this chapter. These factors either lead to a loss or preservation of soft tissues and explain the occurrence of several amber fossil types based on a dichotomous model. In a favourable outcome of this model, amber fossils contain internal tissues. The last part of this chapter discusses the differences of tissue preservation among these fossils.

6.1.1 Early entrapment and mode of fossilisation

The mode of preservation is the central aspect to explain the characteristics of tissues and biomolecular compounds in amber fossils. After examining ultrastructures of a fungus gnat in Miocene Dominican amber, Poinar & Hess (1982, 1985) suggested that amber fossils are predominantly the result of an extreme form of mummification, called inert dehydration. This purely physical process might have been aided by sugars and terpenes in the resin matrix that reacted with water in the tissues. The abdomen of the fungus gnat was damaged and partially filled with amber. The strip of tissue that Poinar & Hess analysed in their studies consisted of hypodermal tissue that was in contact with the resin and located next to the cuticle of the fossil. The presence of lipids, which are usually lost during inert dehydration, led to the conclusion that natural embalming properties of the resin assisted preservation (Poinar & Hess, 1982, 1985).

During the work on this thesis, dehydration was observable in the *Anolis* sp. fossil from Dominican amber (Barthel et al., 2020) in form of shrunken integument. This shrinkage is attributed to post-embedding dehydration, because former imprints of the integument can be recognised in the matrix. The space between the original position of the integument and its

current position is filled by resin, which means that the resin was still viscous when the shrinkage occurred. Henwood (1992a) describes a noticeable volume reduction of myofibrils and mitochondria in dipteran muscle tissues embedded in maple syrup and Dominican amber when compared to wax-embedded and untreated samples. Therefore, she concluded that dehydration is an important factor in the preservation of amber fossils that takes place after embedding of the organisms and is driven by osmosis. McCoy et al. (2018b) could show that dehydration prior to resin-embedding hampers the preservation of internal structures. Grimaldi et al. (1994) did observe minimal tissue shrinkage indicative of dehydration in some samples from Dominican and Baltic amber when analysed via SEM and TEM. In addition, the insect fossils in this thesis did not show any reduction in tissue volume when analysed via synchrotron or light-microscopy and also CT-scans of *Mitosoma* sp. beetles in Defaunation resin were not indicative of tissue shrinkage or displacement. It is possible, though, that the complete assessment of tissue dehydration in amber insects is limited to the magnification scale of the examination method and should be carried out with electron microscopic approaches.

Dehydration is a well-known process that enables a long-term preservation of proteins and also tissues, but is accompanied by a shrinkage of the structures. Therefore, if dehydration is the main mechanism to stabilise tissues in amber, it is necessary that some components counteract the shrinkage of the tissue. In modern fixatives of histochemical studies, this is achieved by adding organic acids like chloroform and acetic acid to the mixture that bind to the tissue via hydrogen bonds (Puchtler et al., 1968; Howat & Wilson, 2014). This role may be served in resins by multiple organic acids of sesqui-, di-, or triterpenoid origin that either act directly as natural fixatives or produce suitable compounds when reacting with additional resin compounds. It can be assumed that dehydration occurs in all amber inclusions as a natural process in their taphonomy but its effect (tissue shrinkage) is not always detected because of the counteracting nature of fixative compounds in the matrix. Therefore, it is hypothesised that dehydration is an important prerequisite for amber fossil preservation, but the crucial step to maintain the three-dimensional tissue structure regards fixation of the material. Additionally, the model properties by Poinar & Hess (1982, 1985) of inert dehydration in combination with natural embalming properties are not sufficient, because they indicate that the resin must be in contact with the preserved tissues. However, as experienced in the experiments presented in this thesis and shown by multiple examples in the literature, resin is not required to be inside the inclusion to enable ultrastructural, or at least internal tissue preservation (Grimaldi et al., 1994; Henwood, 1992a, b; McCoy et al., 2018a, b; Barthel et al., 2021).

Fossilisation through infiltration

Another explanation for the fossilisation mode in amber is provided by Grimaldi et al. (1994), who proposed that due to a lack of shrinkage and autolysis in their samples, a thorough and rapid cellular fixation must have taken place in amber inclusions. They propose that low molecular weight compounds of the resins' volatile fraction (specifically mono and sesquiterpenoids) diffuse through intact body walls and perfuse the tissue of the trapped organism by replacing cellular water. In this case, intersegmental membranes would be an important area of diffusion, because the cuticle is not as thick in these structures as in other areas of the arthropod body (Grimaldi et al., 1994). The authors conclude that the role of monosaccharides and other compounds is not as significant as that of terpenoids in terms of tissue preservation, because of their much lower concentration and thus slower perfusion rates. This hypothesis suggests that the resin (more specifically its non-volatile fraction) does not need to be in direct contact with the tissue to enable its preservation over geologic time scales, which is in accordance with observations of numerous amber fossils. The idea of tissue fixation through volatile resin compounds is supported by Stankiewicz et al. (1998), who showed that bicyclic resin compounds were present in high abundance in tissues of Dominican amber fossils. However, the results by Stankiewicz et al. (1998) do not precisely explain how these volatiles may have reached the tissues. Instead of a direct diffusion of these compounds through the integument or membranes into the haemolymph and tissues (Grimaldi et al., 1994), another mode of action is suggested here. According to the results of Gerolt (1969) on dieldrin uptake and transportation in several insect groups, synchrotron data of Zhangpu amber fossils indicate that volatile resin compounds reach the tissues over the tracheal system (chapter 5.3).

The bicyclic compounds evidenced by Stankiewicz et al. (1998) in their amber fossils had molecular weights of approximately 190, 192, 204, 206, and 220 Da and were even present in tissues that were not in direct contact with the resin. Stankiewicz et al. (1998) assume a formation of cross-links between the tissue of the bioinclusion and these compounds, which would result in the stabilisation of the former. Especially cadinene based bicyclic compounds such as cadalene could be involved in this process, because they are evidenced in *Hymenaea* and dammar resins (Langenheim et al., 1978; Mallick et al., 2014), and have a molecular weight of 198 to 206 Da (Dutta et al., 2009).

With regard to the biomolecular preservation in amber, no intact proteins have been extracted from amber fossils so far. This indicates that, beside cross-linking, denaturation mechanisms

may also be involved in the fossilisation of amber-embedded arthropods. Denaturation accompanies the defunctionalisation of proteins and leads to a loss of their secondary, tertiary, and quaternary structure, but does not act on amino acids (primary structure). As shown within this thesis, amino acids can be extracted from Cambay and Zhangpu amber fossils, but their concentration is too low to allow for protein sequencing.

Endogenous fossilisation in amber?

In order to explain the preservation of amino acids and DNA in amber fossils, Bada et al. (1999) suggested that these original biomolecules undergo Maillard-type condensation reactions. Although reports on DNA preservation have been shown to be the result of contamination or could not be reproduced, Maillard reactions could still be a viable option to explain the preservation of biomolecules in amber. Maillard reactions have been shown to play a role in the preservation of original molecules in vertebrate and invertebrate fossils across different geological periods and fossilise proteins, sugars, and lipids through oxidative cross-linking into heterocyclic compounds rich in O, S, and N (Wiemann et al., 2018, 2020). These compounds are much more stable with respect to hydrolysis and can include high molecular weight compounds of several thousand daltons (Bada et al., 1999). *N*-heterocyclic compounds give rise to a prominent Raman band at around 1570-1580 cm^{-1} (Wiemann et al., 2018, 2020). This band is present as a broad, indistinctive feature in a single spectrum of the fossil anole (Fig. 22), but was not present in any insect tissue spectrum of this thesis, including those from Defaunation resin (Fig. 10). In addition, it is proposed that Maillard reactions do not remodel the sugars, proteins, and lipids of invertebrate tissues (Wiemann et al., 2020), but no traces of proteins were evident in insect tissue from amber (Stankiewicz et al., 1998, Edwards et al., 2007). However, it cannot be excluded that Maillard reactions partially take place in amber fossils, because they are endogenous (Wiemann et al., 2020). In any case, it is strongly indicated by the previous observations that these reactions do not represent the major type of fossilisation in amber.

In summary, the hypothesis of a rapid tissue fixation through volatile resin compounds (Grimaldi et al., 1994) is still valid and represents the best explanation of ultrastructural and biomolecular preservation in amber. Volatile resin compounds likely reach the tissues indirectly by diffusing into the integument and being transported along the tracheal system. Cadinene based bicyclic terpenoids are presumably involved in the fossilisation process, but it has to be examined to which extent additional compounds may contribute. This main mechanism of tissue stabilisation in amber probably involves a combination of cross-linking and denaturing

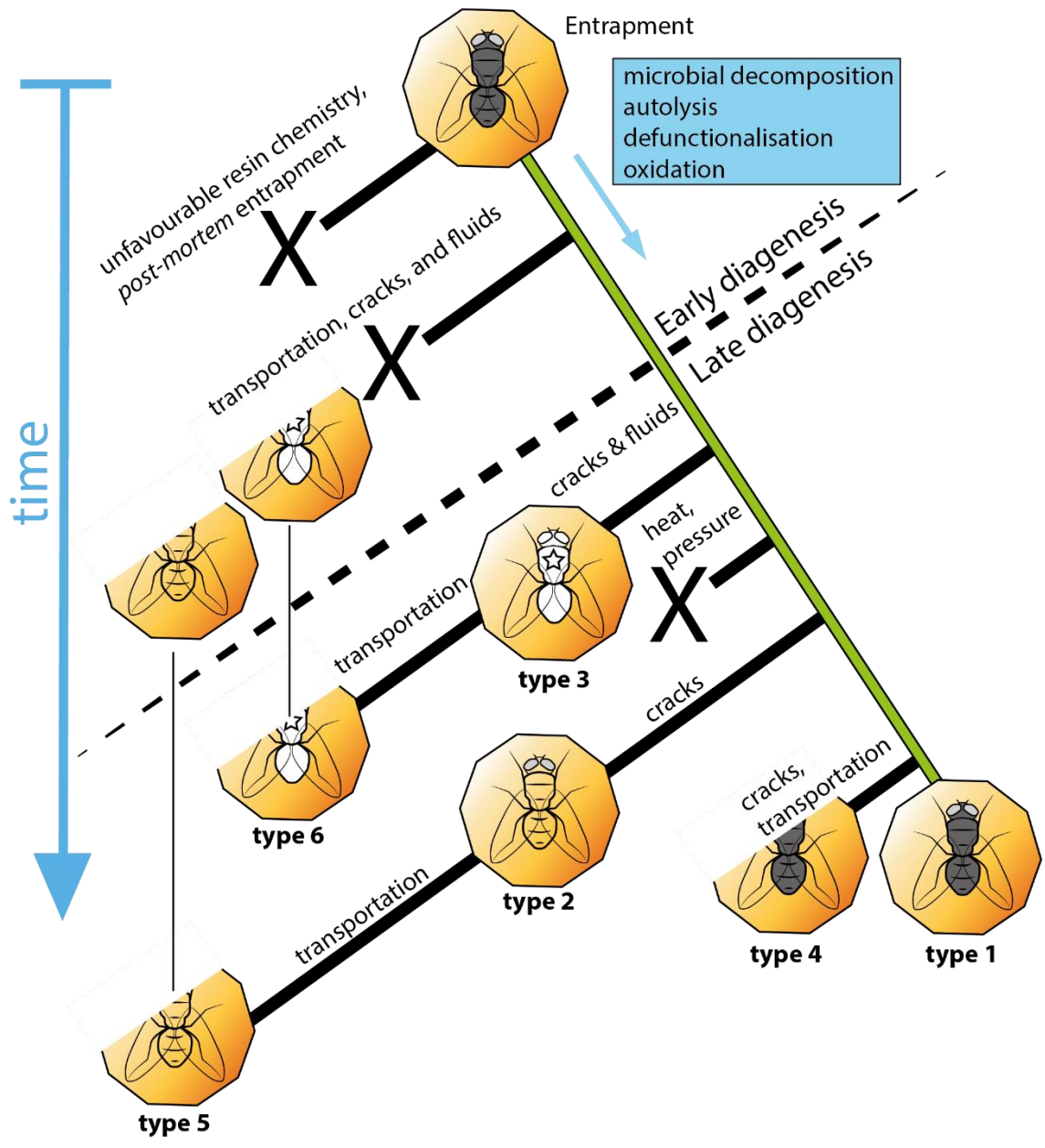
fixation and is accompanied by dehydration and possibly Maillard reactions. It is possible that different types of tissues are preserved by different mechanisms within the same fossil, based on their original composition and characteristics. Although the mode and pathway of fossilisation in amber seem clear, the specific volatile-tissue interactions have to be examined in the future.

6.1.2 Amber fossil types and their diagenetic history

After reviewing collection material and literature reports, six main types of amber fossils can be distinguished (Fig. 23). These types can be further subdivided into completely surrounded specimens and such that are exposed to the surface. The surrounded specimens comprise inclusions with preserved internal tissues (type 1), hollow casts (type 2), and hollow casts with mineral infillings (type 3). Exposed specimens can either contain internal tissues (type 4) or are present as hollow casts (type 5) or only imprints (type 6) of former body parts in the matrix.

The different types are the result of varying taphonomic influences, comprising resin chemistry, autolysis, microbial decomposition, maturation, temperature, formation of cracks, external and internal water availability, and depositional environment.

Type 1 inclusions (completely surrounded inclusions with internal tissues) can be regarded as the favourable outcome of amber taphonomy and represent the best preserved specimens in terms of original tissue structure and composition. Other preservation types can be regarded as taphonomic alterations of this optimal fossilisation pathway whereby the timing of the influencing processes can play a major role (Fig. 23). The process of fossilisation in amber can be best imagined as a dichotomous pathway that either leads to a loss of internal tissues (visualised by a branching, cf. Fig. 23), or their preservation (Barthel et al., 2021). It has to be emphasised that the branching along this pathway (= loss of tissues) can happen at any time during taphonomy, even after excavation of the pieces.



Legend









-  inclusion with internal tissues
-  hollow inclusion
-  mineral formations
-  intact amber piece
-  exposed inclusion (fracturing, cracks)
-  destruction of inclusion or amber piece
-  possible alterations
-  optimal pathway

Figure 23. Fossil types and their origin. The taphonomy of amber fossils can be regarded as the result of a dichotomous branching, caused by diagenetic factors. These factors either lead to tissue preservation or destruction over geological time scales and start with the entrapment of the organism. Their temporal occurrence has a strong influence on the preservation quality.

Previous experiments demonstrate that there must be some chemical interaction between the embedding medium and the inclusion (Henwood, 1992a; Stankiewicz et al., 1998; McCoy et al., 2018b). Therefore, it can be hypothesised that these interactions control the early dichotomous branching between soft tissue preservation and soft tissue degradation in early diagenesis. In this case, resin chemistry would be the most influential factor and is sufficient to explain the fossilisation mechanism. However, it can be expected that resin compounds not only interact with tissues, but also with the microbiota or enzymes of the inclusion. It has been shown that terpenoids inhibit microbiotic (e.g. Savluchinske Feio et al., 1999) and enzymatic (Miyazawa & Yamafuji, 2005; Adamczyk et al., 2015) activity, suggesting that these interactions deserve more study. In any case, it can be expected that the loss or preservation of tissues is already determined during early diagenesis. The fate of tissue preservation over long time periods is then controlled by late diagenetic processes, implying further biochemical changes as the fossil continues down the tissue preservation branch. These biochemical changes do not represent dichotomous branches but rather continuous changes (Barthel et al., 2021) and are responsible for differences in the tissue preservation of type 1 and type 4 amber fossils.

The absence of internal tissues in type 2 amber fossils may be caused by several reasons, for example unfavourable original resin chemistry, leading to insufficient microbial inhibition and/or enzymatic activity, as well as the early diagenetic formation of cracks and fissures that enable infiltration by fluids or microbes. Type 3 fossils (with mineral infillings) are probably affected by the same mechanisms except that infiltrating fluids were rich in ions, enabling mineral replacement of different parts of the animal. Previous studies report only on pyritisation of inclusions (Baroni-Urbani & Graeser, 1987; Schlüter, 1989; Kowalewska & Szwed, 2009) whereas this thesis reports on silica and carbonate phase precipitation in fossils from Baltic and Dominican amber. Screening of Cambay amber material revealed that several pieces contain pyrite, but to date this observation is limited to the matrix, with no pyrite detected within the inclusions. Mineralisation of amber fossils may occur during any point of diagenesis and shows that the depositional environment and its water chemistry have an effect on the chances of tissue preservation in amber.

Type 4 and 5 fossils are interpreted to be the result of transportation processes that either allowed infiltration (type 5, without tissues) or took place in such a late phase of diagenesis that the exposure occurred only recently (type 4). Type 6 fossils represent imprints of former organismal body parts on the amber surface. They must have been exposed for long time spans, because even the cuticle, which is present in all other amber fossil types, is not preserved anymore. These fossils are the result of severe biological or chemical degradation.

Based on the six major fossil types described before, several subtypes may exist. These include isolated organismal remains, fossils covered by fungal mycelium or decay gases (“Verlumung”), and fossils with ruptured abdomens. Isolated legs, antennae, or other body parts can be the result of successful escape attempts from the viscous resin of the formerly trapped arthropod or may derive from formerly isolated body parts that were driven into the resin by wind or other processes (Martínez-Delclós et al., 2004). Fungal coatings of inclusions (e.g. Speranza et al., 2010, 2015; Halbwachs, 2019) or trapped decay gases indicate, that the inclusion was not completely covered by a single resin flow and exposed at the surface until it was finally covered by a subsequent resin flow (Martínez-Delclós et al., 2004). However, fungal mycelia in amber that are limited to the matrix may represent more recent contamination instead of true bioinclusions (Speranza et al., 2015). The time of exposure has a crucial impact on the overall preservation of internal tissues, because during this time, the carcass is subjected to decay processes under usual atmospheric conditions, and the fixing effect of resin is hampered or at least limited to a certain part of the animal’s body.

Ruptured abdomens can be observed in several inclusions of amber and indicate that the microbiota, especially the gut biota, was not sufficiently inhibited by resin compounds (c.f. McCoy et al., 2018b). It is hypothesised that these fossils are the result of gas accumulations in the abdomen as a cause of *post-mortem* microbial activity. It could be that based on their initial gut biota, fossils from different taxa have not the same preservation potential, but this has not been studied so far. With respect to decay gas accumulations, another factor that has not been studied yet is the timely availability of body fluids in amber fossils. It is known that in the early decay process, body fluids are produced by enzymatic breakdown of original tissue (Aufderheide, 2011). These newly produced body fluids may react with the more resistant tissues, leading to complex interactions. The analysis of resin-embedded beetles (chapter 5.5; Peris et al., 2020) showed that their tissues contain internal waters for some years after entrapment. This is problematic with regard to DNA preservation and may be disadvantageous for other tissues or biomolecules as well.

6.1.2 Differences in tissue preservation of amber fossils

Only two out of six types of amber fossils contain internal tissues (type 1 and type 4). The examination of such fossils in this thesis and previous studies indicate that internal tissues do not have the same chance to become preserved, with most records being on tracheal parts or muscle tissue (reviewed in Barthel et al., 2021). This chapter deals with the differences of tissue preservation in amber and lists possible explanations for the observed patterns. In terms of tissue preservation, it is important to distinguish between the tissue and ultrastructural (cellular and sub-cellular) level. Where possible, the chemical composition should be taken into account as well, because the presence of a certain tissue does not necessarily mean that original compounds are preserved. On the tissue level, the preservation of the cuticle, respiratory, nervous, muscle, and digestive tissue could be assessed, whereas on the ultrastructural level only mitochondria were examined in this thesis.

The cuticle is visually present in amber fossils of types 1-5 and appears to be the best preserved tissue. It is not present in type 6 fossils that only consist of imprints in the amber matrix. In addition, it is questionable to which extent the original cuticle is preserved in samples that have been altered by mineral infillings (type 3). Synchrotron scans showed that the cuticle is present in every sample of Zhanpgu amber (chapter 5.3) and extraction of Cambay amber fossils indicate the preservation of cuticle from this deposit as well (Rust et al., 2010; Mazur et al., 2014).

Arthropod cuticle is a composite material consisting of variable amounts of chitin (polysaccharide) and protein (peptides) and is responsible for the different colours of insect bodies. Inorganic compounds like calcite may be incorporated as well, especially in the hard carapaces of crustaceans. The cuticle of amber arthropods exhibits various shades of brown, regardless of the age of the sample or its phylogenetic affiliation, which indicates some degree of alteration or chemical reaction. It has been shown that the cuticle in amber insects does not contain protein signatures, but aliphatic carbon compounds that can be assigned to the original chitin (Stankiewicz et al., 1998). Thus, the uniform colouration of amber insects can be attributed to the degradation of protein complexes in the cuticle, which seem to be less stable than the preserved but severely altered chitin component. Degradation of cuticle components was also apparent in the TEM samples of this thesis (chapter 5.1) where only the epicuticle, the most external part of the structure, was preserved. In consequence, the visual evidence of cuticle in amber fossils is assigned to aliphatic carbon compounds that do not represent intact tissue.

However, chitin and its decay products are stable over geological time scales (Ehrlich et al., 2013) and could be evidenced already in early attempts on exceptional preservation in amber (von Lengerken 1913, 1922).

The stability of chitin is probably also the reason for the common reports on tracheal remains in amber fossils. Trachea are canals of the respiratory system of insects and spiders (tracheal system) and transport oxygen to the internal tissues. They are coated internally and externally with cuticle tissue and can be easily identified via light microscopy after sample preparation. Similar to the case of cuticle preservation, it can be expected that the presence of tracheal remains in amber arthropods is due to aliphatic carbon compounds that are stable enough to reflect the original tissue structure. The respiratory system was not examined with synchrotron scans, but TEM of a Cambay amber spider revealed the presence of the book lung even though the surrounding tissue was absent, which again argues for the stability of these compounds compared to other tissues (chapter 5.1). In addition, it is hypothesised that the transport of external resin compounds takes place along the tracheal system. In this case, the respiratory system is severely exposed to those reactive volatiles, which may further explain the abundant preservation of tracheal remains in amber embedded arthropods.

In contrast to the cuticle, the internal muscle, nervous, and digestive tissue structures are purely composed of various cell types that contain specific protein and membranous components. These tissues are limited to type 1 and type 4 amber fossils. Among internal tissues, muscles are the most commonly reported in previous studies (reviewed in Barthel et al., 2021) and the examination with synchrotron scans supports these observations. The reports on muscle preservation over any other internal tissue in traditional studies (prior to the electron microscopic era) could be due to the characteristic striation of the tissue that can be easier identified during microscopic examination than other structures. The striation of muscle fibers is caused by sarcomeres, which contain parallel-orientated actin-myosin protein to enable the muscles' contraction.

In the synchrotron examination, most records of muscle tissue accord to the thoracic region which contains the strongly developed flight muscles in winged insects (chapter 5.3). Only in a few cases, muscles were evident in the appendages or head capsule.

In the samples of preservation class A (PC A), the nervous tissue of the head capsule, comprising the cerebral ganglia, medulla, and lobula, was nearly as often preserved as the thoracic muscle tissue and far more common than digestive tissue (Table 6). However, nervous tissue was only present when either muscle or digestive tissue was also present within the same

sample. Digestive tissue was by far the least preserved tissue in the Zhangpu amber fossils and is reported only in a few cases (Andrée & Keilbach, 1936; Petrunkevitch, 1950; Henwood, 1992b; Grimaldi et al., 1994).

Remarkably, the fat body is well preserved in an extant ethanol-stored wasp (chapter 5.3; Fig.13) whereas only one specimen of Zhangpu amber probably showed the preservation of this tissue in the abdomen. The fat body of insects consists of trophocytes and has excretory functions in contributing to the storage and synthesis of carbohydrates, lipids, and proteins.

On the ultrastructural level, mitochondria were found in the head region of a Cambay amber nematoceran, but other structures could not be identified (chapter 5.1). Considering the abundance and location of mitochondria in this sample, they must belong to the former cerebral ganglia. Besides mitochondria, reports on cellular components comprise nuclei, ribosomes, and endoplasmic reticuli (Poinar & Hess, 1982, 1985; Henwood, 1992a; Grimaldi et al., 1994). Mitochondria make up the most reports of ultrastructures in amber fossils, which is probably due to a combination of their characteristic shape that makes them and their membrane structure easy to identify. The nucleus and mitochondria of insect cells are the only components that possess a double lipid membrane layer. This double layer may be important in making the cell components more resistant to decay compared to other organelles and could explain why some organelles are more commonly preserved than others. This is in accordance with the observation of Grimaldi et al., (1994) who noted that membranous structures are more commonly preserved than proteinaceous ones in Baltic and Dominican amber fossils. Lipids can be extremely durable and have been evidenced even in fossils from the Ediacarian (Bobrovskiy et al., 2018). However, a degradation sequence of other ultrastructures could not be provided due to limited data.

The favoured preservation of certain structures is also apparent on the tissue level. Synchrotron examination of Zhangpu amber fossils (chapter 5.3) showed that there is a general trend in the frequency of preservation in distinct body parts: thoracic tissues are most commonly preserved, followed by tissues in the head capsule and abdomen. This pattern can be explained with the functionalisation of the different body parts, the structure, function, and abundance of the tissues found within them, and the characteristics of the tracheal system.

Food is transported through the arthropod body by the alimentary canal, but its processing is limited to the digestive organs in the abdomen (or opisthosoma). Here, the concentration of microbes and enzymes should be the highest among the body. In addition, organs that are involved in digestion, like the gut, fat body, or malpighian tubules are commonly folded to

increase their volume and to enhance their capacity of metabolic interactions. Of all the body parts in an arthropod, the probability of microbes or enzymes to be unharmed by infiltrating volatile resin compounds should be the highest within the abdomen. This would mean that although microbial decomposition or autolysis is severely inhibited, small “active” areas may prevail within the digestive tissue. To further test this assumption, it would be necessary to gain more information about the infiltration speed and the overall permeability of the cuticle. With respect to the cuticle thickness, which was also assumed being a factor in amber fossil taphonomy (Grimaldi et al., 1994), mostly weakly sclerotised dipteran fossils were analysed within the frame of this thesis. Although some coleopterans were analysed as well, the sample size is too low to allow any conclusions on a superordinate state regarding the cuticle thickness as an influence on tissue preservation. In addition, it is unclear to which extent molecular water or body liquids are present in entrapped arthropods. These liquid phases may cause complex interactions between the tissues in the abdomen and may contribute towards their degradation or preservation.

In contrast to the abdomen, the tissues in the head and thorax region predominantly consist of locomotory and nervous tissue. These tissues are not involved in synthesising or digesting complex metabolic compounds, which is why the concentration of microbes should be not as high as in the abdomen. The preservation potential of these tissues seems to be controlled more by their structure and physical integrity rather than microbial or enzymatic activity. Muscle tissue is built to last under mechanical pressure and consists of densely packed myofibrils that appear to be more robust than the neurons of the nervous tissue. This physical robustness might be an explanation for the preservation frequency of muscle tissue over nervous tissue. Muscle tissue was most commonly preserved in the thoracic region of Zhangpu amber fossils whereas only some of such fossils contained muscle tissue in the appendages. This discrepancy may derive from the sheer abundance of the tissue in the thorax: the larger the original tissue, the more likely parts of it are preserved.

The pattern of tissue preservation observed in amber fossils can also be explained by the structure and characteristics of the tracheal system. In traditional textbooks on entomology, a passive uptake of gaseous oxygen through the tracheal system is postulated. Although this passive mechanism takes place in insects, it is supported by the extension and contraction of abdominal segments within several groups of insects, especially those with a moderately to extensively sclerotised cuticle, such as Heteroptera, Hymenoptera, Coleoptera, and Blattodea.

Besides these mechanisms of oxygen uptake, it has been shown that active tracheal respiration occurs in the head capsule and thorax of insects, comparable to the inflating and deflating of the vertebrate lung (Westneat et al., 2003). The tracheal system is a complex network and its structure widely varies between insect taxa depending on their lifestyle. The tracheal system of *Drosophila* occurs as a densely packed network especially in the head capsule and thoracic segments, but less so in the abdomen (Pitsouli & Perrimon, 2010). This general structure may be comparable to other dipterans and could explain the favourable preservation of muscle and nervous tissues: infiltrating volatile resin compounds transported along the respiratory system would attain their highest concentration in such tissues that are supported by abundant tracheols. This model is suited to explain the pattern of tissue preservation in Zhangpu amber dipterans and should be tested on other arthropod taxa as well. If applicable, different degrees and frequencies of tissue preservation could be initially controlled by the bauplan of the trapped arthropod and the concentration of volatile compounds in the original resin.

6.2 Evaluation and future perspectives

I Description and documentation of exceptional preservation in amber fossils

This aim was achieved by intensive literature reviews and the projects performed in the frame of this thesis. Overall, six types of amber fossils could be identified. It was shown that ultrastructural preservation is not limited to class I ambers and occurs also in class II Cambay amber samples and much likely also in fossils from Zhangpu amber. For the first time, silicified and calcified fossils could be evidenced in Baltic and Dominican amber. This expands earlier reports on mineralisation processes in amber that were limited to pyritisation. Furthermore, it was proven that bioinclusions from Cambay and Zhangpu amber contain original amino acids.

II Improving the understanding of the taphonomy of resin-embedded arthropods

The model of amber taphonomy could be improved with respect to the early phase of fossilisation. It was shown that the fossilisation of amber arthropods begins with an infiltration by volatile resin compounds along the tracheal system. Therefore, besides other factors, the bauplan of an arthropod impacts its potential to maintain internal tissues over geological time scales. This model can be tested in the future on different arthropod taxa and amber deposits. Fossilisation in amber is a truly unique mode and represents a combination of tissue fixation with a physical sealing, unmatched by any other Konservat-Lagerstätte.

III Comparing the preservation quality between different deposits

Previous studies already showed that the preservation quality varies between amber deposits in respect to morphological and biomolecular preservation. This thesis shows that the frequency of morphological preservation in Zhangpu amber (class II) fossils reaches 90%, which is close to the 94% reported in Dominican amber (class I). Although the results on Dominican amber are based on a smaller data set, these results indicate that the potential for tissue preservation is about the same for ambers of different classes. Remarkably, both deposits are Miocene in age. A comparison with material of older deposits might help to identify age-related or diagenetic differences in the extent and quality of tissue preservation.

The biomolecular preservation also varied between fossils of different amber deposits. No amino acids were detected in a lizard bone from Miocene Dominican amber, whereas arthropod inclusions from Zhangpu (Miocene) and Cambay (Eocene) amber contained original amino

acids. These results indicate that the potential of biomolecular preservation is coupled to diagenetic processes and not only age related. It has to be noted that a comparative study under standardised conditions should be carried out on fossils from different amber deposits in order to quantify and assess the extent of biomolecular preservation.

IV Examining the limits of fossilisation in amber

Investigation of a lizard forelimb in Dominican amber revealed that the mineral and organic phase of the bone has been severely altered. The bone apatite was transformed into francolite and the organic phase consisted only of aliphatic carbon compounds. So far, no evidence of complex biomolecules in Dominican amber has been reported.

Several original amino acids were extracted from fossils of Zhangpu and Cambay amber.

This result holds a lot of potential for further investigations, although some methodological improvements should be carried out beforehand. To date, there is no evidence of macromolecular preservation in different amber deposits and with respect to proteins, the limit of fossilisation in amber represents single amino acids. The preservation of lipids has not been examined so far and the results on polysaccharides (such as chitin) provide an indistinct pattern, ranging from intact chitin in Baltic amber to aliphatic carbon compounds in Dominican amber. Experiments with extant platypodid beetles showed that it is possible to obtain DNA from resin-embedded arthropods. This represents an initial basis for future studies to examine the limits of DNA preservation in amber in a step-by-step approach.

General remarks on future perspectives

Possible factors influencing amber preservation, such as internal and external fluid phases, matrix permeability, sedimentary environment, degree of sclerotization, and thermal history of the sample are discussed in the literature, but have never been studied extensively (Poinar & Hess, 1985; Grimaldi et al., 1994; Martínez-Delclòs et al., 2004; Ragazzi & Schmidt, 2011; McCoy et al., 2018b). Although gas is reported to penetrate amber (Hopfenberg et al., 1988), experiments on the permeability with regard to fluids have never been conducted. Examining these factors in detail would have been far beyond the frame of this thesis but they offer promising perspectives on improving our understanding of amber taphonomy in future studies.

7.0 Conclusions

- Exceptional preservation of ultrastructures is evident in fossils from Eocene Cambay amber and thus is not limited to class I ambers. TEM analyses proved the presence of mitochondria in a chironomid and the preservation of the book lung of a spider.
- In Zhangpu amber fossils, muscle tissue and tracheal remains are most commonly preserved, followed by nervous tissue of the head capsule. Abdominal tissues are infrequently preserved. This is in accordance with a general pattern observed in earlier studies. It is likely that abdominal tissues in Zhangpu amber fossils express the same quality when compared to tissues of other body parts.
- Previous studies report that the potential of internal soft tissue preservation varies between amber deposits of different ages and localities. This thesis shows that the potential of class I and II ambers to preserve internal soft tissues is about the same as long as favourable conditions are met.
- This potential is coupled to the specific arthropod's organisation and external factors, especially composition and concentration of volatile resin compounds. The pattern of internal tissue preservation is explained by an infiltration of volatile resin compounds along the tracheal system of the embedded arthropod.
- With regard to peptides, single amino acids are the limit of fossilisation in amber. No larger protein remains of secondary, tertiary or quaternary structure have been found.
- Deviations in the preservation of biomolecules from different amber deposits are most likely due to age and diagenetic factors.
- Evidence of original biomolecules in amber fossils holds great potential for future analyses.

8.0 References

- Abelson, P.H., 1954. Amino acids in fossils. *Science* 119, 576.
- Adamczyk, S., Adamczyk, B., Kitunen, V., Smolander, A., 2015. Monoterpenes and higher terpenes may inhibit enzyme activities in boreal forest soil. *Soil Biology and Biochemistry* 87, 59–66. <https://doi.org/10.1016/j.soilbio.2015.04.006>
- Aksamija, A., Mathe, C., Vieillescazes, C., 2012. Liquid chromatography of triterpenic resins after derivatiation with dansyl chloride. *Journal of Liquid Chromatography & Related Technologies* 35, 1222–1237. <https://doi.org/10.1080/10826076.2011.619032>
- Alimohammadian, H., Sahni, A., Patnaik, R., Rana, R.S., Singh, H., 2005. First record of an exceptionally diverse and well preserved amber-embedded biota from Lower Eocene (ca. 52 Ma) lignites, Vastan, Gujarat. *Current Science* 89, 1328–1330.
- Allison, P.A., 1988. *Konservat-Lagerstätten: cause and classification*. *Paleobiology* 14, 331–344. <https://doi.org/10.1017/S0094837300012082>
- Anderson, A.B., Riffer, R., Wong, A., 1969. Monoterpenes, fatty and resin acids of *Pinus ponderosa* and *Pinus jeffreyi*. *Phytochemistry* 8, 873–875. [https://doi.org/10.1016/S0031-9422\(00\)85876-8](https://doi.org/10.1016/S0031-9422(00)85876-8)
- Anderson, K., 1994. The nature and fate of natural resins in the geosphere—IV.* Middle and Upper Cretaceous amber from the Taimyr Peninsula, Siberia - evidence for a new form of polyabdanoid of resinite and revision of the classification of Class I resinites. *Organic Geochemistry* 21, 209–212.
- Anderson, K.B., 1996. The nature and fate of natural resins in the geosphere—VII. A radiocarbon (¹⁴C) age scale for description of immature natural resins: an invitation to scientific debate. *Organic Geochemistry* 25, 251–253. [https://doi.org/10.1016/S0146-6380\(96\)00137-4](https://doi.org/10.1016/S0146-6380(96)00137-4)
- Anderson, K.B., Botto, R.E., 1993. The nature and fate of natural resins in the geosphere—III.* Re-evaluation of the structure and composition of Highgate Copalite and Giessite. *Organic Geochemistry* 20, 1027–1038.
- Anderson, K.B., LePage, B., 1995. Analysis of fossil resins from Axel Heiberg Island, Canadian Arctic, in: Anderson, K., Crelling, J.C. (Eds.), *Amber, Resinite, and Fossil Resins*, American Chemical Society Symposium Series. American Chemical Society, Washington D.C., pp. 170–192.
- Anderson, K.B., Muntean, J.V., 2000. The nature and fate of natural resins in the geosphere. Part X.† Structural characteristics of the macromolecular constituents of modern Dammar resin and Class II ambers. *Geochem Trans* 1, 1. <https://doi.org/10.1186/1467-4866-1-1>
- Anderson, K.B., Winans, R.E., 1991. Nature and fate of natural resins in the geosphere. I. Evaluation of pyrolysis-gas chromatography mass spectrometry for the analysis of natural resins and resinites. *Analytical Chemistry* 63, 2901–2908.
- Anderson, K.B., Winans, R.E., Botto, R.E., 1992. The nature and fate of natural resins in the geosphere —II.* Identification, classification and nomenclature of resinites. *Organic Geochemistry* 18, 829–841.
- Andrée, K., 1951. *Der Bernstein. Das Bernsteinland und sein Leben*. Kosmos. Gesellschaft der Naturfreunde, Stuttgart.
- Andrée, K., Keilbach, 1936. Neues über Bernsteineinschlüsse. *Schriften der Physikalisch-Ökonomischen Gesellschaft zu Königsberg in Preußen* 69, 124–128.
- Armbruster, W.S., 1984. The role of resin in angiosperm pollination: ecological and chemical considerations. *American Journal of Botany* 71, 1149–1160. <https://doi.org/10.1002/j.1537-2197.1984.tb11968.x>
- Armbruster, W.S., 1993. Evolution of plant pollination systems: hypotheses and tests with the neotropical vine *Dalechampia*. *Evolution* 47, 1480–1505.

- Arnold, E.N., Azar, D., Ineich, I., Nel, A., 2002. The oldest reptile in amber: a 120 million year old lizard from Lebanon. *Journal of Zoology* 258, 7–10.
<https://doi.org/10.1017/S0952836902001152>
- Asara, J.M., Schweitzer, M.H., Freimark, L.M., Phillips, M., Cantley, L.C., 2007. Protein sequences from *Mastodon* and *Tyrannosaurus rex* revealed by mass spectrometry. *Science* 316, 280–285. <https://doi.org/10.1126/science.1137614>
- Aufderheide, A.C., 2011. Soft tissue taphonomy: A paleopathology perspective. *International Journal of Paleopathology* 1, 75–80. <https://doi.org/10.1016/j.ijpp.2011.10.001>
- Austin, J.J., Smith, A.B., Thomas, R.H., 1997a. Palaeontology in a molecular world: the search for authentic ancient DNA. *Trends in Ecology & Evolution* 12, 303–306.
- Austin, J.J., Ross, A.J., Smith, A.B., Fortey, R.A., Thomas, R.H., 1997b. Problems of reproducibility—does geologically ancient DNA survive in amber-preserved insects? *Proceedings of the Royal Society of London B: Biological Sciences* 264, 467–474.
<https://doi.org/10.1098/rspb.1997.0067>
- Azar, D., 1997. A new method for extracting plant and insect fossils from Lebanese amber. *Palaeontology* 40, 1027–1029.
- Azar, D., Gèze, R., El-Samrani, A., Maalouly, J., Nel, A., 2010a. Jurassic amber in Lebanon. *Acta Geologica Sinica (English Edition)* 84, 977–983.
- Azar, D., Gèze, R., Acra, F., 2010b. Lebanese amber, in: Penney, D. (Ed.), *Biodiversity of Fossils in Amber from the Major World Deposits*. Siri Scientific Press, Manchester, pp. 271–298.
- Bada, J.L., 1971. Kinetics of the nonbiological decomposition and racemization of amino acids in natural water, in: Hem, J.D. (Ed.), *Nonequilibrium Systems in Natural Water Chemistry, Advances in Chemistry*. American Chemical Society, Washington, D. C., pp. 309–331.
<https://doi.org/10.1021/ba-1971-0106>
- Bada, J.L., 1991. Amino acid cosmogeochemistry. *Philosophical Transactions of the Royal Society of London. Series B: Biological Sciences* 333, 349–358.
<https://doi.org/10.1098/rstb.1991.0084>
- Bada, J.L., Schroeder, R.A., 1975. Amino acid racemization reactions and their geochemical implications. *Naturwissenschaften* 62, 71–79. <https://doi.org/10.1007/BF00592179>
- Bada, J.L., Kvenvolden, K.A., Peterson, E., 1973. Racemization of amino acids in bones. *Nature* 245, 308–310.
- Bada, J.L., Wang, X.S., Poinar, H.N., Pääbo, S., Poinar, G.O., 1994. Amino acid racemization in amber-entombed insects: Implications for DNA preservation. *Geochimica et Cosmochimica Acta* 58, 3131–3135.
- Bada, J.L., Wang, X.S., Hamilton, H., 1999. Preservation of key biomolecules in the fossil record: current knowledge and future challenges. *Philosophical Transactions of the Royal Society B: Biological Sciences* 354, 77–87. <https://doi.org/10.1098/rstb.1999.0361>
- Bailleul, A.M., Zheng, W., Horner, J.R., Hall, B.K., Holliday, C.M., Schweitzer, M.H., 2020. Evidence of proteins, chromosomes and chemical markers of DNA in exceptionally preserved dinosaur cartilage. *National Science Review* 7, 815–822. <https://doi.org/10.1093/nsr/nwz206>
- Banerjee, A., Jha, M., Mittal, A.K., Thomas N. J., Misra, K.N., 2001. The effective source rocks in the north Cambay basin, India. *Marine and Petroleum Geology* 17, 1111–1129.
<https://doi.org/10.1306/61EEDB02-173E-11D7-8645000102C1865D>
- Bardet, N., Fernandez, M., 2000. A new ichthyosaur from the Upper Jurassic lithographic limestones of Bavaria. *Journal of Paleontology* 74, 503–511.
- Baroni Urbani, C., Graeser, S., 1987. REM-Analysen an einer pyritisierten Ameise aus Baltischem Bernstein. *Stuttgarter Beiträge zur Naturkunde (B)* 133, 1–16.
- Barthel, H.J., Fougereuse, D., Geisler, T., Rust, J., 2020. Fluoridation of a lizard bone embedded in Dominican amber suggests open-system behavior. *PLoS ONE* 15, e0228843.
<https://doi.org/10.1371/journal.pone.0228843>

- Barthel, H.J., McCoy, V.E., Rust, J., 2021. From ultrastructure to biomolecular composition: taphonomic patterns of tissue preservation in arthropod inclusions in amber, in: Gee, C.T., McCoy, V.E., Sander, P.M. (Eds.), *Fossilization: Understanding the Material Nature of Ancient Plants and Animals*. Johns Hopkins University Press, Baltimore, pp. 115–138.
- Bassolé, I.H.N., Juliani, H.R., 2012. Essential oils in combination and their antimicrobial properties. *Molecules* 17, 3989–4006. <https://doi.org/10.3390/molecules17043989>
- Beck, C.W., Wilbur, E., Meret, S., 1964. Infra-red spectra and origin of amber. *Nature* 201, 256–257.
- Beimforde, C., Seyfullah, L.J., Perrichot, V., Schmidt, K., Rikkinen, J., Schmidt, A.R., 2017. Resin exudation and resinicolous communities on *Araucaria humboldtensis* in New Caledonia. *Arthropod-Plant Interactions* 11, 495–505. <https://doi.org/10.1007/s11829-016-9475-3>
- Beltran, V., Salvadó, N., Butí, S., Pradell, T., 2016. Ageing of resin from *Pinus* species assessed by infrared spectroscopy. *Analytical and Bioanalytical Chemistry* 408, 4073–4082. <https://doi.org/10.1007/s00216-016-9496-x>
- Berryman, A.A., 1972. Resistance of conifers to invasion by bark beetle-fungus associations. *BioScience* 22, 598–602. <https://doi.org/10.2307/1296206>
- Bertazzo, S., Maidment, S.C.R., Kallepitis, C., Fearn, S., Stevens, M.M., Xie, H., 2015. Fibres and cellular structures preserved in 75-million-year-old dinosaur specimens. *Nature Communications* 6, 7352. <https://doi.org/10.1038/ncomms8352>
- Bisset, N.G., Chavanel, V., Lantz, J.-P., Wolff, R.E., 1971. Constituants sesquiterpéniques et triterpéniques des résines du genre *Shorea**. *Phytochemistry* 10, 2451–2463.
- Bisulca, C., Nascimbene, P.C., Elkin, L., Grimaldi, D.A., 2012. Variation in the deterioration of fossil resins and implications for the conservation of fossils in amber. *American Museum Novitates* 3734, 1–19. <https://doi.org/10.1206/3734.2>
- Bobrovskiy, I., Hope, J.M., Ivantsov, A., Nettersheim, B.J., Hallmann, C., Brocks, J.J., 2018. Ancient steroids establish the Ediacaran fossil *Dickinsonia* as one of the earliest animals. *Science* 361, 1246–1249. <https://doi.org/10.1126/science.aat7228>
- Borsuk-Bialynicka, M., Lubka, M., Böhme, W., 1999. A lizard from Baltic amber (Eocene) and the ancestry of the crown group lacertids. *Acta Palaeontologica Polonica* 44, 349–328.
- Brasier, M., Cotton, L., Yenney, I., 2009. First report of amber with spider webs and microbial inclusions from the earliest Cretaceous (c. 140 Ma) of Hastings, Sussex. *Journal of the Geological Society* 166, 989–997. <https://doi.org/10.1144/0016-76492008-158>
- Bray, P.S., Anderson, K.B., 2009. Identification of Carboniferous (320 million years old) Class Ic amber. *Science* 326, 132–134. <https://doi.org/10.1126/science.1177539>
- Bridges, J.R., 1987. Effects of terpenoid compounds on growth of symbiotic fungi associated with the southern pine beetle. *Phytopathology* 77, 83. <https://doi.org/10.1094/Phyto-77-83>
- Briggs, D.E.G., 2003. The role of decay and mineralization in the preservation of soft-bodied fossils. *Annual Review of Earth and Planetary Sciences* 31, 275–301. <https://doi.org/10.1146/annurev.earth.31.100901.144746>
- Briggs, D.E.G., Bottrell, S.H., Raiswell, R., 1991. Pyritization of soft-bodied fossils: Beecher's Trilobite Bed, Upper Ordovician, New York State. *Geology* 19, 1221–1224.
- Briggs, D.E., Moore, R.A., Shultz, J.W., Schweigert, G., 2005. Mineralization of soft-part anatomy and invading microbes in the horseshoe crab *Mesolimulus* from the Upper Jurassic Lagerstätte of Nusplingen, Germany. *Proceedings of the Royal Society B: Biological Sciences* 272, 627–632. <https://doi.org/10.1098/rspb.2004.3006>
- Brody, R.H., Edwards, H.G., Pollard, A.M., 2001. A study of amber and copal samples using FT-Raman spectroscopy. *Spectrochimica Acta Part A: Molecular and Biomolecular Spectroscopy* 57, 1325–1338.
- Brundin, M., Figdor, D., Sundqvist, G., Sjögren, U., 2013. DNA binding to hydroxyapatite: a potential mechanism for preservation of microbial DNA. *Journal of Endodontics* 39, 211–216.

- Buckley, M., Recabarren, O.P., Lawless, C., García, N., Pino, M., 2019. A molecular phylogeny of the extinct South American gomphothere through collagen sequence analysis. *Quaternary Science Reviews* 224, 105882. <https://doi.org/10.1016/j.quascirev.2019.105882>
- Büsse, S., von Grumbkow, P., Mazanec, J., Tröster, G., Hummel, S., Hörnschemeyer, T., 2017. Note on using nuclear 28S rDNA for sequencing ancient and strongly degraded insect DNA: Protocol for aDNA sequencing in insects. *Entomological Science* 20, 137–141. <https://doi.org/10.1111/ens.12242>
- Camargo, J.M.F., Grimaldi, D.A., Pedro, S.R.M., 2000. The extinct fauna of stingless bees (Hymenoptera: Apidae: Meliponini) in Dominican amber: two new species and redescription of the male of *Proplebeia dominica* (Wille and Chandler). *American Museum Novitates* 3293, 1–24.
- Cano, R.J., Poinar, H., Poinar, G.O., 1992a. Isolation and partial characterisation of DNA from the bee *Proplebeia dominicana* (Apidae: Hymenoptera) in 25–40 million year old amber. *Medical Science Research* 20, 249–251.
- Cano, R.J., Poinar, H.N., Roubik, D.W., Poinar Jr, G.O., 1992b. Enzymatic amplification and nucleotide sequencing of portions of the 18s rRNA gene of the bee *Proplebeia dominicana* (Apidae: Hymenoptera) isolated from 25–40 million year old Dominican amber. *Medical Science Research* 20, 249–251.
- Cano, R.J., Poinar, H.N., Pieniasek, N.J., Acra, A., Poinar, G.O., 1993. Amplification and sequencing of DNA from a 120–135-million-year-old weevil. *Nature* 363, 536–538.
- Cano, R.J., Borucki, M.K., Schweitzer, M., Poinar, H.N., Pollard, K.J., 1994. *Bacillus* DNA in fossil bees: an ancient symbiosis? *Applied and Environmental Microbiology* 60, 2164–2167.
- Clifford, D.J., Hatcher, P.G., 1995. Structural transformations of polylabdanoid resinites during maturation. *Organic Geochemistry* 23, 407–418. [https://doi.org/10.1016/0146-6380\(95\)00022-7](https://doi.org/10.1016/0146-6380(95)00022-7)
- Clifford, D.J., Hatcher, P.G., Botto, R.E., Muntean, V., Michels, B., Anderson, K.B., 1997. The nature and fate of natural resins in the geosphere—VIII.* NMR and Py-GC-MS characterization of soluble labdanoid polymers, isolated from Holocene class I resins. *Organic Geochemistry* 27, 449–464.
- Collins, M.J., Gernaey, A.M., Nielsen-Marsh, C.M., Vermeer, C., Westbroek, P., 2000. Slow rates of degradation of osteocalcin: Green light for fossil bone protein? *Geology* 28, 4.
- Collins, M.J., Penkman, K.E.H., Rohland, N., Shapiro, B., Dobberstein, R.C., Ritz-Timme, S., Hofreiter, M., 2009. Is amino acid racemization a useful tool for screening for ancient DNA in bone? *Proceedings of the Royal Society B: Biological Sciences* 276, 2971–2977. <https://doi.org/10.1098/rspb.2009.0563>
- Conway Morris, S., Robison, R.A., 1986. Middle Cambrian priapulids and other soft-bodied fossils from Utah and Spain. *Paleontological Contributions to the University of Kansas* 117, 1–22.
- Conwentz, H.W., 1890. Monographie der Baltischen Bernsteinbäume. Vergleichende Untersuchungen über die Vegetationsorgane und Blüten sowie über das Harz und die Krankheiten der Baltischen Bernsteinbäume. Kommissions-Verlag von Wilhelm Engelmann in Leipzig, Danzig.
- Cunningham, A., Martin, S.S., Langenheim, J.H., 1973. Resin acids from two Amazonian species of *Hymenaea*. *Phytochemistry* 12, 633–635.
- Cunningham, A., Gay, I.D., Oehlschlager, A.C., Langenheim, J.H., 1983. ¹³C NMR and IR analyses of structure, aging and botanical origin of Dominican and Mexican ambers. *Phytochemistry* 22, 965–968. [https://doi.org/10.1016/0031-9422\(83\)85031-6](https://doi.org/10.1016/0031-9422(83)85031-6)
- Cunningham, A., West, P.R., Hammond, G.S., Langenheim, J.H., 1987. The existence and photochemical initiation of free radicals in *Hymenaea* trunk resins. *Phytochemistry* 16, 1142–1143.

- Czapla, D., Natkaniec-Nowak, L., Drzewicz, P., 2016. Microhardness as a method for investigation of fossil resins. *Geology, Geophysics & Environment* 42, 63–64. <https://doi.org/10.7494/geol.2016.42.1.63>
- da Silva Oliveira, F.G., de Souza Araújo, C., Rolim, L.A., Barbosa-Filho, J.M., da Silva Almeida, J.R.G., 2018. The genus *Hymenaea* (Fabaceae): a chemical and pharmacological review, in: *Studies in Natural Products Chemistry*. Elsevier, pp. 339–388. <https://doi.org/10.1016/B978-0-444-64056-7.00012-X>
- Dal Corso, J., Roghi, G., Ragazzi, E., Angelini, I., Giaretta, A., Soriano, C., Delclòs, X., Jenkyns, H.C., 2013. Physico-chemical analysis of Albian (Lower Cretaceous) amber from San Just (Spain): implications for palaeoenvironmental and palaeoecological studies. *Geologica Acta* 11, 359–370.
- Dal Corso, J., Gianolla, P., Newton, R.J., Franceschi, M., Roghi, G., Caggiati, M., Raucsik, B., Budai, T., Haas, J., Preto, N., 2015. Carbon isotope records reveal synchronicity between carbon cycle perturbation and the “Carnian Pluvial Event” in the Tethys realm (Late Triassic). *Global and Planetary Change* 127, 79–90. <https://doi.org/10.1016/j.gloplacha.2015.01.013>
- Dal Corso, J., Bernardi, M., Sun, Y., Song, H., Seyfullah, L.J., Preto, N., Gianolla, P., Ruffell, A., Kustatscher, E., Roghi, G., Merico, A., Hohn, S., Schmidt, A.R., Marzoli, A., Newton, R.J., Wignall, P.B., Benton, M.J., 2020. Extinction and dawn of the modern world in the Carnian (Late Triassic). *Science Advances* 6, eaba0099. <https://doi.org/10.1126/sciadv.aba0099>
- Dauwe, B., Middelburg, J.J., Herman, P.M.J., Heip, C.H.R., 1999. Linking diagenetic alteration of amino acids and bulk organic matter reactivity. *Limnology and Oceanography* 44, 1809–1814. <https://doi.org/10.4319/lo.1999.44.7.1809>
- Daza, J.D., Bauer, A.M., 2012. A new amber-embedded sphaerodactyl gecko from Hispaniola, with comments on morphological synapomorphies of the Sphaerodactylidae. *Breviora* 529, 1–28. <https://doi.org/10.3099/529.1>
- Daza, J.D., Bauer, A.M., Wagner, P., Böhme, W., 2013. A reconsideration of *Sphaerodactylus dommeli* Böhme, 1984 (Squamata: Gekkota: Sphaerodactylidae), a Miocene lizard in amber. *Journal of Zoological Systematics and Evolutionary Research* 51, 55–63. <https://doi.org/10.1111/jzs.12001>
- Daza, J.D., Stanley, E.L., Wagner, P., Bauer, A.M., Grimaldi, D.A., 2016. Mid-Cretaceous amber fossils illuminate the past diversity of tropical lizards. *Science Advances* 2, e1501080–e1501080. <https://doi.org/10.1126/sciadv.1501080>
- De Gelder, J., De Gussem, K., Vandenabeele, P., Moens, L., 2007. Reference database of Raman spectra of biological molecules. *Journal of Raman Spectroscopy* 38, 1133–1147. <https://doi.org/10.1002/jrs.1734>
- de Navarro, J.M., 1925. Prehistoric routes between Northern Europe and Italy defined by the amber trade. *The Geographical Journal* 66, 481. <https://doi.org/10.2307/1783003>
- Delclòs, X., Peñalver, E., Ranaivosoa, V., Solórzano-Kraemer, M.M., 2020. Unravelling the mystery of “Madagascar copal”: Age, origin and preservation of a Recent resin. *PLoS ONE* 15, e0232623. <https://doi.org/10.1371/journal.pone.0232623>
- Dell, B., McComb, A.J., 1978. Biosynthesis of resin terpenes in leaves and glandular hairs of *Newcastelia viscida*. *Journal of Experimental Botany* 29, 89–95.
- Demarchi, B., Hall, S., Roncal-Herrero, T., Freeman, C.L., Woolley, J., Crisp, M.K., Wilson, J., Fotakis, A., Fischer, R., Kessler, B.M., Rakownikow Jersie-Christensen, R., Olsen, J.V., Haile, J., Thomas, J., Marean, C.W., Parkington, J., Presslee, S., Lee-Thorp, J., Ditchfield, P., Hamilton, J.F., Ward, M.W., Wang, C.M., Shaw, M.D., Harrison, T., Domínguez-Rodrigo, M., MacPhee, R.D., Kwekason, A., Ecker, M., Kolska Horwitz, L., Chazan, M., Kröger, R., Thomas-Oates, J., Harding, J.H., Cappellini, E., Penkman, K., Collins, M.J., 2016. Protein sequences bound to mineral surfaces persist into deep time. *eLife* 5, e17092. <https://doi.org/10.7554/eLife.17092>

- DeSalle, R., Gatesy, J., Wheeler, W., Grimaldi, D., 1992. DNA sequences from a fossil termite in Oligo-Miocene amber and their phylogenetic implications. *Science* 257, 1933–1936.
- Dirzo, R., Young, H.S., Galetti, M., Ceballos, G., Isaac, N.J.B., Collen, B., 2014. Defaunation in the Anthropocene. *Science* 345, 401–406. <https://doi.org/10.1126/science.1251817>
- Drzewicz, P., Natkaniec-Nowak, L., Czaplá, D., 2016. Analytical approaches for studies of fossil resins. *Trends in Analytical Chemistry* 85, 75–84. <https://doi.org/10.1016/j.trac.2016.06.022>
- Dumont, M., Kostka, A., Sander, P.M., Borbely, A., Kaysser-Pyzalla, A., 2011. Size and size distribution of apatite crystals in sauropod fossil bones. *Palaeogeography, Palaeoclimatology, Palaeoecology* 310, 108–116. <https://doi.org/10.1016/j.palaeo.2011.06.021>
- Dutta, S., Mallick, M., 2017. Chemical evidence for dammarenediol, a bioactive angiosperm metabolite, from 54Ma old fossil resins. *Review of Palaeobotany and Palynology* 237, 96–99. <https://doi.org/10.1016/j.revpalbo.2016.11.004>
- Dutta, S., Mallick, M., Bertram, N., Greenwood, P.F., Mathews, R.P., 2009. Terpenoid composition and class of Tertiary resins from India. *International Journal of Coal Geology* 80, 44–50. <https://doi.org/10.1016/j.coal.2009.07.006>
- Dutta, S., Mallick, M., Kumar, K., Mann, U., Greenwood, P.F., 2011. Terpenoid composition and botanical affinity of Cretaceous resins from India and Myanmar. *International Journal of Coal Geology* 85, 49–55. <https://doi.org/10.1016/j.coal.2010.09.006>
- Dutta, S., Kumar, S., Singh, H., Khan, M.A., Barai, A., Tewari, A., Rana, R.S., Bera, S., Sen, S., Sahni, A., 2020. Chemical evidence of preserved collagen in 54-million-year-old fish vertebrae. *Palaeontology* 63, 195–202. <https://doi.org/10.1111/pala.12469>
- Dwivedi, S.K., Dey, S., Swarup, D., 1997. Hydrofluorosis in water buffalo (*Bubalus bubalis*) in India. *Science of The Total Environment* 207, 105–109. [https://doi.org/10.1016/S0048-9697\(97\)00247-7](https://doi.org/10.1016/S0048-9697(97)00247-7)
- Edwards, H.G.M., Farwell, D.W., 1996. Fourier transform-Raman spectroscopy of amber. *Spectrochimica Acta Part A: Molecular and Biomolecular Spectroscopy* 52, 1119–1125. [https://doi.org/10.1016/0584-8539\(95\)01643-0](https://doi.org/10.1016/0584-8539(95)01643-0)
- Edwards, H.G.M., Farwell, D.W., Villar, S.E.J., 2007. Raman microspectroscopic studies of amber resins with insect inclusions. *Spectrochimica Acta Part A: Molecular and Biomolecular Spectroscopy* 68, 1089–1095. <https://doi.org/10.1016/j.saa.2006.11.037>
- Edwards, N.P., Barden, H.E., van Dongen, B.E., Manning, P.L., Larson, P.L., Bergmann, U., Sellers, W.I., Wogelius, R.A., 2011. Infrared mapping resolves soft tissue preservation in 50 million year-old reptile skin. *Proceedings of the Royal Society B: Biological Sciences* 278, 3209–3218. <https://doi.org/10.1098/rspb.2011.0135>
- Ehrlich, H., Rigby, J.K., Botting, J.P., Tsurkan, M.V., Werner, C., Schwille, P., Petrášek, Z., Pisera, A., Simon, P., Sivkov, V.N., Vyalikh, D.V., Molodtsov, S.L., Kurek, D., Kammer, M., Hunoldt, S., Born, R., Stawski, D., Steinhof, A., Bazhenov, V.V., Geisler, T., 2013. Discovery of 505-million-year old chitin in the basal demosponge *Vauxia gracilentia*. *Scientific Reports* 3, 3497. <https://doi.org/10.1038/srep03497>
- Eisenreich, W., Schwarz, M., Cartayrade, A., Arigoni, D., Zenk, M.H., Bacher, A., 1998. The deoxyxylulose phosphate pathway of terpenoid biosynthesis in plants and microorganisms. *Chemistry & Biology* 5, 221–233. [https://doi.org/10.1016/S1074-5521\(98\)90002-3](https://doi.org/10.1016/S1074-5521(98)90002-3)
- Elliger, C.A., Zinkel, D.F., Chan, B.G., Waiss, A.C., 1976. Diterpene acids as larval growth inhibitors. *Experientia* 32, 1364–1366.
- Engel, M.S., Grimaldi, D.A., Nascimbene, P.C., Singh, H., 2011. The termites of Early Eocene Cambay amber, with the earliest record of the Termitidae (Isoptera). *ZooKeys* 148, 105–123. <https://doi.org/10.3897/zookeys.148.1797>
- Farrell, B.D., Dussourd, D.E., Mitter, C., 1991. Escalation of plant defense: do latex and resin canals spur plant diversification? *The American Naturalist* 138, 881–900. <https://doi.org/10.1086/285258>

- Feist, M., Lamprecht, I., Müller, F., 2007. Thermal investigations of amber and copal. *Thermochimica Acta* 458, 162–170. <https://doi.org/10.1016/j.tca.2007.01.029>
- Fischer, W.B., Eysel, H.H., 1992. Polarized Raman spectra and intensities of aromatic amino acids phenylalanine, tyrosine and tryptophan. *Spectrochimica Acta Part A: Molecular Spectroscopy* 48, 725–732. [https://doi.org/10.1016/0584-8539\(92\)80216-J](https://doi.org/10.1016/0584-8539(92)80216-J)
- Franzen, J.L., 1985. Exceptional preservation of Eocene vertebrates in the lake deposit of Grube Messel (West Germany). *Philosophical Transactions of the Royal Society of London. B, Biological Sciences* 311, 181–186. <https://doi.org/10.1098/rstb.1985.0150>
- Freire, P.T.C., Barboza, F.M., Lima, J.A., Melo, F.E.A., Filho, J.M., 2017. Raman spectroscopy of amino acid crystals, in: Maaz, K. (Ed.), *Raman Spectroscopy and Applications*. InTech, pp. 201–223. <https://doi.org/10.5772/65480>
- Garg, R., Atequzzaman, K., Prasad, V., Tripathi, S., Singh, I.B., Jauhri, A.K., Bajpai, S., 2008. Age-diagnostic dinoflagellate cysts from the lignite-bearing sediments of the Vastan lignite mine, Surat district, Gujarat, Western India. *Journal of the Paleontological Society of India* 53, 99–105.
- Gerolt, P., 1969. Mode of entry of contact insecticides. *Journal of Insect Physiology* 15, 563–580.
- Gianolla, P., Ragazzi, E., Roghi, G., 1998. Upper Triassic amber from the Dolomites (Northern Italy). A paleoclimatic indicator? *Rivista Italiana di Paleontologia e Stratigrafia* 104, 381–390.
- Girard, V., Schmidt, A.R., Saint Martin, S., Struwe, S., Perrichot, V., Saint Martin, J.-P., Grosheny, D., Breton, G., Neraudeau, D., 2008. Evidence for marine microfossils from amber. *Proceedings of the National Academy of Sciences* 105, 17426–17429. <https://doi.org/10.1073/pnas.0804980105>
- Grantham, P.J., Douglas, A.G., 1980. The nature and origin of sesquiterpenoids in some tertiary fossil resins. *Geochimica et Cosmochimica Acta* 44, 1801–1810. [https://doi.org/10.1016/0016-7037\(80\)90229-X](https://doi.org/10.1016/0016-7037(80)90229-X)
- Greenwalt, D.E., Goreva, Y.S., Siljestrom, S.M., Rose, T., Harbach, R.E., 2013. Hemoglobin-derived porphyrins preserved in a Middle Eocene blood-engorged mosquito. *Proceedings of the National Academy of Sciences* 110, 18496–18500. <https://doi.org/10.1073/pnas.1310885110>
- Grimaldi, D.A., 1995. The age of Dominican amber, in: Anderson, K.B., Crelling, J.C. (Eds.), *Amber, Resinite and Fossil Resins*, American Chemical Society Symposium Series. Washington D.C., pp. 203–217.
- Grimaldi, D.A., 1996. *Amber: window to the past*. Harry N. Abrams, Publishers, in association with the American Museum of Natural History, New York.
- Grimaldi, D.A., Engel, M.S., 2005. *Evolution of Insects*. Cambridge University Press, New York.
- Grimaldi, D.A., Beck, C.W., Boon, J.J., 1989. Occurrence, chemical characteristics and paleontology of the fossil resins from New Jersey. *American Museum Novitates* 2948, 1–28.
- Grimaldi, D.A., Bonwich, E., Delannoy, M., Doberstein, S., 1994. Electron microscopic studies of mummified tissues in amber fossils. *American Museum Novitates* 3097, 1–31.
- Grimaldi, D., Shedrinsky, A., Wampler, T.P., 2000. A remarkable deposit of fossiliferous amber from the Upper Cretaceous (Turonian) of New Jersey, in: Grimaldi, D. (Ed.), *Studies on Fossils in Amber, with Particular Reference to the Cretaceous of New Jersey*. Backhuys Publishing, Leiden, pp. 1–76.
- Grimaldi, D.A., Engel, M.S., Nascimbene, P.C., 2002. Fossiliferous Cretaceous amber from Myanmar (Burma): its rediscovery, biotic diversity, and paleontological significance. *American Museum Novitates* 3361, 1–71.
- Grimalt, J.O., Simoneit, B.R.T., Hatcher, P.G., Nissenbaum, A., 1988. The molecular composition of ambers. *Organic Geochemistry* 13, 677–690.
- Halbwachs, H., 2019. Fungi trapped in amber—a fossil legacy frozen in time. *Mycological Progress* 18, 879–893. <https://doi.org/10.1007/s11557-019-01498-y>

- Hartl, C., Schmidt, A.R., Heinrichs, J., Seyfullah, L.J., Schäfer, N., Gröhn, C., Rikkinen, J., Kaasalainen, U., 2015. Lichen preservation in amber: morphology, ultrastructure, chemofossils, and taphonomic alteration. *Fossil Record* 18, 127–135. <https://doi.org/10.5194/fr-18-127-2015>
- Haug, C., Nyborg, T., Vega, F.J., 2013. An exceptionally preserved upogebiid (Decapoda: Reptantia) from the Eocene of California. *Boletín de la Sociedad Geológica Mexicana* 65, 235–248. <https://doi.org/10.18268/BSGM2013v65n2a5>
- Havelcová, M., Machovič, V., Špaldoňová, A., Lapčák, L., Hendrych, J., Adam, M., 2019. Characterization of Eocene fossil resin from Moravia, Czech Republic: Insights into macromolecular structure. *Spectrochimica Acta Part A: Molecular and Biomolecular Spectroscopy* 215, 176–186. <https://doi.org/10.1016/j.saa.2019.02.058>
- Hebsgaard, M.B., Phillips, M.J., Willerslev, E., 2005. Geologically ancient DNA: fact or artefact? *Trends in Microbiology* 13, 212–220. <https://doi.org/10.1016/j.tim.2005.03.010>
- Henwood, A.A., 1992a. Exceptional preservation of Dipteran flight muscle and the taphonomy of Insects in amber. *PALAIOS* 7, 203–212.
- Henwood, A.A., 1992b. Soft-part preservation of beetles in Tertiary amber from the Dominican Republic. *Palaeontology* 35, 901–912.
- Henwood, A.A., 1993. Recent plant resins and the taphonomy of organisms in amber: a review. *Modern Geology* 35–59.
- Hernández, B., Pflüger, F., Kruglik, S.G., Ghomi, M., 2013. Characteristic Raman lines of phenylalanine analyzed by a multiconformational approach: Multiconformational analysis of the zwitterionic Phe Raman data. *Journal of Raman Spectroscopy* 44, 827–833. <https://doi.org/10.1002/jrs.4290>
- Hofmann, H.J., Fritz, W.H., Narbonne, G.M., 1983. Ediacaran (Precambrian) fossils from the Wernecke Mountains, Northwestern Canada. *Science* 221, 455–457. <https://doi.org/10.1126/science.221.4609.455>
- Hopfenberg, H.B., Witchey, L.C., Poinar, G.O., 1988. Is the air in amber ancient? *Science* 241, 717–718.
- Hota, R.K., Bapuji, M., 1993. Triterpenoids from the resin of *Shorea robusta*. *Phytochemistry* 32, 466–468.
- Howat, W.J., Wilson, B.A., 2014. Tissue fixation and the effect of molecular fixatives on downstream staining procedures. *Methods* 70, 12–19. <https://doi.org/10.1016/j.ymeth.2014.01.022>
- Hueber, F.M., Langenheim, J.H., 1986. Dominican amber tree had African ancestors. *Geotimes* 31, 8–10.
- Hughes, J.M., Rakovan, J., 2002. The crystal structure of apatite, $\text{Ca}_5(\text{PO}_4)_3(\text{F},\text{OH},\text{Cl})$, in: Kohn, M.J., Rakovan, J., Hughes, J.M. (Eds.), *Phosphates: Geochemical, Geobiological, and Materials Importance, Reviews in Mineralogy and Geochemistry, Reviews in Mineralogy and Geochemistry*. Mineralogical Society of America, Washington D.C., pp. 1–12.
- Iturralde-Vinent, M.A., 2001. Geology of the amber-bearing deposits of the Greater Antilles. *Caribbean Journal of Science* 37, 141–167.
- Janssen, A.M., Scheffer, J.J.C., Baerheim Svendsen, A., 1987. Antimicrobial activities of essential oils. *Pharmaceutisch Weekblad Scientific Edition* 9, 193–197.
- Jehlička, J., Jorge Villar, S.E., Edwards, H.G.M., 2004. Fourier transform Raman spectra of Czech and Moravian fossil resins from freshwater sediments. *Journal of Raman Spectroscopy* 35, 761–767. <https://doi.org/10.1002/jrs.1191>
- Jehlička, J., Vitek, P., Edwards, H.G.M., Hargreaves, M., Čapoun, T., 2009. Rapid outdoor non-destructive detection of organic minerals using a portable Raman spectrometer: Rapid outdoor non-destructive detection of organic minerals. *Journal of Raman Spectroscopy* 40, 1645–1651. <https://doi.org/10.1002/jrs.2313>

- Jones, J.M., Murchison, D.G., 1963. The occurrence of resinite in bituminous coals. *Economic Geology* 58, 263–273.
- Joye, N.M., Lawrence, R.V., 1967. Resin acid composition of pine oleoresins. *Journal of Chemical & Engineering Data* 12, 279–282. <https://doi.org/10.1021/jc60033a034>
- Klebs, R., 1910. Über Bernsteineinschlüsse im allgemeinen und die Coleopteren meiner Bernsteinsammlung. *Schriften der Physikalisch-Ökonomischen Gesellschaft zu Königsberg in Preußen* 51, 217–242.
- Kohring, R., 1998. REM-Untersuchungen an harzkonservierten Arthropoden. *Entomologia Generalis* 23, 95–106.
- Koller, B., Schmitt, J.M., Tischendorf, G., 2005. Cellular fine structures and histochemical reactions in the tissue of a cypress twig preserved in Baltic amber. *Proceedings of the Royal Society B: Biological Sciences* 272, 121–126. <https://doi.org/10.1098/rspb.2004.2939>
- Kosanke, R.M. (Robert M., Harrison, J.A., 1957. Microscopy of the resin rodlets of Illinois coal. *Illinois Geological Survey Circular* 234, 1–14.
- Kosmowska-Ceranowicz, B., 1984. Amber and its origins, in: Kosmowska-Ceranowicz, B. (Ed.), *Amber in Nature*, PAN Muzeum Ziemi. pp. 17–18.
- Kowalewska, M., Szwedo, J., 2009. Examination of the Baltic amber inclusion surface using SEM techniques and X-ray microanalysis. *Palaeogeography, Palaeoclimatology, Palaeoecology* 271, 287–291. <https://doi.org/10.1016/j.palaeo.2008.10.025>
- Labandeira, C.C., 2006. The four phases of plant-arthropod associations in deep time. *Geologica Acta* 4, 409–438.
- Labandeira, C.C., 2014. Amber. Reading and Writing of the Fossil record: Preservational Pathways to Exceptional Fossilization, *The Paleontological Society Papers* 20, 163–217.
- Lafuente, B., Downs, R.T., Yang, H., Stone, N., 2015. The power of databases: The RRUFF project, in: Armbruster, T., Danisi, R.M. (Eds.), *Highlights in Mineralogical Crystallography*. Walter de Gruyter, Berlin, pp. 1–30.
- Lak, M., Néraudeau, D., Nel, A., Cloetens, P., Perrichot, V., Tafforeau, P., 2008. Phase contrast X-ray synchrotron imaging: opening access to fossil inclusions in opaque amber. *Microscopy and Microanalysis* 14, 251–259. <https://doi.org/10.1017/S1431927608080264>
- Lambert, J.B., Frye, J.S., 1982. Carbon functionalities in amber. *Science* 217, 55–57.
- Lambert, J.B., Poinar, G.O., 2002. Amber: the organic gemstone. *Accounts of Chemical Research* 35, 628–636. <https://doi.org/10.1021/ar0001970>
- Lambert, J.B., Frye, J.S., Poinar, G.O., 1990. Analysis of North American amber by carbon-13 NMR spectroscopy. *Geoarchaeology* 5, 43–52. <https://doi.org/10.1002/gea.3340050105>
- Lambert, J.B., Johnson, S.C., Poinar, G.O., 1995. Resin from Africa and South America: criteria for distinguishing between fossilized and recent resin based on NMR spectroscopy, in: Anderson, K.B., Crelling, J.C. (Eds.), *Amber, Resinite, and Fossil Resins*. American Chemical Society, Washington, DC, pp. 193–202. <https://doi.org/10.1021/bk-1995-0617.ch010>
- Lambert, J.B., Shaul, C.E., Poinar, G.O., Santiago-Blay, J.A., 1999. Classification of modern resins by solid state nuclear magnetic resonance spectroscopy. *Bioorganic Chemistry* 27, 409–433. <https://doi.org/10.1006/bioo.1999.1147>
- Lambert, J.B., Wu, Y., Santiago-Blay, J.A., 2005. Taxonomic and chemical relationships revealed by nuclear magnetic resonance spectra of plant exudates. *Journal of Natural Products* 68, 635–648. <https://doi.org/10.1021/np050005f>
- Lambert, J.B., Kozminski, M.A., Fahlstrom, C.A., Santiago-Blay, J.A., 2007. Proton nuclear magnetic resonance characterization of resins from the family Pinaceae. *Journal of Natural Products* 70, 188–195. <https://doi.org/10.1021/np060486i>
- Lambert, J.B., Santiago-Blay, J.A., Anderson, K.B., 2008. Chemical signatures of fossilized resins and recent plant exudates. *Angewandte Chemie International Edition* 47, 9608–9616. <https://doi.org/10.1002/anie.200705973>

- Lambert, J.B., Tsai, C.Y.-H., Shah, M.C., Hurltley, A.E., Santiago-Blay, J.A., 2012. Distinguishing amber and copal classes by proton magnetic resonance spectroscopy. *Archaeometry* 54, 332–348. <https://doi.org/10.1111/j.1475-4754.2011.00625.x>
- Lambert, J.B., Levy, A.J., Santiago-Blay, J.A., Wu, Y., 2013. Nuclear magnetic resonance characterization of Indonesian amber. *Life: The Excitement of Biology* 1, 136–155. [https://doi.org/10.9784/LEB1\(3\)Lambert.02](https://doi.org/10.9784/LEB1(3)Lambert.02)
- Lambert, J.B., Santiago-Blay, J.A., Wu, Y., Levy, A.J., 2015. Examination of amber and related materials by NMR spectroscopy. *Magnetic Resonance in Chemistry* 53, 2–8. <https://doi.org/10.1002/mrc.4121>
- Lambert, L.H., Cox, T., Mitchell, K., Rossello-Mora, R.A., Del Cueto, C., Dodge, D.E., Orkand, P., Cano, R.J., 1998. *Staphylococcus succinus* sp. nov., isolated from Dominican amber. *International Journal of Systematic and Evolutionary Microbiology* 48, 511–518.
- Langenheim, J.H., 1969. Amber: a botanical inquiry. *Science* 163, 1157–1169. <https://doi.org/10.1126/science.163.3872.1157>
- Langenheim, J.H., 1990. Plant resins. *American Scientist* 78, 16–24.
- Langenheim, J.H., 1994. Higher plant terpenoids: A phytocentric overview of their ecological roles. *Journal of Chemical Ecology* 20, 1223–1280. <https://doi.org/10.1007/BF02059809>
- Langenheim, J.H., 1995. Biology of amber-producing trees: focus on case studies of *Hymenaea* and *Agathis*, in: Anderson, K.B., Crelling, J.C. (Eds.), *Amber, Resinite, and Fossil Resins*. American Chemical Society, Washington, DC, pp. 1–31. <https://doi.org/10.1021/bk-1995-0617.ch001>
- Langenheim, J.H., 2003. *Plant resins: chemistry, evolution, ecology, and ethnobotany*. Timber Press, Portland, Oregon.
- Langenheim, J.H., Beck, C.W., 1965. Infrared spectra as a means of determining botanical sources of amber. *Science* 149, 52–54.
- Langenheim, J.H., Convis, C.L., Macedo, C.A., Stubblebine, W.H., 1986. *Hymenaea* and *Copaifera* leaf sesquiterpenes in relation to lepidopteran herbivory in Southeastern Brazil. *Biochemical Systematics and Ecology* 14, 41–49.
- Lazell, J.D., 1965. An *Anolis* (Sauria, Iguanidae) in amber. *Journal of Paleontology* 39, 379–382.
- Li, Q., Gao, K.-Q., Vinther, J., Shawkey, M.D., Clarke, J.A., D’Alba, L., Meng, Q., Briggs, D.E.G., Prum, R.O., 2010. Plumage color patterns of an extinct dinosaur. *Science* 327, 1369–1372. <https://doi.org/10.1126/science.1186290>
- Lincoln, D.E., 1985. Host-plant protein and phenolic resin effects on larval growth and survival of a butterfly. *Journal of Chemical Ecology* 11, 1459–1467. <https://doi.org/10.1007/BF01012192>
- Lindahl, T., 1993a. Instability and decay of the primary structure of DNA. *Nature* 362, 709–715.
- Lindahl, T., 1993b. Recovery of antediluvian DNA. *Nature* 365, 700.
- Lindgren, J., Uvdal, P., Engdahl, A., Lee, A.H., Alwmark, C., Bergquist, K.-E., Nilsson, E., Ekström, P., Rasmussen, M., Douglas, D.A., Polcyn, M.J., Jacobs, L.L., 2011. Microspectroscopic evidence of cretaceous bone proteins. *PLoS ONE* 6, e19445. <https://doi.org/10.1371/journal.pone.0019445>
- Litvak, M.E., Monson, R.K., 1998. Patterns of induced and constitutive monoterpene production in conifer needles in relation to insect herbivory. *Oecologia* 114, 531–540. <https://doi.org/10.1007/s004420050477>
- Litwin, R.J., Ash, S.R., 1991. First early Mesozoic amber in the Western Hemisphere. *Geology* 19, 173–276.
- Lorio, P.L., Hodges, J.D., 1968. Microsite effects on oleoresin exudation pressure of large loblolly pines. *Ecology* 49, 1207–1210. <https://doi.org/10.2307/1934519>
- Lyons, P.C., Finkelman, R.B., Thompson, C.L., Brown, F.W., Hatcher, P.G., 1982. Properties, origin and nomenclature of rodlets of the inertinite maceral group in coals of the central Appalachian basin, U.S.A. *International Journal of Coal Geology* 1, 313–346. [https://doi.org/10.1016/0166-5162\(82\)90019-2](https://doi.org/10.1016/0166-5162(82)90019-2)

- Lyons, P.C., Mastalerz, M., Orem, W.H., 2009. Organic geochemistry of resins from modern *Agathis australis* and Eocene resins from New Zealand: Diagenetic and taxonomic implications. *International Journal of Coal Geology* 80, 51–62. <https://doi.org/10.1016/j.coal.2009.07.015>
- Manning, P.L., Morris, P.M., McMahon, A., Jones, E., Gize, A., Macquaker, J.H.S., Wolff, G., Thompson, A., Marshall, J., Taylor, K.G., Lyson, T., Gaskell, S., Reamtong, O., Sellers, W.I., van Dongen, B.E., Buckley, M., Wogelius, R.A., 2009. Mineralized soft-tissue structure and chemistry in a mummified hadrosaur from the Hell Creek Formation, North Dakota (USA). *Proceedings of the Royal Society B: Biological Sciences* 276, 3429–3437. <https://doi.org/10.1098/rspb.2009.0812>
- Martin, R., 1999. *Taphonomy: a process approach*, Cambridge Paleobiology Series. Cambridge University Press, Cambridge.
- Martínez-Delclòs, X., Briggs, D.E., Peñalver, E., 2004. Taphonomy of insects in carbonates and amber. *Palaeogeography, Palaeoclimatology, Palaeoecology* 203, 19–64. [https://doi.org/10.1016/S0031-0182\(03\)00643-6](https://doi.org/10.1016/S0031-0182(03)00643-6)
- Mazur, N., Nagel, M., Leppin, U., Bierbaum, G., Rust, J., 2014. The extraction of fossil arthropods from Lower Eocene Cambay amber. *Acta Palaeontologica Polonica* 59, 455–459.
- McCann, T., 2010. Chenier plain sedimentation in the Palaeogene-age lignite-rich successions of the Surat area, Gujarat, western India. *Zeitschrift der Deutschen Gesellschaft für Geowissenschaften* 161, 335–351.
- McCoy, V.E., Boom, A., Solórzano Kraemer, M.M., Gabbott, S.E., 2017. The chemistry of American and African amber, copal, and resin from the genus *Hymenaea*. *Organic Geochemistry* 113, 43–54. <https://doi.org/10.1016/j.orggeochem.2017.08.005>
- McCoy, V.E., Soriano, C., Gabbott, S.E., 2018a. A review of preservational variation of fossil inclusions in amber of different chemical groups. *Earth and Environmental Science Transactions of the Royal Society of Edinburgh* 107, 203–211. <https://doi.org/10.1017/S1755691017000391>
- McCoy, V.E., Soriano, C., Pegoraro, M., Luo, T., Boom, A., Foxman, B., Gabbott, S.E., 2018b. Unlocking preservation bias in the amber insect fossil record through experimental decay. *PLoS ONE* 13, e0195482. <https://doi.org/10.1371/journal.pone.0195482>
- McCoy, V.E., Gabbott, S.E., Penkman, K., Collins, M.J., Presslee, S., Holt, J., Grossman, H., Wang, B., Solórzano Kraemer, M.M., Delclòs, X., Peñalver, E., 2019. Ancient amino acids from fossil feathers in amber. *Scientific Reports* 9, 6420. <https://doi.org/10.1038/s41598-019-42938-9>
- McKay, S.A.B., Hunter, W.L., Godard, K.-A., Wang, S.X., Martin, D.M., Bohlmann, J., Plant, A.L., 2003. Insect attack and wounding induce traumatic resin duct development and gene expression of (—)-pinene synthase in Sitka spruce. *Plant Physiology* 133, 368–378. <https://doi.org/10.1104/pp.103.022723>
- McKellar, R.C., Wolfe, A.P., 2010. Canadian amber, in: Penney, D. (Ed.), *Biodiversity of Fossils in Amber from the Major World Deposits*. Siri Scientific Press, Manchester, pp. 149–166.
- McKellar, R.C., Wolfe, A.P., Muehlenbachs, K., Tappert, R., Engel, M.S., Cheng, T., Sánchez-Azofeifa, G.A., 2011. Insect outbreaks produce distinctive carbon isotope signatures in defensive resins and fossiliferous ambers. *Proceedings of the Royal Society B: Biological Sciences* 278, 3219–3224. <https://doi.org/10.1098/rspb.2011.0276>
- McKenna, D.D., Farrell, B.D., 2005. Molecular phylogenetics and evolution of host plant use in the Neotropical rolled leaf ‘hispine’ beetle genus *Cephaloleia* (Chevrolat) (Chrysomelidae: Cassidinae). *Molecular Phylogenetics and Evolution* 37, 117–131. <https://doi.org/10.1016/j.ympev.2005.06.011>
- McNamara, M., Orr, P.J., Kearns, S.L., Alcalá, L., Anadón, P., Peñalver-Mollá, E., 2010. Organic preservation of fossil musculature with ultracellular detail. *Proceedings of the Royal Society B: Biological Sciences* 277, 423–427. <https://doi.org/10.1098/rspb.2009.1378>

- McNamara, M.E., van Dongen, B.E., Lockyer, N.P., Bull, I.D., Orr, P.J., 2016. Fossilization of melanosomes via sulfurization. *Palaeontology* 59, 337–350. <https://doi.org/10.1111/pala.12238>
- Messer, A., McCormick, K., Sunjaya, Hagedorn, H.H., Tumbel, F., Meinwald, J., 1990. Defensive role of tropical tree resins: antitermitic sesquiterpenes from Southeast Asian Dipterocarpaceae. *Journal of Chemical Ecology* 16, 3333–3352. <https://doi.org/10.1007/BF00982102>
- Mierzejewski, P., 1978. Electron microscopy study on the milky impurities covering arthropod inclusions in the Baltic amber. *Prace Muzeum Ziemi* 28, 81–84.
- Mierzejewski, P., 1976a. On application of scanning electron microscope to the study of organic inclusions from the Baltic amber. *Rocznik Polskiego Towarzystwa Geologicznego* 46, 291–295.
- Mierzejewski, P., 1976b. Scanning electron microscope studies on the fossilization of Baltic amber spiders (preliminary note). *Annals of the Medical Section of the Polish Academy of Sciences* 21, 81–82.
- Mills, J.S., Werner, A.E.A., 1955. The chemistry of dammar resin. *Journal of the Chemical Society* 1955 (Resumed), 3132–3140. <https://doi.org/10.1039/jr9550003132>
- Mills, J.S., White, R., Gough, L.J., 1984. The chemical composition of Baltic amber. *Chemical Geology* 47, 15–39. [https://doi.org/10.1016/0009-2541\(84\)90097-4](https://doi.org/10.1016/0009-2541(84)90097-4)
- Miyazawa, M., Yamafuji, C., 2005. Inhibition of acetylcholinesterase activity by bicyclic monoterpenoids. *Journal of Agricultural and Food Chemistry* 53, 1765–1768. <https://doi.org/10.1021/jf040019b>
- Moleyar, V., Narasimham, P., 1992. Antibacterial activity of essential oil components. *International Journal of Food Microbiology* 16, 337–342. [https://doi.org/10.1016/0168-1605\(92\)90035-2](https://doi.org/10.1016/0168-1605(92)90035-2)
- Mugu, S., Pistone, D., Jordal, B.H., 2018. New molecular markers resolve the phylogenetic position of the enigmatic wood-boring weevils Platypodinae (Coleoptera: Curculionidae). *Arthropod Systematics & Phylogeny* 76, 45–58.
- Murillo-Barroso, M., Martín-Torres, M., 2012. Amber sources and trade in the prehistory of the Iberian peninsula. *European Journal of Archaeology* 15, 187–216. <https://doi.org/10.1179/1461957112Y.0000000009>
- Murillo-Barroso, M., Peñalver, E., Bueno, P., Barroso, R., de Balbín, R., Martín-Torres, M., 2018. Amber in prehistoric Iberia: New data and a review. *PLoS ONE* 13, e0202235. <https://doi.org/10.1371/journal.pone.0202235>
- Nadein, K.S., Perkovsky, E.E., 2019. Small and common: the oldest tropical Chrysomelidae (Insecta: Coleoptera) from the lower Eocene Cambay amber of India. *Alcheringa: An Australasian Journal of Palaeontology* 43, 597–611. <https://doi.org/10.1080/03115518.2019.1622780>
- Najarro, M., Peñalver, E., Pérez-de la Fuente, R., Ortega-Blanco, J., Menor-Salván, C., Barrón, E., Soriano, C., Rosales, I., López del Valle, R., Velasco, F., Tornos, F., Daviero-Gomez, V., Gomez, B., Delclòs, X., 2010. Review of the El Soplao amber outcrop, Early Cretaceous of Cantabria, Spain. *Acta Geologica Sinica (English Edition)* 84, 959–976.
- Nel, A., de Ploëg, G., Millet, J., Menier, J.-J., Waller, A., 2004. The french ambers: a general conspectus and the lowermost Eocene amber deposit of Le Quesnoy in the Paris basin. *Geologica Acta* 2, 3–8.
- Néraudeau, D., Perrichot, V., Batten, D.J., Boura, A., Girard, V., Jeanneau, L., Nohra, Y.A., Polette, F., Martin, S.S., Saint Martin, J.-P., Thomas, R., 2017. Upper Cretaceous amber from Vendée, north-western France: Age dating and geological, chemical, and palaeontological characteristics. *Cretaceous Research* 70, 77–95. <https://doi.org/10.1016/j.cretres.2016.10.001>
- Otto, A., Wilde, V., 2001. Sesqui-, Di-, and Triterpenoids as chemosystematic markers in extant conifers—a review. *The Botanical Review* 67, 141–238.

- Pääbo, S., Poinar, H., Serre, D., Jaenicke-Després, V., Hebler, J., Rohland, N., Kuch, M., Krause, J., Vigilant, L., Hofreiter, M., 2004. Genetic analyses from ancient DNA. *Annual Review of Genetics* 38, 645–679. <https://doi.org/10.1146/annurev.genet.37.110801.143214>
- Pasteris, J.D., Ding, D.Y., 2009. Experimental fluoridation of nanocrystalline apatite. *American Mineralogist* 94, 53–63.
- Pasteris, J.D., Wopenka, B., Valsami-Jones, E., 2008. Bone and tooth mineralization: Why apatite? *Elements* 4, 97–104.
- Pawlicki, R., Korbel, A., Kubiak, H., 1966. Cells, collagen fibrils and vessels in dinosaur bone. *Nature* 211, 655–657.
- Pawlicki, R., Nowogrodzka-Zagórska, M., 1998. Blood vessels and red blood cells preserved in dinosaur bones. *Annals of Anatomy - Anatomischer Anzeiger* 180, 73–77. [https://doi.org/10.1016/S0940-9602\(98\)80140-4](https://doi.org/10.1016/S0940-9602(98)80140-4)
- Peñalver, E., Delclòs, X., 2010. Spanish amber, in: Penney, D. (Ed.), *Biodiversity of Fossils in Amber from the Major World Deposits*. Siri Scientific Press, Manchester, pp. 236–270.
- Penney, D., 2010a. *Biodiversity of fossils in amber from the major world deposits*. Siri Scientific Press, Manchester.
- Penney, D., 2010b. Dominican Amber, in: Penney, D. (Ed.), *Biodiversity of Fossils in Amber from the Major World Deposits*. Siri Scientific Press, Manchester, pp. 22–41.
- Penney, D., Green, D.I., 2010. Introduction, preparation, study & conservation of amber inclusions, in: Penney, D. (Ed.), *Biodiversity of Fossils in Amber from the Major World Deposits*. Siri Scientific Press, Manchester, pp. 5–21.
- Penney, D., Green, D.I., 2012. Sub-fossils in copal: an undervalued resource. *Deposits Magazine* 14–19.
- Penney, D., Preziosi, R.F., 2010. On inclusions in subfossil resins (copal), in: *Biodiversity of Fossils in Amber from the Major World Deposits*. Siri Scientific Press, Manchester, pp. 299–303.
- Penney, D., Wadsworth, C., Green, D.I., Kennedy, S.L., Preziosi, R.F., Brown, T.A., 2013a. Extraction of inclusions from (sub) fossil resins, with description of a new species of stingless bee (Hymenoptera: Apidae: Meliponini) in Quaternary Colombian copal. *Paleontological Contributions* 2013.
- Penney, D., Wadsworth, C., Fox, G., Kennedy, S.L., Preziosi, R.F., Brown, T.A., 2013b. Absence of ancient DNA in sub-fossil insect inclusions preserved in ‘Anthropocene’ Colombian copal. *PLoS ONE* 8, e73150. <https://doi.org/10.1371/journal.pone.0073150>
- Peris, D., Rust, J., 2020. Cretaceous beetles (Insecta: Coleoptera) in amber: the palaeoecology of this most diverse group of insects. *Zoological Journal of the Linnean Society* 189, 1085–1104. <https://doi.org/10.1093/zoolinnean/zlz118>
- Peris, D., Ruzzier, E., Perrichot, V., Delclòs, X., 2016. Evolutionary and paleobiological implications of Coleoptera (Insecta) from Tethyan-influenced Cretaceous ambers. *Geoscience Frontiers* 7, 695–706. <https://doi.org/10.1016/j.gsf.2015.12.007>
- Peris, D., Janssen, K., Barthel, H.J., Bierbaum, G., Delclòs, X., Peñalver, E., Solórzano-Kraemer, M.M., Jordal, B.H., Rust, J., 2020. DNA from resin-embedded organisms: Past, present and future. *PLoS ONE* 15, e0239521. <https://doi.org/10.1371/journal.pone.0239521>
- Petrunkévitch, A., 1935. Striated muscles of an amber insect. *Nature* 135, 760–761.
- Petrunkévitch, A., 1950. Baltic amber spiders in the Museum of Comparative Zoology. *Bulletin of the Museum of Comparative Zoology* 10, 259–337.
- Pfretzschner, H.-U., 2004. Fossilization of Haversian bone in aquatic environments. *Comptes Rendus Palevol* 3, 605–616.
- Philippe, M., Cuny, G., Suteehorn, V., Teerarungsikul, N., Barale, G., Thévenard, F., Le Loeuff, J., Buffetaut, E., Gaona, T., Košir, A., Tong, H., 2005. A Jurassic amber deposit in Southern Thailand. *Historical Biology* 17, 1–6.

- Phillips, M.A., Croteau, R.B., 1999. Resin-based defenses in conifers. *Trends in Plant Science* 4, 184–190. [https://doi.org/10.1016/S1360-1385\(99\)01401-6](https://doi.org/10.1016/S1360-1385(99)01401-6)
- Phillips, T.L., Avcin, M.J., Berggren, D., 1976. Fossil peat of the Illinois basin : a guide to the study of coal balls of Pennsylvanian age, Educational series. Illinois State Geological Survey, Urbana.
- Piga, G., Santos-Cubedo, A., Moya Solà, S., Brunetti, A., Malgosa, A., Enzo, S., 2009. An X-ray Diffraction (XRD) and X-ray Fluorescence (XRF) investigation in human and animal fossil bones from Holocene to Middle Triassic. *Journal of Archaeological Science* 36, 1857–1868. <https://doi.org/10.1016/j.jas.2009.04.013>
- Pitsouli, C., Perrimon, N., 2010. Embryonic multipotent progenitors remodel the *Drosophila* airways during metamorphosis. *Development* 137, 3615–3624. <https://doi.org/10.1242/dev.056408>
- Poehland, B.L., Carté, B.K., Francis, T.A., Hyland, L.J., Allaudeen, H.S., Troupe, N., 1987. In vitro antiviral activity of dammar resin triterpenoids. *Journal of Natural Products* 50, 706–713. <https://doi.org/10.1021/np50052a022>
- Poinar, G.O., 1991. *Hymenaea protera* sp.n. (Leguminosae, Cesalpinioideae) from Dominican amber has African affinities. *Experientia* 47, 1075–1082.
- Poinar, G.O., 1992. Life in amber. Stanford University Press, Stanford, California.
- Poinar, G.O., Hess, R., 1982. Ultrastructure of 40-million-year-old insect tissue. *Science* 215, 1241–1242.
- Poinar, G.O., Hess, R., 1985. Preservative qualities of recent and fossil resins: Electron micrograph studies on tissue preserved in Baltic amber. *Journal of Baltic Studies* 16, 222–230.
- Poinar, G.O., Poinar, R., 1999. The amber forest: a reconstruction of a vanished world. Princeton University Press, Princeton, N.J.
- Poinar, H.N., Cano, R.J., Poinar, G.O., 1993. DNA from an extinct plant. *Nature* 363, 677.
- Poinar, H.N., Melzer, R.R., Poinar Jr, G.O., 1996. Ultrastructure of 30–40 million year old leaflets from Dominican amber (*Hymenaea protera*, Fabaceae: Angiospermae). *Experientia* 52, 387–390.
- Poinar, H.N., Hofreiter, M., Spaulding, W.G., 1998. Molecular coproscopy: dung and diet of the extinct ground sloth *Nothrotheriops shastensis* 281, 5.
- Polcyn, M.J., Rogers II, J.V., Kobayashi, Y., Jacobs, L.L., 2002. Computed tomography of an Anolis lizard in Dominican amber: systematic, taphonomic, biogeographic, and evolutionary implications. *Palaeontologia Electronica* 5, 1–13.
- Poulin, J., Helwig, K., 2012. Class Id resinite from Canada: a new sub-class containing succinic acid. *Organic Geochemistry* 44, 37–44. <https://doi.org/10.1016/j.orggeochem.2011.11.012>
- Poulin, J., Helwig, K., 2014. Inside amber: the structural role of succinic acid in Class Ia and Class Id resinite. *Analytical Chemistry* 86, 7428–7435. <https://doi.org/10.1021/ac501073k>
- Poulin, J., Helwig, K., 2015. Inside amber: new insights into the macromolecular structure of Class Ib resinite. *Organic Geochemistry* 86, 94–106. <https://doi.org/10.1016/j.orggeochem.2015.05.009>
- Pucéat, E., Reynard, B., Lécuyer, C., 2004. Can crystallinity be used to determine the degree of chemical alteration of biogenic apatites? *Chemical Geology* 205, 83–97. <https://doi.org/10.1016/j.chemgeo.2003.12.014>
- Puchtler, H., Sweat Waldrop, F., Conner, H.M., Terry, M.S., 1968. Carnoy fixation: practical and theoretical considerations. *Histochemie* 16, 361–371. <https://doi.org/10.1007/BF00306359>
- Punekar, J., Saraswati, P.K., 2010. Age of the Vastan lignite in context of some oldest cenozoic fossil mammals from India. *Journal of the Geological Society of India* 76, 63–68. <https://doi.org/10.1007/s12594-010-0076-y>
- Raffa, K.F., Berryman, A.A., 1982. Accumulation of monoterpenes and associated volatiles following inoculation of grand fir with a fungus transmitted by the fir engraver, *Scolytus ventralis* (Coleoptera: Scolytidae). *The Canadian Entomologist* 114, 797–810.

- Ragazzi, E., Schmidt, A.R., 2011. Amber, in: Reitner, J., Thiel, V. (Eds.), *Encyclopedia of Geobiology, Encyclopedia of Earth Sciences*. Springer, Dordrecht, pp. 24–36.
- Ragazzi, E., Roghi, G., Giaretta, A., Gianolla, P., 2003. Classification of amber based on thermal analysis. *Thermochimica Acta* 404, 43–54. [https://doi.org/10.1016/S0040-6031\(03\)00062-5](https://doi.org/10.1016/S0040-6031(03)00062-5)
- Rana, R.S., Kumar, K., Singh, H., 2004. Vertebrate fauna from the subsurface Cambay shale (Lower Eocene), Vastan lignite mine, Gujarat, India. *Current Science* 87, 1726–1733.
- Rao, Z., Dong, K., Yang, X., Lin, J., Cui, X., Zhou, R., Deng, Q., 2013. Natural amber, copal resin and colophony investigated by UV-VIS, infrared and Raman spectrum. *Science China Physics, Mechanics and Astronomy* 56, 1598–1602. <https://doi.org/10.1007/s11433-013-5144-z>
- Rieppel, O., 1980. Green anole in Dominican amber. *Nature* 286, 486–487. <https://doi.org/10.1038/286486a0>
- Roghi, G., Ragazzi, E., Gianolla, P., 2006. Triassic Amber of the Southern Alps (Italy). *PALAIOS* 21, 143–154. <https://doi.org/10.2110/palo.2005.p05-68>
- Ross, A., 1997. Insects in amber. *Geology Today* 13, 24–28.
- Rosselló, J.A., 2014. The never-ending story of geologically ancient DNA: was the model plant *Arabidopsis* the source of Miocene Dominican amber? *Biological Journal of the Linnean Society* 111, 234–240. <https://doi.org/10.1111/bij.12192>
- Rust, J., Singh, H., Rana, R.S., McCann, T., Singh, L., Anderson, K., Sarkar, N., Nascimbene, P.C., Stebner, F., Thomas, J.C., others, 2010. Biogeographic and evolutionary implications of a diverse paleobiota in amber from the early Eocene of India. *Proceedings of the National Academy of Sciences* 107, 18360–18365.
- Sadowski, E.-M., Schmidt, A.R., Seyfullah, L.J., Kunzmann, L., 2017. Conifers of the “Baltic amber forest” and their palaeoecological significance. *Stapfia* 106, 1–73.
- Sahni, A., Saraswati, P.K., Rana, R.S., Kumar, K., Singh, H., Alimohammadian, H., Sahni, N., Rose, K.D., Singh, L., Smith T., 2006. Temporal constraints and depositional palaeoenvironments of the Vastan lignite sequence, Gujarat: analogy for the Cambay shale hydrocarbon source rock. *Indian Journal of Petroleum Geology* 15, 1–20.
- Saitta, E.T., Vinther, J., Crisp, M.K., Abbott, G.D., Kaye, T.G., Pittman, M., Bull, I., Fletcher, I., Chen, X., Collins, M.J., Sakalauskaite, J., Mackie, M., Dal Bello, F., Dickinson, M.R., Stevenson, M.A., Donohoe, P., Heck, P.R., Demarchi, B., Penkman, K.E.H., 2020. Non-avian dinosaur eggshell calcite contains ancient, endogenous Amino acids. *bioRxiv*. <https://doi.org/DOI: 10.1101/2020.06.02.129999>
- Sandermann, W., 1962. Terpenoids, structure and distribution, in: Florkin, M., Mason, H.S. (Eds.), *Comparative Biochemistry*. Academic Press, New York.
- Santos-Sánchez, N.F., Salas-Coronado, R., Hernández-Carlos, B., Villanueva-Cañongo, C., 2019. Shikimic acid pathway in biosynthesis of phenolic compounds, in: Soto-Hernández, M., García-Mateos, R., Palma-Tenango, M. (Eds.), *Plant Physiological Aspects of Phenolic Compounds*, IntechOpen.
- Savluchinske Feio, S., Gigante, B., Carlos Roseiro, J., Marcelo-Curto, M., 1999. Antimicrobial activity of diterpene resin acid derivatives. *Journal of Microbiological Methods* 35, 201–206. [https://doi.org/10.1016/S0167-7012\(98\)00117-1](https://doi.org/10.1016/S0167-7012(98)00117-1)
- Schlee, D., Dietrich, H.G., 1970. Insektenführender Bernstein aus der Unterkreide des Libanon. *Neues Jahrbuch für Geologie und Paläontologie Monatshefte* 40–50.
- Schlee, D., Glöckner, W., 1978. Bernstein. *Bernsteine und Bernsteinfossilien*. *Stuttgarter Beiträge zur Naturkunde (C)* 8, 1–72.
- Schlüter, T., 1989. Neue Daten über harzkonservierte Arthropoden aus dem Cenomanium NW-Frankreichs. *Documenta Naturae* 56, 59–70.
- Schlüter, T., von Gnielinski, F., 1980. The east African copal: its geology, stratigraphy, palaeontological significance and comparison with other fossil resins of similar age. *Occasional Papers of the National Museum of Tanzania* 8, 1–32.

- Schmidt, A.R., Jancke, S., Lindquist, E.E., Ragazzi, E., Roghi, G., Nascimbene, P.C., Schmidt, K., Wappler, T., Grimaldi, D.A., 2012. Arthropods in amber from the Triassic Period. *Proceedings of the National Academy of Sciences* 109, 14796–14801. <https://doi.org/10.1073/pnas.1208464109>
- Schroeder, R., Bada, J., 1976. A review of the geochemical applications of the amino acid racemization reaction. *Earth-Science Reviews* 12, 347–391. [https://doi.org/10.1016/0012-8252\(76\)90011-8](https://doi.org/10.1016/0012-8252(76)90011-8)
- Schweitzer, M.H., 2004. Molecular paleontology: some current advances and problems. *Annales de Paléontologie* 90, 81–102. <https://doi.org/10.1016/j.annpal.2004.02.001>
- Schweitzer, M.H., 2011. Soft tissue preservation in terrestrial Mesozoic vertebrates. *Annual Review of Earth and Planetary Sciences* 39, 187–216. <https://doi.org/10.1146/annurev-earth-040610-133502>
- Schweitzer, M.H., Wittmeyer, J.L., Horner, J.R., Toporski, J.K., 2005. Soft-Tissue Vessels and Cellular Preservation in *Tyrannosaurus rex*. *Science* 307, 1952–1955.
- Schweitzer, M.H., Zheng, W., Organ, C.L., Avci, R., Suo, Z., Freimark, L.M., Lebleu, V.S., Duncan, M.B., Vander Heiden, M.G., Neveu, J.M., Lane, W.S., Cottrell, J.S., Horner, J.R., Cantley, L.C., Kalluri, R., Asara, J.M., 2009. Biomolecular characterization and protein sequences of the Campanian Hadrosaur *B. canadensis*. *Science* 324, 626–631. <https://doi.org/10.1126/science.1165069>
- Schweitzer, M.H., Zheng, W., Cleland, T.P., Goodwin, M.B., Boatman, E., Theil, E., Marcus, M.A., Fakra, S.C., 2013. A role for iron and oxygen chemistry in preserving soft tissues, cells and molecules from deep time. *Proceedings of the Royal Society B: Biological Sciences* 281, 20132741. <https://doi.org/10.1098/rspb.2013.2741>
- Schweitzer, M.H., Schroeter, E.R., Cleland, T.P., Zheng, W., 2019. Paleoproteomics of Mesozoic dinosaurs and other Mesozoic fossils. *Proteomics* 19, 1800251. <https://doi.org/10.1002/pmic.201800251>
- SDBSWeb. 2021. Spectral database for organic compounds. National Institute of Advanced Industrial Science and Technology. Available at <https://sdfs.db.aist.go.jp> (accessed February 11, 2021).
- Seilacher, A., 1970. Begriff und Bedeutung der Fossil-Lagerstätten. *Neues Jahrbuch für Geologie und Paläontologie, Monatshefte* 1, 34–39.
- Seilacher, A., Reif, W.-E., Westphal, F., 1985. Sedimentological, ecological and temporal patterns of fossil Lagerstätten. *Philosophical Transactions of the Royal Society of London. B, Biological Sciences* 311, 5–24. <https://doi.org/10.1098/rstb.1985.0134>
- Selden, P., Nudds, J.R., 2012. *Evolution of Fossil Ecosystems, Second Edition*. ed. Academic Press, London; Waltham, MA.
- Seyfullah, L.J., Beimforde, C., Dal Corso, J., Perrichot, V., Rikkinen, J., Schmidt, A.R., 2018a. Production and preservation of resins - past and present. *Biological Reviews* 93, 1684–1714. <https://doi.org/10.1111/brv.12414>
- Seyfullah, L.J., Roghi, G., Corso, J.D., Schmidt, A.R., 2018b. The Carnian Pluvial Episode and the first global appearance of amber. *Journal of the Geological Society* 175, 1012–1018. <https://doi.org/10.1144/jgs2017-143>
- Sharma, V., Sircar, A., 2019. Mineralogical assemblage of Cambay shale of north Cambay basin, Gujarat, India. *Journal of Petroleum Exploration and Production Technology* 9, 87–95. <https://doi.org/10.1007/s13202-018-0505-9>
- Sherratt, E., del Rosario Castañeda, M., Garwood, R.J., Mahler, D.L., Sanger, T.J., Herrel, A., de Queiroz, K., Losos, J.B., 2015. Amber fossils demonstrate deep-time stability of Caribbean lizard communities. *Proceedings of the National Academy of Sciences* 112, 9961–9966.
- Shi, G., Li, H., 2010. A fossil fruit wing of *Dipterocarpus* from the middle Miocene of Fujian, China and its palaeoclimatic significance. *Review of Palaeobotany and Palynology* 162, 599–606. <https://doi.org/10.1016/j.revpalbo.2010.08.001>

- Shi, G., Dutta, S., Paul, S., Wang, B., Jacques, F.M.B., 2014a. Terpenoid compositions and botanical origins of Late Cretaceous and Miocene amber from China. PLoS ONE 9, e111303. <https://doi.org/10.1371/journal.pone.0111303>
- Shi, G., Jacques, F.M.B., Li, H., 2014b. Winged fruits of *Shorea* (Dipterocarpaceae) from the Miocene of Southeast China: evidence for the northward extension of dipterocarps during the Mid-Miocene climatic optimum. Review of Palaeobotany and Palynology 200, 97–107.
- Smith, A.B., Austin, J.J., 1997. Can ancient DNA be recovered from the fossil record? GeoScientist 7, 58–61.
- Solórzano Kraemer, M.M., 2010. Mexican amber, in: Biodiversity of Fossils in Amber from the Major World Deposits. Siri Scientific Press, Manchester, pp. 42–56.
- Solórzano Kraemer, M.M., Kraemer, A.S., Stebner, F., Bickel, D.J., Rust, J., 2015. Entrapment Bias of Arthropods in Miocene Amber Revealed by Trapping Experiments in a Tropical Forest in Chiapas, Mexico. PLoS ONE 10, e0118820. <https://doi.org/10.1371/journal.pone.0118820>
- Solórzano Kraemer, M.M., Delclòs, X., Clapham, M.E., Arillo, A., Peris, D., Jäger, P., Stebner, F., Peñalver, E., 2018. Arthropods in modern resins reveal if amber accurately recorded forest arthropod communities. Proceedings of the National Academy of Sciences 115, 6739–6744. <https://doi.org/10.1073/pnas.1802138115>
- Sonibare, O.O., Agbaje, O.B., Jacob, D.E., Faithfull, J., Hoffmann, T., Foley, S.F., 2014. Terpenoid composition and origin of amber from the Cape York Peninsula, Australia. Australian Journal of Earth Sciences 61, 979–985. <https://doi.org/10.1080/08120099.2014.960897>
- Soriano, C., Archer, M., Azar, D., Creaser, P., Delclòs, X., Godthelp, H., Hand, S., Jones, A., Nel, A., Néraudeau, D., Ortega-Blanco, J., Pérez-de la Fuente, R., Perrichot, V., Saupe, E., Kraemer, M.S., Tafforeau, P., 2010. Synchrotron X-ray imaging of inclusions in amber. Comptes Rendus Palevol 9, 361–368. <https://doi.org/10.1016/j.crpv.2010.07.014>
- Speranza, M., Ascaso, C., Delclòs, X., Peñalver, E., 2015. Cretaceous mycelia preserving fungal polysaccharides: taphonomic and paleoecological potential of microorganisms preserved in fossil resins. Geologica Acta 13, 363–385.
- Speranza, M., Wierzchos, J., Alonso, J., Bettucci, L., Martín-González, A., Ascaso, C., 2010. Traditional and new microscopy techniques applied to the study of microscopic fungi included in amber, in: Méndez-Vilas, A., Díaz, J. (Eds.), Microscopy: Science, Technology, Applications and Education. pp. 1135–1145.
- Stacey, R.J., Cartwright, C.R., McEwan, C., 2006. Chemical characterization of ancient mesoamerican “copal” resins: preliminary results. Archaeometry 48, 323–340.
- Stach, P., Martinkutė, G., Šinkūnas, P., Natkaniec-Nowak, L., Drzewicz, P., Naglik, B., Bogdasarov, M., 2019. An attempt to correlate the physical properties of fossil and subfossil resins with their age and geographic location. Journal of Polymer Engineering 39, 716–728. <https://doi.org/10.1515/polyeng-2019-0159>
- Stankiewicz, B.A., Briggs, D.E.G., Evershed, R.P., Flannery, M.B., Wuttke, M., 1997. Preservation of chitin in 25-million-year-old fossils. Science 276, 1541–1543. <https://doi.org/10.1126/science.276.5318.1541>
- Stankiewicz, B.A., Poinar, H.N., Briggs, D.E.G., Evershed, R.P., Poinar, G.O., 1998. Chemical preservation of plants and insects in natural resins. Proceedings of the Royal Society B: Biological Sciences 265, 641–647. <https://doi.org/10.1098/rspb.1998.0342>
- Stebner, F., Szadziewski, R., Rühr, P.T., Singh, H., Hammel, J.U., Kvitte, G.M., Rust, J., 2016. A fossil biting midge (Diptera: Ceratopogonidae) from early Eocene Indian amber with a complex pheromone evaporator. Scientific Reports 6, 34352. <https://doi.org/10.1038/srep34352>
- Stebner, F., Szadziewski, R., Singh, H., Gunkel, S., Rust, J., 2017. Biting midges (Diptera: Ceratopogonidae) from Cambay amber indicate that the Eocene fauna of the Indian

- subcontinent was not isolated. *PLoS ONE* 12, e0169144.
<https://doi.org/10.1371/journal.pone.0169144>
- Storch, G., Engesser, B., Wuttke, M., 1996. Oldest fossil record of gliding in rodents. *Nature* 379, 439–441. <https://doi.org/10.1038/379439a0>
- Sturgeon, K.B., 1979. Monoterpene variation in ponderosa pine xylem resin related to Western pine beetle predation. *Evolution* 33, 803–814. <https://doi.org/10.2307/2407647>
- Tahoun, M., Gee, C.T., McCoy, V.E., Sander, P.M., Müller, C.E., 2021. Chemistry of porphyrins in fossil plants and animals. *RSC Advances* 11, 7552–7563.
<https://doi.org/10.1039/D0RA10688G>
- Tanaka, G., Parker, A.R., Siveter, D.J., Maeda, H., Furutani, M., 2009. An exceptionally well-preserved Eocene dolichopodid fly eye: function and evolutionary significance. *Proceedings of the Royal Society B: Biological Sciences* 276, 1015–1019.
<https://doi.org/10.1098/rspb.2008.1467>
- Tappert, R., Wolfe, A.P., McKellar, R.C., Tappert, M.C., Muehlenbachs, K., 2011. Characterizing modern and fossil gymnosperm exudates using micro-fourier transform infrared spectroscopy. *International Journal of Plant Sciences* 172, 120–138. <https://doi.org/10.1086/657277>
- Thomas, B.R., 1969. Kauri resins—modern and fossil, in: Eglinton, G., Murphy, M.T.J. (Eds.), *Organic Geochemistry*. Springer Berlin Heidelberg, Berlin, Heidelberg, pp. 599–618.
https://doi.org/10.1007/978-3-642-87734-6_32
- Thomas, B.R., 1970. Modern and fossil plant resins, in: Harborne, B. (Ed.), *Phytochemical Phylogeny*. Academic Press, New York, pp. 59–79.
- Tomlin, E.S., Antonejevic, E., Alfaro, R.I., Borden, J.H., 2000. Changes in volatile terpene and diterpene resin acid composition of resistant and susceptible white spruce leaders exposed to simulated white pine weevil damage. *Tree Physiology* 20, 1087–1095.
<https://doi.org/10.1093/treephys/20.16.1087>
- Tornquist, A.J.H., 1910. *Geologie von Ostpreussen*. Gebrüder Borntraeger, Berlin.
- Trapp, S.C., Croteau, R.B., 2001. Defensive resin biosynthesis in conifers. *Annual Review of Plant Physiology and Plant Molecular Biology* 52, 689–724.
- Trinajstić, K., Marshall, C., Long, J., Bifield, K., 2007. Exceptional preservation of nerve and muscle tissues in Late Devonian placoderm fish and their evolutionary implications. *Biology Letters* 3, 197–200. <https://doi.org/10.1098/rsbl.2006.0604>
- Trueman, C.N., Behrensmeyer, A.K., Tuross, N., Weiner, S., 2004. Mineralogical and compositional changes in bones exposed on soil surfaces in Amboseli National Park, Kenya: diagenetic mechanisms and the role of sediment pore fluids. *Journal of Archaeological Science* 31, 721–739. <https://doi.org/10.1016/j.jas.2003.11.003>
- Truică, G.I., Ditaranto, N., Caggiani, M.C., Mangone, A., Lițescu, S.C., Teodor, E.D., Sabbatina, L., Radu, G.L., 2014. A multi-analytical approach to amber characterization. *Chemical Papers* 68, 15–21.
- Tuross, N., Stathoplos, L., 1993. Ancient proteins in fossil bones. *Methods in Enzymology* 224, 121–129. [https://doi.org/10.1016/0076-6879\(93\)24010-R](https://doi.org/10.1016/0076-6879(93)24010-R)
- van Bergen, P.F., Collinson, M.E., Scott, A.C., de Leeuw, J.W., 1995. Unusual resin chemistry from Upper Carboniferous pteridosperm resin rodlets, in: Anderson, K.B., Crelling, J.C. (Eds.), *Amber, Resinite, and Fossil Resins*. American Chemical Society, Washington, DC, pp. 149–169. <https://doi.org/10.1021/bk-1995-0617.ch008>
- Vandenabeele, P., Grimaldi, D.M., Edwards, H.G.M., Moens, L., 2003. Raman spectroscopy of different types of Mexican copal resins. *Spectrochimica Acta Part A: Molecular and Biomolecular Spectroscopy* 59, 2221–2229. [https://doi.org/10.1016/S1386-1425\(03\)00066-0](https://doi.org/10.1016/S1386-1425(03)00066-0)
- Vávra, N., 2009. The chemistry of amber – facts, findings and opinions. *Annalen des Naturhistorischen Museum in Wien* 111, 445–474.

- Vítek, P., Ali, E.M.A., Edwards, H.G.M., Jehlička, J., Page, K., 2012. Evaluation of portable Raman spectrometer with 1064 nm excitation for geological and forensic application. *Spectrochimica Acta Part A: Molecular and Biomolecular Spectroscopy* 86, 320–327.
- Voigt, E., 1937. Paläohistologische Untersuchungen an Bernsteineinschlüssen. *Palaeontologische Zeitschrift* 19, 35–46.
- von Lengerken, H., 1913. Etwas über den Erhaltungszustand von Insekten-Inklusen im Bernstein. *Zoologischer Anzeiger* 41, 284–286.
- von Lengerken, H., 1922. Über fossile Chitinstrukturen. *Verhandlungen der Deutschen Zoologischen Gesellschaft* 27, 73–75.
- Vonk, R., Schram, F.R., 2007. Three new tanaid species (Crustacea, Peracarida, Tanaidacea) from the Lower Cretaceous Álava amber in northern Spain. *Journal of Paleontology* 81, 1502–1509. <https://doi.org/10.1666/05-020.1>
- Walden, K.K., Robertson, H.M., 1997. Ancient DNA from amber fossil bees? *Molecular Biology and Evolution* 14, 1075–1077. <https://doi.org/10.1093/oxfordjournals.molbev.a025713>
- Wang, B., Rust, J., Engel, M.S., Szwedo, J., Dutta, S., Nel, A., Fan, Y., Meng, F., Shi, G., Jarzembowski, E.A., Wappler, T., Stebner, F., Fang, Y., Mao, L., Zheng, D., Zhang, H., 2014. A diverse paleobiota in Early Eocene Fushun amber from China. *Current Biology* 24, 1606–1610. <https://doi.org/10.1016/j.cub.2014.05.048>
- Wang, D., Hamm, L.M., Bodnar, R.J., Dove, P.M., 2012. Raman spectroscopic characterization of the magnesium content in amorphous calcium carbonates: Raman spectroscopic characterization. *Journal of Raman Spectroscopy* 43, 543–548. <https://doi.org/10.1002/jrs.3057>
- Wang, X.S., Poinar, H.N., Poinar, G.O., Bada, J.L., 1995. Amino acids in the amber matrix and in entombed insects, in: Anderson, K.B., Crelling, J.C. (Eds.), *Amber, Resinite, and Fossil Resins*. American Chemical Society, Washington, DC, pp. 255–262. <https://doi.org/10.1021/bk-1995-0617.ch014>
- Weitschat, W., Wichard, W., 1998. *Atlas der Pflanzen und Tiere im Baltischen Bernstein*. Pfeil, München.
- Weitschat, W., Wichard, W., 2010. Baltic amber, in: Penney, D. (Ed.), *Biodiversity of Fossils in Amber from the Major World Deposits*. Siri Scientific Press, Manchester, pp. 80–115.
- Westneat, M.W., Betz, O., Blob, R.W., Fezzaa, K., Cooper, W.J., Lee, W.-K., 2003. Tracheal respiration in insects visualized with synchrotron X-ray imaging. *Science* 299, 558–560. <https://doi.org/10.1126/science.1078008>
- Wichard, W., Gröhn, C., Seredszus, F., 2009. Aquatic insects in Baltic amber. *Kessel, Remagen-Oberwinter*.
- Wiemann, J., Crawford, J.M., Briggs, D.E.G., 2020. Phylogenetic and physiological signals in metazoan fossil biomolecules. *Science Advances* 6, eaba6883. <https://doi.org/10.1126/sciadv.aba6883>
- Wiemann, J., Fabbri, M., Yang, T.-R., Stein, K., Sander, P.M., Norell, M.A., Briggs, D.E.G., 2018. Fossilization transforms vertebrate hard tissue proteins into N-heterocyclic polymers. *Nature Communications* 9, 4741. <https://doi.org/10.1038/s41467-018-07013-3>
- Wilby, P.R., Briggs, D.E.G., Riou, B., 1996. Mineralization of soft-bodied invertebrates in a Jurassic metalliferous deposit. *Geology* 24, 847–850.
- Willerslev, E., Cooper, A., 2005. Ancient DNA. *Proceedings of the Royal Society B: Biological Sciences* 272, 3–16. <https://doi.org/10.1098/rspb.2004.2813>
- Winkler, W., Kirchner, E.C., Asenbaum, A., Musso, M., 2001. A Raman spectroscopic approach to the maturation process of fossil resins. *Journal of Raman Spectroscopy* 32, 59–63.
- Wolfe, A.P., Tappert, R., Muehlenbachs, K., Boudreau, M., McKellar, R.C., Basinger, R.J.F., Garrett, A., 2009. A new proposal concerning the botanical origin of Baltic amber. *Proceedings of the Royal Society of London B: Biological Sciences* 276, 3403–3412.

- Wopenka, B., Pasteris, J.D., 2005. A mineralogical perspective on the apatite in bone. *Materials Science and Engineering: C* 25, 131–143. <https://doi.org/10.1016/j.msec.2005.01.008>
- Xing, L., McKellar, R.C., Xu, X., Li, G., Bai, M., Persons, W.S., Miyashita, T., Benton, M.J., Zhang, J., Wolfe, A.P., Yi, Q., Tseng, K., Ran, H., Currie, P.J., 2016. A feathered dinosaur tail with primitive plumage trapped in Mid-Cretaceous amber. *Current Biology* 26, 3352–3360. <https://doi.org/10.1016/j.cub.2016.10.008>
- Xing, L., O'Connor, J.K., McKellar, R.C., Chiappe, L.M., Tseng, K., Li, G., Bai, M., 2017. A mid-Cretaceous enantiornithine (Aves) hatchling preserved in Burmese amber with unusual plumage. *Gondwana Research* 49, 264–277. <https://doi.org/10.1016/j.gr.2017.06.001>
- Yu, T., Kelly, R., Mu, L., Ross, A., Kennedy, J., Broly, P., Xia, F., Zhang, H., Wang, B., Dilcher, D., 2019. An ammonite trapped in Burmese amber. *Proceedings of the National Academy of Sciences* 116, 11345–11350. <https://doi.org/10.1073/pnas.1821292116>
- Zhu, M., Babcock, L.E., Steiner, M., 2005. Fossilization modes in the Chengjiang Lagerstätte (Cambrian of China): testing the roles of organic preservation and diagenetic alteration in exceptional preservation. *Palaeogeography, Palaeoclimatology, Palaeoecology* 220, 31–46. <https://doi.org/10.1016/j.palaeo.2003.03.001>

9.0 Appendix

9.1 TEM protocol for amber samples

Osmium staining & dehydration

1. Dissolving of the amber piece with orange oil (CASRN: 8008-57-9) for 2-5 h.
2. Flush with dry acetone until the yellow colouring vanishes. Transfer the sample into a small polystyrene container.
3. Dehydration of the sample with an acetone series from 100% to 40% (100%, 90%, 80%, 75%, 50%, 40%). Interval: 3 min. Caution: during the change from 75% to 50% acetone, the sample may begin to float.
4. Transfer into 40% ethanol (cooled). For this step, the polystyrene container is removed and the sample is put into a small snap-on jar.
5. Stain the sample in osmium mixture (cooled) for 1 h. Osmium mixture = 1% OsO₄ + 40% ethanol.
6. Flushing with 50% acetone (cooled)
7. Acetone series from 50% to 100% (same steps as in point 3). Interval: 3 min. Optional: Acetone series, from 50% to 75%. Sample can be stored overnight.

Embedding with epoxy resin

The embedding of the samples was carried out with the Epoxy resin (Araldite CY212) Kit[®] of Agar Scientific. Besides the epoxy resin, 500 g DDSA, 100 g dibutylphthalate, and 50 g BDMA are included. All mixtures have been prepared as recommended by the manual.

1. Preparation of 25ml Mixture A.
Mixture A consists of Araldite CY 212 and DDSA, but not BDMA.
2. 3 glasses with snap-on lids are prepared with Mixture A + propylene oxide in varying proportions (1/3; 1/2; 3/1; proportions).

Mix in the 1/3 mixture; let stand for 10 min before removing the supernatant. Subsequently close the glass and let stand for 30 min.

Mix in the 1/2 mixture; let stand for 10 min before removing the supernatant. Subsequently close the glass and let stand for 60 min.

Mix in the 3/1 mixture; let stand for 10 min before removing the supernatant. Subsequently close the glass and let stand for 60 min.

3. Transfer the sample into pure Mixture A; let stand overnight with opened lid.
4. Prepare Mixture B (Mixture A + BDMA (dimethylbenzylamine). BDMA starts the polymerisation reaction of the epoxy resin mixture.
5. Put the sample together with Mixture B into a curved glass and let stand for 6 h in a laboratory hood. Prepare the bases of the sample holders with Mixture B and put into drying oven for 6 h.
6. Transfer the sample onto the prepared sample holders. Keep the sample in a drying oven for 3-4 d at 50-60° C.
7. After this preparation, the sample can be processed as extant samples for TEM analysis (e.g. Winey et al., 2014 and references therein). This includes the production of ultramicrotome sections, which are then placed on copper grids. To enhance the contrast, the sections should be stained with uranyl acetat (CASRN: 6159-44-0) for 10 minutes and lead citrate (after Reynolds, 1963) for 8 – 10 minutes.

References

- Reynolds, E.S., 1963. The use of lead citrate at high pH as an electron-opaque stain in electron microscopy. *Journal of Cell Biology* 17, 208-212.
- Winey, M., Meehl, J.B., O'Toole, E.T., Giddings, T.H., 2014. Conventional transmission electron microscopy. *Molecular Biology of the Cell* 25, 319–323.
<https://doi.org/10.1091/mbc.e12-12-0863>

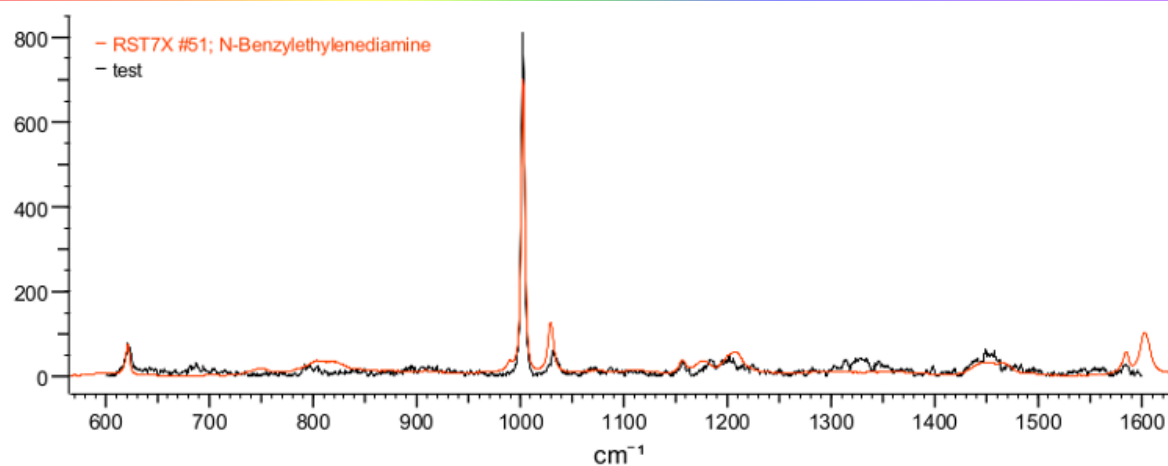
9.2 Bio-Rad spectra

Raman spectrum of N-Benzylethylenediamine



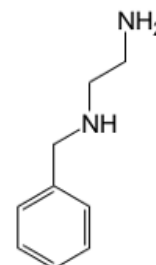
Bio-Rad Laboratories
Informatics Division

19/01/2021 11:06



Manual Corrections: None
Ranges: Full
Search Algorithm: Correlation
Query Path: C:\Users\Analysis-PC\Desktop\test.txt

Name	Value
Resulting HQI	91.32
Database Abbreviation	RST7X
Database Title	Raman - Standards 7 - Bio-Rad Sadtler
Record ID	51
Name	N-Benzylethylenediamine
<unknown>	<a
Boiling Point	250 °C
CAS Registry Number	4152-09-4
Catalog Number	A13262
Color Properties	Yellow
Density	1.00 g/cm ³
Flash Point	95 °C
Formula	C ₉ H ₁₄ N ₂
InChI	InChI=1S/C ₉ H ₁₄ N ₂ /c10-6-7-11-8-
InChIKey	ACYBVNYNIZTUIL-
Instrument Name	Bruker MultiRAM Stand Alone FT-Raman Spectrometer
Lot Number	10141033

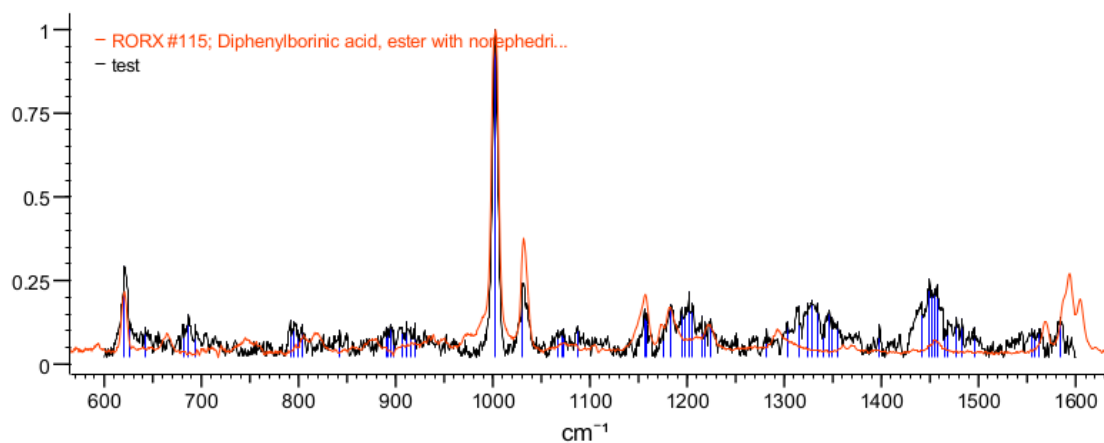


Raman spectrum of Diphenylborinic acid



Bio-Rad Laboratories
Informatics Division

19/01/2021 11:07



Manual Corrections: None

Ranges: Full

Search Algorithm: Correlation

Query Path: C:\Users\Analysis-PC\Desktop\test.txt

Classification	Group	Bond	Range	Intensity	Mode	Notes
Sulfur Con	R-N=S=O					

9.3 HPLC results

Appendix Table 1. Total amino acid concentrations (picomole / mg) of fossils from Cambay and Zhangpu amber. Specimens without L-hArg repression are marked in green.

Sample name	Description	concentration in picomoles / mg												
		Asx	Glx	Ser	L-Thr	L-His	Gly	L-Arg	Ala	Tyr	Val	Phe	Leu	Ile
10013A	Brachycera	420	836	485	177	0	2200	147	409	0	478	629	685	318
10013B	Brachycera	411	809	478	173	59	2295	177	415	34	500	684	662	0
10040A	Nematocera	233	463	284	89	0	927	60	250	0	247	324	280	203
10040B	Nematocera	267	461	290	94	0	966	61	221	0	267	0	446	488
11614A	plant fragment	507	2801	489	254	0	5063	204	995	0	1400	1553	649	196
11614B	plant fragment	540	2824	528	239	0	5003	232	1013	0	1423	0	720	1520
11614C	plant fragment	277	1793	486	150	0	4682	178	637	76	761	2931	1174	97
11614D	plant fragment	315	2014	452	174	0	5427	1887	751	119	844	3304	1705	0
11614E	plant fragment	17	108	29	0	0	332	0	0	0	17	62	0	42
11697A	Nematocera	580	1140	1017	279	182	2448	298	465	197	408	327	817	611
11697B	Nematocera	617	1180	972	278	183	2380	299	468	189	439	341	773	546
11706A	Nematocera	527	828	656	216	0	1839	177	321	0	270	259	626	408
11706B	Nematocera	521	831	663	215	88	1812	175	336	0	262	263	587	418
STB-011-T'10A	Acari	137	289	217	87	0	861	43	139	0	140	0	421	293
STB-011-T'10B	Acari	65	138	185	76	0	776	37	139	0	115	0	180	201
STB-039-T'12A	Araneae	351	657	632	181	156	1646	140	290	0	364	82	495	500
STB-039-T'12B	Araneae	303	613	641	166	0	1427	132	266	0	358	0	515	688
STB-0041-T'12A	plant fragment	241	440	505	177	97	2222	200	455	0	206	153	400	273
STB-0041-T'12B	plant fragment	147	250	430	155	0	1150	196	469	0	214	175	377	297
STB-0291-T'09A	Nematocera	449	937	982	151	0	2621	229	363	0	247	197	548	297
STB-0291-T'09B	Nematocera	386	928	937	153	0	2564	233	350	0	250	213	519	291
STB-0291-T'09C	Nematocera	0	971	840	0	0	4709	0	0	0	0	0	0	0
STB-0291-T'09D	Nematocera	394	1004	794	243	0	4625	285	364	0	323	560	1062	0
STB-0291-T'09E	Nematocera	356	1054	765	157	0	2966	285	380	0	278	260	1116	165
STB-0291-T'09F	Nematocera	27	54	46	9	0	251	14	25	0	13	0	40	0
Tad'10 spider 02A	Arachnida	639	1033	1279	218	0	2665	311	459	0	313	245	628	324
Tad'10 spider 02B	Arachnida	621	1030	1112	223	0	2554	288	444	0	315	245	640	303
Tad'10 spider 02C	Arachnida	426	915	943	277	0	3861	310	394	0	286	248	1016	191
Tad'10 spider 02D	Arachnida	443	970	966	314	0	3982	323	392	0	314	340	1095	290
Tad'10 spider 02E	Arachnida	436	932	1048	0	0	2875	231	396	0	292	0	978	506
Tad'10 spider 02F	Arachnida	79	136	142	33	0	384	36	53	0	39	33	84	43

Appendix Table 2. Amino acid percent concentrations of fossils from Cambay and Zhangpu amber. Specimens without L-hArg repression are marked in green.

Sample name	Description	Asx (%)	Glx (%)	Ser (%)	L-Thr (%)	L-His (%)	Gly (%)	L-Arg (%)	Ala (%)	Tyr (%)	Val (%)	Phe (%)	Leu (%)	Ile (%)
10013A	Brachycera	6.0	12.0	7.0	3.0	0.0	32.0	2.0	6.0	0.0	7.0	9.0	10.0	5.0
10013B	Brachycera	6.0	12.0	7.0	3.0	1.0	34.0	3.0	6.0	1.0	7.0	10.0	10.0	0.0
10040A	Nematocera	7.0	14.0	8.0	3.0	0.0	28.0	2.0	7.0	0.0	7.0	10.0	8.0	6.0
10040B	Nematocera	8.0	13.0	8.0	3.0	0.0	27.0	2.0	6.0	0.0	7.0	0.0	13.0	14.0
11614A	plant fragment	4.0	20.0	3.0	2.0	0.0	36.0	1.0	7.0	0.0	10.0	11.0	5.0	1.0
11614B	plant fragment	4.0	20.0	4.0	2.0	0.0	36.0	2.0	7.0	0.0	10.0	0.0	5.0	11.0
11614C	plant fragment	2.0	14.0	4.0	1.0	0.0	35.0	1.0	5.0	1.0	6.0	22.0	9.0	1.0
11614D	plant fragment	2.0	13.0	3.0	1.0	0.0	35.0	1.0	5.0	1.0	6.0	22.0	11.0	0.0
11614E	plant fragment	3.0	18.0	5.0	0.0	0.0	55.0	0.0	0.0	0.0	3.0	10.0	0.0	7.0
11697A	Nematocera	7.0	13.0	12.0	3.0	2.0	28.0	3.0	5.0	2.0	5.0	4.0	9.0	7.0
11697B	Nematocera	7.0	14.0	11.0	3.0	2.0	27.0	3.0	5.0	2.0	5.0	4.0	9.0	6.0
11706A	Nematocera	9.0	14.0	11.0	4.0	0.0	30.0	3.0	5.0	0.0	4.0	4.0	10.0	7.0
11706B	Nematocera	8.0	13.0	11.0	3.0	1.0	29.0	3.0	5.0	0.0	4.0	4.0	10.0	7.0
STB-011-T'10A	Acari	5.0	11.0	8.0	3.0	0.0	33.0	2.0	5.0	0.0	5.0	0.0	16.0	11.0
STB-011-T'10B	Acari	3.0	7.0	10.0	4.0	0.0	41.0	2.0	7.0	0.0	6.0	0.0	9.0	11.0
STB-039-T'12A	Araneae	6.0	12.0	12.0	3.0	3.0	30.0	3.0	5.0	0.0	7.0	1.0	9.0	9.0
STB-039-T'12B	Araneae	6.0	12.0	13.0	3.0	0.0	28.0	3.0	5.0	0.0	7.0	0.0	10.0	13.0
STB-0041-T'12A	plant fragment	4.0	8.0	9.0	3.0	2.0	41.0	4.0	8.0	0.0	4.0	3.0	7.0	5.0
STB-0041-T'12B	plant fragment	4.0	6.0	11.0	4.0	0.0	30.0	5.0	12.0	0.0	6.0	5.0	10.0	8.0
STB-0291-T'09A	Nematocera	6.0	13.0	14.0	2.0	0.0	37.0	3.0	5.0	0.0	4.0	3.0	8.0	4.0
STB-0291-T'09B	Nematocera	6.0	14.0	14.0	2.0	0.0	38.0	3.0	5.0	0.0	4.0	3.0	8.0	4.0
STB-0291-T'09C	Nematocera	0.0	15.0	13.0	0.0	0.0	72.0	0.0	0.0	0.0	0.0	0.0	0.0	0.0
STB-0291-T'09D	Nematocera	4.0	10.0	8.0	3.0	0.0	48.0	3.0	4.0	0.0	3.0	6.0	11.0	0.0
STB-0291-T'09E	Nematocera	5.0	14.0	10.0	2.0	0.0	38.0	4.0	5.0	0.0	4.0	3.0	14.0	2.0
STB-0291-T'09F	Nematocera	6.0	11.0	10.0	2.0	0.0	52.0	3.0	5.0	0.0	3.0	0.0	8.0	0.0
Tad'10 spider 02A	Arachnida	8.0	13.0	16.0	3.0	0.0	33.0	4.0	6.0	0.0	4.0	3.0	8.0	4.0
Tad'10 spider 02B	Arachnida	8.0	13.0	14.0	3.0	0.0	33.0	4.0	6.0	0.0	4.0	3.0	8.0	4.0
Tad'10 spider 02C	Arachnida	5.0	10.0	11.0	3.0	0.0	44.0	3.0	4.0	0.0	3.0	3.0	11.0	2.0
Tad'10 spider 02D	Arachnida	5.0	10.0	10.0	3.0	0.0	42.0	3.0	4.0	0.0	3.0	4.0	12.0	3.0
Tad'10 spider 02E	Arachnida	6.0	12.0	13.0	0.0	0.0	37.0	4.0	5.0	0.0	4.0	0.0	13.0	7.0
Tad'10 spider 02F	Arachnida	7.0	13.0	13.0	3.0	0.0	36.0	3.0	5.0	0.0	4.0	3.0	8.0	4.0

Appendix Table 3. L and D amino acid concentrations (picomole / mg) of fossils from Cambay and Zhangpu amber. Specimens without L-hArg repression are marked in green.

Sample name	Description	LAsx	DAsx	LGlx	DGlu	LSer	DSer	LArg	DArg	LAla	DAla	LTyr	DTyr	LVal	DVal	LPhe	DPhe	LLeu	DLeu	Llle	Dlle
10013A	Brachycera	363	57	745	92	441	43	147	466	338	71	0	0	281	197	629	0	685	0	318	0
10013B	Brachycera	356	55	722	87	440	38	177	474	340	75	34	0	287	214	670	14	662	0	0	0
10040A	Nematocera	233	0	434	28	242	42	60	110	188	62	0	0	144	102	324	0	280	0	203	0
10040B	Nematocera	235	32	432	29	249	41	61	106	190	32	0	0	151	116	0	0	446	0	356	132
11614A	plant fragment	398	109	1750	1050	489	0	204	618	731	264	0	0	489	911	1478	76	649	0	0	196
11614B	plant fragment	414	125	1770	1054	528	0	232	609	739	274	0	0	501	922	0	0	720	0	1335	185
11614C	plant fragment	217	60	1129	664	349	137	178	690	465	173	76	0	306	455	2888	43	174	1000	0	97
11614D	plant fragment	247	68	1267	747	452	0	187	916	541	210	119	0	367	476	3304	0	513	1192	0	0
11614E	plant fragment	17	0	71	37	29	0	0	0	0	0	0	0	17	0	62	0	0	0	42	0
11697A	Nematocera	536	44	1066	74	991	25	298	252	406	59	197	0	320	88	327	0	817	0	479	132
11697B	Nematocera	566	51	1104	76	951	21	299	263	412	57	189	0	331	107	341	0	773	0	463	83
11706A	Nematocera	482	45	787	41	656	0	177	160	321	0	0	0	270	0	259	0	626	0	339	69
11706A	Nematocera	477	44	791	40	648	16	175	150	313	22	0	0	262	0	263	0	587	0	347	72
STB-011-T'10A	Acari	137	0	268	21	217	0	43	86	139	0	0	0	107	33	0	0	421	0	225	69
STB-011-T'10B	Acari	65	0	138	0	185	0	37	0	139	0	0	0	115	0	0	0	180	0	201	0
STB-039-T'12A	Araneae	320	30	613	44	607	25	140	138	261	29	0	0	187	177	82	0	495	0	500	0
STB-039-T'12B	Araneae	303	0	572	41	616	25	132	152	266	0	0	0	187	171	0	0	515	0	489	199
STB-0041-T'12A	plant fragment	224	18	424	16	505	0	200	103	455	0	0	0	206	0	153	0	400	0	215	58
STB-0041-T'12B	plant fragment	147	0	250	0	430	0	196	116	447	22	0	0	214	0	175	0	377	0	241	56
STB-0291-T'09A	Nematocera	399	50	836	101	982	0	229	0	363	0	0	0	247	0	197	0	548	0	297	0
STB-0291-T'09B	Nematocera	386	0	828	100	937	0	233	186	350	0	0	0	250	0	213	0	519	0	291	0
STB-0291-T'09C	Nematocera	0	0	971	0	840	0	0	0	0	0	0	0	0	0	0	0	0	0	0	0
STB-0291-T'09D	Nematocera	394	0	1004	0	794	0	285	601	364	0	0	0	323	0	560	0	512	550	0	0
STB-0291-T'09E	Nematocera	356	0	958	96	765	0	285	561	380	0	0	0	278	0	260	0	632	483	165	0
STB-0291-T'09F	Nematocera	27	0	54	0	46	0	14	0	25	0	0	0	13	0	0	0	40	0	0	0
Tad'10 spider 02A	Arachnida	589	49	1033	0	1279	0	311	134	459	0	0	0	313	0	245	0	628	0	324	0
Tad'10 spider 02B	Arachnida	578	43	1030	0	1112	0	288	132	444	0	0	0	315	0	245	0	640	0	303	0
Tad'10 spider 02C	Arachnida	426	0	915	0	943	0	310	364	394	0	0	0	286	0	248	0	617	399	191	0
Tad'10 spider 02D	Arachnida	443	0	970	0	966	0	323	459	392	0	0	0	314	0	340	0	666	429	290	0
Tad'10 spider 02E	Arachnida	436	0	932	0	1048	0	321	370	396	0	0	0	292	0	0	0	621	357	506	0
Tad'10 spider 02F	Arachnida	79	0	136	0	142	0	36	0	53	0	0	0	39	0	33	0	84	0	43	0

Appendix Table 4. D/L ratios of amino acids of fossils from Cambay and Zhangpu amber. Specimens without L-hArg repression are marked in green.

Sample name	Description	Asx D/L	Glx D/L	Ser D/L	Arg D/L	Ala D/L	Tyr D/L	Val D/L	Phe D/L	Leu D/L	Ile D/L
10013A	Brachycera	0.16	0.12	0.1	3.17	0.21	0	0.7	0	0	0
10013B	Brachycera	0.15	0.12	0.09	2.68	0.22	0	0.75	0.02	0	0
10040A	Nematocera	0	0.07	0.17	1.83	0.33	0	0.71	0	0	0
10040B	Nematocera	0.14	0.07	0.16	1.73	0.17	0	0.77	0	0	0.37
11614A	plant fragment	0.27	0.6	0	3.03	0.36	0	1.86	0.05	0	0
11614B	plant fragment	0.3	0.6	0	2.63	0.37	0	1.84	0	0	0.14
11614C	plant fragment	0.28	0.59	0.39	3.87	0.37	0	1.49	0.01	5.74	0
11614D	plant fragment	0.28	0.59	0	4.9	0.39	0	1.3	0	2.33	0
11614E	plant fragment	0	0.52	0	0	0	0	0	0	0	0
11697A	Nematocera	0.08	0.01	0.03	0.85	0.15	0	0.27	0	0	0.28
11697B	Nematocera	0.09	0.01	0.02	0.88	0.14	0	0.32	0	0	0.18
11706A	Nematocera	0.09	0.05	0	0.91	0	0	0	0	0	0.2
11706A	Nematocera	0.09	0.05	0.02	0.86	0.07	0	0	0	0	0.21
STB-011-T'10A	Acari	0	0.08	0	2.02	0	0	0.31	0	0	0.31
STB-011-T'10B	Acari	0	0	0	0	0	0	0	0	0	0
STB-039-T'12A	Araneae	0.09	0.07	0.01	0.99	0.11	0	0.95	0	0	0
STB-039-T'12B	Araneae	0	0.07	0.01	1.15	0	0	0.91	0	0	0.41
STB-0041-T'12A	plant fragment	0.08	0.04	0	0.52	0	0	0	0	0	0.27
STB-0041-T'12B	plant fragment	0	0	0	0.59	0.05	0	0	0	0	0.23
STB-0291-T'09A	Nematocera	0.12	0.12	0	0	0	0	0	0	0	0
STB-0291-T'09B	Nematocera	0	0.12	0	0.8	0	0	0	0	0	0
STB-0291-T'09C	Nematocera	0	0	0	0	0	0	0	0	0	0
STB-0291-T'09D	Nematocera	0	0	0	2.11	0	0	0	0	1.08	0
STB-0291-T'09E	Nematocera	0	0.1	0	1.97	0	0	0	0	0.76	0
STB-0291-T'09F	Nematocera	0	0	0	0	0	0	0	0	0	0
Tad'10 spider 02A	Arachnida	0.08	0	0	0.43	0	0	0	0	0	0
Tad'10 spider 02B	Arachnida	0.07	0	0	0.46	0	0	0	0	0	0
Tad'10 spider 02C	Arachnida	0	0	0	1.17	0	0	0	0	0.65	0
Tad'10 spider 02D	Arachnida	0	0	0	1.42	0	0	0	0	0.64	0
Tad'10 spider 02E	Arachnida	0	0	0	1.15	0	0	0	0	0.58	0
Tad'10 spider 02F	Arachnida	0	0	0	0	0	0	0	0	0	0

10.0 Publications

10.1 Publicaton 1

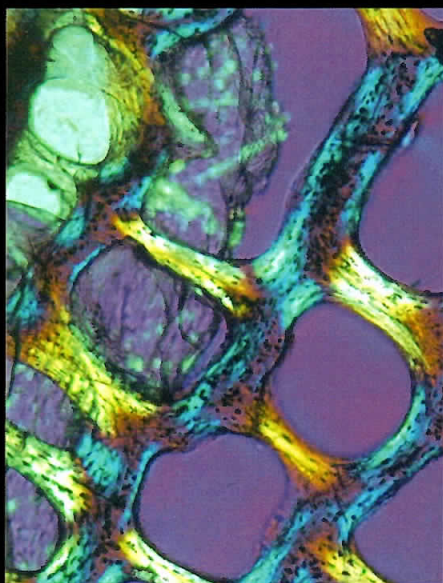
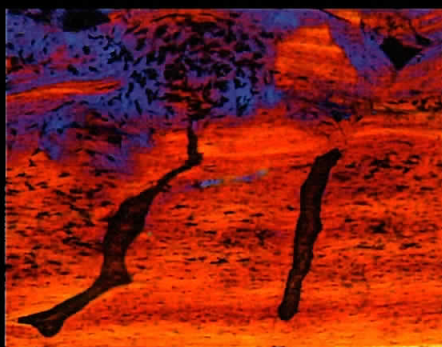
Barthel, H.J., McCoy, V.E., Rust, J., 2021. From ultrastructure to biomolecular composition: taphonomic patterns of tissue preservation in arthropod inclusions in amber, in: Gee, C.T., McCoy, V.E., Sander, P.M. (Eds.), *Fossilization: Understanding the Material Nature of Ancient Plants and Animals*. Johns Hopkins University Press, Baltimore, pp. 115–138.

FOSSILIZATION

UNDERSTANDING THE MATERIAL NATURE OF
ANCIENT PLANTS AND ANIMALS

Edited by

CAROLE T. GEE, VICTORIA E. MCCOY and P. MARTIN SANDER



FOSSILIZATION

Understanding the Material Nature
of Ancient Plants and Animals

EDITED BY
CAROLE T. GEE,
VICTORIA E. MCCOY,
AND P. MARTIN SANDER



JOHNS HOPKINS
UNIVERSITY PRESS



JOHNS HOPKINS UNIVERSITY PRESS
BALTIMORE

This book has been brought to publication with the generous assistance of Darlene Bookoff.

© 2021 Johns Hopkins University Press
All rights reserved. Published 2021
Printed in the United States of America on acid-free paper
9 8 7 6 5 4 3 2 1

Johns Hopkins University Press
2715 North Charles Street
Baltimore, Maryland 21218-4363
www.press.jhu.edu

Library of Congress Cataloging-in-Publication Data

Names: Gee, Carole T., editor. | McCoy, Victoria E., editor | Sander, Martin P., editor

Title: Fossilization : understanding the material nature of ancient plants and animals /
edited by Carole T. Gee, Victoria E. McCoy, and P. Martin Sander.

Description: Baltimore : Johns Hopkins University Press, 2021. |

Includes bibliographical references and index.

Identifiers: LCCN 2020015932 | ISBN 9781421440217 (hardcover) |

ISBN 9781421440224 (ebook)

Subjects: LCSH: Fossilization. | Taphonomy.

Classification: LCC QE721.2.F6 F67 2021 | DDC 560/.41—dc23

LC record available at <https://lccn.loc.gov/2020015932>

A catalog record for this book is available from the British Library.

*Special discounts are available for bulk purchases of this book. For more information,
please contact Special Sales at specialsales@jh.edu.*

Johns Hopkins University Press uses environmentally friendly book materials,
including recycled text paper that is composed of at least 30 percent post-consumer
waste, whenever possible.

Contents

Preface *vii*

CAROLE T. GEE

1 Introduction to the Limits of the Fossil Record 1

P. MARTIN SANDER AND CAROLE T. GEE

2 Organic Phase Preservation in Fossil Dinosaur and Other Tetrapod Bone from Deep Time: Extending the Probable Osteocyte Record to the Early Permian 16

KAYLEIGH WIERSMA, SASHIMA LÄBE, AND P. MARTIN SANDER

3 Fossilization of Reproduction-Related Hard and Soft Tissues and Structures in Non-Avian Dinosaurs and Birds 55

TZU-RUEI YANG AND AURORE CANOVILLE

4 Raman Spectroscopy in Fossilization Research: Basic Principles, Applications in Paleontology, and a Case Study on an Acanthodian Fish Spine 73

THORSTEN GEISLER AND MARTINA MENNEKEN

5 From Ultrastructure to Biomolecular Composition: Taphonomic Patterns of Tissue Preservation in Arthropod Inclusions in Amber 115

H. JONAS BARTHEL, VICTORIA E. MCCOY, AND JES RUST

6 Experimental Silicification of Wood in the Lab and Field: Pivotal Studies and Open Questions 139

CAROLE T. GEE AND MORITZ LIESEGANG

7 The Structure and Chemistry of Silica in Mineralized Wood: Techniques and Analysis 159

MORITZ LIESEGANG, FRANK TOMASCHEK, AND JENS GÖTZE



JOHNS HOPKINS
UNIVERSITY PRESS

**8 Exceptional Fossilization of Ecological Interactions: Plant
Defenses during the Four Major Expansions of Arthropod
Herbivory in the Fossil Record 187**

VICTORIA E. MCCOY, TORSTEN WAPPLER, AND CONRAD C. LABANDEIRA

**9 Color in Living and Fossil Plants: The Search for Biological
Pigments in the Paleobotanical Record 221**

CAROLE T. GEE AND VICTORIA E. MCCOY

10 The Future of Fossilization 249

VICTORIA E. MCCOY

Contributors 257

Index 265



From Ultrastructure to Biomolecular Composition

Taphonomic Patterns of Tissue Preservation in Arthropod Inclusions in Amber

H. JONAS BARTHEL, VICTORIA E. MCCOY, AND JES RUST

ABSTRACT | Amber and copal represent unique and important sources of fossil arthropods. Their extraordinary preservation of morphological characters and internal tissues is well known and unrivaled by any other type of *Konservat-Lagerstätte*. Thus, amber is regarded as an ideal source for ancient biomolecules such as lipids, proteins, and DNA. Here we review the state of knowledge of amber and copal preservation, placing particular emphasis on evidence for a dichotomous pathway of soft tissue preservation in amber. Hypotheses to explain the outstanding preservation of inclusions focus on the resin chemistry and specifically volatile compounds that perfuse the tissue. These volatile compounds have effects that range from the active inhibition of decay enzymes and microorganisms to the inert dehydration caused by the reactions of terpenes and sugars with water in the tissues. However, chemical analysis of inclusions from various deposits indicates that the process of preserving arthropods in amber does not always follow the same exact taphonomic pathway. Furthermore, the quality of the amber fossils varies morphologically, from hollow inclusions to three-dimensional bodies of fossil arthropods exquisitely preserved with all their internal organs. Very early after entrapment, fossilization follows one of two pathways: either decay is severely inhibited, resulting in the preservation of soft tissues complete with ultrastructure, or decay proceeds as usual and the inclusion loses all soft tissues. If the inclusion follows the first, decay-inhibited, pathway, there are then further slow changes in tissue chemistry and biomolecule preservation during diagenesis. In this review, we also summarize previous studies that document internal tissue preservation in amber inclusions and discuss several factors that are likely the major drivers of this phenomenon, such as resin chemistry and microbial gut composition of the entrapped arthropods. It is clear that more extensive taphonomic experimentation is necessary to understand the role of these major drivers in the fine ultrastructural preservation of fossil arthropods in amber. |

Introduction

Resin is a viscous plant exudate produced by trees primarily as a defense against herbivores and pathogens (Hinejima et al. 1992; Langenheim 1994; Lange 2015; Pichersky and Raguso 2018; McCoy et al., chap. 8). Fossil and ancient forms of resin (amber and copal, respectively) are well known and important archives of terrestrial arthropods, plants, and fungi from the Mesozoic to the present day. With their characteristic three-dimensional inclusions—some even fossilized during an ephemeral moment of behavior, such as a parasitic worm emerging from its host (Poinar and Buckley 2006)—and the preservation of minute, even subcellular, detail, the amber fossil record is a powerful tool for answering phylogenetic and paleoecological questions (Labandeira 2014). The uniquely detailed preservation of labile soft-bodied organisms, tissues, and tissue ultrastructure is so exceptional as to suggest that fossil organisms in amber or copal may even preserve ancient biomolecules such as DNA and proteins (an idea most famously suggested in the 1993 blockbuster movie *Jurassic Park*).

Most studies on amber focus on arthropods, which are the dominant group of organisms found as inclusions. The prevalence of arthropod inclusions is due to several factors, such as their ecology and small size, which make them more likely to be entrapped than other taxa like vertebrates (Martínez-Delclòs et al. 2004). However, there is also variation in entrapment frequencies within the arthropod clade that are based on further differences in ecology and size (Martínez-Delclòs et al. 2004; Solórzano Kraemer et al. 2015, 2018). Consequently, if fossilization can be considered a sieve that only allows certain organisms to pass from an ecosystem into the fossil record, amber is a sieve with a particularly fine mesh. The amber fossil record therefore represents only a very small, incomplete slice of a paleocommunity (Solórzano Kraemer et al. 2015, 2018). Fossil organisms in amber and copal have been extensively studied and reviewed in the past (Larsson 1978; Poinar 1992; Solórzano Kraemer 2007; Vávra 2009; Penney 2010; Soriano et al. 2010; Labandeira 2014; McCoy et al. 2018a; Seyfullah et al. 2018a, b), but studies emphasizing taphonomic aspects are relatively sparse compared to studies on taxonomy and ecology. Nevertheless, as with all exceptional fossils, the utility of inclusions in amber in any research context (taxonomic, ecological, etc.) depends on the quality of the preservation.

Chemical and microscopic investigations suggest that the quality of preservation in amber is not uniform and depends on several factors, such as the chemistry of the resin, the grade of dehydration of the inclusion, or the soil composition (Kohring 1998; Stankiewicz et al. 1998; Martínez-Delclòs

et al. 2004; Koller et al. 2005; McCoy et al. 2018a, b). Many questions arise from this observation: How are the fossils preserved? What is the degree of alteration? Do original biomolecules get preserved? Are some structures (or tissues) generally “better” preserved than others? Are there differences in preservation between amber deposits of the same or different ages, or based on geographical origin and resin-producing tree origin? Understanding the process of fossilization in resin would allow us to answer these questions and therefore target the most suitable deposits for specific research questions, which may require the preservation of specific tissues or biomolecules.

Here we summarize the current state of research on the taphonomy of inclusions in amber and combine these data into a unified picture of taphonomic patterns in amber. While we focus primarily upon investigations of arthropods because these are the most widely studied taxa, we also occasionally include information on other taxa to strengthen our conclusions and clarify the patterns that we identify. Further, we present a hypothesis for a general dichotomous pathway of fossilization in amber that results in either the presence or absence of soft tissue preservation, and we focus particularly upon several factors that we think are likely to most strongly influence the quality of preservation when soft tissues remain. Finally, we suggest the most productive future pathways for research into amber taphonomy.

Tissue Ultrastructure

Ultrastructural preservation is absent in fossils from most amber deposits (Martínez-Delclòs et al. 2004; Soriano et al. 2010; Labandeira 2014; McCoy et al. 2018a). Recent large-scale investigations of amber taphonomy have revealed that the majority of amber deposits have no fossils, and the majority of fossiliferous amber sites are characterized by “empty” inclusions, that is, inclusions that are empty molds with just external tissue preservation (Martínez-Delclòs et al. 2004; Soriano et al. 2010; Labandeira 2014; McCoy et al. 2018a). However, for inclusions in amber with preserved tissues, the ultrastructural details of those tissues can be used as a valuable tool for understanding the process of fossilization in amber.

The earliest pioneers in the study of tissue ultrastructure in amber fossils looked at arthropods—the most common type of inclusion—and used traditional study methods such as thin-sectioning, light microscopy, scanning electron microscopy (SEM), and transmission electron microscopy (TEM). These studies usually utilized only one method, and at most a few specimens, and were focused on whether tissue ultrastructure is preserved in

fossil animals in amber. As described by Grimaldi et al. (1994), Kornilowitsch was the first to recognize the importance of studying tissue ultrastructure; in 1903, he thin-sectioned legs from both neuropteran and dipteran inclusions in Baltic amber and identified striated muscle tissue in both types of insects. However, his results were not widely accepted due to the poor quality of his images and the fact that the piece exhibited surface crazing. At the time, surface crazing was thought to be specific to copal alteration, but it has since been realized that it occurs in poorly looked-after ambers as well, such as historic Baltic amber collections (e.g. Kettunen et al. 2019). Nineteen years after Kornilowitsch's study, von Lengerken (1922) successfully extracted the tracheal parts of beetles from Baltic amber, although he was less interested in ultrastructural preservation and more interested in the chemical preservation of chitin.

Andrée and Keilbach (1936) and Voigt (1937) presented new results on ultrastructural preservation in amber and showed that it is not a rare occurrence in inclusions with preserved soft tissues. The first set of authors reported the preservation of tissue ultrastructure in parts of the tracheal system, musculature, and "soft tissue" (gut material and ovarioles) (Andrée and Keilbach 1936); they also indicated that they had evidence for chitin preservation. However, they do not clearly state their methods, neither for extracting the inclusions from the amber nor for analyzing the inclusions, although Voigt (1937) notes that Andrée and Keilbach achieved their results by dissolving the amber. Voigt (1937) himself applied the "lacquer film method," which he developed as an improvement over previous iterations of this technique in order to prepare insects, spiders, plants, and fecal pellets in numerous pieces of Baltic amber. Using light microscopy, Voigt identified muscle tissue, trachea, and gland epithelia from the insects, and noted that while even badly preserved samples yielded ultrastructural details, small insects generally seemed to be better preserved than large ones.

After these two studies, there was a long hiatus of 39 years before the advent of newer technology, specifically SEM, facilitated the investigation of tissue ultrastructure in fossils. Mierzejewski (1976a, b) was one of the first to apply this new technology to amber, focusing on arthropod and wood inclusions in Baltic amber. He accessed the tissues by grinding and polishing the outer covering of amber until only a thin layer remained over the inclusion, which he then removed manually with a thin needle. With this technique, Mierzejewski documented the ultrastructural details of the eye of a dolichopodid fly, the elytra of a beetle, and the book lungs of a spider, as well as of the wood of *Pinus succinifera*. A few years later, Poinar and Hess (1982, 1985) and Poinar (1992) applied TEM to elucidate the ultra-

structure of a single specimen of a fungus gnat. They were able to identify various cellular remains containing muscle fibers, nuclei, ribosomes, lipid droplets, endoplasmic reticula, and even mitochondria. Using the same method, Poinar (1992) also identified cellular-level structures in tissues of a braconid wasp in Cretaceous amber from Canada.

The era of ultrastructural studies that started in the 1970s is rounded out by a few analyses of mineralized arthropod inclusions in amber. Mineralized tissues are rare in amber but not unknown (Labandeira 2014); it is more common for minerals to replicate fine-scale tissue ultrastructure outside of amber (e.g., Martill 1990; Gee and Liesegang, chap. 6). Baroni-Urbani and Graeser (1987) used SEM to describe a pyritized cast of an ant in Baltic amber; the pyrite replicated the surface microsculptural features of the integument. A few years later, Schlüter (1989) also employed SEM to investigate the wing venation of three termites from the Cenomanian amber of France, whereby one sample was covered with marcasite and pyrite. He also showed images of two other mineralized specimens—an insect head that may have belonged to an ant, although definite identification was not possible, and the elytra of a beetle—both of which preserved surface microsculpture.

These studies unequivocally demonstrate the preservation of exceptional microscopic ultrastructural details in fossils from various amber sites, including Eocene Baltic amber, Cretaceous French amber, and Cretaceous Canadian amber. More importantly, all authors emphasized that the preserved ultrastructures were identical to those in extant groups, even though the documentation of extant samples was not included in these publications.

The next major advancement in the study of tissue ultrastructure in amber involved the first direct comparison of fossil and extant material by Henwood (1992a), who removed inclusions from amber by cutting or fracturing the specimen through the insect body and analyzing the inclusions with TEM or SEM. Henwood (1992a) also carried out decomposition experiments under varying conditions to develop an understanding of different decay sequences in the flight muscles of living blowflies. She then compared the end results with preserved muscle tissues from similar brachyceran flies in Dominican amber. Although muscle fibers and the finest detail of mitochondria (their internal membranes or cristae) were still preserved in the fossil fly in amber, they were not identical to those in freshly dead flies. However, they were comparable to these structures after some experimental decay in extant flies.

Specifically, Henwood noted that the experimental pathways involving dehydration resulted in the best-preserved tissues but also led to the shrinkage of muscle fibers and mitochondria. The fossil fly embedded in Domin-

ican amber also exhibited these features, which may have been due to the dehydrating effects of resin. Henwood expanded her studies by using SEM to describe the internal tissue preservation of essentially all organ systems in a beetle in Dominican amber (Henwood 1992b). As would be expected, the ultrastructure of all tissues was well preserved. Thus, these results somewhat contradict the previous conclusions: although ultrastructure is recognizable and well preserved, it may not be exactly identical to the ultrastructure observed in the tissues of a living organism.

Shortly after Henwood's experiments, the most comprehensive study of internal tissue preservation in amber was published by Grimaldi et al. (1994). Grimaldi et al. addressed the question of consistency and patterns in soft tissue preservation in amber based on a large number of organisms embedded in two types of amber. Altogether, the sample set included 16 specimens of arthropods from Baltic and Dominican amber that varied in several aspects, such as size and degree of cuticle sclerotization (bees, beetles, termites, gnats, flies). Furthermore, the sample set also included one leaflet and seven anthers of the leguminous tree *Hymenaea* from Dominican amber. The inclusions were manually extracted by fracturing the amber: a groove was first circumscribed around the midsagittal line of the specimens, which in the end formed a circle less than 1 mm from the inclusion. With the help of a sharp blade, the internal edge of the groove was scored until slight leverage caused the piece to split, exposing the inclusions for SEM and TEM analysis. Soft tissue preservation was more common in Dominican than in Baltic amber; all the Dominican amber specimens had internal soft tissues, whereas half of the Baltic amber samples were just empty molds. However, in both ambers, when soft tissues were preserved, air sacs, tracheae, parts of the gut, remains of the brain, and muscle fibers were found in their original position and insertions.

Since then, a few other studies have demonstrated similarly exceptional preservation of tissue ultrastructure in a variety of inclusions from many sites. Kohring (1998) documented the preservation of various arthropod structures, such as alae, muscle tissue with myofibrils, cornea cells, dorsal vessels, and trachea, in inclusions in Baltic, Bitterfeld, and Dominican ambers. Using a method similar to that of Mierzejewski, Kohring exposed the inclusion by putting mechanical pressure on the amber piece, relying on the fact that inclusions represent discontinuities that favor the splitting of the amber along the main axis of the embedded organisms. Just over a decade later, Kowalewska and Szwedo (2009) combined SEM with energy-dispersive X-ray spectroscopy (EDS) analysis and examined the surface of a leafhopper from Baltic amber, revealing the presence of marcasite. In that same

year, Tanaka et al. (2009) published SEM and TEM images of dolichopodid fly eyes. They examined two specimens trapped together in the same piece of Baltic amber and report a completely preserved visual system in both animals. A radial section through ommatidia revealed the presence of a basement membrane, rhabdomeres, trachea, and pigment cells (primary and secondary).

These studies reveal an interesting pattern of tissue preservation. First, they unambiguously demonstrate the exceptional preservation of tissue ultrastructure in fossil inclusions in amber. Second, they indicate a dichotomy in the preservation of tissue ultrastructure: either no soft tissue is preserved or tissue morphology is exquisitely preserved, even including subcellular structures (although they may be slightly altered in morphology due to shrinkage). Third, this dichotomy is apparent even within the same amber site; for example, Baltic amber inclusions are an even mix of empty molds and tissues preserved with ultrastructural details (Grimaldi et al. 1994). This suggests that there is a dichotomous pathway to tissue preservation: depending on fossilization variables (specific variables discussed in more detail below), there is either a rapid preservation or a rapid decay of soft tissues.

Biomolecular Composition

Fossil arthropods in amber have an exquisite life-like preservation, as if they were frozen in time, unchanged since the day they were first trapped in resin. As discussed above, the life-like nature of tissue preservation can even extend to microscopic ultrastructural details, which immediately prompts follow-up questions: Does the preservational fidelity of amber-embedded tissues extend beyond the ultrastructural scale into the molecular level? In other words, do amber-entombed tissues retain remnants of the original chemical composition?

The question of the chemical preservation of tissues was raised very early on in the study of amber. Alexander Tornquist, professor and head of the amber collection of the Albertus University Königsberg in the early 20th century, states in his monograph on the geology of East Prussia (Tornquist 1910) that no original material is preserved in amber (as mentioned earlier in this chapter, Kornilowitsch's success in extracting muscle tissue from Baltic amber was doubted by the majority of the scientific community at this time). In that same year, Klebs tested Tornquist's hypothesis by examining bone in Baltic amber to determine if original tissues in bone were still preserved (Klebs 1910). This study was carried out on the only lizard in am-

ber known at that time (the “Königsberg specimen”), which had to be sacrificed for the cause; the mechanical opening of the amber to expose the inclusions resulted in the partial destruction of this unique specimen. Without the benefit of modern technology, his conclusions were limited. Klebs reported “coaly remains,” but he did not check for muscle preservation; the rest of the inclusion was simply a hollow void.

Initial studies on the preservation of chitin in amber were carried out by von Lengerken (1913, 1922). In his first attempt, von Lengerken examined pieces that had been stored in alcohol for years. All of these inclusions showed no evidence of chitin preservation and were either hollow inside or contained coaly remains that could not be assigned to any specific organ (von Lengerken 1913). In contrast to this, an inclusion that was stored under dry conditions did yield chitin and had preserved partial remains of abdominal segments, including a ventral porus (von Lengerken 1913). It was reported that the chitin was not strongly altered in this specimen but had in some places transformed into brown coal. Later, von Lengerken successfully analyzed chitin of beetles from Baltic amber, which he extracted manually through needle preparation (von Lengerken 1922); in these specimens, the structure of the chitin could be observed under a microscope. In addition to the chitin, von Lengerken also extracted tracheal remains.

The geochemical basis of tissue fixation and preservation in inclusions in amber is not fully understood. It has been suggested that biomolecules in the fossil tissues might have undergone extensive polymerization, similar to nonenzymatic Maillard reactions (Bada et al. 1999; Briggs 1999), which would lead to chemical and mechanical fixation. This hypothesis was supported by the detection of volatile compounds released from ancient plants found in Egyptian graves, which are characteristic of Maillard reaction products (Evershed et al. 1997). High molecular weight Maillard polymers have been dissolved in *in vitro* experiments with the chemical phenacyl thiazolium bromide (PTB), which breaks specific crosslinks and allows for the release of the trapped proteins and DNA (Vasan et al. 1996). In accordance with this reaction, incubation with PTB released polymerase chain reaction-amplifiable DNA from insoluble polymers in ancient feces that were about 10,000 years old (Poinar et al. 1998). These results have led to the hypothesis that the carbohydrates, peptides, or short chains of DNA or RNA in the tissue of amber fossils may also be trapped in a three-dimensional insoluble network of geopolymers formed by Maillard reactions and therefore cannot be detected as native biological molecules (Bada et al. 1999). This hypothesis is supported by the observation that the color of amber-embedded tissues seen in thin section consists of various shades of brown, which is rem-

iniscient of melanoidins, the insoluble products of the Maillard reaction (browning reaction).

Modern investigations of tissue composition of fossil inclusions in amber started with techniques such as pyrolysis–gas chromatography–mass spectrometry (Py-GC-MS), Raman spectroscopy (see Geisler and Menneken, chap. 4, for a more in-depth discussion of Raman spectroscopy), and histochemical staining to determine the major organic composition of fossils in amber and specifically to look for remnants of original tissue moieties. Stanekiewicz et al. (1998) used Py-GC-MS to investigate cuticle preservation in arthropods (bees and beetles) and leaves from Dominican amber, as well as subfossil and ancient resin from Kenya. The younger (2–20 ka) samples from Kenya retained some of their original composition, including chitin (but not protein) in the arthropod cuticle and lignocellulose in the plants. The inclusions in the much older Dominican amber (ca. 15–20 Ma; Iturralde-Vinent and MacPhee 1996) had no recognizable remnants of original chemistry. Edwards et al. (2007) used Raman spectroscopy to investigate insects in Mexican and Baltic ambers. They found evidence of severely degraded proteins in the insect in Mexican amber (22 Ma; de Lourdes Serrano-Sánchez et al. 2015) and no evidence of original biomolecules in the insect in Baltic amber (45 Ma). However, they suggest their Baltic amber specimen was hollow and that a specimen with preserved internal tissue would have yielded different results. These two amber studies of arthropod tissue chemistry give variable and contradictory results because they are based on multiple amber sites and methods, which makes it challenging to draw any conclusions about the patterns of chemical preservation of tissues in amber.

We will now briefly mention the results from studies on other tissues to help resolve these issues and clarify the patterns. Hartl et al. (2015) used Raman spectroscopy to analyze the tissue chemistry of lichens in amber and determined that the cortex and medulla can be distinguished on the basis of Raman spectra. However, these differences in the spectra could not be interpreted to determine if they retain some remnants of original chemistry, or if diagenesis and alteration had not yet completely obscured any original differences. Similarly, Koller et al. (2005) used histochemical staining on a cypress twig in Baltic amber to demonstrate the presence of some unidentified tissue biomolecules. They suggested that these represent original tissue moieties, but it is not clear to what extent the stains would also react to diagenetically altered biomolecules. In general, the results of Koller et al. (2005) suggest significant alteration or loss of original tissue chemistry during fossilization in amber, but also offer some hope that the inclusions may retain some trace remnants of original biomolecules.

Based on the likelihood of finding biochemical remnants, more recent studies have focused on targeted techniques to isolate and characterize specific molecules of interest. This was first attempted for DNA preservation in Dominican amber, using what was at the time the most up-to-date techniques for DNA purification, amplification, and sequencing (Cano et al. 1992; DeSalle et al. 1992; Poinar et al. 1996). Although the results initially looked exciting, later advances in our understanding of contamination and appropriate methods for ancient DNA analysis showed that the nucleotides recovered were contaminants (Gutiérrez et al. 1998). In addition, all later studies that tried to recover DNA from amber under strict laboratory conditions were unsuccessful (Austin et al. 1997a, b; Smith and Austin 1997; Walden and Robertson 1997; Hebsgaard et al. 2005). These results were further supported by a more recent study that failed to extract DNA from fossil inclusions in much younger copal, suggesting that DNA preserves very poorly in amber (Penney et al. 2013).

Protein and amino acid extraction from fossils in amber has been more successful, most likely due to the higher preservation potential of proteins relative to DNA. Bada et al. (1994) found amino acids in arthropod inclusions in copal, as well as in Dominican, Baltic, and Lebanese ambers, but not in Mexican amber. The amino acids were localized in the inclusion rather than in the amber matrix, and their degree of racemization indicated that the amino acids came from intact protein fragments. Smejkal et al. (2011) obtained ancient amino acids and sequenced protein fragments from fossil fungal inclusions in amber, giving more support to the idea that these inclusions can contain intact protein fragments. More recently, McCoy et al. (2019) found similar results for fossil feathers in Burmese and Baltic ambers: ancient amino acids with low degrees of racemization and a composition similar to that expected for feathers degraded in resin. These results suggest that trace amounts of original biomolecules can be preserved in fossils in amber and can be identified using targeted, highly sensitive chemical techniques.

Taphonomic Pattern: The Dichotomous Pathway to Preservation

The primary goal in investigating the patterns of preservation of tissue ultrastructure and tissue chemistry is to understand the process of fossilization in amber. This process can be divided into three phases (Martínez-Delclòs et al. 2004; Labandeira 2014): entrapment, in which an insect or other organism is trapped in resin; early diagenesis, which occurs immediately

after entrapment, when the resin is still rich in original volatiles that interact with the tissues; and late diagenesis, after the resin has lost many of its volatiles but during which chemical changes related to polymerization may still be occurring. The boundary between early diagenesis and late diagenesis, like the boundary between copal and amber, is not clearly defined (Labandeira 2014). Entrapment is the best studied of these three phases, having been thoroughly investigated and summarized in a few recent studies (Martínez-Delclòs et al. 2004; Solórzano Kraemer et al. 2015, 2018). Entrapment biases are unlikely to be a major factor influencing the patterns of tissue preservation in fossil inclusions in amber; if the amber has an inclusion, then by default an organism has been trapped.

The second phase, early diagenesis, is most strongly characterized by the interaction of resin volatiles with the tissues and microbiota of any entrapped organism. Through chemical analysis of inclusions in resin, various resin specialists have noted that the tissues are perfused with resin compounds (Grimaldi et al. 1994; Stankiewicz et al. 1998), indicating that resin chemicals can reach and interact with all organic tissues (Poinar and Hess 1985). Moreover, Henwood (1992a) demonstrated the importance of resin chemistry in preserving tissues by evaluating the decay of flies entrapped in a variety of substances. The flies in wax decayed more quickly and had relatively poorer tissue preservation than a control group left open in the air, and the slowest decay and best preservation were found in flies embedded in maple syrup. In other words, physical sealing of organic matter from oxygen alone is not a guarantee of inhibited decay and high-fidelity tissue preservation, rather, there must be some chemical interaction with the embedding medium (Henwood 1992a). The exact mechanism of decay inhibition is unclear and likely includes some combination of tissue dehydration and inhibition of microbial or enzymatic activity.

These analyses and experiments demonstrate the importance of early diagenesis in fossilization in amber, as well as the role of resin volatiles in exceptional tissue preservation. We further hypothesize that interactions between the tissue, bacteria, and volatiles (e.g. dehydration, enzyme inhibition, growth inhibition of bacteria) control the early dichotomous branching on the fossilization pathway. These interactions will determine if soft tissues (with their attendant ultrastructures) preserve over geological time-scales or degrade. Previous authors have noted this dichotomous pattern of tissue loss or preservation in ambers of all ages (Grimaldi et al. 1994; Labandeira 2014), and we have observed it in young resin from Madagascar as well. Thus, this split in the taphonomic pathway must happen fairly early in diagenesis. More support comes from McCoy et al. (2018b), who observed

this dichotomy after less than two years of experimental decay in resin: fruit flies encased in *Pinus* resin resulted in empty molds, whereas fruit flies in *Wollemia* resin retained all their tissues. The analytical method used by McCoy et al. (2018b)—synchrotron tomography—precluded the assessment of tissue ultrastructural preservation, but given the preservation of tissue ultrastructure in, for example, 45-million-year-old Baltic amber (Grimaldi et al. 1994), it was likely preserved in the fruit flies in *Wollemia* resin as well.

Based on our hypothesis that chemical interactions with resin determine the loss or preservation of tissues, the most obvious influential factor would be resin chemistry, which is complex and can differ significantly between resin-producing taxa and even within an individual tree (Anderson and Winans 1991; Anderson et al. 1992; Langenheim 2003; Lambert et al. 2008, 2012, 2015). This also proved to be the most important factor in the experiments by McCoy et al. (2018b) that resulted in the dichotomous pattern of tissue loss or preservation analogous to what is observed in the amber fossil record. This factor alone would be sufficient to explain the pattern if the mechanism of decay inhibition is a straightforward interaction between tissues and volatile resin compounds, such as dehydration. However, a more complex scenario involving the interaction of resin compounds with the microbiota in the inclusions suggests alternative factors, such as the composition of the gut microbiota, which can be very different between taxa or even within a single individual. McCoy et al. (2018b) noted differences in the extent of decay based on the formation of decay gas bubbles between fruit flies with no gut biota and fruit flies with a gut biota embedded in *Wollemia* resin; however, all still retained their internal soft tissues.

There is extensive literature on the interaction of various resins and resin constituents with various bacteria (e.g., Lang and Buchbauer 2012; Shuaib et al. 2013), but there is no clear pattern: any particular resin may inhibit the activity of some bacteria and promote the growth of other bacteria, and these bacterial assemblages vary among different resins. Experiments involving resins that are known precursors to amber along with bacteria common in arthropod guts may help untangle this complicated set of interactions. Even less well-understood is the role that resin volatiles may play in inhibiting autolytic decay; there is some evidence that chemical compounds in plant tissues, including those such as terpenoids and terpenes, which are also the primary components of resin, can inhibit enzymatic activity (e.g., Miyazawa and Yamafuji 2005; Chang et al. 2006; Bustanji et al. 2011; Adamczyk et al. 2015), suggesting this interaction deserves more study. Other less well-supported factors have been suggested as well, for example, dehydration

prior to entrapment (Coty et al. 2014), the degree of sclerotization of the cuticle (Poinar and Hess 1985; Grimaldi et al. 1994), and the physical prevention of external bacteria from interacting with the inclusions, which is related to resin permeability (Smith 1880). We expect factors arising from the depositional environment, such as sediment interactions, heat, and pressure, to play a more important role in late diagenesis, but of course they may also have an impact on early diagenesis.

Resin polymerization during late diagenesis is a prerequisite for producing a fossil inclusion in amber, but we expect that there are still changes in the preservation of inclusions during this stage of fossilization in amber. Specifically, although the preservation of tissues and their ultrastructures seems to be determined during early diagenesis, we hypothesize that this phase, late diagenesis, controls the loss or preservation of original tissue chemistry over long time periods. In other words, if an inclusion continues down the tissue preservation branch of the dichotomous pathway of fossil preservation, it may experience further biochemical changes. These do not represent further dichotomous branches, but rather continuous changes.

Original tissue chemistry is more commonly preserved in copal than in amber, but remnants may remain even in Cretaceous amber (e.g., Bada et al. 1994; McCoy et al. 2019). Factors influencing the degradation of tissue chemistry in amber have been less well-studied than variables influencing the preservation of tissues in amber; this field is still in the early stages, and most studies are focused simply on investigating the extent of original tissue chemistry in fossils in amber (Bada et al. 1994; Stankiewicz et al. 1998; Koller et al. 2005; Edwards et al. 2007; Penney et al. 2013; Thomas et al. 2014; Hartl et al. 2015; McCoy et al. 2019). However, the degradation of biomolecules, such as proteins, is strongly influenced by environmental factors, such as temperature and water, which correspond to variables such as burial depth, diagenetic history, sediment composition, and amber permeability (Martínez-Delclòs et al. 2004; McCoy et al. 2018b).

Amber permeability has been briefly investigated within the context of determining whether air and water inclusions in amber are original, resulting in the conclusion that amber is a somewhat open, permeable system (Beck 1988; Hopfenberg et al. 1988). Further investigations to understand variations in permeability throughout the process of polymerization and between different resins would be a valuable addition to the field. Similarly, there have been a few studies subjecting resin to different temperatures, pressures, and sediments to understand how these variables influence polymerization and amberization (Gold et al. 1999; Poinar and Mastalerz 2000;

Winkler et al. 2001; Scalarone et al. 2003a, b; Bisulca et al. 2012; Saitta et al. 2019); applying these methods to resin with inclusions would help understand the role of these particular factors in the fossilization of inclusions.

Future Perspectives

We must emphasize that all previous studies of tissue ultrastructure obtained access to the tissues through the sawing, cutting, or cracking of the amber—methods that are inherently destructive to the inclusion. It may be possible to extract complete, undamaged inclusions by dissolving the amber around them (fig. 5.1; plate 5.1), but this method is restricted to samples of a few

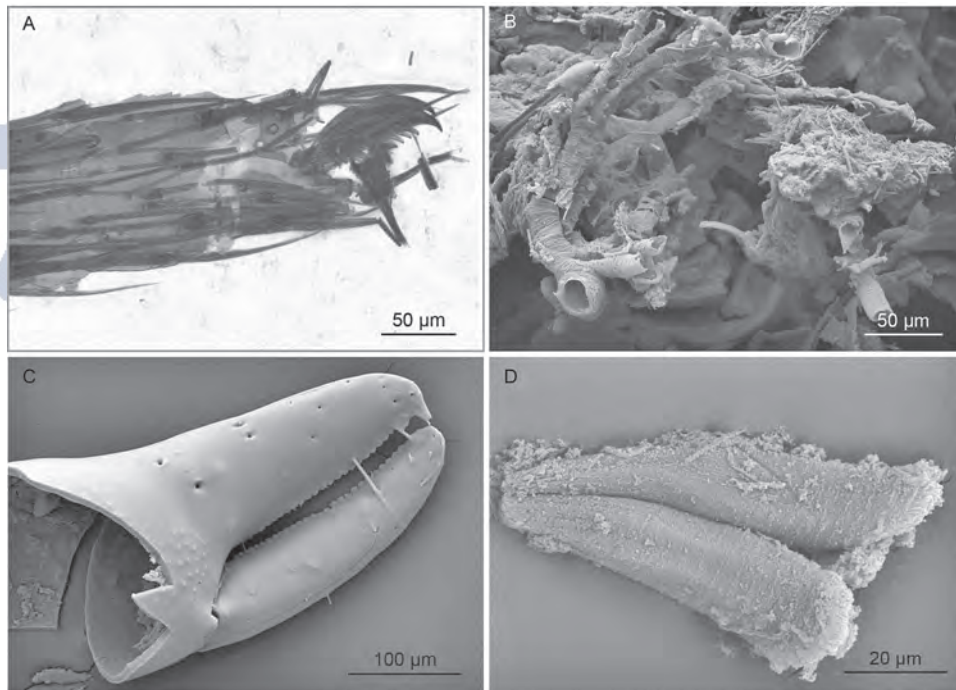


Figure 5.1. Inclusions extracted from Eocene Indian Cambay amber (ca. 53 Ma). (A) Light microscope image of an isolated insect leg. (B) SEM image showing parts of the tracheal system of an extracted beetle. (C) SEM image of a pedipalp of a pseudoscorpion. (D) SEM image showing the preservation of the muscular tissue that was removed from the pedipalp shown in C.



Plate 5.1. Nematoceran fly extracted from Indian Cambay amber (ca. 53 Ma). Except for the antennae, the anterior-most part of the body is nicely preserved and projects above the amber matrix. The abdomen is still enclosed by the resinous residue of the original amber.

localities and depends on the composition of the resin. Viehmeyer (1913), in his study of Sulawesi copal; Azar (1997), in his study of Lower Cretaceous Lebanese amber; Andrée and Keilbach (1936), in their study of Eocene Baltic amber; and Mazur et al. (2014), in their study of Eocene Indian amber, developed protocols for dissolving their respective type of amber and were thereby able to recover more or less complete arthropod remains. Viehmeyer (1913), for example, exhumed complete, three-dimensional specimens and even large parts of insects by completely dissolving the amber matrix with different organic solvents; although the plant and insect remains were fragile, they could be mounted on microscope slides.

To date, all of these studies have only developed dissolution methods and

observed the preservation of soft tissues; however, such extracted arthropod remains are an obvious target for future tissue ultrastructure studies. Younger ambers and copals, or just “ancient resins,” are less polymerized than fossil resins such as amber and can be more easily dissolved, although some highly viscous nondissolvable fraction may remain in the vial (Viehmeyer 1913; Penney et al. 2013; Mazur et al. 2014; Barthel, own data). Over time, the resins start to polymerize and become amber, making it difficult or impossible to dissolve most ambers (Mazur et al. 2014). Dutta et al. (2010) and Dutta and Mallick (2017) have theorized that, due to their unique chemical composition, dammar resins undergo only minimal polymerization during fossilization. Therefore, these and similar class II resins originating from angiosperms (van Aarssen et al. 1990) are the most promising target for dissolution experiments.

Another approach is to apply newer methods such as high-resolution X-ray microcomputed tomography (micro-CT or CT scanning) and synchrotron X-ray tomographic microscopy (SRXTM, or synchrotron tomography) to amber inclusions (Dierick et al. 2007; Soriano et al. 2010; Kehlmaier et al. 2014; Sherratt et al. 2015; Pepinelli and Currie 2017). These two imaging techniques are nondestructive methods that can be used to develop three-dimensional models of the internal and external features of the inclusion. At the moment, these three-dimensional reconstructions are a powerful tool for taxonomy. It should be pointed out, however, that while synchrotron tomography can clearly show images of tissue ultrastructure (Zehbe et al. 2010), this method has not yet been applied to specimens in amber. Synchrotron tomography at these very detailed scales may prove to be an imaging tool as equally powerful as CT scanning for studying ultrastructure.

Further research is needed to understand the patterns of chemical preservation in fossils in amber. In particular, there are still several unresolved issues. Can remnants of original biomolecules preserve even when soft tissues have decayed away? Are there trace remnants of original chemical composition that characterize all arthropod fossils in amber with tissues preserved to the ultrastructure level? Or, are there one or more additional taphonomic filters that control the biomolecule preservation?

Fossilization of soft tissues in resin is most likely a complex process involving a number of factors. Further taphonomic experimentation is needed to understand the effects of these factors in isolation and in combination with one another. Previous experiments have been sufficient to confirm that some factors—specifically chemistry of the embedding resin and the composition of the gut microbiota of the entrapped arthropods—are likely to

play a major role in tissue preservation and the early diagenetic phases of fossilization. These factors should be investigated in greater detail in a series of taphonomic experiments to develop a more complete understanding of their influence on decay and their interactions with one another.

As of yet, there have not been any experiments on the late diagenesis phase of fossilization in amber, and any attempts in this direction would be a major step forward. There are a number of experiments on the diagenesis of nonfossiliferous resin (Scalarone et al. 2003a, b; Pastorelli 2011; Beltran et al. 2017; Saitta et al. 2019) that could provide a good basis for experimentation on resin with inclusions.

Conclusions

Amber and its inclusions have been extensively studied for over a hundred years. Initially, most investigations were either chemical analyses of the amber or taxonomic and ecological investigations of the inclusions (ignoring the amber). In the past few decades, more emphasis has been placed on the unit of amber and its inclusions rather than focusing on one or the other in isolation, revealing a unique and interesting taphonomic pathway (Poinar and Hess 1985; Henwood 1992a; Grimaldi et al. 1994; Stankiewicz et al. 1998; McCoy et al. 2018a, b). Recent integrative investigations have revealed a robust taphonomic pattern in the fossilization of entrapped organisms: an early dichotomy between the loss or preservation of tissues and tissue ultrastructure, which corresponds to early diagenetic interactions with resin volatiles, and a later, more complex pattern of loss or preservation of original tissue chemistry, which corresponds to a variety of later diagenetic interactions.

While this sounds straightforward, the taphonomic pattern in amber fossilization may be influenced by a wide array of complex factors, such as resin chemistry, composition of the microbiota in the inclusions, and parameters of the depositional environment. A deeper analysis of localities with amber fossils in order to understand these taphonomic patterns would be useful and extremely interesting. However, concurrent taphonomic experiments in the laboratory to better understand and quantify the effect of the resin chemistry and microbiota would help with understanding the taphonomic processes of fossilization in amber even more. Finally, we encourage amber researchers to consider both the amber and the inclusions together, rather than viewing them in isolation.

ACKNOWLEDGMENTS

The authors thank Kerstin Koch and Axel Huth (Rhine-Waal University of Applied Sciences) for access to the Centre for Microscopy and supporting the senior author by taking images of the extracted inclusions. Furthermore, thank you to reviewers Leyla Seyfullah (University of Vienna) and an anonymous colleague for their helpful comments on the manuscript. This work was funded by the Deutsche Forschungsgemeinschaft (DFG, German Research Foundation), Project number 396704064 to Jes Rust for HJB and Project number 396637283 to Jes Rust for VEM (both at the University of Bonn). This is contribution number 19 of DFG Research Unit FOR 2685, “The Limits of the Fossil Record: Analytical and Experimental Approaches to Fossilization.”

WORKS CITED

- Adamczyk, S., Adamczyk, B., Kitunen, V., and Smolander, A. 2015. Monoterpenes and higher terpenes may inhibit enzyme activities in boreal forest soil. *Soil Biology & Biochemistry*, 87: 59–66.
- Anderson, K.B., and Winans, R.E. 1991. Nature and fate of natural resins in the geosphere. I. Evaluation of pyrolysis–gas chromatography mass spectrometry for the analysis of natural resins and resinates. *Analytical Chemistry*, 63: 2901–2908.
- Anderson, K.B., Winans, R.E., and Botto, R.E. 1992. The nature and fate of natural resins in the geosphere—II. Identification, classification and nomenclature of resinates. *Organic Geochemistry*, 18: 829–841.
- Andrée, K., and Keilbach, R. 1936. Neues über Bernsteineinschlüsse. *Schriften der Physikalisch-Ökonomische Gesellschaft zu Königsberg*, 69: 124–128.
- Austin, J.J., Ross, A.J., Smith, A.B., Fortey, R.A., and Thomas, R.H. 1997a. Problems of reproducibility—Does geologically ancient DNA survive in amber-preserved insects? *Proceedings of the Royal Society B*, 264: 467–474.
- Austin, J.J., Smith, A.B., and Thomas, R.H. 1997b. Palaeontology in a molecular world: The search for authentic ancient DNA. *Trends in Ecology & Evolution*, 12: 303–306.
- Azar, D. 1997. A new method for extracting plant and insect fossils from Lebanese amber. *Palaeontology*, 40: 1027–1060.
- Bada, J.L., Wang, X.S., and Hamilton, H. 1999. Preservation of key biomolecules in the fossil record: Current knowledge and future challenges. *Philosophical Transactions of the Royal Society of London B*, 354: 77–86.
- Bada, J.L., Wang, X.S., Poinar, H.N., Paabo, S., and Poinar, G.O. 1994. Amino acid racemization in amber-entombed insects: Implications for DNA preservation. *Geochimica et Cosmochimica Acta*, 58: 3131–3135.
- Baroni-Urbani, C., and Graeser, S. 1987. REM-Analysen an einer pyritisiereten Ameise aus Baltischem Bernstein. *Stuttgarter Beiträge zur Naturkunde B*, 133: 1–16.
- Beck, C.W. 1988. In reply: Is the air in amber ancient? *Science*, 241: 718–719.
- Beltran, V., Salvadó, N., Butí, S., Cinque, G., and Pradell, T. 2017. Markers, reactions,

- and interactions during the aging of *Pinus* resin assessed by Raman spectroscopy. *Journal of Natural Products*, 80: 854–863.
- Bisulca, C., Nascimbene, P.C., Elkin, L., and Grimaldi, D.A. 2012. Variation in the deterioration of fossil resins and implications for the conservation of fossils in amber. *American Museum Novitates*, 3734: 1–19.
- Briggs, D.E.G. 1999. Molecular taphonomy of animal and plant cuticles: Selective preservation and diagenesis. *Philosophical Transactions of the Royal Society of London B*, 354: 7–17.
- Bustanji, Y., Al-Masri, I.M., Mohammad, M., Hudaib, M., Tawaha, K., Tarazi, H., and Alkhatib, H.S. 2011. Pancreatic lipase inhibition activity of trilactone terpenes of *Ginkgo biloba*. *Journal of Enzyme Inhibition and Medicinal Chemistry*, 26: 453–459.
- Cano, R.J., Poinar, H., and Poinar, G.O. 1992. Isolation and partial characterisation of DNA from the bee *Proplebeia dominicana* (Apidae: Hymenoptera) in 25–40 million year old amber. *Medical Science Research*, 20: 249–251.
- Chang, T.K.H., Chen, J., and Yeung, E.Y.H. 2006. Effect of *Ginkgo biloba* extract on procarcinogen-bioactivating human CYP1 enzymes: Identification of isorhamnetin, kaempferol, and quercetin as potent inhibitors of CYP1B1. *Toxicology and Applied Pharmacology*, 213: 18–26.
- Coty, D., Aria, C., Garrouste, R., Wils, P., Legendre, F., and Nel, A. 2014. The first ant-termite syninclusion in amber with CT-scan analysis of taphonomy. *PLOS ONE*, 9: e104410.
- de Lourdes Serrano-Sánchez, M., Hegna, T.A., Schaaf, P., Pérez, L., Centeno-García, E., and Vega, F.J. 2015. The aquatic and semiaquatic biota in Miocene amber from the Campo LA Granja mine (Chiapas, Mexico): Paleoenvironmental implications. *Journal of South American Earth Sciences*, 62: 243–256.
- DeSalle, R., Gatesy, J., Wheeler, W., and Grimaldi, D. 1992. DNA sequences from a fossil termite in Oligo-Miocene amber and their phylogenetic implications. *Science*, 257: 1933–1936.
- Dierick, M., Cnudde, V., Masschaele, B., Vlassenbroeck, J., Van Hoorebeke, L., and Jacobs, P. 2007. Micro-CT of fossils preserved in amber. *Nuclear Instruments & Methods in Physics Research. Section A, Accelerators, Spectrometers, Detectors and Associated Equipment*, 580: 641–643.
- Dutta, S., and Mallick, M. 2017. Chemical evidence for dammarenediol, a bioactive angiosperm metabolite, from 54 Ma old fossil resins. *Review of Palaeobotany and Palynology*, 237: 96–99.
- Dutta, S., Mallick, M., Mathews, R.P., Mann, U., Greenwood, P.F., and Saxena, R. 2010. Chemical composition and palaeobotanical origin of Miocene resins from Kerala-Konkan Coast, western India. *Journal of Earth System Science*, 119: 711–716.
- Edwards, H.G.M., Farwell, D.W., and Villar, S.E.J. 2007. Raman microspectroscopic studies of amber resins with insect inclusions. *Spectrochimica Acta. Part A, Molecular and Biomolecular Spectroscopy*, 68: 1089–1095.
- Evershed, R.P., Bland, H.A., van Bergen, P.F., Carter, J.F., Horton, M.C., and Rowley-Conwy, P.A. 1997. Volatile compounds in archaeological plant remains and the Maillard reaction during decay of organic matter. *Science*, 278: 432–433.

- Gold, D., Hazen, B., and Miller, W.G. 1999. Colloidal and polymeric nature of fossil amber. *Organic Geochemistry*, 30: 971–983.
- Grimaldi, D.A., Bonwich, E., Delannoy, M., and Doberstein, S. 1994. Electron microscopic studies of mummified tissues in amber fossils. *American Museum Novitates*, 3097: 1–31.
- Gutiérrez, G., and Marín, A. 1998. The most ancient DNA recovered from an amber-preserved specimen may not be as ancient as it seems. *Molecular Biology and Evolution*, 15: 926–929.
- Hartl, C., Schmidt, A.R., Heinrichs, J., Seyfullah, L.J., Schäfer, N., Gröhn, C., Rikkinen, J., and Kaasalainen, U. 2015. Lichen preservation in amber: Morphology, ultrastructure, chemofossils, and taphonomic alteration. *Fossil Record*, 2: 127–135.
- Hebsgaard, M.B., Phillips, M.J., and Willerslev, E. 2005. Geologically ancient DNA: Fact or artefact? *Trends in Microbiology*, 13: 212–220.
- Henwood, A. 1992a. Exceptional preservation of dipteran flight muscle and the taphonomy of insects in amber. *Palaos*, 7: 203–212.
- Henwood, A. 1992b. Soft-part preservation of beetles in Tertiary amber from the Dominican Republic. *Palaontology*, 35: 901–912.
- Hinejima, M., Hobson, K.R., Otsuka, T., Wood, D.L., and Kubo, I. 1992. Antimicrobial terpenes from oleoresin of ponderosa pine tree *Pinus ponderosa*: A defense mechanism against microbial invasion. *Journal of Chemical Ecology*, 18 (10): 1809–1818.
- Hopfenberg, H.B., Witchev, L.C., Poinar, G.O., Beck, C.W., Chave, K.E., Smith, S.V., Horibe, Y., and Craig, H. 1988. Is the air in amber ancient? *Science*, 241: 717–721.
- Iturralde-Vinent, M.A., and MacPhee, R.D.E. 1996. Age and paleogeographical origin of Dominican amber. *Science*, 273: 1850–1852.
- Kehlmaier, C., Dierick, M., and Skevington, J.H. 2014. Micro-CT studies of amber inclusions reveal internal genitalic features of big-headed flies, enabling a systematic placement of *Metanephrocerus* Aczél, 1948 (Insecta: Diptera: Pipunculidae). *Arthropod Systematics & Phylogeny*, 72: 23–36.
- Kettunen, E., Sadowski, E.-M., Seyfullah, L.J., Dörfelt, H., Rikkinen, J., and Schmidt, A.R. 2019. Caspary's fungi from Baltic amber: historic specimens and new evidence. *Papers in Palaeontology*, 5: 365–389.
- Klebs, R. 1910. Über Bernsteineinschlüsse im allgemeinen und die Coleopteren meiner Bernsteinsammlung. *Schriften der physikalischen-ökonomischen Gesellschaft zu Königsberg*, 51: 217–242.
- Kohring, R. 1998. REM-Untersuchungen an harzkonservierten Arthropoden. *Entomologia Generalis*, 23: 95–106.
- Koller, B., Schmitt, J.M., and Tischendorf, G. 2005. Cellular fine structures and histochemical reactions in the tissue of a cypress twig preserved in Baltic amber. *Proceedings of the Royal Society B*, 272: 121–126.
- Kowalewska, M., and Szewdo, J. 2009. Examination of the Baltic amber inclusion surface using SEM techniques and X-ray microanalysis. *Palaogeography, Palaeoclimatology, Palaeoecology*, 271: 287–291.
- Labandeira, C.C. 2014. Amber. Reading and writing of the fossil record: Preservation pathways to exceptional fossilization. *Paleontological Society Papers*, 20: 163–216.
- Lambert, J.B., Santiago-Blay, J.A., and Anderson, K.B. 2008. Chemical signatures of fossilized resins and recent plant exudates. *Angewandte Chemie*, 47: 9608–9616.

- Lambert, J.B., Santiago-Blay, J.A., Wu, Y., and Levy, A.J. 2015. Examination of amber and related materials by NMR spectroscopy. *Magnetic Resonance in Chemistry*, 53: 2–8.
- Lambert, J.B., Tsai, C.Y.-H., Shah, M.C., Hurtley, A.E., and Santiago-Blay, J.A. 2012. Distinguishing amber and copal classes by proton magnetic resonance spectroscopy. *Archaeometry*, 54: 332–348.
- Lang, G., and Buchbauer, G. 2012. A review on recent research results (2008–2010) on essential oils as antimicrobials and antifungals. A review. *Flavour and Fragrance Journal*, 27: 13–39.
- Lange, B.M. 2015. The evolution of plant secretory structures and emergence of terpenoid chemical diversity. *Annual Review of Plant Biology*, 66: 19.1–19.21.
- Langenheim, J.H. 1994. Higher plant terpenoids: A phyto-centric overview of their ecological roles. *Journal of Chemical Ecology*, 20 (6): 1–58.
- Langenheim, J.H. 2003. *Plant Resins: Chemistry, Evolution, Ecology, and Ethnobotany*. Timber Press, Oregon, USA.
- Larsson, S.G. 1978. *Baltic Amber: A Paleobiological Study*. Scandinavian Scientific Press, Klampenborg, Denmark.M;
- Martill, D.M. 1990. Macromolecular resolution of fossilized muscle tissue from an elopomorph fish. *Nature*, 346: 171–172.
- Martínez-Delclòs, X., Briggs, D.E.G., and Peñalver, E. 2004. Taphonomy of insects in carbonates and amber. *Palaeogeography, Palaeoclimatology, Palaeoecology*, 203: 19–64.
- Mazur, N., Nagel, M., Leppin, U., Bierbaum, G., and Rust, J. 2014. The extraction of fossil arthropods from Lower Eocene Cambay amber. *Acta Palaeontologica Polonica*, 59: 455–460.
- McCoy, V.E., Soriano, C., and Gabbott, S.E. 2018a. A review of preservational variation of fossil inclusions in amber of different chemical groups. *Earth and Environmental Science, Transactions of the Royal Society of Edinburgh*, 107 (2–3): 203–211.
- McCoy, V.E., Soriano, C., Pegoraro, M., Luo, T., Boom, A., Foxman, B., and Gabbott, S.E. 2018b. Unlocking preservation bias in the amber insect fossil record through experimental decay. *PLOS ONE*, 13: e0195482.
- Mierzejewski, P. 1976a. On application of scanning electron microscope to the study of organic inclusions from the Baltic amber. *Rocznik Polskiego Towarzystwa Geologicznego*, 46: 291–295.
- Mierzejewski, P. 1976b. Scanning electron microscope studies on the fossilization of Baltic amber spiders (preliminary note). *Annals of the Medical Section of the Polish Academy of Sciences*, 21: 81–82.
- Miyazawa, M., and Yamafuji, C. 2005. Inhibition of acetylcholinesterase activity by bicyclic monoterpenoids. *Journal of Agricultural and Food Chemistry*, 53: 1765–1768.
- Pastorelli, G. 2011. A comparative study by infrared spectroscopy and optical oxygen sensing to identify and quantify oxidation of Baltic amber in different ageing conditions. *Journal of Cultural Heritage*, 12: 164–168.
- Penney, D. 2010. *Biodiversity of Fossils in Amber from the Major World Deposits*. Siri Scientific Press, Manchester.
- Penney, D., Wadsworth, C., Fox, G., Kennedy, S.L., Preziosi, R.F., and Brown, T.A. 2013. Absence of ancient DNA in sub-fossil insect inclusions preserved in “Anthropocene” Colombian copal. *PLOS ONE*, 8: e73150.

- Pepinelli, M., and Currie, D.C. 2017. The identity of giant black flies (Diptera: Simuliidae) in Baltic amber: Insights from large-scale photomicroscopy, micro-CT scanning and geometric morphometrics. *Zoological Journal of the Linnean Society*, 181: 846–866.
- Pichersky, E., and Raguso, R.A. 2018. Why do plants produce so many terpenoid compounds? *New Phytologist*, 220: 692–702.
- Poinar, G.O. 1992. *Life in Amber*. Stanford University Press, Stanford, California.
- Poinar, G.O., and Buckley, R. 2006. Nematode (Nematoda: Mermithidae) and hair-worm (Nematomorpha: Chordodidae) parasites in Early Cretaceous amber. *Journal of Invertebrate Pathology*, 93: 36–41.
- Poinar, G.O., and Hess, R. 1982. Ultrastructure of 40-million-year-old insect tissue. *Science*, 215: 1241–1242.
- Poinar, G.O., and Hess, R. 1985. Preservative qualities of recent and fossil resins: Electron micrograph studies on tissue preserved in Baltic amber. *Journal of Baltic Studies*, 16: 222–230.
- Poinar, G.O., and Mastalerz, M. 2000. Taphonomy of fossilized resins: Determining the biostratigraphy of amber. *Acta Geológica Hispánica*, 35: 171–182.
- Poinar, H.N., Hofreiter, M., Spaulding, W.G., Martin, P.S., Stankiewicz, B.A., Bland, H., Evershed, R.P., Possnert, G., and Pääbo, S. 1998. Molecular coproscopy: Dung and diet of the extinct ground sloth *Nothrotheriops shastensis*. *Science*, 281: 402–406.
- Poinar, H.N., Höss, M., Bada, J.L., and Pääbo, S. 1996. Amino acid racemization and the preservation of ancient DNA. *Science*, 272: 864–866.
- Saitta, E.T., Kaye, T.G., and Vinther, J. 2019. Sediment-encased maturation: A novel method for simulating diagenesis in organic fossil preservation. *Palaeontology*, 62: 135–150.
- Scalabrone, D., Lazzari, M., and Chiantore, O. 2003a. Ageing behaviour and analytical pyrolysis characterisation of diterpenic resins used as art materials: Manila Copal and Sandarac. *Journal of Analytical and Applied Pyrolysis*, 68–69: 115–136.
- Scalabrone, D., van der Horst, J., Boon, J.J., and Chiantore, O. 2003b. Direct-temperature mass spectrometric detection of volatile terpenoids and natural terpenoid polymers in fresh and artificially aged resins. *Journal of Mass Spectrometry*, 38: 607–617.
- Schlüter, T. 1989. Neue Daten über harzkonservierte Arthropoden aus dem Cenomanium NW-Frankreichs. *Documenta Naturae*, 56: 59–70.
- Seyfullah, L.J., Beimforde, C., Dal Corso, J., Perrichot, V., Rikkinen, J., and Schmidt, A.R. 2018a. Production and preservation of resins—Past and present. *Biological Reviews of the Cambridge Philosophical Society*, 93: 1684–1714.
- Seyfullah, L.J., Roghi, G., Dal Corso, J., and Schmidt, A.R. 2018b. The Carnian pluvial episode and the first global appearance of amber. *Journal of the Geological Society*, 175: 1012–1018.
- Sherratt, E., del Rosario Castañeda, M., Garwood, R.J., Mahler, D.L., Sanger, T.J., Herrel, A., de Queiroz, K., and Losos, J.B. 2015. Amber fossils demonstrate deep-time stability of Caribbean lizard communities. *Proceedings of the National Academy of Sciences of the United States of America*, 112: 9961–9966.
- Shuaib, M., Ali, A., Ali, M., Panda, B.P., and Ahmad, M.I. 2013. Antibacterial activity of resin rich plant extracts. *Journal of Pharmacy & Bioallied Sciences*, 5: 265–269.
- Smejkal, G.B., Poinar, G.O., Righetti, P.G., and Chu, F. 2011. Revisiting Jurassic Park: The isolation of proteins from amber encapsulated organisms millions of years

- old, pp. 925–938. In: Ivanov, A.R., and Lazarev, A.V., eds. *Sample Preparation in Biological Mass Spectrometry*. Springer, Dordrecht.
- Smith, A.B., and Austin, J.J. 1997. Can ancient DNA be recovered from the fossil record? *GeoScientist*, 7: 58–61.
- Smith, E.A. 1880. Concerning amber. *The American Naturalist*, 14: 179–190.
- Solórzano Kraemer, M.M. 2007. Systematic, palaeoecology, and palaeobiogeography of the insect fauna from Mexican amber. *Palaeontographica Abteilung A*, 282: 1–133.
- Solórzano Kraemer, M.M., Kraemer, A.S., Stebner, F., Bickel, D.J., and Rust, J. 2015. Entrapment bias of arthropods in Miocene amber revealed by trapping experiments in a tropical forest in Chiapas, Mexico. *PLOS ONE*, 10: e0118820.
- Solórzano Kraemer, M.M., Martínez-Delclos, X., Clapham, M.E., Arillo, A., Peris, D., Jäger, P., Stebner, F., and Peñalver, E. 2018. Arthropods in modern resins reveal if amber accurately recorded forest arthropod communities. *Proceedings of the National Academy of Sciences*, 115: 6739–6744.
- Soriano, C., Archer, M., Azar, D., Creaser, P., Delclòs, X., Godthelp, H., Hand, S., J Jones, A., Nel, A., Néraudeau, D., Ortega-Blanco, J., Pérez-de la Fuente, R., Perichot, V., Saupe, E., Solórzano Kraemer, M., and Tafforeau, P. 2010. Synchrotron X-ray imaging of inclusions in amber. *Comptes Rendus Palevol*, 9: 361–368.
- Stankiewicz, B.A., Poinar, H.N., Briggs, D.E.G., Evershed, R.P., and Poinar, G.O. 1998. Chemical preservation of plants and insects in natural resins. *Proceedings of the Royal Society B*, 265: 641–647.
- Tanaka, G., Parker, A.R., Siveter, D.J., Maeda, H., and Furutani, M. 2009. An exceptionally well-preserved Eocene dolichopodid fly eye: Function and evolutionary significance. *Proceedings of the Royal Society B*, 276: 1015–1019.
- Thomas, D.B., Nascimbene, P.C., Dave, C.J., Grimaldi, D.A., and James, H.F. 2014. Seeking carotenoid pigments in amber-preserved fossil feathers. *Scientific Reports*, 4: 5226.
- Tornquist, A.J.H. 1910. *Geologie von Ostpreussen*. Gebrüder Borntraeger, Berlin.
- van Aarssen, B.G.K., Cox, H.C., Hoogendoorn, P., and de Leeuw, J.W. 1990. A cadinene biopolymer in fossil and extant dammar resins as a source for cadinanes and bicadinanes in crude oils from South East Asia. *Geochimica et Cosmochimica Acta*, 54: 3021–3031.
- Vasan, S., Zhang, X., Zhang, X., Kapurniotu, A., Bernhagen, J., Teichberg, S., Basgen, J., Wagle, D., Shih, D., Terlecky, I., Bucala, R., Cerami, A., Egan, J., and Ulrich, P.W. 1996. An agent cleaving glucose-derived protein crosslinks *in vitro* and *in vivo*. *Nature*, 382: 275–278.
- Vávra, N. 2009. The chemistry of amber—Facts, findings and opinions. *Annalen des Naturhistorischen Museums in Wien Serie A*, 111: 445–473.
- Viehmeyer, H. 1913. Ameisen aus dem Kopal von Celebes. *Stettiner Entomologische Zeitung*, 74: 141–155.
- Voigt, E. 1937. Paläohistologische Untersuchungen an Bernstein-Einschlüssen. *Palaeontologische Zeitschrift*, 19: 35–46.
- von Lengerken, H. 1913. Etwas über den Erhaltungszustand von Insekten-Inklusen im Bernstein. *Zoologischer Anzeiger*, 41: 284–286.
- von Lengerken, H. 1922. Über fossile Chitinstrukturen. *Verhandlungen der Deutschen Zoologischen Gesellschaft*, 27: 73.
- Walden, K.O.O., and Robertson, H.M. 1997. Ancient DNA from amber fossil bees? *Molecular Biology and Evolution*, 14: 1075–1077.

Winkler, W., Kirchner, E.C., Asenbaum, A., and Musso, M. 2001. A Raman spectroscopic approach to the maturation process of fossil resins. *Journal of Raman Spectroscopy*, 32: 59–63.

Zehbe, R., Haibel, A., Riesemeier, H., Gross, U., Kirkpatrick, C.J., Schubert, H., and Brochhausen, C. 2010. Going beyond histology. Synchrotron micro-computed tomography as a methodology for biological tissue characterization: From tissue morphology to individual cells. *Journal of the Royal Society Interface*, 7: 49–59.





Plate 5.1. Nematoceran fly extracted from Indian Cambay amber (ca. 53 Ma). Except for the antennae, the anterior-most part of the body is nicely preserved and projects above the amber matrix. The abdomen is still enclosed by the resinous residue of the original amber.

10.2 Publication 2

Peris, D., Janssen, K., **Barthel, H.J.**, Bierbaum, G., Delclòs, X., Peñalver, E., Solórzano-Kraemer, M.M., Jordal, B.H., Rust, J., 2020. DNA from resin-embedded organisms: Past, present and future. PLoS ONE 15, e0239521. <https://doi.org/10.1371/journal.pone.0239521>

RESEARCH ARTICLE

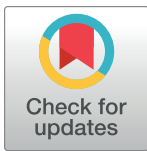
DNA from resin-embedded organisms: Past, present and future

David Peris¹*, Kathrin Janssen²*, H. Jonas Barthel¹, Gabriele Bierbaum², Xavier Delclòs³, Enrique Peñalver⁴, Mónica M. Solórzano-Kraemer⁵, Bjarte H. Jordal⁶, Jes Rust¹

1 Section Paleontology, Institute of Geosciences, University of Bonn, Bonn, Germany, **2** Institute of Medical Microbiology, Immunology and Parasitology, Medical Faculty, University of Bonn, Bonn, Germany, **3** Department of Earth and Ocean Dynamics and Biodiversity Research Institute (IRBio), Faculty of Earth Sciences, Universitat de Barcelona, Barcelona, Spain, **4** Geological and Mining Institute of Spain (Geominero Museum), Valencia, Spain, **5** Department of Palaeontology and Historical Geology, Senckenberg Research Institute, Frankfurt am Main, Germany, **6** Museum of Natural History, University Museum of Bergen, University of Bergen, Bergen, Norway

* These authors contributed equally to this work.

* daperce@gmail.com (DP); Kathrin.Janssen@ukbonn.de (KJ)



OPEN ACCESS

Citation: Peris D, Janssen K, Barthel HJ, Bierbaum G, Delclòs X, Peñalver E, et al. (2020) DNA from resin-embedded organisms: Past, present and future. PLoS ONE 15(9): e0239521. <https://doi.org/10.1371/journal.pone.0239521>

Editor: David Caramelli, University of Florence, ITALY

Received: January 28, 2020

Accepted: September 9, 2020

Published: September 28, 2020

Copyright: © 2020 Peris et al. This is an open access article distributed under the terms of the [Creative Commons Attribution License](https://creativecommons.org/licenses/by/4.0/), which permits unrestricted use, distribution, and reproduction in any medium, provided the original author and source are credited.

Data Availability Statement: All relevant data are within the manuscript and its Supporting Information files.

Funding: DP - Alexander von Humboldt Foundation (Germany). <https://www.humboldt-foundation.de/web/home.html>. DP, KJ, HJB, GB, JR - German Research Foundation Research Unit 2685 (Germany). This is contribution no. 25 of Research Unit 2685 (Projektnummer 396704301). <https://www.dfg.de/en/>. DP, XD, EP, MMSK - CRE project funded by the Spanish AEI/FEDER, EU Grant CGL2017-84419. <http://www.idi.mineco.gob.es>.

Abstract

Past claims have been made for fossil DNA recovery from various organisms (bacteria, plants, insects and mammals, including humans) dating back in time from thousands to several million years BP. However, many of these recoveries, especially those described from million-year-old amber (fossil resin), have faced criticism as being the result of modern environmental contamination and for lack of reproducibility. Using modern genomic techniques, DNA can be obtained with confidence from a variety of substrates (e.g. bones, teeth, gum, museum specimens and fossil insects) of different ages, albeit always less than one million years BP, and results can also be obtained from much older materials using palaeoproteomics. Nevertheless, new attempts to determine if ancient DNA (aDNA) is present in insects preserved in 40 000-year old sub-fossilised resin, the precursor of amber, have been unsuccessful or not well documented. Resin-embedded specimens are therefore regarded as unsuitable for genetic studies. However, we demonstrate here, for the first time, that although a labile molecule, DNA is still present in platypodine beetles (Coleoptera: Curculionidae) embedded in six-year-old and two-year-old resin pieces from *Hymenaea verrucosa* (Angiospermae: Fabaceae) collected in Madagascar. We describe an optimised method which meets all the requirements and precautions for aDNA experiments for our purpose: to explore the DNA preservation limits in resin. Our objective is far from starting an uncontrolled search for aDNA in amber as it was in the past, but to start resolving basic aspects from the DNA preservation in resin and search from the most modern samples to the ancient ones, step by step. We conclude that it is therefore possible to study genomics from resin-embedded organisms, although the time limits remain to be determined.

XD, EP, MMSK - National Geographic Global Exploration Fund Northern Europe, Grant GEFNE 127-14. <https://www.nationalgeographic.org/funding-opportunities/grants/what-we-fund/>. MMSK - VolkswagenStiftung (Germany) Grant 90946. <https://www.volkswagenstiftung.de/>.

Competing interests: The authors have declared that no competing interests exist.

Introduction

Deoxyribonucleic acid (DNA) contains the genetic information that allows all life forms to function, grow and reproduce; in addition, it is present in all cells and thus forms part of the tissues. Ideally, fossil—or ancient—DNA (aDNA) might serve as an alternative to morphological analysis and palaeoethology, which for centuries have served as the only tools available for scientists to determine the phylogenetic relationships between past organisms. Genomic sequences also provide insights into molecular evolutionary changes over time, clarify evolutionary relationships among taxa and yield information on mutualism rates [1, 2].

Amber is fossilised tree resin that may preserve deep time fauna in exceptionally clear morphological detail [3–5], and therefore appeared a promising material for preserving aDNA. It was hoped that DNA could easily be extracted from ancient soft tissue remains that were desiccated and macroscopically well preserved [6], because the complete and rapid engulfment of arthropods in resin and their hypothetically rapid fixation and dehydration—a type of mummification—promised to promote the preservation of DNA [7, 8]. Claims for DNA preserved in amber samples were rapidly made [9–12] in some cases with samples more than 125 million years old [13]. These studies overshadowed other less well-known studies on younger aDNA [14, 15]. However, amber claims are suspected of being the result of modern environmental DNA contamination because authentication procedures were not followed [16–22].

Natural resins are secreted from parenchymal cells in plants and trees and comprise complex mixtures of terpenoid compounds, including acids, alcohols and saccharides, some of which have preservative and antimicrobial properties [5, 23]. It has been observed that modern resin and amber both exhibit extensive chemical variations [24], which may influence preservation processes and therefore the quality of embedded organisms [25, 26]. Furthermore, DNA is a particularly labile macromolecule. In living cells, specific repair mechanisms act on damaged DNA, but these processes cease after cell death and DNA is naturally degraded [27]. Besides active cleavage of DNA by nucleases shortly after cell death [28, 29], long-term DNA degradation by hydrolytic processes (initiating double-strand breaks) or oxidative dinucleotide modification and depurination (removal of the guanine and adenine bases from the sugar-phosphate backbone) highly affect the stability of DNA molecules [16, 30–33]. Additionally, it seems that diagenetic events, including overburden pressure and heat generated through orogenesis over millions of years, affect amber permeability [34] and minimise the likelihood of DNA preservation in amber [21, 35].

The resin samples used in this study came from *Hymenaea verrucosa* Gaertner, 1791 [36] trees (Fabaceae), which produce copious amounts of resin that contains different types of sesquiterpene hydrocarbons and diterpenoid resin acids [23, 37]. Plants from this genus are the source plant of Miocene amber deposits in Mexico, the Dominican Republic, Peru and Ethiopia, and of sub-fossil resin deposits in different parts of the world [38]. Cenozoic amber from India and China was produced by some species of Angiospermae: Dipterocarpaceae [39, 40]. By contrast, the major Mesozoic amber deposits mainly derive from Coniferales [38]. The different plant group origin of the resin implies different sets of compounds in their chemical composition: monosaccharides, alcohols, aldehydes and esters [23]. The participation of esters in resin fossilisation (amberisation) and the biomolecules of the inclusions is still unknown [26]. Resin is a very complex (and not completely studied) preservation source with many variables simultaneously influencing preservation processes.

Distinguishing ancient DNA from recent contamination may be difficult while no strict correlation exists between DNA degradation and the age of the studied organism [41]. Although a comparison of modern and older mitochondrial DNA (mtDNA) showed significant differences in average fragment size, there is no direct correlation between age and

fragmentation, and it is assumed that the main processes affecting DNA fragmentation occur rapidly after cell death [41, 42]. Heintzman et al. [43] found a time-dependent decrease in the concentration of amplifiable DNA in museum specimens. As mtDNA degrades more slowly than nuclear DNA (nuDNA), presumably due to additional protection of mtDNA by the double membranes of the mitochondrion, and is present in many more copies per cell, mtDNA may be more useful for aDNA studies [43–45]. Many different factors influence the state of preservation [3, 4]; therefore, the conditions under which individual specimens have been preserved are of decisive importance [20].

Attempts in various laboratories to repeat aDNA extraction from amber or from younger resin that will become amber have not been successful [21, 46, 47], which has raised further doubts about claims that aDNA was isolated from various fossilised insects in amber. Penney et al. [21] used next generation sequencing to analyse two Colombian sub-fossil resin bees, dated as less than 60 years and around 10 600 years BP, respectively. The young age of these resins means that they were not subjected to any extreme processes. Nevertheless, no convincing evidence was obtained for the preservation of endogenous DNA in either of the two studied sub-fossil resin inclusions. The clear conclusion of this study was that DNA is not preserved in insect inclusions in sub-fossil resin and amber [21]. After publication of these (and previous) results, the hypothesis that preserved DNA could be extracted and studied from animal remains in amber, or in younger resin, was totally discarded. However, these studies did provide negative evidence, demonstrating that DNA was not preserved in these samples.

Some success with DNA amplification has been reported with pinned museum and permafrost-preserved invertebrates [43, 48–51], and some of these samples were older than the oldest specimens analysed by Penney et al. [21]. These studies concluded that museum specimens could serve as a source of molecular information [48–50]. Of all recent publications, the sole hypothetical success with aDNA extraction from sub-fossil specimens embedded in resin was reported by Büsse et al. [51], who claimed to have successfully amplified aDNA from 61 species of 46 higher arthropod taxa from ca. 200-year-old dried museum specimens, as well as from two beetles embedded in sub-fossil resin. The two samples of ancient resin (*sensu* [52]) were analysed via accelerator mass spectrometry (standard-AMS) radiocarbon and dated to 790–700 years BP and 4030–3900 years BP. However, the positive results reported by Büsse et al. [51] should be viewed with caution as the publication does not contain a detailed discussion of the authentication procedures employed. The greatest problem with many studies of insect aDNA is their lack of reproducibility [47], a requirement for scientific evidence. Further limitations of studies of specimens embedded in resin include the implicit destruction of the samples and the small size and often uniqueness of the specimen analysed. Here, we discuss possible ways to solve these questions and limitations.

Fortunately, many studies conducted since 2005 have analysed aDNA using more specific methods, such as next generation sequencing, which not only yields massive amounts of sequencing data and amplification of highly degraded DNA, but also enables more efficient exclusion of modern contamination [53, 54]. Additionally, aDNA research has yielded promising results [e.g. 18, 54–57]; positive studies have been reported for aDNA from beetles in museum collections and permafrost [43, 49] and more recently, novel insights have been obtained into biomolecule preservation in amber samples [58] and other fossils [2, 59], including chewed birch pitch [60].

Here, we describe attempts to amplify DNA from ambrosia beetles embedded in six-year-old and two-year-old resins (modern resin, *sensu* [52]) from Madagascar collected *in situ* from the producing trees. Authentication and potential contamination with modern DNA were taken carefully into consideration. Our objective was to explore the potential limits of DNA

preservation in resins and to develop a standardised protocol for DNA extraction from these samples, which could guarantee unambiguous and independent verification of fossil DNA following the authentication procedures for aDNA research, but applied to a more modern samples by the moment.

Material and methods

Samples

We used platypodine beetles of the genus *Mitosoma* Chapuis, 1865 [61] (Coleoptera: Curculionidae: Platypodinae) embedded in resin (Fig 1). *Mitosoma* is an endemic genus from Madagascar and is abundantly found embedded in resin drops from *Hymenaea verrucosa* (Angiospermae: Fabales: Fabaceae). We collected specimens in resins from a lowland forest close to the Pangalanes Canal, in Ambahy (Nosy Varika, Mananjary) (20°46' S, 48°28' W) and Andranotsara (Sambava) (14°37' S, 050°11' W) on the east coast of Madagascar. The Government of Madagascar authorised sampling (permit no. 160/13 /MEF/SG/DGF/DCB.SAP/SCB and no. 192/17/ MEEF/SG/DGF/DSAP/SCB.Re) and exportation (permit no. 186 N.EA10/MG13 and no. N. 249/17/MEEF/SG/DREEF-SAVA) of samples. The specimens embedded in resin were collected by X.D., E.P. and M.S.K. directly from *H. verrucosa* trees in Madagascar in October 2013 and September–October 2017, respectively. Resin samples were stored at room temperature until commencing the study in February 2019, which increased the risk of greater DNA degradation [27]. After the first experiments, all resin samples were stored at -20°C.

We used specimens of *Mitosoma lobatum* Schedl, 1961 [62], *M. excisum* Schaufuss, 1897 [63] and *M. obconiceps* Schedl, 1970 [64] as positive controls, collected in 2012 by B.J. when on a fieldtrip in Ranomafana National Park (Madagascar). Specimens were stored in >96% ethanol immediately after collection and preserved at -20°C prior to DNA extraction.



Fig 1. Resin samples from *Hymenaea* trees in Madagascar with embedded platypodine beetle specimens of the genus *Mitosoma*, sampled during fieldtrips in 2013 and 2017.

<https://doi.org/10.1371/journal.pone.0239521.g001>

Table 1. Specimens of *Mitosoma* sp. used for DNA extraction and DNA concentration of the eluted DNA [ng/μl].

Year	Specimen	Body Part	DNA-Conc. [ng/μl]	260/280
2012	In ethanol	head	3.20 ng/μl	2.20
		thorax	6.90 ng/μl	1.70
		abdomen	27.30 ng/μl	2.04
	In ethanol	head	9.44 ng/μl	1.87
		thorax	15.67 ng/μl	2.20
		abdomen	66.24 ng/μl	2.00
	In ethanol	head	11.32 ng/μl	1.86
		abdomen	111.58 ng/μl	2.10
	In ethanol	head	13.86 ng/μl	1.99
thorax		38.54 ng/μl	2.12	
abdomen		105.45 ng/μl	2.09	
2013	Resin	whole body	6.67 ng/μl	1.64
	Resin	whole body	9.34 ng/μl	1.86
	Resin	whole body	17.88 ng/μl	1.93
2017	Resin	whole body	21.17 ng/μl	2.13
	Resin	whole body	33.95 ng/μl	2.07
	Resin	whole body	47.35 ng/μl	2.01
	Resin	whole body	48.90 ng/μl	2.06
	Resin + chloroform	whole body	2.90 ng/μl	1.87
	Resin + chloroform	whole body	3.60 ng/μl	1.63
	Resin + chloroform	whole body	3.95 ng/μl	1.67

DNA purity is depicted by the absorbance ratio at 260 nm and 280 nm (260/280).

<https://doi.org/10.1371/journal.pone.0239521.t001>

DNA extraction was performed at the Institute of Medical Microbiology, Immunology and Parasitology (University Clinic Bonn, Germany) from ten adult specimens in resin and four adult specimens in ethanol, all representing the same genus and body size, but different localities (see above) and ages (Table 1).

Only resin pieces with two or more complete specimens as syninclusions were selected in order to use some of them for analysis and store the other(s) at -20°C at the Senckenberg Research Institute (Frankfurt, Germany) under the collection numbers SMF Be 13578–13584. We hoped thereby to halt degradation of the hypothetically preserved biomolecules [27] and to preserve the specimen(s) for future controls and experiments. These specimens are available to other researchers/laboratories upon request, for suitable research projects aimed at determining reproducibility. Different specimens from other resin samples collected at the same time (three from 2013 and four from 2017) were treated as independent replicates (Table 1, Fig 1).

Sample preparation and DNA extraction

All samples used in this study were entirely encased within *H. verrucosa* resin. The resins with insect inclusions were cut into small cubes with a sterile scalpel, leaving a few millimetres around the insect. The surfaces were sterilised with 0.1 M HCl and then washed in sterile water. All the following procedures were carried out under a laminar flow hood in a microbiology laboratory without any contact with entomological experiments. The resin cubes were ground with a micro-pestle in a 1.5 ml reaction tube to which 180 μl ATL-buffer with 20 μl proteinase K (Qiagen, Germany) was added. After incubation at 56°C for 72 h and occasional

vortexing, the DNA was extracted using the DNeasy® Blood & Tissue kit (Qiagen, Germany), following the manufacturer's instructions. DNA was eluted in DNase- and RNase free water and stored at -20°C until further experiments. DNA concentration was measured using the NanoDrop™ One/OneC microvolume-UV/VIS-spectrophotometer (Thermo Scientific, USA). DNA extraction from beetles in ethanol was performed using an identical procedure except for a reduced lysis step of 24 h. To test an alternative methodology some cubes were incubated in 5 ml 100% chloroform (AppliChem GmbH, Germany) for 3 days at 40°C to dissolve the resin. After the chloroform treatment the beetle was washed in ≥ 99% EtOH and further processed as described above. Precautions to eliminate contamination included regular disinfection of all surfaces and working materials with Freka®-NOL AF (Dr. Schumacher GmbH, Germany) and the use of dedicated protective clothing, equipment and reagents. In addition, prior to DNA extraction and amplification experiments, working materials and surfaces were cleaned with DNA-ExitusPlus™ IF (AppliChem GmbH, Germany) to avoid contamination with extrinsic DNA.

Primers

Primers and protocols were selected from previously published studies on the weevil subfamily Platypodinae [65–67], or newly designed based on Platypodinae DNA sequences. The primer pairs S3690F and A4285R, targeting the D2–D3 domains of the large nuclear ribosomal subunit (28S), and S2442F with A3014R, targeting the 3' end of the mitochondrial cytochrome oxidase I (COI), efficiently detected DNA from extant *Mitosoma* samples and were therefore selected for further experiments (Table 2). Two additional COI primers (COIRes F and COIRes R2; COInew) were designed based on sequences from the resin-embedded beetles collected in 2013. These enabled amplification of a much smaller fragments than the standardised primers used in previous studies (160 base pairs (bp) vs. more than 600 bp) and were more suitable for new experiments with older (and theoretically more fragmented) material.

Polymerase Chain Reaction (PCR) amplification

The PCR reaction mixture used to amplify genes of interest was composed of 12.5 µl One-Taq® 2X Master Mix with Standard Buffer (New England Biolabs, Germany), 0.5 µl of each primer (10 µM) and 50 ng DNA, adding water to a final volume of 25 µl. Addition of 1 µl bovine serum albumin (BSA) (10 mg/ml) to the PCR reaction mixture improved efficiency and enabled a reduction in PCR cycles. In each PCR, a negative (sterile water) and a positive control (beetle DNA from specimens in ethanol) were included. PCR was performed in a Gradient LabCycler (SensoQuest, Germany) with the standard cycle program: initial denaturation step at 95°C for 5 min, followed by 30–50 cycles of denaturation at 95°C for 30 s, annealing at specific temperatures (Table 2) for 30 s and elongation at 68°C for 60 s, and a final elongation

Table 2. Primer sequences for DNA extraction selected from the literature and two new sequences tested here.

Targeted Gene		Sequence	Fragment Size	Annealing Temperature	Reference
Large ribosomal subunit (28S)	28S	(S3690F) GAG AGT TMA ASA GTA CGT GAA AC	~ 800 bp	55°C	[66]
		(A4285R) CTG ACT TCG TCC TGA CCA GGC		55°C	[66]
Cytochrome oxidase I (COI)	COI (original primer pair)	(S2442F) CCA ACA GGA ATT AAA ATT TTT AGA TGA TTA GC	~ 600 bp	49°C	[67]
		(A3014R) TCC AAT GCA CTA ATC TGC CAT ATT A		49°C	[67]
	COInew (modified primer pair)	(COIRes F) CAG TAT TTG CTA TCT TAG CTG G	~ 160 bp	50°C	This work
		(COIRes R2) CGT GGT ATT CCT CTT AAA CC		50°C	This work

<https://doi.org/10.1371/journal.pone.0239521.t002>

step at 68°C for 5 min. Further optimisation included different cycles and gradient PCRs to determine the annealing temperature. The PCR results were analysed by means of agarose gel electrophoresis (1.5%). The PCR products were purified using the GeneJet PCR Purification Kit or GeneJet Gel Extraction Kit (Thermo Scientific, USA), in case that fragments had to be extracted directly from the agarose gel, following the manufacturer's instructions. Sanger sequencing was performed by Eurofins Genomics GmbH (Germany) with the amplification primers for 28S and COI (Table 2). Alignments between DNA sequences from beetles in EtOH and resin-embedded specimens to analyse the sequence data and investigate potential contamination with modern DNA were performed with Geneious R10 (<https://www.geneious.com>).

Authentication of DNA sequences

We applied the following criteria to authenticate the amplified DNA sequences recovered from the beetles [41, 68]:

1. Negative controls, extraction blanks and PCR negative controls should be devoid of specific PCR amplification products.
2. Amplified sequences should be consistently and reproducibly obtained from the same extract(s) from one specimen and from different samples of the same species to guarantee reproducibility.
3. All procedures should be repeated three times in different laboratory rooms (in our case, at the Institute of Medical Microbiology, Immunology and Parasitology).
4. All PCR products should be controlled and analysed via sequencing for quality, assembly and specificity.

Illustrations

General pictures of the resin samples were taken using a Nikon D3X with an AF-S Micro-NIKKOR 60 mm 1:2.8 G ED lens. Gel electrophoresis pictures were created using the FastGene FAS-Digi imaging system (NIPPON Genetics Europe). Detailed pictures of the beetle specimen were taken in the laboratory using a Keyence VHX1000 digital microscope under incident light (general body) and using a stereomicroscope in combination with a smartphone adapter. All figures were edited using CorelDraw-X8 software.

Original uncropped and unadjusted images underlying all gel results reported in this work may be found in the [S1 Raw](#) images.

Statistics

Significant differences between DNA concentrations from the analysed samples were calculated by an unpaired t-test using GraphPad Prism version 5.00 for Windows (GraphPad Software, La Jolla, California, USA; www.graphpad.com).

Results

Contrary to some previous experiments using insects in modern resin and sub-fossil resin [21, 47], we successfully amplified DNA sequences from beetles preserved in resins that were six and two years old (Fig 2).

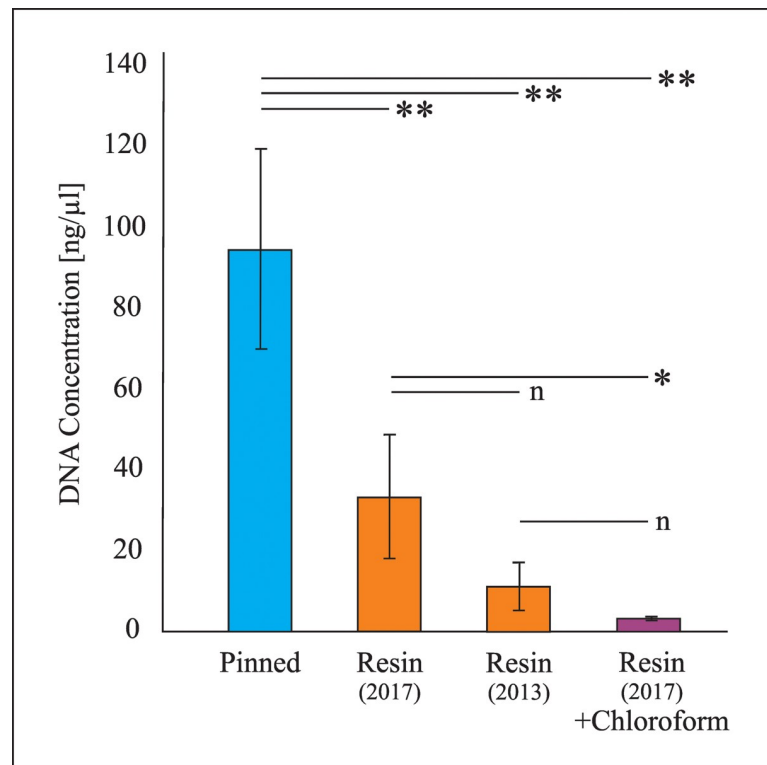


Fig 2. Mean DNA concentration in the different samples analysed. * = Significant differences $P < 0.05$; ** = Significant differences $P < 0.01$; n = Non-significant differences.

<https://doi.org/10.1371/journal.pone.0239521.g002>

DNA extraction

DNA was extracted from beetle specimens of *Mitosoma* sp. and from specimens of the same genus preserved in resin of the same origin (*H. verrucosa*) but differing in age (2013 and 2017 fieldtrips) and collection site. DNA concentrations differed significantly between recent and resin-embedded beetles (Table 1). We observed a time-correlated decrease, albeit not significant, in the amount of DNA obtained from resin beetles (Table 1, Fig 2). The lowest DNA concentration was detected in resin beetles when the resin encasing the specimens had been dissolved in chloroform prior to DNA extraction (Table 1, Fig 2).

PCR amplification

Initial attempts to amplify DNA from two- and six-year-old resin samples, using the PCR protocol normally employed with recent DNA, were unsuccessful, whereas amplification of recent samples (beetles in ethanol) was positive with the original primer pairs COI and 28S. As DNA extraction from the resin samples was performed with completely ground insect together with remaining resin portions, it was suspected that the resin components might inhibit the PCR. This was tested by the addition of different proportions of resin to beetle samples at different time points during DNA extraction. Neither addition of resin to the sample before DNA extraction nor mixing of extracted DNA from resin and recent samples (Table 3) supported the hypothesis of PCR inhibition by resin components. In further experiments, BSA was added to the PCR mixture to avoid any possible inhibition of the DNA polymerase (Fig 3). The blood plasma protein efficiently binds to inhibitors and thereby prevents a negative impact of these molecules on the DNA polymerase [69–71]. After that, two different

Table 3. Inhibition test performed with the primer combination COI for different proportions of DNA from beetles in ethanol and resin beetles.

Test	Proportion of DNA from resin beetles	Proportion of DNA from beetles in ethanol	DNA amplification result
1	1 μ l (50 ng)	0 μ l (0 ng)	Negative
2	0.8 μ l (40 ng)	0.2 μ l (10 ng)	Positive (weak)
3	0.5 μ l (25 ng)	0.5 μ l (25 ng)	Positive
4	0.2 μ l (10 ng)	0.8 μ l (40 ng)	Positive
5	0 μ l (0 ng)	1 μ l (50 ng)	Positive

<https://doi.org/10.1371/journal.pone.0239521.t003>

approaches to amplify the specific DNA fragments were tested: a) two consecutive PCRs of 30 cycles each with a PCR product purification step in between, and b) an increase in the number of PCR cycles up to 50. Both strategies resulted in positive amplifications (Fig 4). Whereas the addition of BSA increased the amplification efficiency of the primer combination targeting the large fragment of COI and enabled successful amplification with a lower number of cycles (≥ 35 cycles), no product could be detected for 28S with less than 45 PCR cycles (Fig 3).

Negative amplification was obtained when the DNA from beetles in ethanol was absent, weak positive result when the proportion was low and positive in the remainder of tests, even when resin remains were included.

Control for contamination

Authentication procedures in aDNA studies are aimed at avoiding sample contamination with modern environmental DNA and detecting this should it occur. Therefore, each PCR product was purified and then sequenced by Sanger sequencing. To analyse the sequences several alignments were performed. Besides alignment of the sequences to Platypodinae sequences in the NCBI database BLAST to test for specificity, all products were checked for contamination with modern DNA. We especially examined the risk of inter-sample contamination from the positive control (beetles in ethanol) to the tested samples by multiple alignments of all sequences. Whereas the similarity between the sequences of insects extracted from resin in 2013 and 2017 was $\geq 97.4\%$ with both primer combinations, a comparison between resin beetles and the sequence of beetles in ethanol yielded a similarity of only 73.7% for the original primer pair COI and 52.5% for primer combination 28S, respectively (Table 4), excluding any contamination with DNA from beetles in ethanol.

Discussion

Contamination occurring during analysis

A major handicap in aDNA research, especially when using resin samples, is contamination with modern environmental DNA [16–20]. The selection of gene sequences for DNA amplification is a crucial step before working with genetically unknown organisms, as is the case of extinct organisms. Here, the closest living relatives often form the basis for identification of homologous sequences. In this study, primers were selected and specifically designed for beetles of the subfamily Platypodinae [66, 67], to prevent amplification of contaminating modern DNA. Furthermore, our experiments were performed in a microbiology laboratory experienced in molecular methods, but which had never worked with entomological DNA before.

To avoid contamination with modern DNA in the experiments presented here, several control procedures at different stages of the isolation and amplification processes were included in the experimental setup. Besides precautions for working with DNA, all PCR products were purified, sequenced and controlled for sequence specificity and inter-sample contamination.

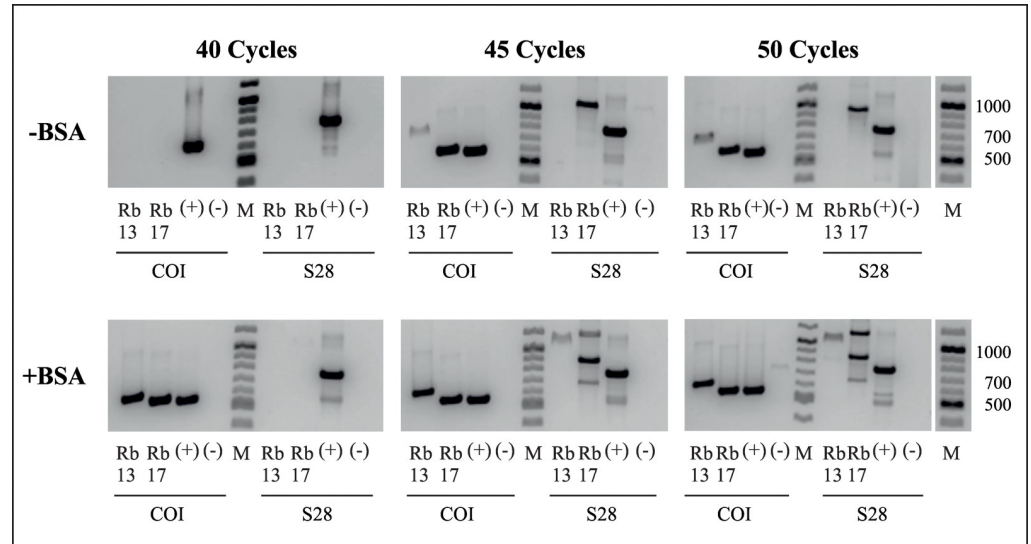


Fig 3. Gel electrophoresis of specific DNA fragments amplified with the original primer combinations COI and 28S with different numbers of cycles. Comparison of PCR products with and without the addition of BSA to prevent DNA polymerase inhibition. Rb13 = Resin beetle (collected in 2013); Rb17 = Resin beetle (collected in 2017); (+) = positive control, DNA from beetles in ethanol; (-) = negative control, DNase- & RNase-free water; M = 100 bp DNA ladder (New England Biolabs).

<https://doi.org/10.1371/journal.pone.0239521.g003>

Relatively long fragments of the 28S ribosomal subunit (~ 800 bp) and the mitochondrial gene oxidase (~ 600 bp) (Table 1, Fig 2) were successfully amplified.

To take into account aDNA fragmentation due to decay, the primer used for amplification should encase small sequences. A basic premise is that primers should amplify fragments up to about 160 bp, because longer aDNA sequences become damaged and degraded and have

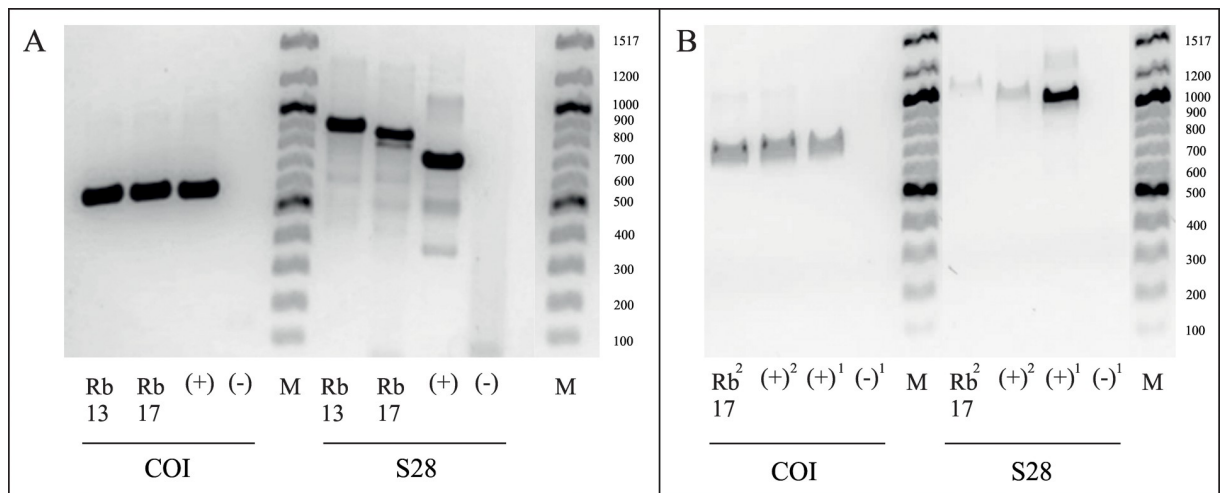


Fig 4. Gel electrophoresis of specific DNA fragments amplified with original primer combinations COI and 28S. A. Positive results with an increase in number of cycles to 50. Rb13 = Resin beetle (collected in 2013); Rb17 = Resin beetle (collected in 2017); (+) = positive control, DNA from beetle in ethanol; (-) = negative control, DNase- & RNase-free water; M = 100 bp DNA ladder (New England Biolabs). B. Two-step PCR with a PCR product purification step in between. Rb17² = Resin beetle (collected in 2017) after two consecutive PCRs of 30 cycles each; (+)¹ = positive control, DNA from beetle in ethanol after one PCR of 30 cycles; (+)² = positive control, DNA from beetle in ethanol after two consecutive PCRs of 30 cycles each; (-)¹ = negative control, DNase- & RNase-free water after one PCR of 30 cycles; M = 100 bp DNA ladder (New England Biolabs).

<https://doi.org/10.1371/journal.pone.0239521.g004>

Table 4. Multiple alignments of all analyzed sequences and the similarity value for the different combinations.

Alignment	Primer-combination	Similarity [%]
Resin beetle (2013 + 2017)	original COI	97.4
Resin beetle (2013 + 2017)	28S	97.8
Resin beetle (2013 + 2017) alignment to beetles in ethanol	original COI	73.7
Resin beetle (2013 + 2017) alignment to beetles in ethanol	28S	52.5

<https://doi.org/10.1371/journal.pone.0239521.t004>

generally proved impossible to amplify [18, 41, 68]. We designed primers for the amplification of small fragments (~ 160 bp) (Table 2; COInew) for future experiments. The new primers were tested successfully in first experiments with resin-embedded platypodine specimens from 2017 (Fig 5) and therefore, build a fundament for future experiments with aDNA using the same insects after confirming the results obtained by longer fragments.

Reproducibility

Entomological studies can easily implement most recommended aDNA authentication procedures to increase the degree of reliability [18–20]. However, other criteria, such as reproducibility or independent replication, are difficult to meet with insect samples due to the small size and frequent uniqueness of the samples. The methodology entailed with samples embedded in resin renders the research even more difficult. The establishment of authentication procedures for aDNA from small samples requires further consideration [27]. Since aDNA isolation in amber insects requires the complete destruction of fossil material, which is obviously undesirable when dealing with rare and very old species stored in museum collections, a more feasible approach would be to analyse several individuals of the species of interest or individuals of any related species of a group [68]. A taxonomic group with relatively abundant representatives would be the perfect target for these experiments; when a specimen is truly unique, samples cannot be used for this purpose because of obvious methodological and ethical problems [27]. The problem of reproducibility is solved here by the selection of insect samples in resin that contain co-specific syninclusions (minimum 2), with a comparable degree of preservation. After cutting the resin sample, the remaining syninclusions were stored at -20°C to maintain their stability as far as possible and thereby preserve the DNA for future tests. Although they do exist, it is difficult to find similar syninclusions in older resins. For rare or unique finds, the approved protocol is to archive independent similar results in two independent laboratories [17, 68]. However, it is extremely challenging to achieve this when using insects from resin or amber deposits because it is difficult to independently replicate DNA extraction from the same fossil insect. In addition, resins of different origin should be treated as independent experiments because of the different nature of their chemical compounds.

Taking into account all the authentication procedures to increase the degree of reliability and avoid contamination in aDNA studies [17–20, 27, 68], we summarise here the optimal method that we employed, which we consider should become standard practice in taphonomic research on DNA preservation in modern and ancient resins:

1. Analyse the sample in a DNA laboratory that has not previously worked with organisms similar to the target specimens, preferably with previous experience in aDNA research.
2. Select a taxonomic group with abundant representatives as syninclusions in modern resin, sub-fossil resin or amber.
3. Include negative controls, extraction blanks and PCR negative controls.

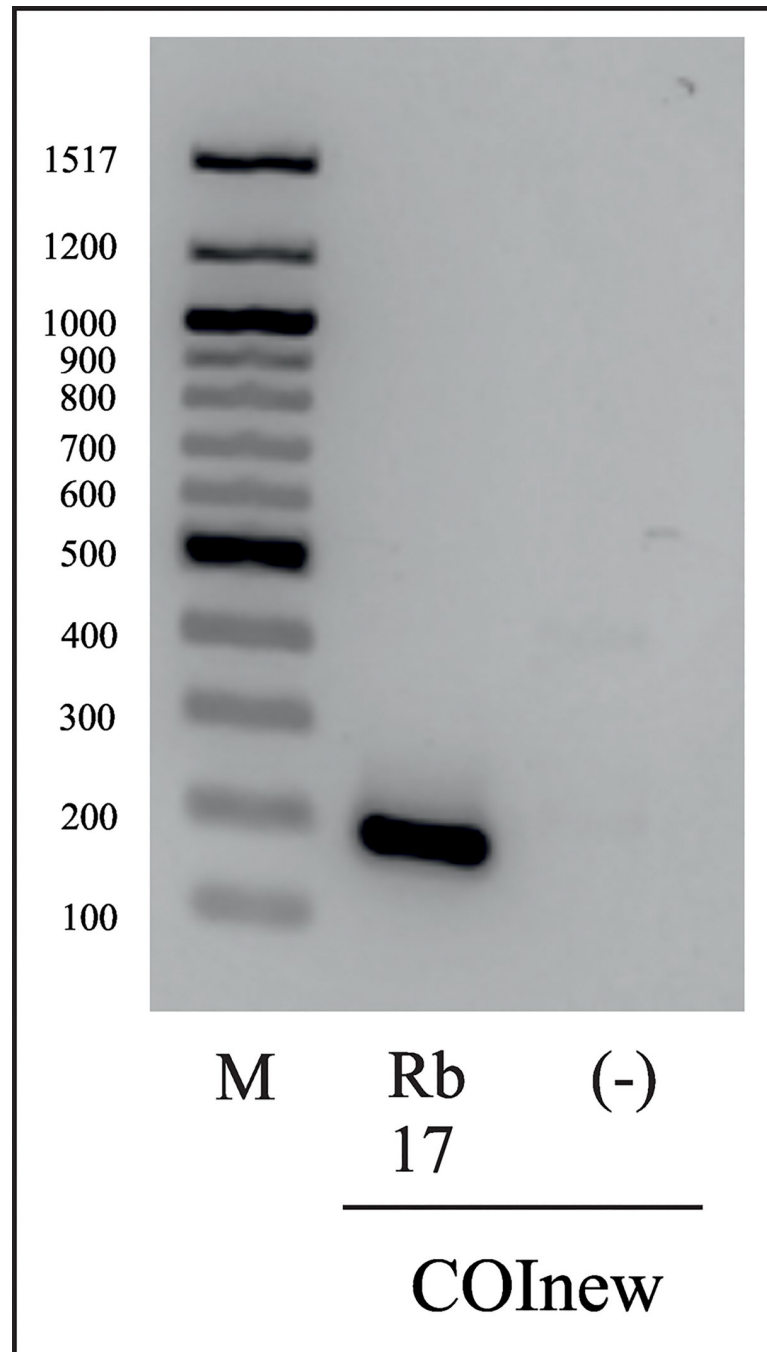


Fig 5. Gelelectrophoresis of the specific DNA fragments amplified with primer combination COInew. The primers were designed based on specific DNA sequences from resin-embedded beetles (collected in 2017) to amplify smaller DNA fragments. Rb17 = Resin beetle (collected in 2017); (-) = negative control, DNase- & RNase free water; M = 100 bp DNA ladder (New England Biolabs).

<https://doi.org/10.1371/journal.pone.0239521.g005>

4. Use specific primers for the target specimens instead of more general primers which amplify a broader range of genomes.
5. Include a sequencing analysis for quality, assembly and specificity control.

6. Repeat the experiment, ideally with similar specimens from the same sample. Close taxonomic groups from the same sample and corroboration with a sequencing process may be sufficient to demonstrate reliability and discard contamination.
7. Include a detailed list of the protocols used in the experiments with a clear discussion of the authentication procedures employed.

The use of chloroform in DNA extraction from specimens embedded in resin

The dissolution of resin, sub-fossil resin and amber in chloroform is a typical procedure to release the embedded insects for further analysis [21, 72]. Penney et al. [21] were unable to detect any insect DNA via next generation sequencing after the use of chloroform to dissolve the resin, and thus concluded that DNA was absent. Chloroform:phenol mixtures are frequently used for DNA extraction [73–75] and one might assume that the difference in age between the youngest sample analysed in Penney et al. [21] and the oldest one in this study (6 years vs. 60 years) could be a key factor in our successful amplification. Surprisingly, we found that the use of chloroform to dissolve the resin surrounding the specimens compromised DNA concentration (Table 1, Fig 2). During work with DNA samples, the use of 70% ethanol also poses a problem as DNA precipitates at this ethanol concentration [47]. Therefore, only $\geq 80\%$ ethanol should be used to sterilise resin surfaces. Büsse et al. [51] reported the amplification of DNA sequences from specimens preserved inside sub-fossil resin samples, but the lack of information about the methodology used with the specimens embedded in resin precludes comparisons. Further experiments are required to obtain more strongly supported conclusions about the effects of chloroform and ethanol on DNA extraction from resin-embedded material.

Dehydration of specimens

The life-like preservation of many amber inclusions is accompanied by preservation of ultra-structural details such as muscle fibres [76], mitochondria [77], brain tissue [3], and internal genitalia [78]. After the death of an organism, enzymes such as DNases rapidly degrade the DNA, but some repair mechanisms, if active, can revert this process. Under rare circumstances, tissue rapidly desiccates after death [8, 79] and DNA is absorbed by a mineral matrix [80]; in addition, rapid burial may change surrounding conditions, significantly reducing or completely inhibiting enzymatic and microbial degradation [81, 82]. On such occasions, slow but still manifest chemical processes start to affect the DNA [18, 83, 84]. Cano [85] stated that sugars such as arabinose, galactose and sucrose, which are components of natural resins, increase osmotic pressure on cells and thereby draw out the water, which results in tissue dehydration and inhibition of biochemical reactions. Additionally, alcohols and terpenes may act as fixatives to preserve tissues.

Dehydration and preservation in resin or permafrost are the three modes of preservation that retain more life-like organisms than any other kind of fossil, maintaining tissues over time [3]. While promising results have been obtained from permafrost-preserved invertebrates [43], none of the claims of DNA isolated from million-year-old amber samples could be independently replicated [21, 47]. In a recent study, amplified fossil genomes were extracted from birch pitch [60], another organic plant substance like resin, but obtained by heating birch bark. Supposedly, volatile compounds cause thorough and rapid dehydration and fixation of tissue once the trapped organism comes into contact with the resin [3]. This contrasts with our



Fig 6. Different specimens of *Mitosoma* sp. preserved in resin from *Hymenaea verrucosa* collected in the Sambava region (Madagascar) in 2017. A. Lateral view of a complete specimen. B. Dorsal view of a complete specimen. C. Photomicrograph of the sectioned head of one *Mitosoma* beetle in resin, showing the still fleshy internal tissue after two years inside the resin.

<https://doi.org/10.1371/journal.pone.0239521.g006>

observations of resin-embedded *Mitosoma* sp. specimens from Madagascar (Fig 6). Two-year-old ground specimens still contained apparently flesh-like tissue without any indication of dehydration or shrinkage (Fig 6C). Therefore, hypothetical dehydration in the resin is not as rapid as was thought and must be regarded as the result of a process lasting for several years. Although the mono- and sesquiterpenoid volatile compounds in resins are known to have antimicrobial and enzyme inhibiting characteristics [23, 86, 87], it is possible that the di- and triterpenoid non-volatile compounds, some of which are also antimicrobial, are crucial to stabilise tissue over longer timescales. The lack of preservation of other molecules, such as chitin and lignin, which are more time-resistant than DNA, in Miocene amber-embedded insects and plants [88] has also been used to argue against the preservation of DNA in these particular fossils [18]. However, β -1,3 and β -1,4-linked polysaccharides, and specifically N-acetylglucosamine residues from chitin, have been detected in fungal mycelia in resinicolous fungi from Spanish amber [89]. One explanation for the better preservation of aDNA in bones than in resins may be hydroxyapatite. This mineral, which predominates in bone, is known for its very strong binding affinity to DNA [15, 80, 90]. Our observations indicate that there is still no satisfactory explanation for preservation in amber, but imply that water is available in the system for longer than previously thought, which has a negative effect on DNA stability in specimens embedded in resin.

Future approach to determine the time limits of DNA preservation in resin specimens

There are broad areas where further progress in studying aDNA from resin-embedded insects can be expected. Decay experiments provide a useful means to investigate variations in the preservation quality of different resin types [26] and offer a promising subject for future analysis. The preservation of inner structures of insects was highly compromised after only a few months embedded in different kinds of resin [26], but to the best of our knowledge, DNA preservation has never been tested. A comparison of DNA preservation in dead specimens of varying ages (such as those from museums and collections) [91], or specimens fixed in paraffin or embedded epoxy resin from less than one hundred years ago, would be highly interesting. Based on the positive results from this study, future experiments could investigate the limits of the DNA preservation in resin embedded specimens in short-time intervals. For future approaches with samples highly sensitive to contaminations, it will be required further adjustments of the methodology. For instance, the DNA concentration was measured via a microvolume-UV/VIS-spectrophotometer in this study, which lacks specificity, being unable to distinguish between DNA (single- and double-stranded), RNA and nucleotides, and is prone to contamination. Therefore, we recommend to use a fluorometer, which is highly accurate detecting fluorescent nucleic acids. Additionally, DNA of older resin embedded specimens

should be analysed with more sensitive next generation sequencing technologies such as shot-gun sequencing. This method is more specific, enabling distinction between modern contaminations and ancient DNA and provides further possibilities, e.g. analysis of fragmentation or degradation patterns. Proteins are thought to be more stable than DNA [92, 93] and seem to provide similar phylogenetic information [2]. Some experiments detected biomolecules such as chitin-protein complexes in insect cuticle from sub-fossil resin but failed to do so when Dominican amber samples were tested [88], while other more recent studies found amino acids from fossil feathers in amber from almost 100 million years BP [58]. Therefore, proteins may be a promising target for the study of deep time specimens [94]. However, if the objective is DNA, it may be more effective to amplify mitochondrial DNA since this is present in higher copy numbers than nuclear DNA, rendering it a more promising candidate for genetic analyses of aDNA [43–45].

The experiments presented here were performed using the commercial DNeasy® Blood & Tissue Kit (Qiagen, Germany), which was recommended for the extraction of beetle DNA [65, 66]. Other studies have also tested DNeasy® extraction systems, which are based on the binding of DNA to silica membranes, for other types of sample, such as bones or other insects [69, 95]. As a beetle embedded in resin is a mixture of two sample types, tissue (insect) and environmental (resin), selection of the most suitable extraction kit must be carefully assessed. Environmental kits offer the advantage of additional steps to avoid PCR inhibitors [96–98], whereas tissue kits are specifically designed for DNA extraction from tissue samples. Other aspects such as choice of DNA polymerase can significantly affect PCR efficiency [69], and should be further investigated to identify the ideal DNA extraction and PCR amplification protocol.

The interaction between a fossil sample and its environment following death of the specimen determines the preservation state of the biomolecules; age *per se* is not an absolute indicator of quantity or quality, at least over a longer timescale [18]. Storage conditions also play a crucial role in preservation, and dry, cold conditions are best for DNA preservation [27]. Since each case is unique, attending to our results, no biological sample should be disregarded as a potential source for recovery [15].

Conclusions

The existence of aDNA in amber specimens is dependent on the possibility that the resin provides a protected environment for DNA preservation (both protective, through encapsulated conditions, and chemically favourable). In previous studies, no aDNA could be amplified either in amber or in specimens embedded in resin, suggesting that the protective and preservative environment in resin prevents tissue but not DNA degradation. However, modern techniques are more powerful and more sensitive. Recently, Büsse et al. [51] reported successful amplification of aDNA from sub-fossil specimens, but limited information was given about extraction methods, the exclusion of contamination or aspects of reproducibility; therefore, the positive results obtained in that study should be viewed with caution. By contrast, the methodology discussed here is intended for future use as a guide and base for studies of specimens embedded in resin. In future investigations next generation sequencing should be included into the methodology as this technique provides more possibilities when working with aDNA. Our study was designed to clarify fundamental aspects about DNA preservation in resin-embedded insects, including an evident experimental support, that was absent until now. Our positive amplification demonstrates that resin inclusions can also be a resource to explore in aDNA studies, albeit with caution. The risk of contamination demands the design of suitable authentication procedures and the possibility to re-evaluate the inclusion of further

analysis once the method is established. Subjects for future studies include the time limits for aDNA detection in resins, the preservation state and assessment of possible taxonomic bias (both entomological and plants) in long-term DNA integrity. With this in mind, a new research project has been launched, moving from newer to older resin samples in order to determine the time limits of DNA preservation in resins.

Supporting information

S1 Raw images.
(PDF)

Acknowledgments

The first author (DP) thanks Francisco Rodríguez (Vall d'Hebron University Hospital, Barcelona, Spain), Victoria McCoy (University of Wisconsin, Milwaukee, USA), Jesús Gómez-Zurita (Institute of Evolutionary Biology, Barcelona, Spain), and Peter D. Heintzman (Royal Holloway University of London, Egham, UK) for their help and discussion in the early stages of writing this manuscript. We thank Georg Oleschinski (Rheinische Friedrich-Wilhelms-Universität Bonn, Germany) for the pictures of the resin pieces. Finally, we would like to thank the work from the two anonymous reviewers who improved a first version of this manuscript.

Author Contributions

Conceptualization: David Peris, Kathrin Janssen, Gabriele Bierbaum, Xavier Delclòs, Enrique Peñalver, Jes Rust.

Data curation: Kathrin Janssen, Xavier Delclòs, Enrique Peñalver, Mónica M. Solórzano-Kraemer, Bjarte H. Jordal.

Formal analysis: David Peris, Kathrin Janssen, H. Jonas Barthel.

Funding acquisition: David Peris, Gabriele Bierbaum, Xavier Delclòs, Mónica M. Solórzano-Kraemer, Bjarte H. Jordal, Jes Rust.

Investigation: David Peris, Kathrin Janssen, H. Jonas Barthel, Enrique Peñalver.

Methodology: David Peris, Kathrin Janssen, Mónica M. Solórzano-Kraemer, Jes Rust.

Project administration: David Peris.

Supervision: David Peris, Gabriele Bierbaum, Jes Rust.

Validation: David Peris, Kathrin Janssen, Bjarte H. Jordal.

Writing – original draft: David Peris, Kathrin Janssen.

Writing – review & editing: David Peris, Kathrin Janssen, H. Jonas Barthel, Gabriele Bierbaum, Xavier Delclòs, Enrique Peñalver, Mónica M. Solórzano-Kraemer, Bjarte H. Jordal, Jes Rust.

References

1. Bokelmann L, Hajdinjak M, Peyrégne S, Brace S, Essel E, de Filippo C, et al. A genetic analysis of the Gibraltar Neanderthals. *PNAS*. 2019; 116: 15610–15615. <https://doi.org/10.1073/pnas.1903984116> PMID: 31308224
2. Cappellini E, Welker F, Pandolfi L, Madrigal JR, Fotakis AK, Lyon D, et al. Early Pleistocene enamel proteome sequences from Dmanisi resolve *Stephanorhinus* phylogeny. *Nature*. 2019; 574: 103–107. <https://doi.org/10.1038/s41586-019-1555-y> PMID: 31511700

3. Grimaldi DA, Bonwich E, Delannoy M, Doberstein S. Electron microscopic studies of mummified tissues in amber fossils. *Am Mus Novit*. 1994; 3097: 1–31.
4. Martínez-Delclòs X, Briggs DEG, Peñalver E. Taphonomy of insects in carbonates and amber. *Palaeogeogr Palaeoclimatol Palaeoecol*. 2004; 203: 19–64.
5. Amber Labandeira C. In: Laflamme M, Schiffbauer JD, Darroch SAF, editors. *Reading and Writing of the Fossil Record: Preservational Pathways to Exceptional Fossilization*. *Paleontol Soc Pap*. 2014; 20: 163–216.
6. Pääbo S. Ancient DNA: extraction, characterization, molecular cloning, and enzymatic amplification. *PNAS*. 1989; 86: 1939–1943. <https://doi.org/10.1073/pnas.86.6.1939> PMID: 2928314
7. Bada JL, Wang XS, Poinar HN, Pääbo S, Poinar GO Jr. Amino acid racemization in amber-entombed insects: Implications for DNA preservation. *Geochim Cosmochim Acta*. 1994; 58: 3131–3135. [https://doi.org/10.1016/0016-7037\(94\)90185-6](https://doi.org/10.1016/0016-7037(94)90185-6) PMID: 11539553
8. Mandrioli M. Insect collections and DNA analyses: How to manage collections? *Mus Manag Curatorship*. 2008; 23: 193–199.
9. Cano RJ, Poinar HN, Roubik DW, Poinar GO Jr. Enzymatic amplification and nucleotide sequencing of portions of the 18s rRNA gene of the bee *Proplebeia dominicana* (Apidae: Hymenoptera) isolated from 25–40 million year old Dominican amber. *Med Sci Res*. 1992; 20: 249–251.
10. Cano RJ, Poinar HN, Poinar GO Jr. Isolation and partial characterization of DNA from the bee *Proplebeia dominicana* (Apidae: Hymenoptera) in 25–40 million year old amber. *Med Sci Res*. 1992; 20: 619–623.
11. DeSalle R, Gatesy J, Wheeler W, Grimaldi D. DNA sequences from a fossil termite in Oligomiocene amber and their phylogenetic implication. *Science*. 1992; 257: 1933–1936 <https://doi.org/10.1126/science.1411508> PMID: 1411508
12. Poinar HN, Cano RJ, Poinar GO Jr. DNA from an extinct plant. *Nature*. 1993; 363: 677.
13. Cano RJ, Poinar HN, Pieniazek NJ, Acra A, Poinar GO Jr. Amplification and sequencing of DNA from a 120–135-million-year-old weevil. *Nature*. 1993; 363: 536–538. <https://doi.org/10.1038/363536a0> PMID: 8505978
14. Thomas RH, Schaffner W, Wilson AC, Pääbo S. DNA phylogeny of the extinct marsupial wolf. *Nature*. 1989; 340: 465–467. <https://doi.org/10.1038/340465a0> PMID: 2755507
15. Parsons TJ, Weeden VW. Preservation and recovery of DNA in postmortem specimens and trace samples. In: Haglund W, Sorg M, editors. *Advances in Forensic Taphonomy: The Fate of Human Remains*. New York: CPR Press; 1996. pp. 109–138.
16. Instability Lindahl T. and decay of the primary structure of DNA. *Nature*. 1993; 362: 709–715. <https://doi.org/10.1038/362709a0> PMID: 8469282
17. Lindahl T. Recovery of antediluvian DNA. *Nature*. 1993; 365: 700. <https://doi.org/10.1038/365700a0> PMID: 8413647
18. Pääbo S, Poinar HN, Serre D, Janicke-Després V, Hebler J, Rohland N, et al. Genetic analyses from ancient DNA. *Annu Rev Genet*. 2004; 38: 645–679. <https://doi.org/10.1146/annurev.genet.37.1.10801.143214> PMID: 15568989
19. Hebsgaard MB, Phillips MJ, Willerslev E. Geologically ancient DNA: fact or artefact? *Trends Microbiol*. 2005; 13: 212–220. <https://doi.org/10.1016/j.tim.2005.03.010> PMID: 15866038
20. Willerslev E, Cooper A. Ancient DNA. *Proc R Soc B*. 2005; 272: 3–16. <https://doi.org/10.1098/rspb.2004.2813> PMID: 15875564
21. Penney D, Wadsworth C, Fox G, Kennedy SL, Preziosi RF, Brown AT. Absence of ancient DNA in sub-fossil insect inclusions preserved in ‘Anthropocene’ Colombian copal. *PLoS ONE*. 2013; 8: e73150. <https://doi.org/10.1371/journal.pone.0073150> PMID: 24039876
22. Rosselló JA. The never-ending story of geologically ancient DNA: was the model plant *Arabidopsis* the source of Miocene Dominican amber? *Biol J Linn Soc*. 2014; 111: 234–240.
23. Langenheim JH. *Plant resins: chemistry, evolution, ecology and ethnobotany*. Cambridge: Timber Press; 2003.
24. Lambert JB, Santiago-Blay JA, Wu Y, Levy AJ. Examination of amber and 490 related materials by NMR spectroscopy. *Magn Reson Chem*. 2015; 53: 2–8. <https://doi.org/10.1002/mrc.4121> PMID: 25176402
25. McCoy VE, Soriano C, Gabbott SE. A review of preservational variation of fossil inclusions in amber of different chemical groups. *Earth Environ Sci Trans R Soc Edinb*. 2018; 107: 203–211.
26. McCoy VE, Soriano C, Pegoraro M, Luo T, Boom A, Foxman B, et al. Unlocking preservation bias in the amber insect fossil record through experimental decay. *PLoS ONE*. 2018; 13: e0195482. <https://doi.org/10.1371/journal.pone.0195482> PMID: 29621345

27. Reiss RA. Ancient DNA from ice age insects: proceed with caution. *Quat Sci Rev.* 2006; 25: 1877–1893.
28. Darzynkiewicz Z, Juan G, Li X, Gorczyca W, Murakami T, Traganos F. Cytometry in cell necrobiology: Analysis of apoptosis and accidental cell death (necrosis). *Cytometry.* 1997; 27: 1–20. PMID: [9000580](#)
29. Nagata S. Apoptotic DNA fragmentation. *Exp Cell Res.* 2000; 256: 12–18. <https://doi.org/10.1006/excr.2000.4834> PMID: [10739646](#)
30. Lindahl T, Andersson A. Rate of chain breakage at apurinic sites double-stranded deoxyribonucleic acid. *Biochemistry.* 1972; 11: 3618–3623. <https://doi.org/10.1021/bi00769a019> PMID: [4559796](#)
31. Lindahl T, Nyberg B. Rate of depurination of native deoxyribonucleic acid. *Biochemistry* 1972; 11: 3610–3618. <https://doi.org/10.1021/bi00769a018> PMID: [4626532](#)
32. Briggs AW, Stenzel U, Johnson PLF, Green RE, Kelso J, Prüfer K, et al. Patterns of damage in genomic DNA sequences from a Neandertal. *PNAS.* 2007; 104: 14616–14621. <https://doi.org/10.1073/pnas.0704665104> PMID: [17715061](#)
33. Dabney J, Meyer M, Pääbo S. Ancient DNA damage. *Cold Spring Harb Perspect Biol.* 2013; 5: a012567. <https://doi.org/10.1101/cshperspect.a012567> PMID: [23729639](#)
34. Hopfenberg HB, Witchev LC, Poinar GO, Beck CW, Chave KE, Smith SV, et al. Is the air in amber ancient? *Science.* 1988; 241: 717–721. <https://doi.org/10.1126/science.241.4866.717> PMID: [17839082](#)
35. Smith CI, Chamberlain AT, Riley MS, Stringer C, Collins MJ. The thermal history of human fossils and the likelihood of successful DNA amplification. *J Hum Evol.* 2003; 45: 203–217. [https://doi.org/10.1016/s0047-2484\(03\)00106-4](https://doi.org/10.1016/s0047-2484(03)00106-4) PMID: [14580590](#)
36. Gaertner J. *De Fructibus et Seminibus Plantarum.* Stuttgart: Stutgardie Typis Academie Caroline; 1791.
37. Anderson KB, Winans RE, Botto RB. The nature and fate of natural resins in the geosphere—II. Identification, classification and nomenclature of resinites. *Org Geochem.* 1992; 18: 829–841.
38. Penney D. *Biodiversity of fossils in amber from the major world deposits.* Manchester: Siri Scientific Press; 2010.
39. Rust J, Singh H, Rana RS, McCann T, Singh L, Anderson K, et al. Biogeographic and evolutionary implications of a diverse paleobiota in amber from the early Eocene of India. *PNAS.* 2010; 107: 18360–18365. <https://doi.org/10.1073/pnas.1007407107> PMID: [20974929](#)
40. Shi G, Dutta S, Paul S, Wang B, Jacques FMB. Terpenoid compositions and botanical origins of Late Cretaceous and Miocene amber from China. *PLoS ONE.* 2014; 9: e111303. <https://doi.org/10.1371/journal.pone.0111303> PMID: [25354364](#)
41. Pääbo S, Higuchi RG, Wilson AC. Ancient DNA and the polymerase chain reaction. *J Biol Chem.* 1989; 264: 9709–9712. PMID: [2656708](#)
42. Sawyer S, Krause J, Guschanski K, Savolainen V, Pääbo S. Temporal patterns of nucleotide misincorporations and DNA fragmentation in ancient DNA. *PLoS ONE.* 2012; 7: e34131. <https://doi.org/10.1371/journal.pone.0034131> PMID: [22479540](#)
43. Heintzman PD, Elias SA, Moore K, Paszkiewicz K, Barnes I. Characterizing DNA preservation in degraded specimens of *Amara alpina* (Carabidae: Coleoptera). *Mol Ecol Resour.* 2014; 14: 606–615. <https://doi.org/10.1111/1755-0998.12205> PMID: [24266987](#)
44. Schwarz C, Debruyne R, Kuch M, McNally E, Schwarcz H, Aubrey AD, et al. New insights from old bones: DNA preservation and degradation in permafrost preserved mammoth remains. *Nucleic Acids Res.* 2009; 37: 3215–3229. <https://doi.org/10.1093/nar/gkp159> PMID: [19321502](#)
45. Allentoft ME, Collins M, Harker D, Haile J, Oskam CL, Hale ML, et al. The half-life of DNA in bone: Measuring decay kinetics in 158 dated fossils. *Proc R Soc B.* 2012; 279: 4724–4733. <https://doi.org/10.1098/rspb.2012.1745> PMID: [23055061](#)
46. Pawlowski J, Kmiecik D, Szadziewski R, Burkiewicz A. Attempted isolation of DNA from insects embedded in Baltic amber. *Inclusion-WrosteK.* 1996; 26: 12–13.
47. Austin JJ, Ross AJ, Smith AB, Fortey RA, Thomas RH. Problems of reproducibility—does geologically ancient DNA survive in amber-preserved insects? *Proc R Soc B.* 1997; 264: 467–474. <https://doi.org/10.1098/rspb.1997.0067> PMID: [9149422](#)
48. Gilbert MTP, Moore W, Melchior L, Worobey M. DNA extraction from dry museum beetles without conferring external morphological damage. *PLoS ONE.* 2007; 3: e272.
49. Thomsen PF, Elias S, Gilbert MT, Haile J, Munch K, Svetlana K, et al. Non-destructive sampling of ancient insect DNA. *PLoS ONE.* 2009; 4: e5048. <https://doi.org/10.1371/journal.pone.0005048> PMID: [19337382](#)

50. Tagliavia M, Massa B, Albanese I, La Farina M. DNA extraction from Orthoptera museum specimens. *Anal Lett.* 2011; 44: 1058–1062.
51. Büsse S, von Grumbkow P, Mazanec J, Tröster G, Hummel S, Hörschemeyer T. Note on using nuclear 28S rDNA for sequencing ancient and strongly degraded insect DNA. *Entomol Sci.* 2017; 20: 137–141.
52. Anderson KB. The nature and fate of natural resins in the geosphere. VII. A radiocarbon (¹⁴C) age scale for description of immature natural resins. An invitation to scientific debate. *Org Geochem.* 1996; 25: 251–253.
53. Bunning SL, Jones G, Brown TA. Next generation sequencing of DNA in 3300-year-old charred cereal grains. *J Archaeol Sci.* 2012; 39: 2780–2784.
54. Hofreiter M, Paijmans JLA, Goodchild H, Speller CF, Barlow A, Fortes GG, et al. The future of ancient DNA: Technical advances and conceptual shifts. *BioEssays.* 2014; 37: 284–293. <https://doi.org/10.1002/bies.201400160> PMID: 25413709
55. Pääbo S. Neanderthal man: In search of lost genomes. New York: Basic Books; 2014.
56. Slon V, Mafessoni F, Vernot B, de Filippo C, Grote S, Viola TB, et al. The genome of the offspring of a Neanderthal mother and a Denisovan father. *Nature.* 2018; 561: 113–116. <https://doi.org/10.1038/s41586-018-0455-x> PMID: 30135579
57. Bailleul AM, Zheng W, Horner JR, Hall BK, Holliday CM, Schweitzer MH. *Natl Sci Rev.* 2020; nwz206. <https://doi.org/10.1093/nsr/nwz206>
58. McCoy VE, Gabott SE, Penkman K, Collins MJ, Presslee S, Holt J, et al. Ancient amino acids from fossil feathers in amber. *Scientific Reports.* 2019; 9: 6420. <https://doi.org/10.1038/s41598-019-42938-9> PMID: 31015542
59. Boatman EM, Goodwin MB, Holman H-Y, Fakra S, Zheng W, Gronsky R, et al. Mechanisms of soft tissue and protein preservation in *Tyrannosaurus rex*. *Sci Rep.* 2019; 9: 15678. <https://doi.org/10.1038/s41598-019-51680-1> PMID: 31666554
60. Jensen TZT, Niemann J, Iversen KH, Fotakis AK, Gopalakrishnan S, Vågene AJ, et al. A 5700 year-old human genome and oral microbiome from chewed birch pitch. *Nat Commun.* 2019; 10: 5520. <https://doi.org/10.1038/s41467-019-13549-9> PMID: 31848342
61. Chapuis F. Monographie des Platypides. Liège: H. Dessain; 1865.
62. Schedl KE. Fauna Madagascariensis IV: 188. Contribution à la morphologie et à la systématique des coléoptères scolytoidea. *Mém Inst Sci Madag.* 1961; 12: 127–170.
63. Schaufuss CFC. Beitrag zur Kaferfauna Madagascars. III. Missions scientifiques de M. Ch. Alluaud aux îles Séchelles (1892) et a Diego-Suarez, Madagascar (1893) (Scolytidae et Platypodidae). *Tijdschr. Entomol.* 1897; 40: 209–225.
64. Schedl KE. Fauna Madagascariensis, V, Coleopteres, Scolytoidea. *Ann Soc Entomol Fr.* 1970; 6: 233–241.
65. Pistone D, Mugu S, Jordal BH. Genomic mining of phylogenetically informative nuclear markers in bark and ambrosia beetles. *PLoS ONE.* 2016; 11: e0163529. <https://doi.org/10.1371/journal.pone.0163529> PMID: 27668729
66. Mugu S, Pistone D, Jordal BH. New molecular markers resolve the phylogenetic position of the enigmatic wood-boring weevils Platypodinae (Coleoptera: Curculionidae). *Arthropod Syst Phylo.* 2018; 76: 45–58.
67. McKenna DD, Farrell BD. Molecular phylogenetics and evolution of host plant use in the Neotropical rolled leaf ‘hispine’ beetle genus *Cephaloleia* (Chevrolat) (Chrysomelidae: Cassidinae). *Mol Phylogenet Evol.* 2005; 37: 117–131. <https://doi.org/10.1016/j.ympev.2005.06.011> PMID: 16054400
68. Handt O, Höss M, Krings M, Pääbo S. Ancient DNA: Methodological challenges. *Experientia.* 1994; 50: 524–529. <https://doi.org/10.1007/BF01921720> PMID: 8020612
69. Rohland N, Hofreiter M. Comparison and optimization of ancient DNA extraction. *BioTechniques.* 2007; 42: 343–352. <https://doi.org/10.2144/000112383> PMID: 17390541
70. Farrell EM, Alexandre G. Bovine serum albumin further enhances the effects of organic solvents on increased yield of polymerase chain reaction of GC-rich templates. *BMC Res Notes.* 2012; 5: 257. <https://doi.org/10.1186/1756-0500-5-257> PMID: 22624992
71. Sidstedt M, Steffen CR, Kiesler KM, Vallone PM, Rådström P, Hedman J. The impact of common PCR inhibitors on forensic MPS analysis. *Forensic Sci Int.* 2019; 40: 182–191.
72. Mazur N, Nagel M, Leppin U, Bierbaum G, Rust J. The extraction of fossil arthropods from Lower Eocene Cambay amber. *Acta Palaeontol Pol.* 2014; 59: 455–459.
73. Gaikwad AB. DNA extraction: Comparison of methodologies. *PLoS Biol.* 2002; 20: 162–173.

74. Köchl S, Niederstätter H, Parson W. DNA extraction and quantitation of forensic samples using the phenol-chloroform method and real-time PCR. *Methods Mol Biol.* 2005; 297: 13–29. <https://doi.org/10.1385/1-59259-867-6:013> PMID: 15570097
75. Barnett R, Larson G. A phenol-chloroform protocol for extracting DNA from ancient samples. In: Shapiro B, Hofreiter M, editors. *Ancient DNA*. Totowa: Humana Press; 2012. pp. 13–19.
76. Henwood AA. Exceptional preservation of Dipteran flight muscle and the taphonomy of insects in amber. *Palaios.* 1992; 7: 203–212.
77. Poinar HN, Melzer RR, Poinar GO Jr. Ultrastructure of 30–40 million year old leaflets from Dominican amber (*Hymenaea protera*, Fabaceae: Angiospermae). *Experientia.* 1996; 52: 387–390.
78. Perreau M, Tafforeau P. Virtual dissection using phase-contrast X-ray synchrotron microtomography: reducing the gap between fossils and extant species. *Syst Entomol.* 2011; 36: 573–580.
79. Shirkey B, McMaster NJ, Smith SC, Wright DJ, Rodriguez H, Jaruga P, et al. Genomic DNA of *Nostoc commune* (Cyanobacteria) becomes covalently modified during long-term (decades) desiccation but is protected from oxidative damage and degradation. *Nucleic Acids Res.* 2003; 31: 2995–3005. <https://doi.org/10.1093/nar/gkg404> PMID: 12799425
80. Brundin M, Figdor D, Sundqvist G, Sjögren, U. DNA binding to hydroxyapatite: A potential mechanism for preservation of microbial DNA. *J Endod.* 2013; 39: 211–216. <https://doi.org/10.1016/j.joen.2012.09.013> PMID: 23321233
81. Seilacher A, Reif WE, Westphal F. Sedimentological, ecological and temporal patterns of fossil Lagerstätten. *Philos T R Soc B.* 1985; 311: 5–24.
82. Briggs DEG. The role of decay and mineralization in the preservation of soft-bodied fossils. *Annu Rev Earth Planet Sci.* 2003; 31: 275–301.
83. Hofreiter M, Serre D, Pääbo S. Ancient DNA. *Nat Rev.* 2001; 2: 353–359.
84. Willerslev E, Hansen AJ, Poinar HN. Isolation of nucleic acids and cultures from fossil ice and permafrost. *Trends Ecol Evol.* 2004; 19: 141–147. <https://doi.org/10.1016/j.tree.2003.11.010> PMID: 16701245
85. Cano RJ. Analysing ancient DNA. *Endeavour.* 1996; 20: 162–167. [https://doi.org/10.1016/s0160-9327\(96\)10031-4](https://doi.org/10.1016/s0160-9327(96)10031-4) PMID: 9022353
86. Deans SG, Ritchie G. Antibacterial properties of plant essential oils. *Int J Food Microbiol.* 1987; 5: 165–180.
87. Ryan MF, Byrne O. Plant-insect coevolution and inhibition of acetylcholinesterase. *J Chem Ecol.* 1988; 14: 1965–1975. <https://doi.org/10.1007/BF01013489> PMID: 24277106
88. Stankiewicz BA, Poinar HN, Briggs DEG, Evershed RP, Poinar GO Jr. Chemical preservation of plants and insects in natural resins. *Proc R Soc B.* 1998; 265: 641–647.
89. Speranza M, Ascaso C, Delclòs X, Peñalver E. Cretaceous mycelia preserving fungal polysaccharides: Taphonomic and paleoecological potential of microorganisms preserved in fossil resins. *Geol Acta.* 2015; 13: 363–385.
90. Adegoke JA, Ighavini BO, Onuigbo RO. Characteristic features of the sonicated DNA of *Agama agama* L. (Reptilia, Agamidae) on hydroxyapatite columns, using mouse DNA as a reference. *Generica.* 1991; 83: 171–80.
91. Goldstein PZ, DeSalle R. Calibrating phylogenetic species formation in a threatened insect using DNA from historical specimens. *Mol Ecol.* 2003; 12: 1993–1998. <https://doi.org/10.1046/j.1365-294x.2003.01860.x> PMID: 12803647
92. Nielsen-Marsh C. Biomolecules in fossil remains: Multidisciplinary approach to endurance. *Biochemist.* 2002; 24: 12–14.
93. Wadsworth C, Procopio N, Anderung C, Carretero J-M, Iriarte E, Valdiosera C, et al. Comparing ancient DNA survival and proteome content in 69 archaeological cattle tooth and bone samples from multiple European sites. *J Proteom.* 2017; 158: 1–8.
94. Schweitzer MH, Schroeter ER, Cleland TP, Zheng W. Paleoproteomics of Mesozoic dinosaurs and other Mesozoic fossils. *Proteomics.* 2019; 19: 1800251.
95. Chen H, Rangasamy M, Tan SY, Wang H, Siegfried BD. Evaluation of five methods for total DNA extraction from western corn rootworm beetles. *PLoS ONE.* 2010; 5: e11963. <https://doi.org/10.1371/journal.pone.0011963> PMID: 20730102
96. Whitehouse CA, Hottel HE. Comparison of five commercial DNA extraction kits for the recovery of *Francisella tularensis* DNA from spiked soil samples. *Mol Cell Probe.* 2007; 21: 92–96.
97. Dineen SM, Aranda R, Anders DL, Robertson JM. An evaluation of commercial DNA extraction kits for the isolation of bacterial spore DNA from soil. *J Appl Microbiol.* 2010; 109: 1886–1896. <https://doi.org/10.1111/j.1365-2672.2010.04816.x> PMID: 20666869

98. Faber KL, Person EC, Hudlow WR. PCR inhibitor removal using the NucleoSpin® DNA Clean-Up XS kit. *Forensic Sci Int Genet.* 2013; 7: 209–213. <https://doi.org/10.1016/j.fsigen.2012.06.013> PMID: [22784879](https://pubmed.ncbi.nlm.nih.gov/22784879/)

Supporting Information for

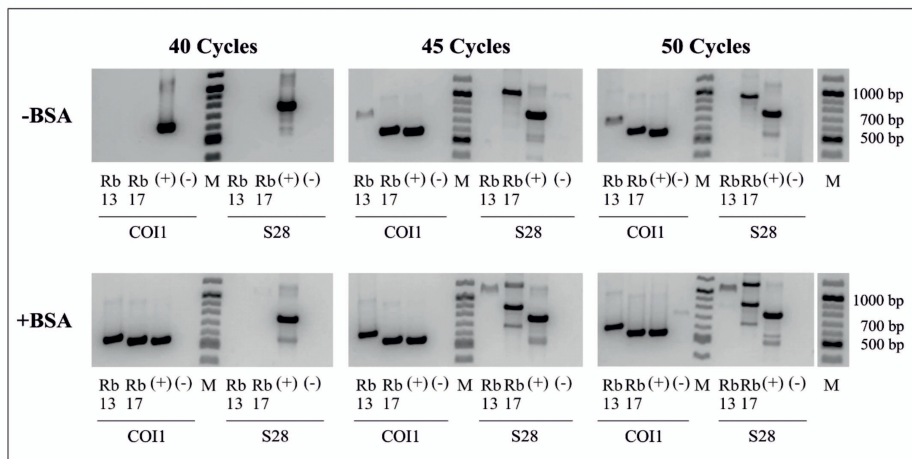
DNA from resin-embedded organisms: Past, present and future

David Peris, Kathrin Janssen, H. Jonas Barthel, Gabriele Bierbaum, Xavier Delclòs, Enrique Peñalver, Mónica M. Solórzano-Kraemer, Bjarte H. Jordal, Jes Rust

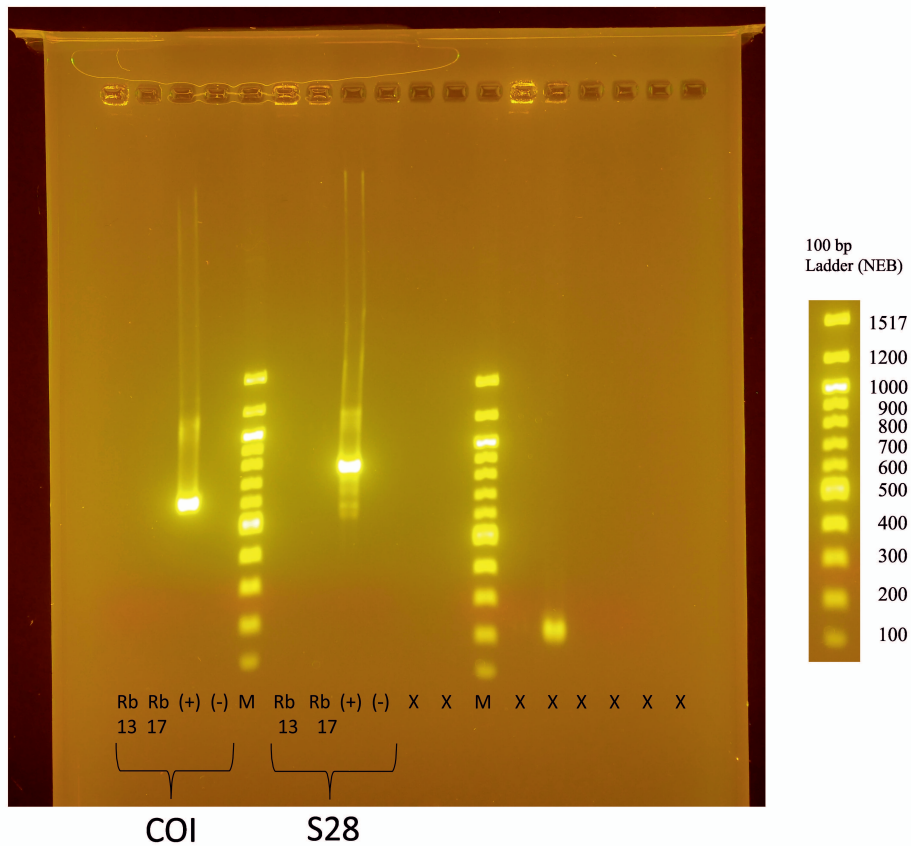
Email: daperce@gmail.com; Kathrin.Janssen@ukbonn.de

Fig. 3, pictures were taken with FastGene FAS-Digi (NIPPON Genetics Europe). As molecular marker 100 bp ladder (New England Biolabs) was used. The color was changed to Black and White and inverted.

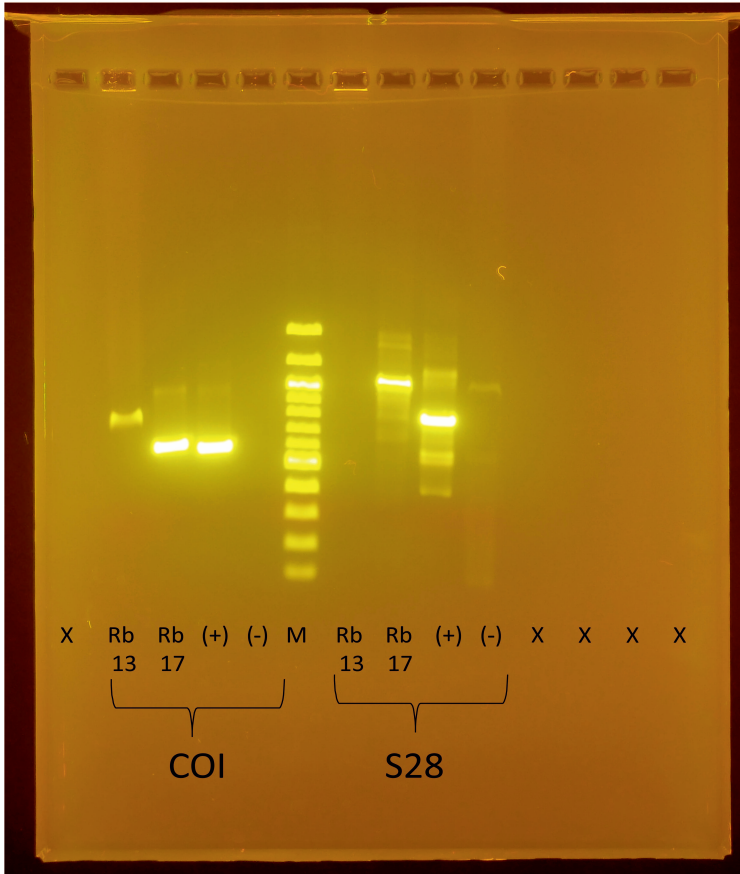
Figure 3. Gelelectrophoresis of the specific DNA fragments amplified with primer combinations COI1 and S28 with different amounts of cycles. Comparison of the products of PCR reactions with and without the addition of BSA to prevent inhibition of the DNA polymerase. Rb13 = Resin beetle (collected in 2013); Rb17 = Resin beetle (collected in 2017); (+) = positive control, DNA from pinned beetle; (-) = negative control, DNase- & RNase free water; M = 100 bp DNA ladder (New England Biolabs).



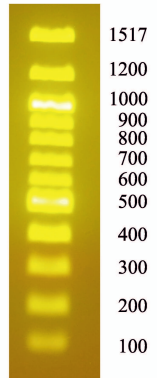
-BSA / 40 Cycles



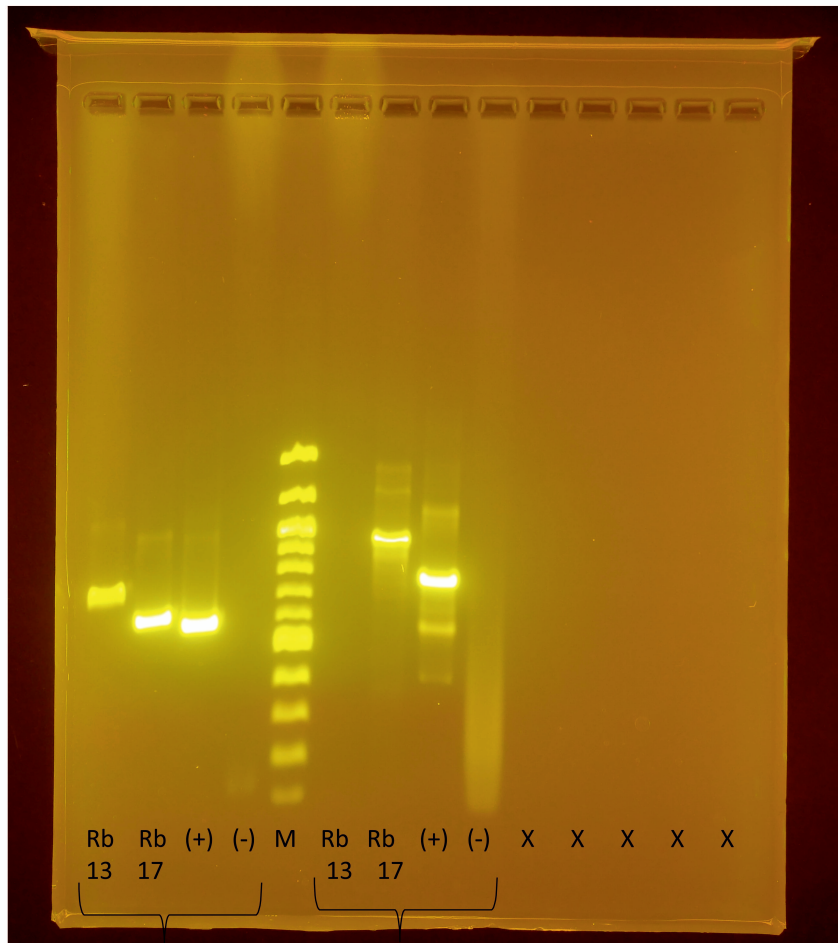
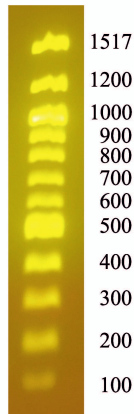
-BSA / 45 Cycles



100 bp
Ladder (NEB)



-BSA / 50 Cycles

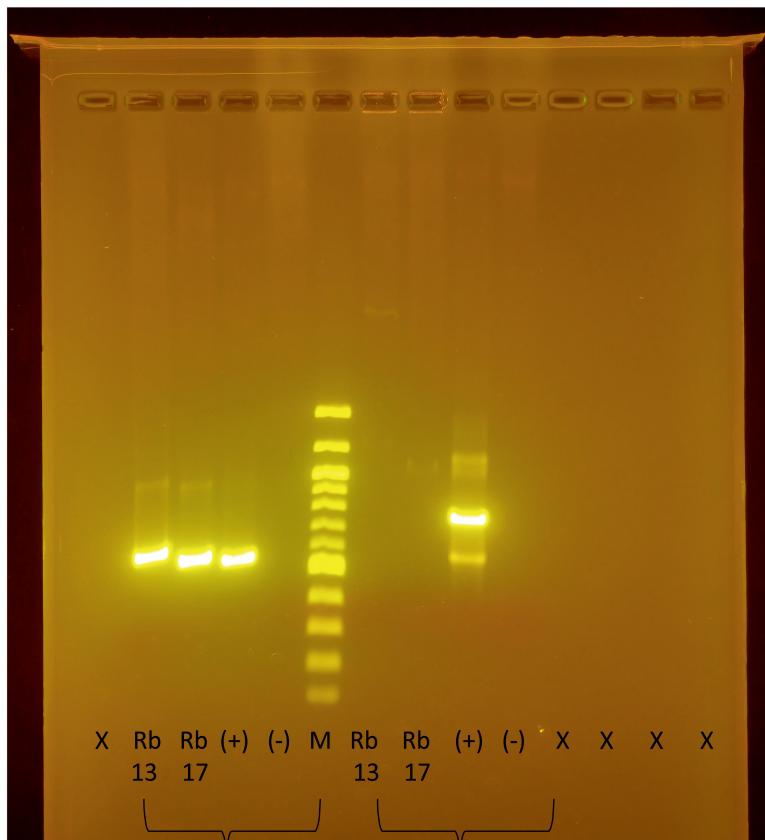
100 bp
Ladder (NEB)

Rb Rb (+) (-) M Rb Rb (+) (-) X X X X X
13 17 13 17

COI

S28

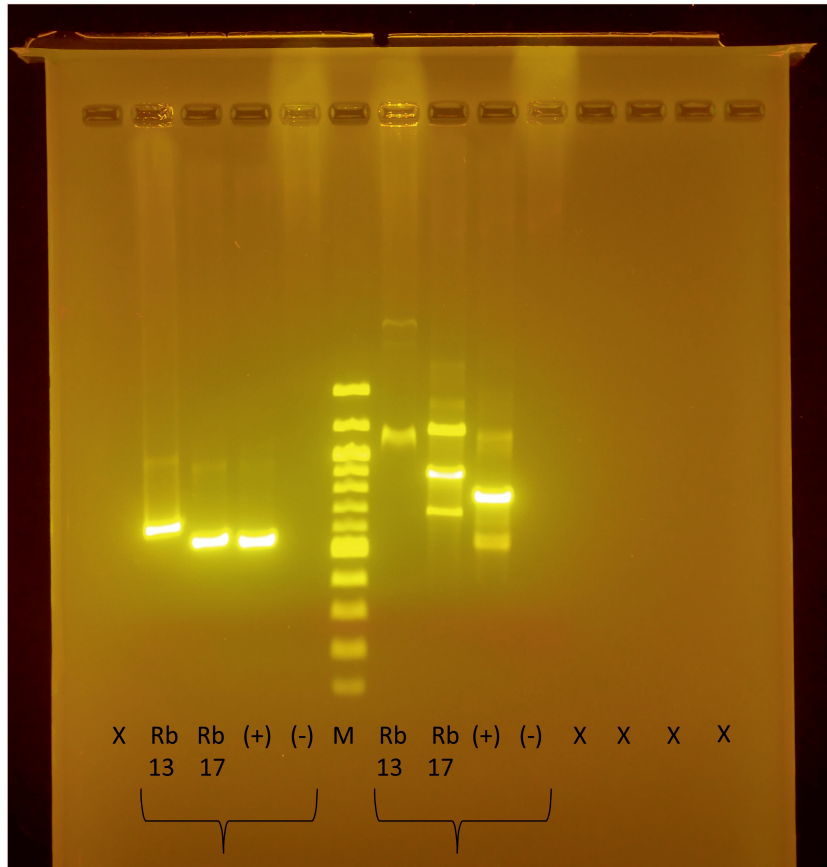
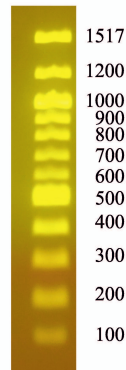
+BSA / 40 Cycles

100 bp
Ladder (NEB)1517
1200
1000
900
800
700
600
500
400
300
200
100

COI

S28

+BSA / 45 Cycles

100 bp
Ladder (NEB)

COI

S28

+BSA / 50 Cycles

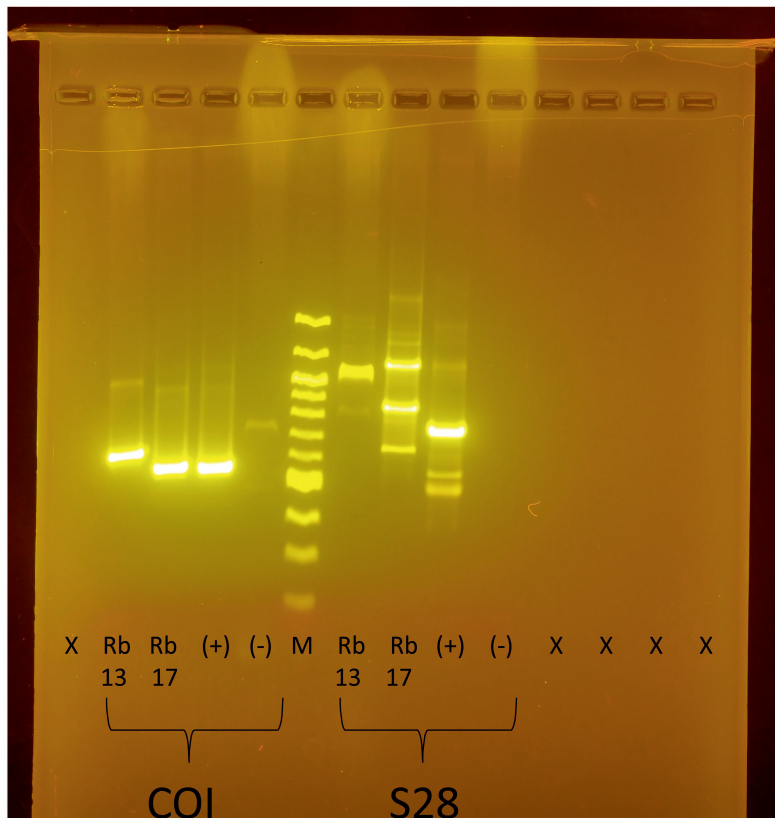
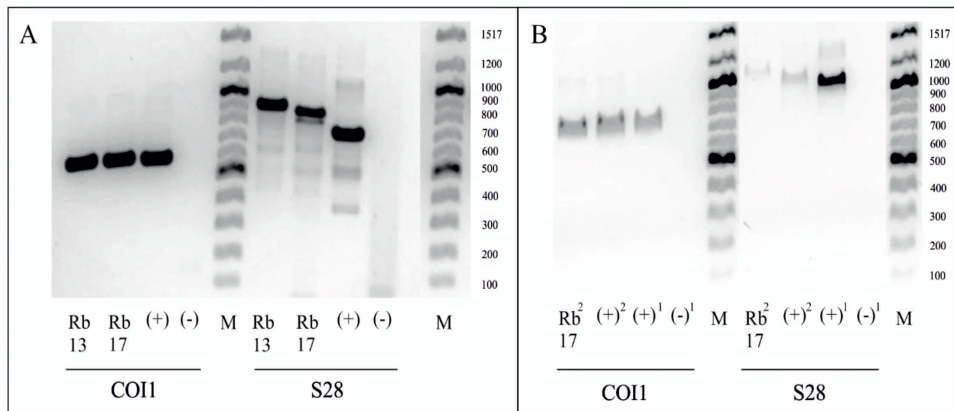
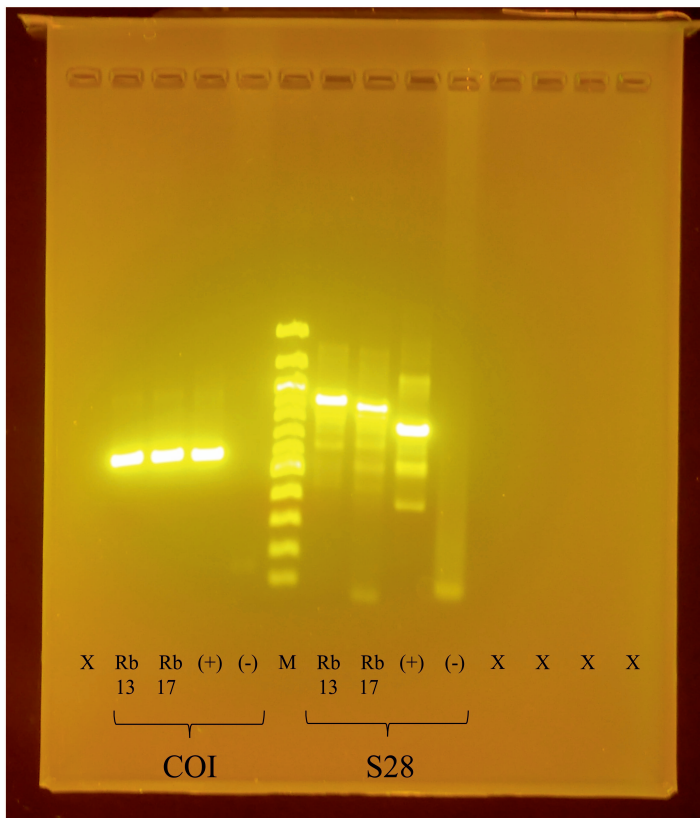


Fig. 4, pictures were taken with FastGene FAS-Digi (NIPPON Genetics Europe). As molecular marker 100 bp ladder (New England Biolabs) was used. The color was changed to Black and White and inverted.

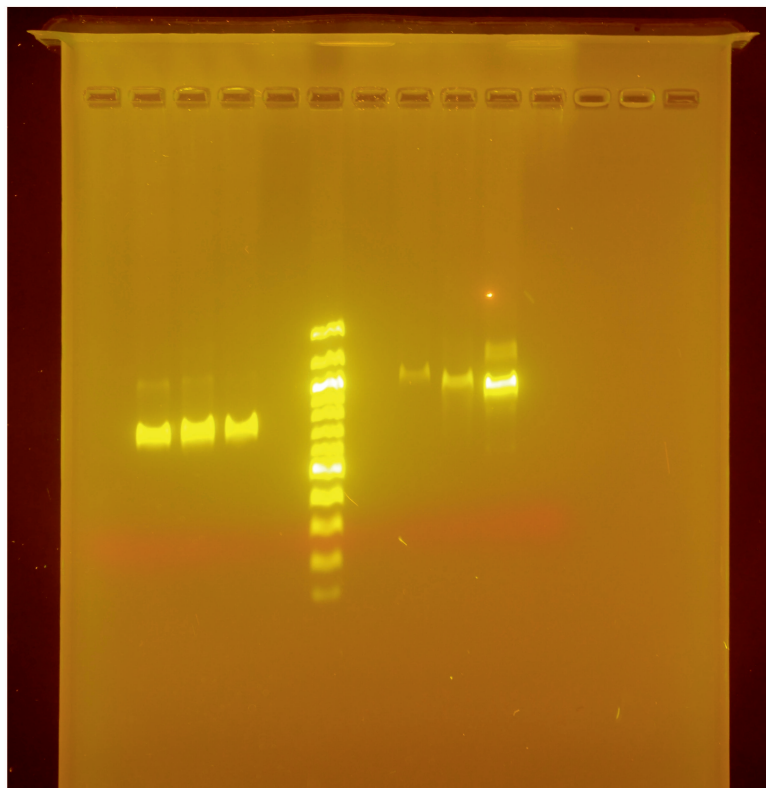
Figure 4. Gelelectrophoresis of the specific DNA fragments amplified with primer combinations COI1 and S28. A. Positive results with an increase of amounts of cycles to 50. Rb13 = Resin beetle (collected in 2013); Rb17 = Resin beetle (collected in 2017); (+) = positive control, DNA from pinned beetle; (-) = negative control, DNase- & Rnase free water; M = 100 bp DNA ladder (New England Biolabs). B. Two-step PCR with a purification step of the PCR products in between. Rb172= Resin beetle (collected in 2017) after two consecutive PCR with 30 cycles each; (+)1 = positive control, DNA from pinned beetle after one PCR with 30 cycles; (+)2 = positive control, DNA from pinned beetle after two consecutive PCR with 30 cycles each; (-)1 = negative control, DNase- & RNase free water after one PCR with 30 cycles; M = 100 bp DNA ladder (New England Biolabs).



A. 50 Cycles



B. 2-Step-PCR



100 bp
Ladder (NEB)

1517

1200

1000

900

800

700

600

500

400

300

200

100

X Rb² (+)² (+)¹ (-)¹ M X Rb² (+)² (+)¹ (-)¹ X X X

17

COI

17

S28

Fig. 5, pictures were taken with FastGene FAS-Digi (NIPPON Genetics Europe). As molecular marker 100 bp ladder (New England Biolabs) was used. The color was changed to Black and White and inverted.

Figure 5. Gelelectrophoresis of the specific DNA fragments amplified with primer combination COInew. The primers were designed based on specific DNA sequences from resin entombed beetles (collected in 2017) to amplify smaller DNA fragments. Rb17 = Resin beetle (collected in 2017); (-) = negative control, DNase- & RNase free water; M = 100 bp DNA ladder (New England Biolabs).

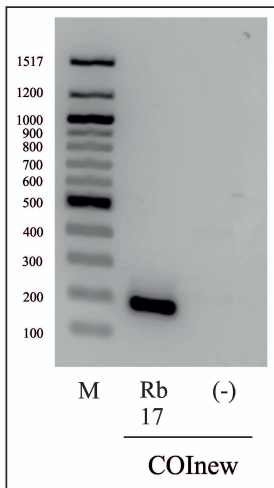
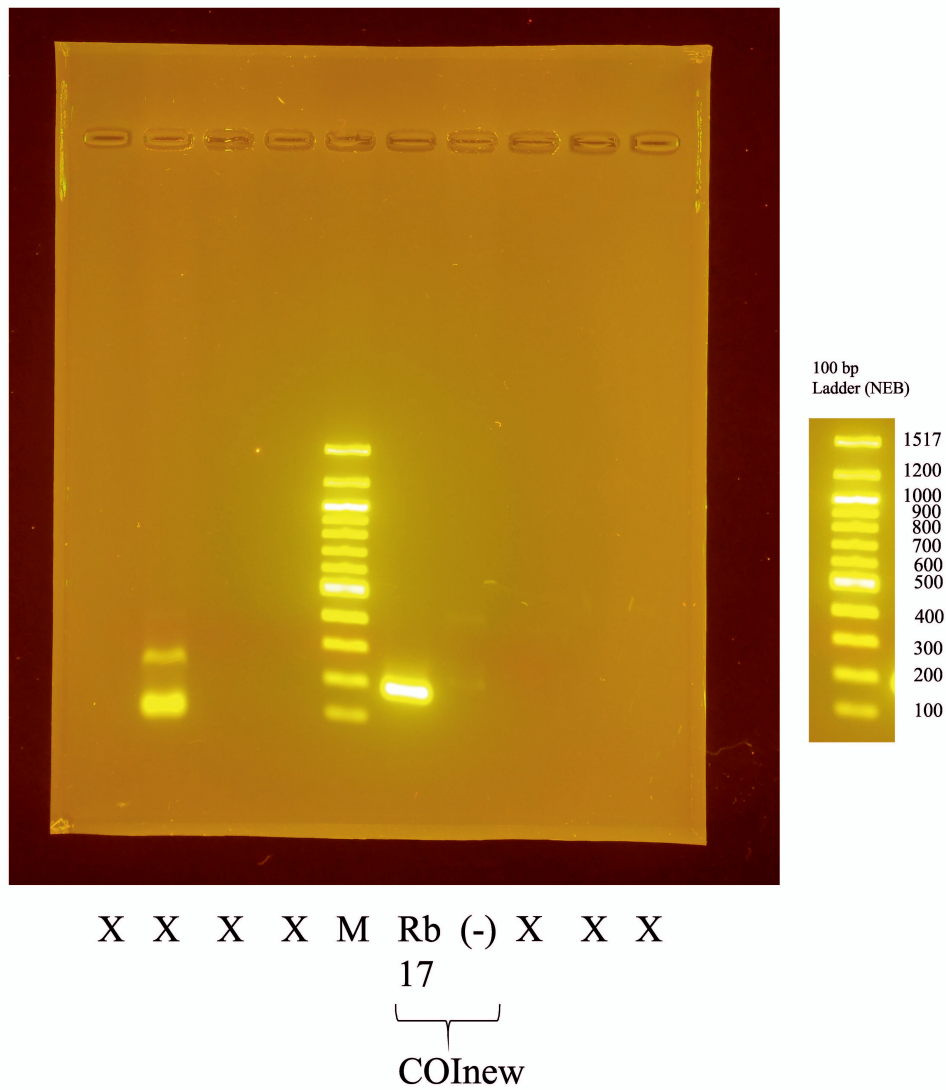


Fig 5



10.3 Publication 3

Barthel, H.J., Fougrouse, D., Geisler, T., Rust, J., 2020. Fluoridation of a lizard bone embedded in Dominican amber suggests open-system behavior. PLoS ONE 15, e0228843. <https://doi.org/10.1371/journal.pone.0228843>.

RESEARCH ARTICLE

Fluoridation of a lizard bone embedded in Dominican amber suggests open-system behavior

H. Jonas Barthel^{1*}, Denis Fougerouse², Thorsten Geisler³, Jes Rust¹

1 Paleontology Section, Institute of Geosciences, RheinischeFriedrich-Wilhelms-Universität Bonn, Bonn, Germany, **2** School of Earth and Planetary Sciences, Curtin University, Perth, Australia, **3** Geochemistry/Petrology Section, Institute of Geosciences, RheinischeFriedrich-Wilhelms-Universität Bonn, Bonn, Germany

* jbarthel@uni-bonn.de



OPEN ACCESS

Citation: Barthel HJ, Fougerouse D, Geisler T, Rust J (2020) Fluoridation of a lizard bone embedded in Dominican amber suggests open-system behavior. PLoS ONE 15(2): e0228843. <https://doi.org/10.1371/journal.pone.0228843>

Editor: Justin W. Adams, Monash University, AUSTRALIA

Received: November 3, 2019

Accepted: January 23, 2020

Published: February 26, 2020

Copyright: © 2020 Barthel et al. This is an open access article distributed under the terms of the [Creative Commons Attribution License](https://creativecommons.org/licenses/by/4.0/), which permits unrestricted use, distribution, and reproduction in any medium, provided the original author and source are credited.

Data Availability Statement: All relevant data are within the paper and its Supporting Information files.

Funding: JR obtained funding by the Deutsche Forschungsgemeinschaft (DFG, German Research Foundation; url: <https://www.dfg.de/>) project number 396704064. DF obtained funding by the Australian Research Council (ARC; url: <https://www.arc.gov.au/>) grant number DE190101307. The funders had no role in study design, data collection and analysis, decision to publish, or preparation of the manuscript.

Abstract

Vertebrate fossils embedded in amber represent a particularly valuable paleobiological record as amber is supposed to be a barrier to the environment, precluding significant alteration of the animals' body over geological time. The mode and processes of amber preservation are still under debate, and it is questionable to what extent original material may be preserved. Due to their high value, vertebrates in amber have never been examined with analytical methods, which means that the composition of bone tissue in amber is unknown. Here, we report our results of a study on a left forelimb from a fossil *Anolis* sp. indet. (Squamata) that was fully embedded in Miocene Dominican amber. Our results show a transformation of the bioapatite to fluorapatite associated with a severe alteration of the collagen phase and the formation of an unidentified carbonate. These findings argue for a poor survival potential of macromolecules in Dominican amber fossils.

Introduction

Fossil bones represent valuable paleontological archives for reconstructing the paleobiology and -environments of vertebrates throughout geological time and thus also represent an important window into the evolution of life on Earth. The preservation of organisms or parts of them over long geological timescales requires exceptional conditions before and after death of the organism. During diagenesis, the remains are affected by various chemical processes like dissolution or pseudomorphosis, so the original material, especially the organic soft tissue, is often lost or severely modified. However, a detailed understanding of the preservation and fossilization of bone at the microscopic scale is still lacking. This is partly because bone is a complex hierarchical composite material. It consists of a nano-crystalline, hydrated, hydroxylated, and carbonated calcium phosphate phase (hydroxylapatite (HAp)-like) that is embedded in a fibrous organic matrix of predominately collagen and subordinately lipids. A recent vibrational spectroscopic study [1] suggested that molecular water is a stabilising component of biogenic apatite (bioapatite), which has also been postulated in previous studies based on nuclear magnetic resonance spectroscopy [2]. Pasteris et al. [1] proposed that the chemical formula of

Competing interests: The authors have declared that no competing interests exist.

bioapatite should be $\text{Ca}_{10-x}[(\text{PO}_4)_{6-x}(\text{CO}_3)_x](\text{OH})_{2-x} \cdot n\text{H}_2\text{O}$, where $n \approx 1.5$ and x ranges between 0.1 and 0.3. The OH group in bioapatite can be replaced by F, whereas Ca may partly be substituted by, e.g., Mg, Zn, Sr, Na, and K [3]. Fluorine was found of particular importance for the preservation of bone and teeth during diagenesis [4, 5] as well as for caries prevention by transforming HAp to more stable, i.e., less soluble fluorapatite (FAp) [6]. Bone apatite is thus a complex solid solution that occurs as nano-crystals with sizes in the order of 20 to 150 nm. Due to its crystal-chemical properties, bioapatite is a highly reactive phase that, if its physicochemical environment is changing (for instance, after death of the organism), has a high thermodynamic driving force to dissolve [4] or to react in aqueous solutions that are (super) saturated with respect to apatite. Under certain conditions original bone tissues survive over geological time scales, including organic components (e.g., collagen) that could still be detected in dinosaur bone [7, 8]. Such bone specimens are often characterised by a larger average crystallite size, a higher crystallinity, and a different apatite chemistry with respect to the original bone [9–12].

The entrapment of an organism in viscous tree resin is a unique prerequisite in terms of fossilization, with the chance to preserve embedded organisms in a three-dimensional, life-like posture. In public perception, amber is therefore often referred to as a “time capsule,” prohibiting the majority of decay processes. Amber represents a strong taphonomic filter and favors the conservation of small organisms such as insects and spiders, which are often extremely well preserved with ultrastructural detail [13, 14, 15]. The liquid resin initially protects entrapped organisms from microbial attack and predators, which represents an important basis for preservation. However, evidence has been reported showing that even air can pass through amber, which may cause oxidation reactions [16]. In general, it is well known that the preservation of fossils in amber differs largely throughout specimens and amber deposits. The degree of preservation ranges from the relict occurrence of straight chain hydrocarbons and altered macromolecules of beetles in Dominican amber to still reacting cellular components of cypress twigs in Baltic amber [17, 18].

Compared to the large amounts of arthropods reported as inclusions in amber, only a small number of vertebrate remains of frogs, lizards, birds, mammals, and dinosaurs has been reported from different amber deposits from the Cretaceous to the Neogene around up to 120 million years old [19–27]. Most of these findings refer to small arboreal lizards of the family Gekkonidae and the genus *Anolis*, comprising partial remains to complete specimens [28–38]. X-ray scans revealed that parts of the skeleton are preserved in most of these specimens [28, 39, 40], but despite this observation, nothing is known about the degree of preservation of bone material in amber. One obvious hypothesis is that bones that were embedded in amber and thus shielded against aqueous solutions, may show a high degree of preservation, including their collagen matrix.

To address this question, we examine the left forelimb of an *Anolis* sp. indet. in a piece of 15 to 20 Million years old Dominican amber, also including a fairy wasp (Mymaridae, Fig 1A and S1 Fig), by micro-Raman spectroscopy, electron microprobe, and time-of-flight secondary ion mass spectroscopy (ToF-SIMS). A detailed description of the fossil specimen is provided in the Supporting Information (S1 Appendix, S1–S3 Figs).

Microtome cuttings of the fossil bone reveal a brittle tissue that might be attributed to contact with acidic resin compounds shortly after entombment. The alteration of the bone is confirmed by our spectral Raman data, and electron microprobe measurements, which indicate a transformation of the original bioapatite into fluorapatite. Furthermore, the collagen matrix is largely degraded to possibly C-H-C aliphatic compounds. Measurements in the bone cavity revealed complex spectra that have to be interpreted in the future and are likely the product of epoxy resin compounds and original material. We discuss several possible sources of the

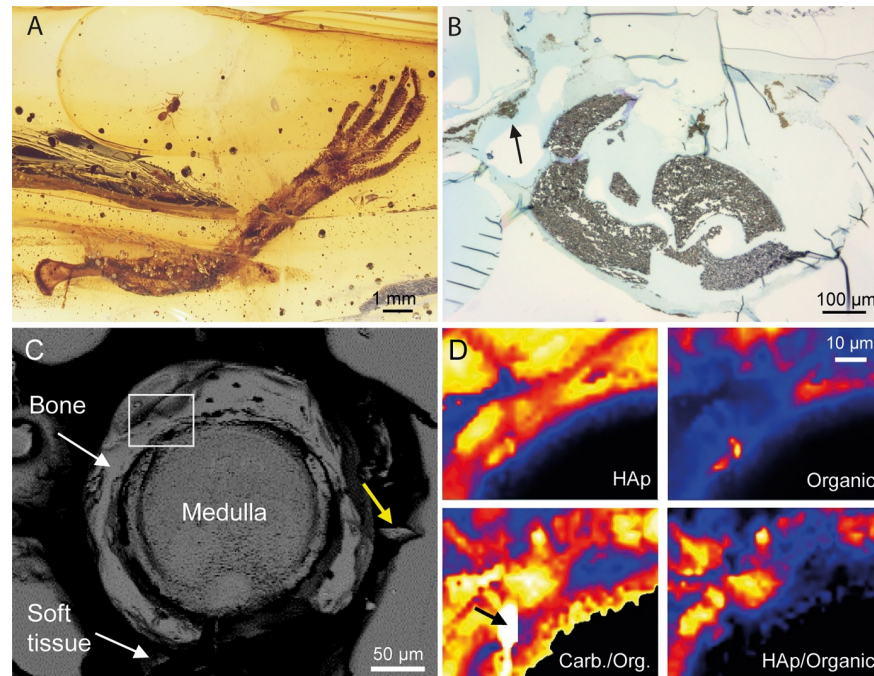


Fig 1. (A) Light microscopic image of the investigated sample DHQ-4924-H. The piece contains a fairy wasp and the left forelimb of an anole lizard. Several flow structures can be recognized in the resin. (B) Optical image of a microtome slice of the fossil humerus, showing fragmented bone tissue (dark in the image). During the cutting of the sample, the fragile bone broke because of the increasing tension in the material. The black arrow points to epidermal remains in the resinous matrix. (C) Backscattered electron image of the fossil bone surface. The yellow arrow shows a bone fragment that was pressed into the material during preparation of the sample. The white rectangle marks the area that was imaged by Raman spectroscopy: (D) False-coloured hyperspectral Raman images of a bone area, showing (upper left) the integrated intensity of the $\nu_1(\text{PO}_4)$ apatite band ($A_{\nu_1(\text{PO}_4)}$), (lower left) the intensity ratio of the $\nu_1(\text{CO}_3)$ band of carbonate near 1070 cm^{-1} ($A_{\nu_1(\text{CO}_3)}$) and the total intensity between 1150 and 1700 cm^{-1} , reflecting the organic content ($A_{1150-1700}$), (upper right) $A_{1150-1700}$, and (lower right) $A_{\nu_1(\text{PO}_4)} / A_{1150-1700}$. An unknown carbonate phase is marked by a black arrow.

<https://doi.org/10.1371/journal.pone.0228843.g001>

fluorine but expect an allochthon origin to be most likely, based on our ToF-SIMS analysis. Although we cannot explain the bone fluoridation and alteration in detail, it is important to note that evidently the presence of a resinous matrix does not necessarily inhibit chemical exchange between fossil and the environment of the amber. Therefore, vertebrate fossils in amber must be considered as the result of open-system processes which severely limits the potential of original macromolecular compounds.

Results

After light microscopic and μ -CT examinations, the sample was cut and polished so that a portion of the humerus was exposed and polished perpendicular to its longitudinal axis (Fig 1C). Raman spectroscopy was then used to first characterize the embedding amber close to the fossil. The most obvious features in the amber spectrum (Fig 2A) are the (fingerprint) bands at 1644 , 1660 , and 1450 cm^{-1} , resulting from the exomethylene stretching $\nu(\text{C}=\text{C})$ and the scissoring type deformation $\delta(\text{CH}_2)$ vibration in the resin structure, respectively [40, 41, 42]. It has been demonstrated that the integrated intensity ratio of the doublet near 1650 cm^{-1} and the band at 1450 cm^{-1} is a good indicator of the maturity of fossilized resins. In general, the ratio is >1 for immature resins such as copal and <1 for mature (fossil) resins such as amber [41, 43]. From a least-squares fit of Gauss-Lorentz functions to the three bands along with a

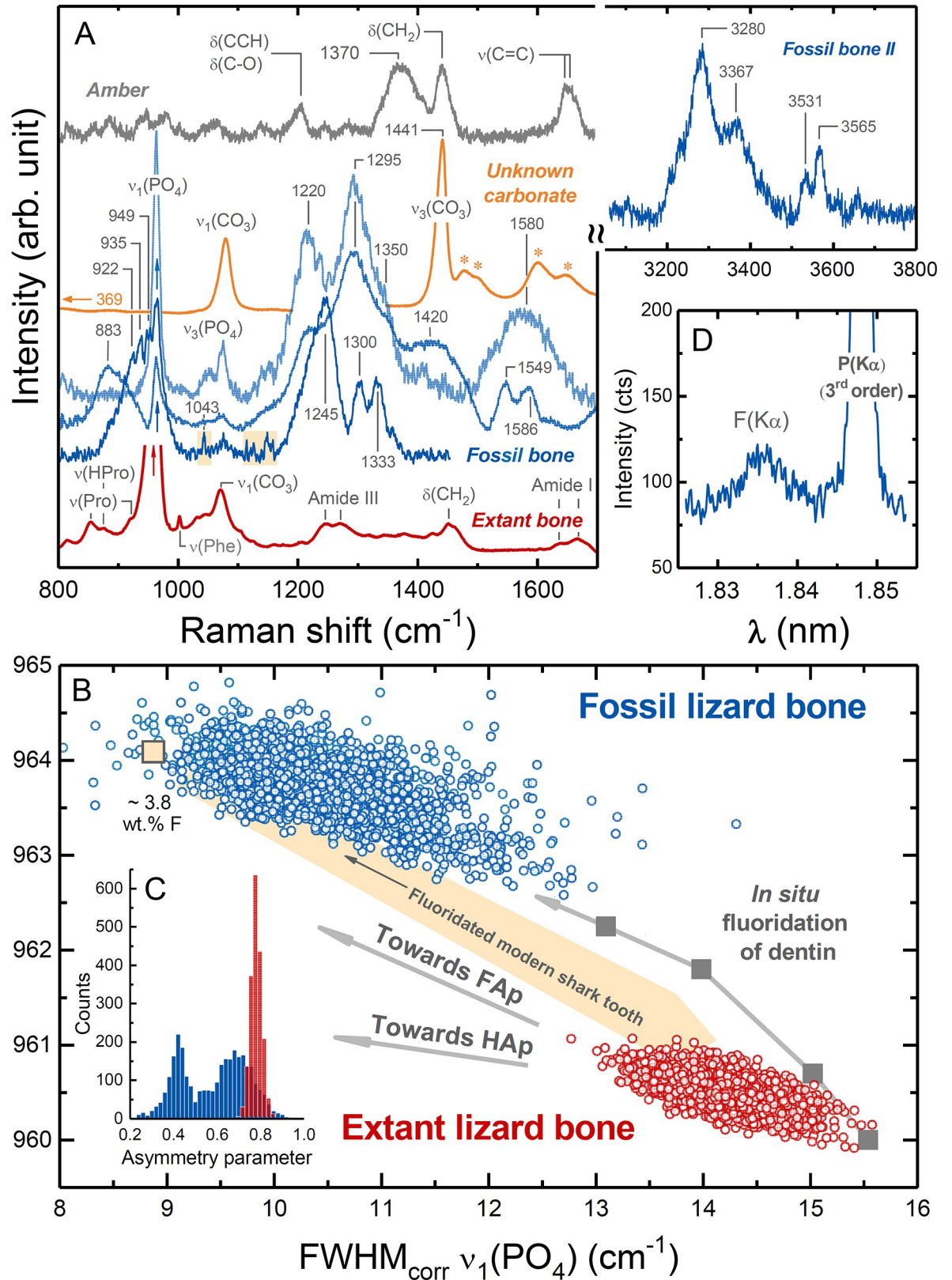


Fig 2. (A) Raman spectra of the fossil bone (blue), extant bone (red), the unknown carbonate (yellow) and the amber matrix (grey). (B) The relationship between the width, given as full width at half (FWHM), and frequency of the $\nu_1(\text{PO}_4)$ mode for bone apatite shows that the fossil

bone (4,323 analyses) is associated with higher frequencies and overall smaller FWHM values compared to the extant sample (2,527 analyses). In comparison with data from an extant shark tooth and experimental bone fluoridation data [49], this observation suggests the formation of fluorapatite. (C) The distribution of the asymmetry parameter of the $\nu_1(\text{PO}_4)$ band of fossil and extant bone spectra. The asymmetry parameter of the fitted asymmetric Gauss-Lorentz function varies between -1 and +1 with 0 referring to a symmetric profile. Negative values skew the spectrum toward higher while positive values, as observed here, skew it toward lower wavenumbers. The multimodal distribution observed for the fossil bone indicates variable degrees of crystallinity and/or crystallite size. (D) An electron microprobe wavelength-dispersive X-ray scan from the fossil bone, which further verifies the occurrence of F in the fossil bone. See text for further discussions.

<https://doi.org/10.1371/journal.pone.0228843.g002>

polynomial background, we obtained a ratio of 0.92 ± 0.09 for our sample that agrees very well with published values from Dominican amber which range between 0.91 and 1.00 [41]. A noticeable difference with published amber spectra, however, is the occurrence of a broad band near 1370 cm^{-1} . Moreover, the bands at 1355 , 1384 , and 1408 cm^{-1} , assigned to $\delta(\text{CH}_2)$ and $\delta(\text{CH}_3)$ deformation modes, are significantly more intense, even reaching the same height as the neighboring $\nu(\text{C}=\text{C})$ band at 1450 cm^{-1} . These spectral differences indicate that the amber has chemically been modified.

The generally good preservation property of the amber is noticeable by the conservation of skin soft tissue that caused problems with the polishing of the bone due to the difference in the hardness between amber, tissue, and bone, so that the sample surface is not perfectly flat (Fig 1C). However, the bone itself also exhibited brittle behaviour during polishing as reflected by cracks and broken bone pieces that are partly pressed into the surrounding amber (yellow arrow in Fig 1C), indicating that some alteration occurred that affected the mechanical properties of the bone. This observation is further confirmed by the histological slices of the fossil. Except for one slice (Fig 1B), the fossil bone tissue was highly fragile and was lost from the microscope slices during preparation. This can be explained by an extensive fragmentation of the bone tissue (Fig 1B) that we expect to stem from the contact with acidic compounds in the resin. Unexpectedly, hyperspectral Raman images from a $50 \times 50 \mu\text{m}^2$ area of the bone further revealed an unusually heterogeneous distribution of organic and inorganic phases (Fig 1D), including the occurrence of a new, yet unidentified carbonate mineral (black arrows in Fig 1D). This phase is unambiguously identified as a carbonate by the $\nu_1(\text{CO}_3)$ band near 1079 cm^{-1} (Fig 2A) and shows only two further Raman bands near 369 and 1441 cm^{-1} , the latter of which can be assigned to the antisymmetric $\nu_4(\text{CO}_3)$ stretching motion of the carbonate group. All three bands are relative broad with linewidths between 20 and 30 cm^{-1} (Fig 2A), suggesting a rather disordered carbonate structure. Unfortunately, its Raman spectrum is not comparable to any of the known (carbonate) minerals that are included in the RRuff Raman spectral data base containing more than 8000 Raman spectra of minerals [44].

From a comparison of representative Raman spectra of the fossil bone with a typical Raman spectrum of an extant lizard bone it is evident that both the inorganic and organic phases in the fossil bone are strongly modified (Fig 2A). In the Raman spectra of the extant bone, bands related to collagen vibrations, such as methylene side chains (CH_2 at 1450 cm^{-1}), amide III ($1243\text{--}1320 \text{ cm}^{-1}$), phenylalanine ($\sim 1002 \text{ cm}^{-1}$), CH stretch ($\sim 2940 \text{ cm}^{-1}$), or the combined proline (921 and 855 cm^{-1}) and hydroxyproline (876 cm^{-1}) vibrations, can clearly be identified (Fig 2A). In contrast, Raman spectra from the fossil do not show any of the collagen bands anymore, but are characterized by a number of new broad bands between 1200 and 1500 cm^{-1} which can be assigned to $\nu_s(\text{C}\text{--}\text{O})$ and/or $\nu_s(\text{C}\text{--}\text{N})$ vibrations. In some spectra, sharper but weak bands can be identified at 1043 , 1115 , 1125 , and 1148 cm^{-1} (marked yellow in Fig 2A). These spectra also show overlapping bands near 922 , 935 , and 949 cm^{-1} , whereas in other spectra a broad band near 883 with a shoulder near 920 cm^{-1} is visible in the wavenumber range between 800 and 1000 cm^{-1} , i.e., at typical frequencies of aliphatic C–C chain vibrations.

Some spectra show a broad band near 1580 cm^{-1} and a shoulder near 1350 cm^{-1} (Fig 2A) that may tentatively be assigned to the D_1 and G band of amorphous sp^2 carbon, respectively [45]. However, the spectra vary in different locations with some spectra showing two distinguishable bands near 1549 and 1586 cm^{-1} rather than a broad band centred near 1580 cm^{-1} , which possibly reflect aliphatic $\nu(N=N)$ modes. Noticeably, no Raman signals were detected in the frequency region between 1650 and 3100 cm^{-1} , suggesting the absence of, e.g., aliphatic C–H bonds and carboxyl functional groups. Relative weak bands could be detected in the fossil bone between 3200 and 3600 cm^{-1} , indicating the occurrence of O–H and/or N–H bonds. It follows from these observations that regardless of the exact composition and structure of these organic compounds, they obviously do not represent typical collagen degradation products such as polypeptides, smaller peptides, or amino acids.

The most intense and sharpest band in the spectra from the extant lizard bone is located near 960 cm^{-1} and reflects the fully symmetric $\nu_1(\text{PO}_4)$ stretching motions of the phosphate tetrahedra in the bone apatite structure (Fig 2A). The carbonate group in the apatite structure generates a $\nu_1(\text{CO}_3)$ band near 1070 cm^{-1} [46] that is, however, partially overlapped by $\nu_3(\text{PO}_4)$ stretching bands, making a quantitative assessment of the carbonate content challenging [47, 48]. All these apatite-related bands also occur in the Raman spectra of the fossil bone. However, here the $\nu_1(\text{PO}_4)$ band is (i) significantly shifted to higher frequencies, (ii) narrower, (iii) significantly less intense when compared to the Raman intensities from the organic material, and (iv) on average less asymmetric (Fig 2C). To quantify these visible differences, we fitted an asymmetric Gauss-Lorentz function to the $\nu_1(\text{PO}_4)$ band along with a 3rd order polynomial background between 930 and 990 cm^{-1} to account for the asymmetry of this band, basically caused by a contribution from a band near 950 cm^{-1} of still unknown origin [49], and any non-linearity in the background of some spectra, respectively. The data from both specimens define non-overlapping, linear arrays in the plot of the frequency of the $\nu_1(\text{PO}_4)$ band versus its full width at half maximum (FWHM), with fossil bone data covering a larger range of frequency and FWHM values (Fig 2B). This and the broad multimodal distribution of the asymmetry parameter (Fig 2C) suggest a heterogeneous bone microstructure that is composed of domains showing variable structural disorder and/or crystallite size. Thereby, the frequency and FWHM values from the fossil bone are significantly higher respectively lower than those from the extant bone and cover values that are typical for highly fluoridated bones and teeth in which the bone apatite is transformed to FAp (Fig 2B) [49]. Due to the significance of such an observation, the occurrence of F was further verified by wavelength-dispersive X-ray scans that unambiguously verify the occurrence of F in the bone (Fig 2D).

Now the question arises about the source of the fluorine. In this respect, the occurrence of a crack in the amber piece is an important observation (S2 Fig), as it potentially represents a favored pathway for chemical transport. As determined by μ -CT scans, radius and ulna of the lizard are broken in the same plane of the crack (S1 and S2 Figs), which suggests cracking after the resin has cured and thus completely polymerized. To find evidence of chemical exchange along the crack, we analyzed this structure with focused ion beam based time-of-flight secondary ion mass spectrometry (FIB ToF-SIMS). The crack is filled with residues of epoxy resin and an aluminosilicate mineral phase (S4 Fig). ToF-SIMS analyses confirmed the presence of O, Mg, Al, Si, K and Na as major elements in the mineral. Traces of F can be observed as elongated features, likely in the cleavage planes of the mineral phase (S4 Fig). The epoxy resin is clearly a preparation artefact, and was used to stabilize the sample prior to the cutting. The epoxy is enriched in O and Cl compared to the host amber and although enrichment of Cl can be observed between the mineral phase and the amber, it remains unclear if this is the result of the epoxy contamination or is indicative of fluid infiltration (S4 Fig).

Discussion

Although optical microscopy and μ -CT imaging revealed a high degree of morphological preservation of the fossil fore limb (S2 and S3 Figs), our Raman and X-ray data (Fig 1) from the bone surprisingly demonstrate the unambiguous formation of FAp in the fossil lizard bone. Fluoridation of bone is a process that involves the transformation or replacement of the carbonated bone HAp to a FAp structure. Fluoridation is commonly observed in fossils from clastic sedimentary environments, where it takes place during an early diagenetic stage by the infiltration of F-rich ground or soil water, and is accompanied by a simultaneous loss of the structurally incorporated carbonate groups and collagen matrix [50, 51], i.e., fluoridation is usually a *post mortem* process. However, teeth and bones may also fluoridate during the lifetime of the individual [51, 52]. Replacement of OH^- by F^- in teeth enamel can have the advantage of producing a harder more resistant enamel. For this reason, F has been added to municipal water supplies in some countries (USA, UK, Australia) as well as to toothpaste [53]. Experiments have confirmed that nanocrystalline hydroxylapatite in dental enamel can be replaced by fluorapatite even at room temperature within laboratory time scales [49]. It has been proposed that the replacement is pseudomorphic with the original morphology of the hydroxylapatite crystallites preserved [49].

The detection of F along the crack in the amber piece (S2 Fig) suggests that F could have been transported as F^- species dissolved in water along the crack that extends to the lizard bone, but it remains unclear in which stage of diagenesis this could have happened. The polymeric and unipolar nature of the fresh and matured resin structure must have generally shielded the lizard bone against the infiltration of free water in an early diagenetic phase. The presence of flow patterns in the amber piece (S1 Appendix and S1 Fig) points to an accumulation of resin on the outer surface of the bark of the tree, and not within the bark, wood, or root area. Consequently, the piece was exposed to air, rain water, and UV-radiation before it was buried in the soil where it may have been in contact to soil or ground water. The fossil humerus is broken in its middle part (S2 Fig) and the formation of an edema (S2B Fig) in this region implies that the resin was still deformable at this time. This interpretation is supported by peeled off parts of the skin “floating” in the matrix around the bone (S1 and S2 Figs). Furthermore, an edema indicates that the lizard was not dehydrated or dead when it entered the fresh tree resin (S1 Appendix), which means that early decay processes of the fossil took place while it was fully embedded within a viscous, non-polymerized resin that included gas bubbles (S1 and S3A Figs), which prevented the escape of the body fluid. It is thus possible that internal body fluids may have played an important role by altering the mineral and organic phases of the mineralized and non-mineralized tissue.

However, it seems unlikely that the fluoridation is solely caused by body fluids, because in this case fluorine must have been locally concentrated in the liquid phase. An autochthonous origin of F may derive from an uptake of F-rich drinking water by the living lizard. In this case, the animal would have suffered from severe fluorosis before it died. Fluoride can be found in the lithosphere and natural waters in varying concentrations, with high amounts being reported from sediments of marine origin in mountainous areas, volcanic rocks, and granitic and gneissic rocks [54, 55]. With the exception of the large lakes in the East African Rift Valley system, high concentrations of F are usually associated with ground waters and not surface waters [54]. Generally, rivers and lakes have a fluoride concentration of less than 0.5 mg l^{-1} . Seawater contains 1.0 mg l^{-1} of fluoride, whereas the concentration in drinking water (ground water) can reach up to 50 mg l^{-1} [54]. If no specialized structures for water uptake are present, most lizards lick water from wet leaves or drink from small ponds or rainwater. These surface waters have a low (if any) concentration of fluorine which means that their effect on

the bone tissue should be negligible. In theory, another source of autochthonous fluorine can be found in the dentition of the animal, but the forelimb was separated from the body, which excludes this possibility in our case.

Conclusions

Although at this stage of investigation the source of F remains somewhat speculative, we expect an allochthon origin to be most likely based on our ToF-SIMS analysis. However, regardless of the exact mode of fluoridation, the alteration process did not alter the bone on a large scale because lacunae of osteocytes are still visible (S3D Fig), which excludes an extensive remodeling of the structure. Furthermore, Raman spectroscopy revealed that the transformation of the nanocrystalline, carbonated bone HAp to FAp was accompanied by severe alteration of the collagen matrix, possibly to aliphatic C-N-H compounds. The intergrowth of the mineral and organic phase in bone suggests that the degradation of collagen must have taken place at the same time as the recrystallization of the carbonated bone HAp to FAp, which apparently releases carbonate groups into the surrounding solution which locally precipitated as a yet unidentified carbonate phase. In nature the chemical breakdown and loss of collagen may occur slowly in soil or groundwater via pH-dependent hydrolysis reactions (proteolysis), producing smaller peptides and amino acids, or later through conditions in a burial environment, where the degradation of collagen may increasingly be controlled by temperature [56]. In archaeological samples of Holocene bones, microbial proteolysis has been identified as the main process of collagen degradation and loss [57]. This pathway is unlikely for our sample due to the antiseptic properties of organic compounds in tree resins such as non-polymerized diterpenoids. However, a previous study focusing on ancient amino acid preservation of insects in amber [58] failed to detect any remains in the samples from Dominican amber, which is in contrast to other deposits and indicates a protein-degrading environment. On the other hand, volatile resin compounds such as mono-, and sesquiterpenoids may have already reacted with the collagen matrix during entrapment of the lizard, i.e., during the early polymerization and solidification process, but without any significant mass loss as indicated by the histological slice (Fig 1B). Some monoterpenoids and sesquiterpenoids possess enzyme inhibiting properties, which might contribute to the generally observed exceptional preservation of soft tissue in amber.

Although the exact mechanism of bone fluoridation and alteration remains unresolved at this stage, it is important to note that evidently the presence of a resinous matrix (later forming copal and amber) does not necessarily inhibit chemical exchange between fossil and the environment of the amber. As a result, fossil inclusions of vertebrates in amber must be considered as the result of complex (open-system) transport and reaction processes involving the interaction of bone tissue with (i) external chemical elements and substances, including aqueous solutions, (ii) the aqueous body fluid of the fossil itself, and (iii) highly reactive, organic resin compounds. As this is the first detailed study on fossil bone material embedded in amber, future studies on different vertebrate inclusions in amber from different deposits will show which of the above processes dominate and whether there is still a chance to find intact macromolecules in amber fossils.

Material & methods

Sample preparation

The investigated piece of Dominican amber is part of the paleontological collection of the State Museum of Natural History Stuttgart (SMNS, collection number DHQ-4924-H). All necessary permits were obtained for the described study, which complied with all relevant

regulations. The piece contains a Mymaridae (fairy wasps, Hymenoptera) and the left forelimb of an *Anolis* sp. indet. The sample has been covered with two glass sheets on either side which have been fixed with some glutinous material (maybe Canada balsam) by its former owner. We removed the glass with a grinding machine and embedded the whole sample again in epoxy resin (Araldite2020®). Documentation took place between consumptive preparation steps and comprises μ -CT scans and optical images taken at different magnifications. We then cut the specimen in half, resulting in a piece containing the head of the humerus and a piece with the distal part of the specimen, including humerus, radius, ulna, and manus from which a polished thin section was prepared. In addition to the fossil specimen, we obtained a dead *Anolis carolinensis* (56 mm snout-vent length) from a private breeder. For comparison, the left forelimb (length: 15 mm) was separated from the trunk with a scalpel and then processed in the same way as the fossil specimen to produce a polished thin section. Raman spectroscopy was then used to first characterize the polished thin sections of the fossil and the recent lizard (Fig 1C).

Furthermore, we used the other half of the sample (including only the head of the humerus) to produce histological thin sections with a microtome, following roughly the same protocol as for extant specimens. An exception was the infiltration of the sample with artificial resin with the help of a desiccator. This was done to seal void spaces in the matrix that would have caused problems during the cutting.

Optical imaging

The images of the osteocyte lacunae and thin sections were taken with a Leica DMLP polarizing microscope and the software Image Access. The lacunae are recognizable in light microscopic images, but they are better visible in polarized images.

Micro-CT (computed X-ray tomography)

The sample was scanned with a General Electronix v-tome-xs micro-CT at the Institute of Geosciences, University of Bonn, Germany. The amber piece was irradiated at a voltage of 105 kV and a current of 105 mA with an exposure time of 1000 ms with a voxel size down to $11.15 \mu\text{m}^3$.

Raman spectroscopy

Raman measurements were performed with a Horiba Scientific LabRam HR800 confocal Raman spectrometer at the Institute of Geosciences, University of Bonn, Germany. Raman scattering was excited with a diode-pumped solid-state laser (783.976 nm) with less than 20 mW at the sample surface. A 100 times objective with a numerical aperture of 0.9 and a confocal hole of $1000 \mu\text{m}$ was used for all measurements, resulting in a theoretical, diffraction-limited lateral and axial resolution of $\sim 1 \mu\text{m}$ and less $1 \mu\text{m}$, respectively. The scattered Raman light was collected in a 180° backscattering geometry by an electron-multiplier charge-coupled device detector after having passed through a $200 \mu\text{m}$ spectrometer entrance slit and being dispersed by a grating of 600 grooves/mm. This yielded a spectral resolution of 2.07 cm^{-1} , as determined by the full width at half maximum of Ne lines that were continuously monitored by placing a Ne lamp inside the beam path of the scattered light. The Ne lines were used to correct for any non-linear spectrometer drift during long term mapping. To correct for the effect of the finite slit width on measured linewidth (given as full width at half maximum, FWHM) following equation was used^(Tanabe & Hiraishi 1980): $\text{FWHM}_c = \text{FWHM}_m [1 - (S / \text{FWHM}_m)^2]$, where FWHM_c , FWHM_m , and S are the corrected linewidth of the Raman band, the measured linewidth, and the spectral slit width ($= 2.07 \text{ cm}^{-1}$), respectively. All spectra were further

corrected by a wavelength-dependent instrumental response function (white light correction). The measurements were performed in the point-by-point mapping mode at different locations of the bone. The total acquisition time of a single spot analysis was between 60 and 300 s.

Electron microprobe (EMP)

To further check the occurrence of F in the bone apatite, suggested by the Raman data, the sample was coated with a thin layer of gold and wavelength-dispersive X-ray spectra were recorded with a JEOL 8200 Superprobe and a TAP crystal in the wavelength range between 1.82 and 1.86 nm, in which the F-K α line (1.832 nm) is located. The measurements were performed with a step size of 9.2×10^{-5} nm and a dwell time of 5 s per wavelength step. The acceleration voltage and beam current were set to 15 keV and 15 nA, respectively.

Time-of-flight secondary ion mass spectrometry (ToF-SIMS)

High spatial resolution maps of $^{19}\text{F}^-$, $^{35}\text{Cl}^-$, $^{28}\text{Si}^+$ and $^{27}\text{Al}^+$ were performed using the Ga $^+$ Tescan Lyra3 Focused Ion Beam Scanning Electron Microscope (FIB-SEM) equipped with a ToF-werk ToF-SIMS detector at Curtin University in Perth, Australia. An accelerating voltage of 20 kV and a current of 500 pA was used for the Ga $^+$ primary ion beam. Maps of $40 \times 40 \mu\text{m}^2$ were acquired with a pixel resolution of 40 nm. A total of 100 frames were collected for the negative ion maps ($^{19}\text{F}^-$ and $^{35}\text{Cl}^-$) and 20 frames for the positive ion maps ($^{28}\text{Si}^+$ and $^{27}\text{Al}^+$). ToF-SIMS Explorer version 1.3 software was used for acquisition and processing of the data. Backscattered and secondary electron images were acquired with the same instrument. The electron beam was operated at 10 kV.

Supporting information

S1 Appendix. Description of DHQ-4924-H and implications on its taphonomy. (DOCX)

S1 Fig. (A) Optical microscope transmission image of the entire sample DHQ-4924-H prior to cutting and grinding. Several flow structures can be recognized in the matrix alongside the fossil inclusions. Detailed images of (B) the forelimb in lateral and (C) medial view were taken under crossed polarized light. (DOCX)

S2 Fig. μ -CT images of sample DHQ-2924-H. (A) Reconstruction of the bone tissue revealed two broken parts of the forelimb (white and blue arrows). (B) The green areas resemble a large crack (blue arrow) as well as parts of the soft tissue. The crack cuts the radius and ulna and continues through the whole amber piece (not fully shown in B). A swelling of the soft tissue can be recognized opposite to the damaged part of the humerus, which we interpret as an edema (white arrow). (DOCX)

S3 Fig. Optical transmission images of sample DHQ-4924-H. (A) Exposed head of the humerus surrounded by peeled off parts of skin and air bubbles. (B) Large crack (black arrow) that cuts through radius and ulna (also shown in the CT-images, S2 Fig). (C) Skin remains and numerous bubbles within the matrix. The tiny black spots are likely sheds that formerly have been part of the integument. (D) Proximal part of the humerus under crossed polarized light. Note the presence of lacunae (blue arrow) which are visible in the middle part of the bone. (DOCX)

S4 Fig. Time-of-flight secondary ion mass spectrometry (ToF-SIMS) measurements of sample DHQ-4924-H. (A) Backscattered electron and (B) secondary electron images of the region around the crack. (C-F) Elemental maps of Silicate, Aluminium, Fluorine, and Chlorine in the region of interest shown in B. (DOCX)

Acknowledgments

We thank the Institute of Evolutionary Biology and Zooecology (University of Bonn) for providing lab supplies and working space and are in particular grateful to Tatjana Bartz for preparing the microtome cuttings. We thank Olaf Dülfer (Institute of Geosciences, University of Bonn) for his help in preparing the thin section. Furthermore, we thank Marie K. Hörnig (Zoological Institute and Museum, Cytology and Evolutionary Biology, University of Greifswald) for the detailed images of the specimen that are shown in the Supplementary Information and Beate Spiering for acquiring the electron microprobe data. We thank P. Martin Sander and Bastian Mähler (Institute of Geosciences, University of Bonn) for discussions on an early version of this work. We are grateful to both anonymous reviewers who helped to improve the manuscript. This is contribution number 26 of DFG Research Unit FOR2685 “The Limits of the Fossil Record: Analytical and Experimental Approaches to Fossilization.”

Author Contributions

Conceptualization: H. Jonas Barthel.

Data curation: Denis Fougerouse.

Funding acquisition: Denis Fougerouse, Jes Rust.

Investigation: H. Jonas Barthel, Thorsten Geisler.

Methodology: Denis Fougerouse, Thorsten Geisler.

Project administration: Jes Rust.

Writing – original draft: H. Jonas Barthel, Thorsten Geisler.

Writing – review & editing: Denis Fougerouse, Jes Rust.

References

1. Pasteris JD, Yoder CH, Wopenka B. Molecular water in nominally unhydrated carbonated hydroxylapatite: The key to a better understanding of bone mineral. *Am Mineral*. 2014; 99(1): 16–27. <https://doi.org/10.2138/am.2014.4627>
2. Wilson EE, Awonusi A, Morris MD, Kohn DH, Tecklenburg MMJ, Beck LW. Three structural roles for water in bone observed by solid-state NMR. *Biophys J*. 2006; 90(10): 3722–31. <https://doi.org/10.1529/biophysj.105.070243> PMID: 16500963
3. Boanini E, Gazzano M, Bigi A. Ionic substitutions in calcium phosphates synthesized at low temperature. *Acta Biomater*. 2010; 6: 1882–94. <https://doi.org/10.1016/j.actbio.2009.12.041> PMID: 20040384
4. Berna F, Matthews A, Weiner S. Solubilities of bone mineral from archaeological sites: the recrystallization window. *Journal Archaeol Sci*. 2004; 31(7): 867–82. <https://doi.org/10.1016/j.jas.2003.12.003>
5. Nemliher JG, Baturin GN, Kallaste TE, Murdmaa IO. Transformation of hydroxyapatite of bone phosphate from the ocean bottom during fossilization. *Lithol Miner Resour*. 2004; 39(5): 468–79. <https://doi.org/10.1023/B:LIMI.0000040736.62014.2d>
6. Rošin-Grgel K, Linčir I. Current concept on the anticaries fluoride mechanism of the action. *Coll Antropol*. 2001; 25(2): 703–12. PMID: 11811302

7. Lee Y-C, Chiang C-C, Huang P-Y, Chung C-Y, Huang TD, Wang C-C, et al. Evidence of preserved collagen in an Early Jurassic sauropodomorph dinosaur revealed by synchrotron FTIR microspectroscopy. *Nat Commun*. 2017; 8: 14220. <https://doi.org/10.1038/ncomms14220> PMID: 28140389
8. Pawlicki R, Korbek A, Kubiak H. Cells, collagen fibrils and vessels in dinosaur bone. *Nature*. 1966; 211(5049): 655–7. <https://doi.org/10.1038/211655a0> PMID: 5968744
9. Trueman CN., Behrensmeier AK, Tuross N, Weiner S. Mineralogical and compositional changes in bones exposed on soil surfaces in Amboseli National Park, Kenya: diagenetic mechanisms and the role of sediment pore fluids. *J Archaeol Sci*. 2004; 31(6): 721–39.
10. Pucéat E, Reynard B, Lécuyer C. Can crystallinity be used to determine the degree of chemical alteration of biogenic apatites? *Chem Geol*. 2004; 205(1–2): 83–97. <https://doi.org/10.1016/j.chemgeo.2003.12.014>
11. Piga G, Santos-Cubedo A, Moya Solà S, Brunetti A, Malgosa A, Enzo S. An X-ray Diffraction (XRD) and X-ray Fluorescence (XRF) investigation in human and animal fossil bones from Holocene to Middle Triassic. *J Archaeol Sci*. 2009; 36(9): 1857–68. <https://doi.org/10.1016/j.jas.2009.04.013>
12. Dumont M, Kostka A, Sander PM, Borbely A, Kaysser-Pyzalla A. Size and size distribution of apatite crystals in sauropod fossil bones. *Palaeogeogr Palaeoclimatol Palaeoecol*. 2011; 310(1–2): 108–16. <https://doi.org/10.1016/j.palaeo.2011.06.021>
13. Henwood AA. Exceptional preservation of Dipteran flight muscle and the taphonomy of Insects in amber. *PALAIOS*. 1992; 7: 203–12. <https://doi.org/10.2307/3514931>
14. Henwood AA. Soft-part preservation of beetles in Tertiary amber from the Dominican Republic. *Palaeontology*. 1992; 35(4): 901–12.
15. Grimaldi DA, Bonwich E, Delannoy M, Doberstein S. Electron microscopic studies of mummified tissues in amber fossils. *American Museum Novitates*. 1994; 3097: 1–31.
16. Hopfenberg HB, Witchev LC, Poinar GO. Is the air in amber ancient? *Science*. 1988; 241(4866): 717–718. <https://doi.org/10.1126/science.241.4866.717> PMID: 17839082
17. Stankiewicz BA, Poinar HN, Briggs DEG, Evershed RP, Poinar GO. Chemical preservation of plants and insects in natural resins. *Proc Royal Soc Lond B: Biological Sciences*. 1998; 265(1397): 641–7. pmcid: PMC1689027
18. Koller B, Schmitt JM, Tischendorf G. Cellular fine structures and histochemical reactions in the tissue of a cypress twig preserved in Baltic amber. *Proc Royal Soc Lond B: Biological Sciences*. 2005; 272(1559): 121–6. <https://doi.org/10.1098/rspb.2004.2939> PMID: 15695201
19. Schlee D. Bernstein-Neuigkeiten. *Stutt Beitr Naturkd Ser C*. 1984; 18:1–100.
20. Eckstein K. Thierische Haareinschlüsse im baltischen Bernstein. *Schrift Naturforsch Gesell Dan*. 1890; 7: 90–3.
21. Peñalver E, Grimaldi DA. Assemblages of mammalian hair and blood-feeding midges (Insecta: Diptera: Psychodidae: Phlebotominae) in Miocene amber. *Trans Roy Soc Edinb: Earth Sci*. 2005; 96: 177–95. <https://doi.org/10.1017/S0263593300001292>
22. MacPhee RDE, Grimaldi DA. Mammal bones in Dominican amber. *Nature*. 1996; 380: 489–90. <https://doi.org/10.1038/380489b0>
23. Schlee D. Harzkonservierte fossile Vogelfedern aus der untersten Kreide. *J Ornithol*. 1973; 114(2):207–19.
24. Perrichot V, Marion L, Neraudeau D, Vullo R, Tafforeau P. The early evolution of feathers: fossil evidence from Cretaceous amber of France. *Proc Royal Soc Lond B: Biological Sciences*. 2008; 275(1639): 1197–202. <https://doi.org/10.1098/rspb.2008.0003> PMID: 18285280
25. Xing L, McKellar RC, Wang M, Bai M, O'Connor JK, Benton MJ, et al. Mummified precocial bird wings in mid-Cretaceous Burmese amber. *Nat Commun*. 2016; 7: 12089. <https://doi.org/10.1038/ncomms12089> PMID: 27352215
26. Xing L, McKellar RC, Xu X, Li G, Bai M, Persons WS, et al. A feathered dinosaur tail with primitive plumage trapped in Mid-Cretaceous amber. *Curr Biol*. 2016; 26(24): 3352–60. <https://doi.org/10.1016/j.cub.2016.10.008> PMID: 27939315
27. Xing L, O'Connor JK, McKellar RC, Chiappe LM, Tseng K, Li G, et al. A mid-Cretaceous enantiornithine (Aves) hatchling preserved in Burmese amber with unusual plumage. *Gondwana Res*. 2017; 49:264–77. <https://doi.org/10.1016/j.gr.2017.06.001>
28. Sherratt E, del Rosario Castañeda M, Garwood RJ, Mahler DL, Sanger TJ, Herrel A, et al. Amber fossils demonstrate deep-time stability of Caribbean lizard communities. *Proc Natl Acad Sci U.S.A.* 2015; 112(32): 9961–9966. <https://doi.org/10.1073/pnas.1506516112> PMID: 26216976
29. Lazell JD Jr. An *Anolis* (Sauria, Iguanidae) in amber. *J Paleontol*. 1965; 39(3): 379–382.

30. Arnold EN, Azar D, Ineich I, Nel A. The oldest reptile in amber: a 120 million year old lizard from Lebanon. *J Zool.* 2002; 258(1): 7–10. <https://doi.org/10.1017/S0952836902001152>
31. Arnold EN, Poinar GO Jr. A 100 million year old gecko with sophisticated adhesive toe pads, preserved in amber from Myanmar. *Zootaxa.* 2008; 1847: 62–8.
32. Böhme W, Weitschat W. New finds of lizards in Baltic amber (Reptilia: Squamata: Sauria: Lacertidae). *Faun Abh Mus Tierkd Dresden.* 2002; 23: 117–30.
33. Borsuk-Bialynicka M, Lubka M, Böhme W. A lizard from Baltic amber (Eocene) and the ancestry of the crown group lacertids. *Acta Palaeontol Pol.* 1999; 44(4): 349–328.
34. Bauer AM, Böhme W, Weitschat W. An Early Eocene gecko from Baltic amber and its implications for the evolution of gecko adhesion. *J Zool.* 2005; 265(4): 327–32.
35. Rieppel O. Green anole in Dominican amber. *Nature.* 1980; 286(5772): 486–7.
36. Daza JD, Stanley EL, Wagner P, Bauer AM, Grimaldi DA. Mid-Cretaceous amber fossils illuminate the past diversity of tropical lizards. *Sci Adv.* 2016; 2(3): e1501080–e1501080. <https://doi.org/10.1126/sciadv.1501080> PMID: 26973870
37. Daza JD, Bauer AM. A new amber-embedded sphaerodactyl gecko from Hispaniola, with comments on morphological synapomorphies of the Sphaerodactylidae. *Breviora.* 2012; 529: 1–28. <https://doi.org/10.3099/529.1>
38. Klebs R. Über Bernsteineinschlüsse im allgemeinen und die Coleopteren meiner Bernsteinsammlung. *Schrif Phyk-Ökon Ges zu Königsb Preußen.* 1910; 51: 217–42.
39. Polcyn MJ, Rogers II JV, Kobayashi Y, Jacobs LL. Computed tomography of an Anolis lizard in Dominican amber: systematic, taphonomic, biogeographic, and evolutionary implications. *Palaeontol Electron.* 2002; 5(1): 1–13.
40. Daza JD, Bauer AM, Wagner P, Böhme W. A reconsideration of *Sphaerodactylus dommeli* Böhme, 1984 (Squamata: Gekkota: Sphaerodactylidae), a Miocene lizard in amber. *J Zool Syst and Evol Res.* 2013; 51(1): 55–63. <https://doi.org/10.1111/jzs.12001>
41. Brody RH, Edwards HG, Pollard AM. A study of amber and copal samples using FT-Raman spectroscopy. *Spectrochim Acta A.* 2001; 57(6): 1325–1338. [https://doi.org/10.1016/s1386-1425\(01\)00387-0](https://doi.org/10.1016/s1386-1425(01)00387-0) PMID: 11419475
42. Edwards HGM, Farwell DW, Villar SEJ. Raman microspectroscopic studies of amber resins with insect inclusions. *Spectrochim Acta A.* 2007; 68(4): 1089–95. <https://doi.org/10.1016/j.saa.2006.11.037> PMID: 17320468
43. Winkler W, Kirchner EC, Asenbaum A, Musso M. A Raman spectroscopic approach to the maturation process of fossil resins. *J Raman Spectrosc.* 2001; 32(1): 59–63. [https://doi.org/10.1002/1097-4555\(200101\)32:1<59::AID-JRS670>3.0.CO;2-D](https://doi.org/10.1002/1097-4555(200101)32:1<59::AID-JRS670>3.0.CO;2-D)
44. Lafuente B, Downs RT, Yang H, Stone N. 1. The power of databases: The RRUFF project. In: Armbruster T, Danisi RM, editors. *Highlights in Mineralogical Crystallography.* Berlin: Walter de Gruyter GmbH; 2015. p. 1–30.
45. Marshall CP, Olcott Marshall A. The potential of Raman spectroscopy for the analysis of diagenetically transformed carotenoids. *Philos Trans Royal Soc A.* 2010; 368(1922): 3137–44. <https://doi.org/10.1098/rsta.2010.0016> PMID: 20529950
46. France CAM, Thomas DB, Doney CR, Madden O. FT-Raman spectroscopy as a method for screening collagen diagenesis in bone. *J Archaeol Sci.* 2014; 42: 346–55. <https://doi.org/10.1016/j.jas.2013.11.020>
47. de Aza PN, Santos C, Pazo A, de Aza S, Cuscó R, Artús L. Vibrational properties of calcium phosphate compounds. 1. Raman spectrum of β -tricalcium phosphate. *Chem Mat.* 1997; 9(4): 912–5. <https://doi.org/10.1021/cm960425d>
48. Awonusi A, Morris MD, Tecklenburg MMJ. Carbonate assignment and calibration in the Raman spectrum of apatite. *Calcif Tissue Int.* 2007; 81(1): 46–52. <https://doi.org/10.1007/s00223-007-9034-0> PMID: 17551767
49. Pasteris JD, Ding DY. Experimental fluoridation of nanocrystalline apatite. *Am Mineral.* 2009; 94(1): 53–63. <https://doi.org/10.2138/am.2009.2926>
50. Pfretzschner H-U. Fossilization of Haversian bone in aquatic environments. *CR Palevol.* 2004; 3(6–7): 605–16. <https://doi.org/10.1016/j.crpv.2004.07.006>
51. Wopenka B, Pasteris JD. A mineralogical perspective on the apatite in bone. *Mater Sci Eng C.* 2005; 25(2): 131–43. <https://doi.org/10.1016/j.msec.2005.01.008>
52. Freeman JJ, Wopenka B, Silva MJ, Pasteris JD. Raman spectroscopic detection of changes in bioapatite in mouse femora as a function of age and in vitro fluoride treatment. *Calcif Tissue Int.* 2001; 68(3): 156–62. <https://doi.org/10.1007/s002230001206> PMID: 11351499

53. Cheng KK, Chalmers I, Sheldon TA. Adding fluoride to water supplies. *BMJ*. 2007; 335(7622): 699–702. <https://doi.org/10.1136/bmj.39318.562951.BE> PMID: 17916854
54. Fawell JK, Bailey K, Chilton J, Dahi E, Fewtrell L, Magara Y, ed. *Fluoride in drinking-water*. London; Seattle: IWA Pub; 2006. 134 p. (WHO drinking water quality series).
55. Petrone P, Guarino FM, Giustino S, Gombos F. Ancient and recent evidence of endemic fluorosis in the Naples area. *J Geochem Explor*. 2013; 131: 14–27. <https://doi.org/10.1016/j.gexplo.2012.11.012>
56. Collins MJ, Nielsen–Marsh CM, Hiller J, Smith CI, Roberts JP, Prigodich RV, et al. The survival of organic matter in bone: a review. *Archaeometry*. 2002; 44(3): 383–394. <https://doi.org/10.1111/1475-4754.t01-1-00071>
57. Hedges RE. Bone diagenesis: an overview of processes. *Archaeometry*. 2002; 44(3): 319–328. <https://doi.org/10.1111/1475-4754.00064>
58. Bada JL, Wang XS, Poinar HN, Pääbo S, Poinar GO. Amino acid racemation in amber-entombed insects: Implications for DNA preservation. *Geochim Cosmochim Acta*. 1994; 58(14): 3131–35. [https://doi.org/10.1016/0016-7037\(94\)90185-6](https://doi.org/10.1016/0016-7037(94)90185-6) PMID: 11539553

Supporting Information for

Fluoridation of a lizard bone embedded in Dominican amber suggests open-system behavior

Hans Jonas Barthel, Denis Fougereuse, Thorsten Geisler, Jes Rust

Email: jbarthel@uni-bonn.de

S1 Appendix. Description of DHQ-4924-H and implications on its taphonomy

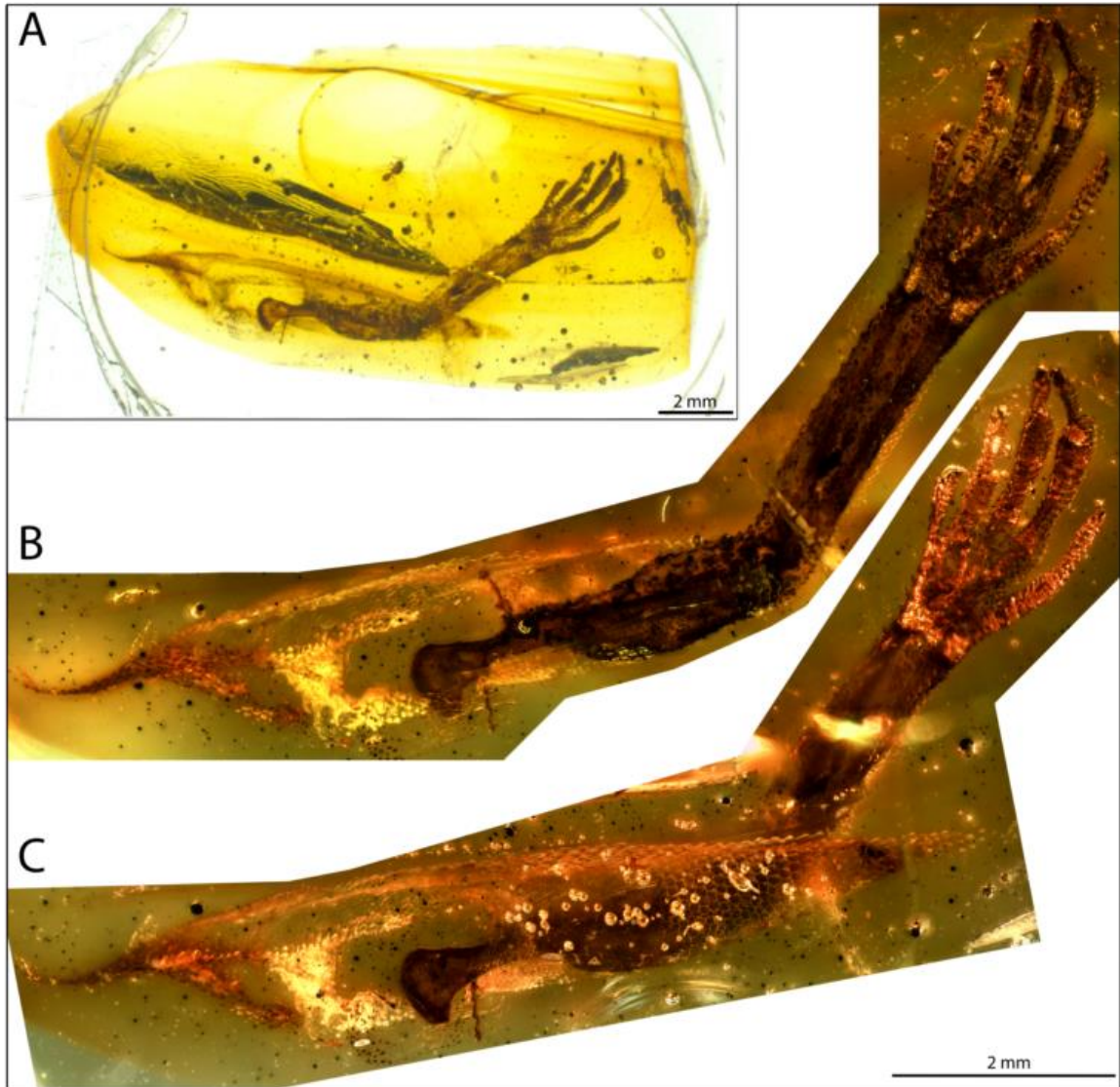
The amber piece DHQ-2924-H contains inclusions of a fore limb of an undetermined species of *Anolis* (Squamata, Dactyloidae) and an undetermined fairy wasp (Hymenoptera, Mymaridae, S1 Fig). The piece is built up of a succession of flows (“Schlauben”) which can be seen by naked-eye observation and were also detectable during segmentation of the CT slides. In total four major flow patterns can be identified whereas only the last two patterns contain the fossils. They are embedded within separate flows and the fore limb lies on the surface of one of these structures. The presence of “Schlauben” is important for two reasons: (i) they indicate an accumulation of resin at the surface of the stem which means (ii) that the lizard got actively into the resin because a dead lizard would not adhere to a vertical plane.

A large crack runs through the piece of amber and even cuts through the lizard limb at the proximal part of radius and ulna (S2B and S3 Figs). The crack must have been formed by the time the resin was completely hardened and represents a favored pathway for diffusional processes.

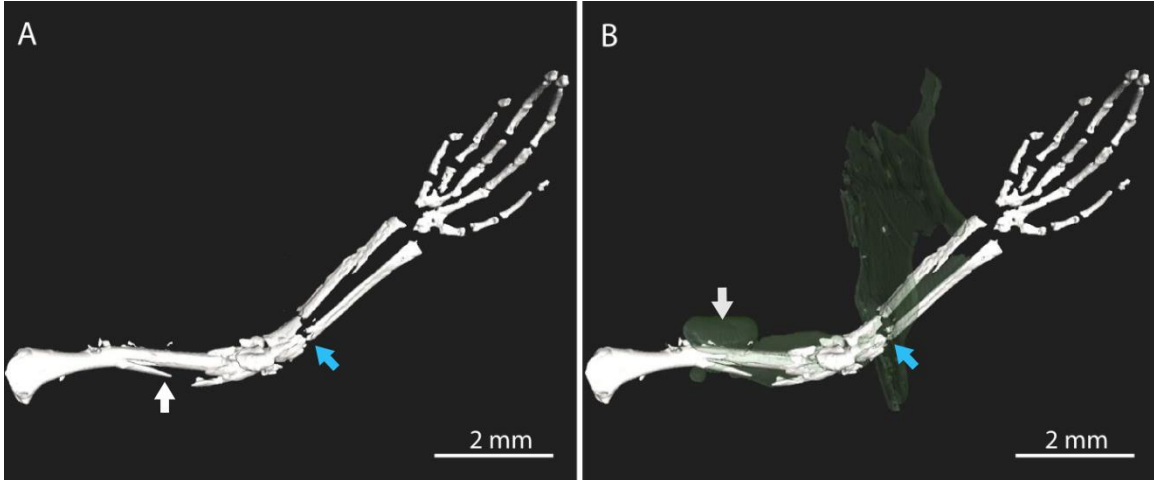
Sheds of skin are present in the matrix, especially in the region of the exposed head of the humerus (S3 Fig). The peeled off parts of the skin, together with the numerous air bubbles, indicate that the resin did not harden fast after the forelimb had been trapped.

CT-scans reveal that the humerus is broken in its middle part (S2 Fig). As there is no large crack to be observed that could have caused this injury *post mortem*, it must have happened shortly before the embedding of the sample or when the resin was still viscous. This assumption is supported by the presence of a roughly ellipsoid shaped area which has a higher density than most of the other soft tissue (cf. S2B Fig). Due to its different physical properties, we interpret this structure as an edema (a local assemblage of body fluids cf. S2B Fig) especially because it is directly opposite to the damaged spot.

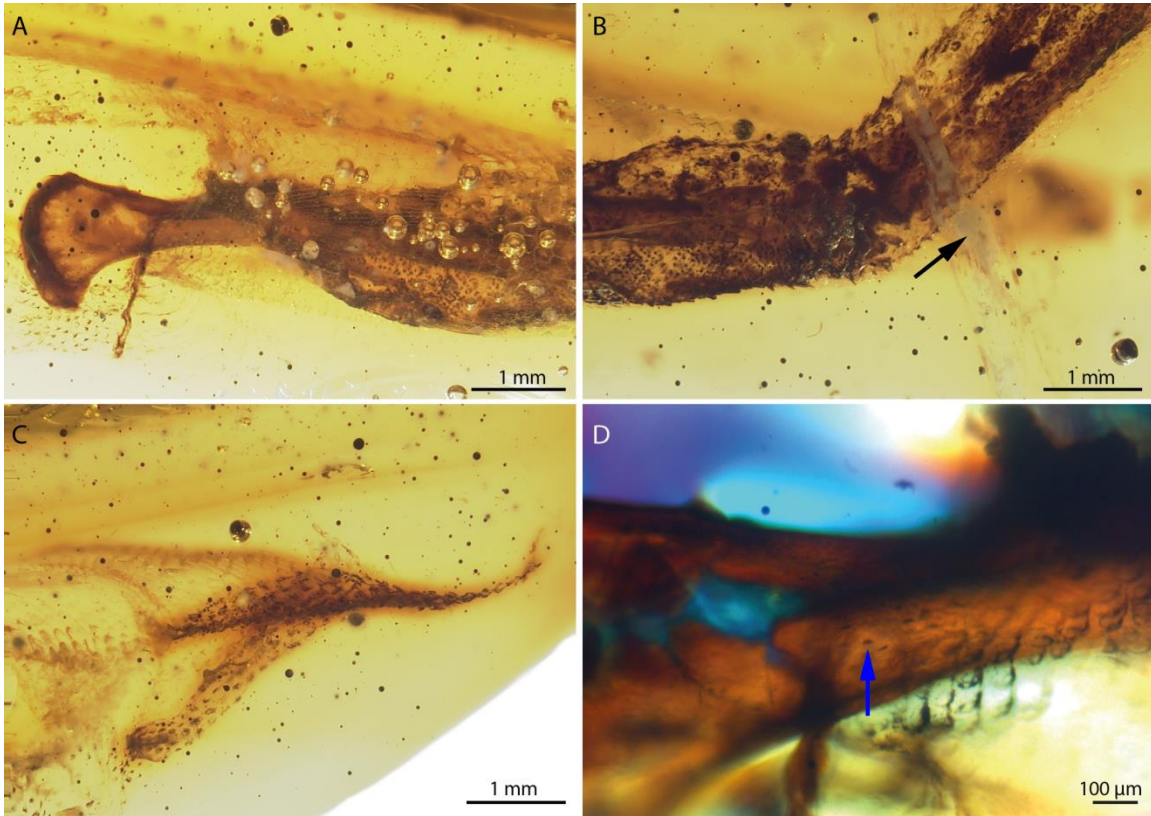
Taking all these observations into account, we propose the following model for our observations: While climbing the tree, the lizard got into contact with a flow of resin and could not escape its sticky trap (note the small size of the lizard). After some time, it attracted the attention of a predator that ripped off the lizard, leaving solely the fore limb in the resin. Later on, the resin hardened and became deposited within the surrounding soil which represents the starting point of its diagenesis. The presence of “Schlauben”, the splintered humerus, the edema, the peeled off parts of the skin, and lastly the numerous air bubbles strongly support this model.



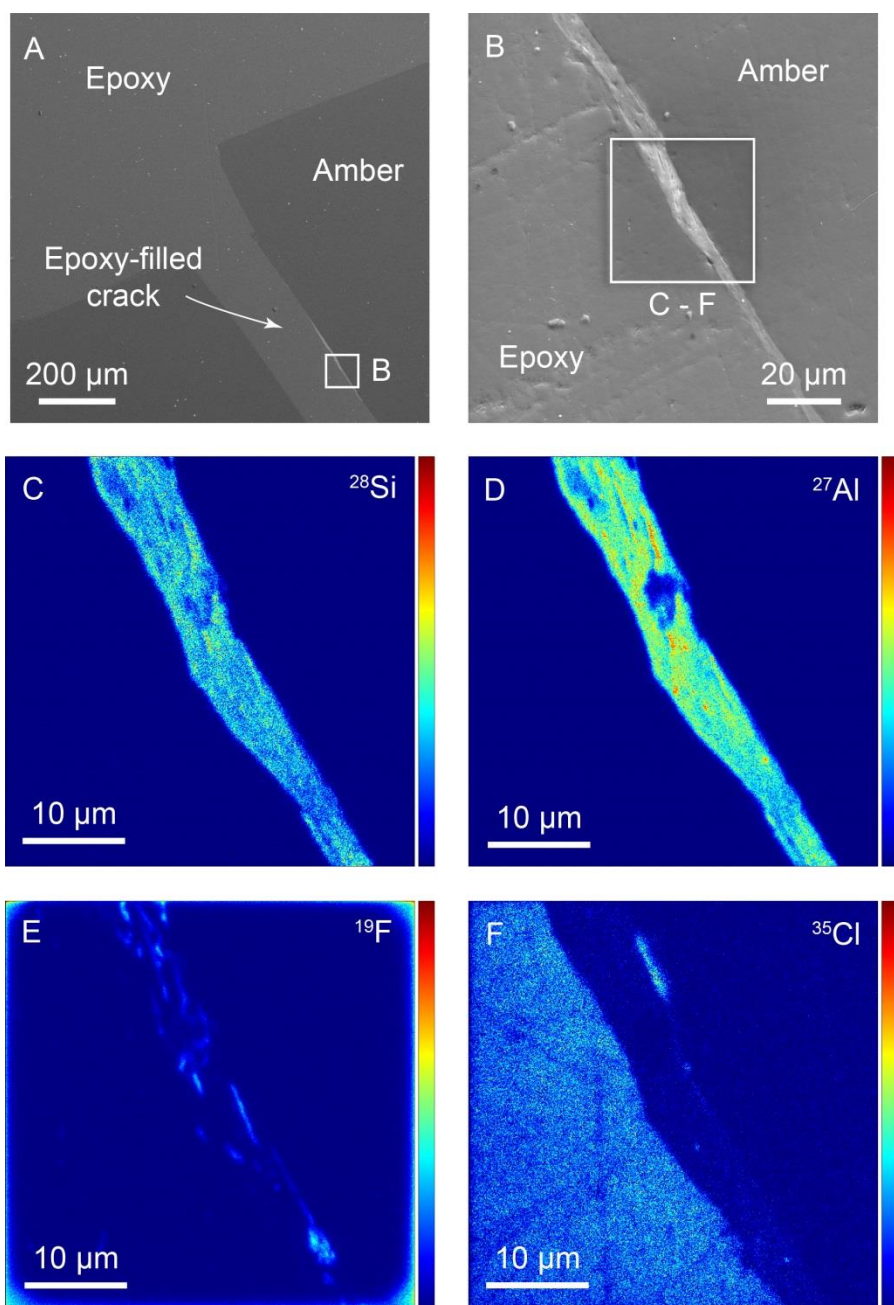
S1 Fig (A) Optical microscope transmission image of the entire sample DHQ-4924-H prior to cutting and grinding. Several flow structures can be recognized in the matrix alongside the fossil inclusions. Detailed images of **(B)** the forelimb in lateral and **(C)** medial view were taken under crossed polarized light.



S2 Fig μ -CT images of sample DHQ-2924-H. **(A)** Reconstruction of the bone tissue revealed two broken parts of the forelimb (white and blue arrows). **(B)** The green areas resemble a large crack (blue arrow) as well as parts of the soft tissue. The crack cuts the radius and ulna and continues through the whole amber piece (not fully shown in B). A swelling of the soft tissue can be recognized opposite to the damaged part of the humerus, which we interpret as an edema (white arrow).



S3 Fig Optical transmission images of sample DHQ-4924-H. **(A)** Exposed head of the humerus surrounded by peeled off parts of skin and air bubbles. **(B)** Large crack (black arrow) that cuts through radius and ulna (also shown in the CT-images, Fig. S2.). **(C)** Skin remains and numerous bubbles within the matrix. The tiny black spots are likely sheds that formerly have been part of the integument. **(D)** Proximal part of the humerus under crossed polarized light. Note the presence of lacunae (blue arrow) which are visible in the middle part of the bone.



S4 Fig Time-of-flight secondary ion mass spectrometry (ToF-SIMS) measurements of sample DHQ-4924-H. **(A)** Backscattered electron and **(B)** secondary electron images of the region around the crack. **(C-F)** Elemental maps of Silicate, Aluminium, Fluorine, and Chlorine in the region of interest shown in B.